Modulation of energy substrate transport by cAMP-hydrolysing phosphodiesterases in cardiac myocytes



Anna Zerio

Balliol College

University of Oxford

A thesis submitted for the degree of

Doctor of Philosophy

Hilary Term 2025

Dedicated to my parents, Dina and Claudio

"Cosimo non volle più salire in casa e s'arrampicò sugli alberi. [...] Aveva scelto di vivere tra le fronde e da lì non scese più."

– Italo Calvino, Il barone rampante

Acknowledgements

The work presented in this thesis was undertaken at the Department of Physiology, Anatomy and Genetics, University of Oxford, in the laboratory of Professor Manuela Zaccolo. All work presented is my own with the following exceptions where work was carried out in close collaboration: i) the data on the fatty acid oxidation in Chapter 5, performed in collaboration with Dr Ujang Purnama from Professor Carolyn Carr's group, and ii) the seahorse experiments in Chapter 5, performed in collaboration with Dr Thomas Nicol from Dr Mark Crabtree's group. Additionally, mouse embryonic fibroblasts (MEF) isolation was performed by Dr. Stefania Monterisi, previous member of the Zaccolo group. Human induced pluripotent stem cells were differentiated and cultured by Dr Koshinski previous member of the Zaccolo group. Adult rat ventricular myocytes were isolated by either Dr Chao, Alexander Demby or Heeseung Jo from the Zaacolo group. This work has not been submitted for any other degree at this University or any other institution.

The work presented in this thesis could not have been completed without the help and support of many individuals.

First and foremost, I would like to thank my supervisor, Professor Manuela Zaccolo, for her unwavering support, guidance, and mentorship. Manuela is not only an exceptional scientist, as evidenced by her outstanding contributions to research, but also a genuinely kind and generous person. I am especially grateful to her for instilling in me the importance of maintaining high standards in science, for ourselves and for others.

I am also deeply thankful to my co-supervisor, Professor Duncan Sparrow, who has followed my scientific journey with steadfast encouragement and passion.

I will always fondly remember our thoughtful discussions, especially when I pass by the Natural History Museum with a coffee in hand. Duncan's advice and support were especially invaluable during the writing of this thesis.
To everyone in the Zaccolo laboratory, thank you for creating a space where I could grow as a scientist. To Andreas in particular, a truly exceptional scientist, thank you for teaching me that true understanding comes from the ability to deconstruct a mechanism and rebuild it, and for reminding me to question everything, no matter how established.

To my Balliol friends and peers, especially Matilde and Klara, thank you for walking this path with me. Completing a DPhil was an adventure full of excitement, joy, and challenges. Sharing both the highs and lows with you brought me immense comfort and strength.
To all my friends who made Oxford feel like home,thank you for the memories, the laughter, and the warmth. A special thank you goes to Luna, now the brightest star in the sky. Thank you for showing us the true meaning of strength, kindness, and passion. All the most beautiful words in the dictionary belong to you.

Special thanks go to Snapper: partner, proofreader, code debugger, cheerleader, and the very best co-pilot I could have hoped for. Thank you for navigating life's challenges with me and celebrating every success, no matter how small.

Finally, to my family, every achievement of mine is rooted in your love and support. To my brother Andrea, thank you for setting an outstanding example of diligence and kindness, whilst being incredibly loving and caring. I wish the world could see me through your eyes, where the best version of myself lives. And to my mother Dina and father Claudio, thank you for your unconditional love and immeasurable support. Words fall short in capturing the depth of

your commitment to giving me a joyful, carefree, and loving life, whilst always standing by me through every step. None of this would have been possible without you. I carry you with me in every accomplishment.

Abstract

cAMP is a key second messenger responsible for mediating a myriad of cellular processes. cAMP signalling is compartmentalised, as different levels of this second messenger are achieved at different subcellular nanodomains within the cell. The tight spatial and temporal organisation of cAMP signals is what allows the specificity of cAMP signalling, avoiding spillage of information amongst different branches of this pathway which occur independently but concurrently to the β-adrenergic regulation of cardiac myocyte contraction and relaxation. It is the distribution and activity of different phosphodiesterases that ultimately defines the topography of active subcellular cAMP nanodomains, by locally degrading cAMP at specific sites. Even though this is now an established concept, only a very limited number of nanodomains have been characterised. The aim of this project is to further validate and characterise novel PDE-dependent cAMP nanodomains in charge of the transport of metabolites for energy production in the cardiac myocyte. The results from this work validate the interaction of PDE2A2 and PDE3A1 with several elements involved in the transport of energy substrates. PDE2A2 is also shown to form a macromolecular complex with transporters of fatty acids, glucose, and pyruvate, suggesting a novel mechanism by which this enzyme may coordinate substrate uptake and mitochondrial import. Functional analyses demonstrate that PDE2A2 modulates fatty acid uptake and oxidation, likely through regulation of AMPK-dependent phosphorylation of acetyl-CoA carboxylase and subsequent modulation of CPT1 activity. These findings support a model in which PDE2A2 contributes to the modulation of a cAMP nanodomain at the mitochondrial outer membrane, positioning it as a critical regulator of cardiac metabolic flexibility and a potential therapeutic target in heart failure.

Contents

1 Introduction **1**

1.1 List of abbreviations 1

1.2 The cAMP signalling pathway 4

1.3 cAMP compartmentalisation 6

1.3.1 G-protein-coupled receptors 7

1.3.2 Adenylyl Cyclases 7

1.3.3 Protein kinase A and PKA anchoring proteins 8

1.3.4 Exchange Protein directly Activated by cAMP 11

1.3.5 Phosphatases 12

1.3.6 Phosphodiesterases 13

1.3.6.1 PDE2A 15

1.3.6.2 PDE2A Structure 15

1.3.6.3 PDE2A Contribution to cAMP compartmentalisation . . . 15

1.3.6.4 PDE2A Isoforms 16

1.3.6.5 PDE2A2 at the mitochondria 16

1.3.6.6 Pharmacology 17

1.3.6.7 Interplay with PDE3A and role in cAMP/cGMP crosstalk 17

1.4 cAMP signalling and energy metabolism 19

1.4.1 GPCR in energy metabolism 19

1.4.2 Adenylyl cyclases in energy metabolism 23

1.4.3 Protein kinase A in energy metabolism 23

1.4.4 A kinase anchoring proteins in energy metabolism 26

1.4.5 EPAC in energy metabolism . . . 27
1.4.6 Phosphatases in energy metabolism . . . 28
1.5 Mitochondrial cAMP subcellular compartment . . . 28
1.5.1 Mitochondrial Outer Membrane . . . 29
1.5.2 Mitochondrial Intermembrane Space . . . 30
1.5.3 Mitochondrial Matrix . . . 31
1.6 Aims of the project . . . 31

2 Materials and methods 35

2.1 Antibodies . . . 35
2.2 Cell culture . . . 37
2.2.1 NRVM isolation and culture . . . 37
2.2.2 ARVM isolation and culture . . . 38
2.2.3 Human Induced Pluripotent Stem Cell-Derived Cardiomyocytes . . . 39
2.2.4 Cell lines . . . 39
2.3 Biochemistry . . . 40
2.3.1 Immunoprecipitation and western blot . . . 40
2.3.2 Mitochondrial fractionation . . . 41
2.3.3 Lipid droplets staining, imaging and analysis . . . 41
2.3.4 CPT1 activity assay . . . 42
2.3.5 ^{3}H-Palmitate and ^{3}H-Oleate Oxidation . . . 44
2.3.6 Seahorse assay . . . 45
2.3.7 Extracellular glucose measurements . . . 46
2.3.8 Extracellular lactate measurements . . . 46
2.3.9 Mouse tissue homogenization . . . 46
2.4 Statistical analysis . . . 47

3 PDE2A2 metabolic interactors 48

3.1 Background . . . 48
3.2 Aims . . . 50

3.3 Identification of potential PDE2A2 interactors 50
3.4 Mitochondrial hits 52
3.4.1 The carnitine palmitoyl transferase shuttle 53
3.4.1.1 Carnitine palmitoyl-transferase 1 (CPT1) 53
3.4.1.2 CPT1A 54
3.4.1.3 CPT1B 56
3.4.1.4 PDE2A2 interacts with CPT1B through the GAF domains 59
3.4.2 SLC25A20 61
3.4.3 SLC25A 64
3.4.3.1 SLC25A4 64
3.4.3.2 SLC25A11 65
3.4.4 MPC2 68
3.5 Other putative interactors 70
3.5.1 SLC27A 70
3.5.1.1 SLC27A1 70
3.5.1.2 SLC27A4 71
3.5.2 SLC2A1 72
3.5.3 SLC16A1 73
3.6 A metabolon at the mitochondrial outer membrane 74
3.7 Summary of results and discussion 79
3.7.1 PDE2A2 interacts with elements involved in trafficking FA 81
3.7.2 PDE2A2 interactions with elements involved in alternative energy production pathways 82
3.7.3 A metabolon-like complex at the mitochondrial outer membrane . . 84

4 PDE3A1 interactors **88**

4.1 Background 88
4.1.1 PDE3A1 in cAMP/cGMP cross-talk 89
4.1.2 PDE3 and RNA binding proteins 90
4.2 Aims 92

4.3 Metabolic proteins . . . 95
4.3.1 Carnitine palmitoyl-transferase 1 (CPT1) . . . 95
4.3.1.1 CPT1A . . . 95
4.3.1.2 CPT1B . . . 96
4.3.2 SLC27A4 . . . 97
4.3.3 SLC16A1 . . . 98
4.4 RNA-binding proteins . . . 99
4.4.1 EIF3C . . . 100
4.4.2 RBM39 . . . 101
4.4.3 YBX and AKT . . . 103
4.4.4 ILF2 . . . 106
4.5 Summary of results and discussion . . . 107
4.5.1 PDE3A1 interacts with elements involved in trafficking different metabolites . . . 109
4.5.2 PDE3A1 interacts with RNA binding proteins . . . 111

5 PDE2A2 regulation of the fatty acid uptake machinery 114

5.1 Background . . . 114
5.2 Aims . . . 116
5.3 Does PDE2A modulate CPT1 activity? . . . 117
5.4 Does PDE2A affect CPT1 activity through a malonyl CoA/acetyl-CoA carboxylase axis? . . . 122
5.5 Is PDE2A required for CPT1A expression? . . . 127
5.6 Does PDE2A regulate fatty acid oxidation? . . . 129
5.7 Does impaired mitochondrial FA oxidation result in FA accumulation in the cytosol? . . . 130
5.8 Could the PDE2A-dependent cAMP nanodomain regulate PLIN 5 activity through PLIN 5 phosphorylation? . . . 135
5.9 Does inhibition of PDE2A increases ACSL1 phosphorylation? . . . 139
5.10 Does PDE2A affect mitochondrial respiration? . . . 141

5.11 Summary of results and discussion . . . 145
5.11.1 Characterisation of PDE2A2 and CPT1 interaction . . . 146
5.11.2 PDE2A2 as a modulator of CPT1 through an ACC/Malonyl-CoA axis 149
5.11.3 PDE2A2 affects CPT1A expression . . . 150
5.11.4 PDE2A regulates FAO . . . 151
5.11.5 PDE2A absence or inhibition results in cytosolic lipid accumulation, and may affect PLIN5 phosphorylation . . . 151
5.11.6 PDE2A inhibition may result in an increase in ACSL1 phosphorylation 153
5.11.7 PDE2A effect on mitochondrial respiration . . . 155

6 Conclusions **157**

6.1 Background . . . 157
6.2 Aims of the project . . . 158
6.3 Summary of Results, limitations and future work . . . 159
6.3.1 Chapter 3, PDE2A2 metabolic interactors . . . 159
6.3.2 Chapter 4, PDE3A1 interactors . . . 160
6.3.3 Chapter 5, PDE2A2 regulation of the fatty acid uptake machinery . 161
6.3.4 Concluding remarks . . . 163

Bibliography **164**

Chapter 1

Introduction

1.1 List of abbreviations

Table 1.1. Abbreviations with their corresponding fully written names in alphabetical order.

Abbreviation	Name
AAC1	ADP/ATP Carrier 1
AC	Adenylyl Cyclase
AC10/sAC	Soluble Adenylyl Cyclase
ACC	Acetyl-CoA Carboxylase
ACSL1	Acyl-CoA Synthetase Long Chain Family Member 1
AKAP	A-Kinase Anchoring Protein
AMPK	AMP-Activated Protein Kinase
ANT1	Adenine Nucleotide Translocator 1
ARVM	Adult Rat Ventricular Myocytes
ATP	Adenosine Triphosphate
CaMKII	Calcium/Calmodulin-Dependent Protein Kinase II
CACT	Carnitine-Acylcarnitine Translocase
CBD	cAMP Binding Domain
CFP	Cyan Fluorescent Protein

Abbreviation	Name
CPT1	Carnitine Palmitoyltransferase 1
CPT1A	Carnitine Palmitoyltransferase 1A
CPT1B	Carnitine Palmitoyltransferase 1B
cAMP	Cyclic Adenosine Monophosphate
cGMP	Cyclic Guanosine Monophosphate
CREB	cAMP Response Element-Binding Protein
DRP1	Dynamin-1-Like Protein
DTNB	5,5'-Dithio-bis(2-nitrobenzoic Acid)
EDTA	Ethylenediaminetetraacetic Acid
EPAC	Exchange Protein Directly Activated by cAMP
ERK	Extracellular Signal-Regulated Kinase
ETC	Electron Transport Chain
FA	Fatty Acid
FAO	Fatty Acid Oxidation
FATP1	Fatty Acid Transport Protein 1
FATP4	Fatty Acid Transport Protein 4
FCCP	Carbonyl Cyanide-p-trifluoromethoxyphenylhydrazone
FRET	Fluorescence Resonance Energy Transfer
GAF	cGMP-stimulated PDE–Anabaena Adenylyl Cyclase–E. coli FhlA Domain
GFP	Green Fluorescent Protein
GLP-1	Glucagon-Like Peptide 1
GLP-1R	Glucagon-Like Peptide 1 Receptor
GLP-1RA	Glucagon-Like Peptide 1 Receptor Agonist
GLUT1	Glucose Transporter Type 1
GPCR	G Protein-Coupled Receptor
GRK	G Protein-Coupled Receptor Kinase

Abbreviation	Name
HEK293T	Human Embryonic Kidney 293T Cells
hiPSC	Human Induced Pluripotent Stem Cell
hiPSC-CM	Human Induced Pluripotent Stem Cell-Derived Cardiomyocyte
IF1	ATPase Inhibitory Factor 1
ILF2	Interleukin Enhancer Binding Factor 2
IMM	Inner Mitochondrial Membrane
LD	Lipid Droplet
MEF	Mouse Embryonic Fibroblast
MOM	Mitochondrial Outer Membrane
MPC2	Mitochondrial Pyruvate Carrier 2
MPTP	Mitochondrial Permeability Transition Pore
NADH	Nicotinamide Adenine Dinucleotide (Reduced Form)
NFAT	Nuclear Factor of Activated T-cells
OCR	Oxygen Consumption Rate
OPA1	Optic Atrophy Protein 1
OXPHOS	Oxidative Phosphorylation
PBS	Phosphate Buffered Saline
PDE	Phosphodiesterase
PDE2A2	Phosphodiesterase 2A Isoform 2
PDE3A1	Phosphodiesterase 3A Isoform 1
PFK	Phosphofructokinase
PGC1α	Peroxisome Proliferator-Activated Receptor Gamma Coactivator 1-α
PI3K	Phosphoinositide 3-Kinase
PKA	Protein Kinase A
PKC	Protein Kinase C

Abbreviation	Name
PLIN5	Perilipin 5
PLN	Phospholamban
PP1	Protein Phosphatase 1
PP2A	Protein Phosphatase 2A
RBM39	RNA Binding Motif Protein 39
RI/RII	PKA Regulatory Subunit Type I/II
RFP	Red Fluorescent Protein
ROS	Reactive Oxygen Species
SLC16A1	Solute Carrier Family 16 Member 1
SLC2A1	Solute Carrier Family 2 Member 1
SLC25A4	Solute Carrier Family 25 Member 4
SLC25A11	Solute Carrier Family 25 Member 11
SLC25A20	Solute Carrier Family 25 Member 20
SLC27A1	Solute Carrier Family 27 Member 1
SLC27A4	Solute Carrier Family 27 Member 4
SLC54A2	Solute Carrier Family 54 Member 2
SR	Sarcoplasmic Reticulum
TCA	Tricarboxylic Acid Cycle
TX	Triton X-100
YBX1	Y-box-binding Protein 1
YFP	Yellow Fluorescent Protein

1.2 The cAMP signalling pathway

In order to communicate, cells rely on signal transducers to convert extracellular stimuli, most commonly carried by hormones and neurotransmitters, into specific cellular responses through a cascade of biochemical reactions. These transducers are known as "`second`

messengers". This fundamental notion in cell biology was first characterised by Earl Sunderland. Over half a century ago, he realised that hormone induced breakdown of glycogen in the liver is dependent on a small molecule, named Cyclic 3',5'-adenosine monophosphate, or simply cAMP (Sutherland and Rall, 1958). cAMP was first observed to be produced by the plasma membrane bound enzyme adenylyl cyclase (AC). Subsequently, cAMP was shown to regulate a plethora of cellular processes which can result in opposing functional outcomes, following activation of a G protein-coupled receptor (GPCR). These include cell proliferation and differentiation (Stork and Schmitt, 2002), gene expression (Yamamoto et al., 1988), apoptosis (Weissinger et al., 1997; Suen et al., 2008) and several metabolic processes such as insulin secretion (Brisson et al., 1972), glycogen synthesis (Rous, 1970) and lipogenesis (Geelen and Vaartjes, 1977). Once produced, cAMP activates a series of effector proteins, including Protein Kinase A (PKA) (Walsh et al., 1968), the Exchange Protein directly Activated by cAMP (EPAC) (de Rooij et al., 1998) , cyclic nucleotide-gated ion channels (Fesenko et al., 1985), and the Popeye domain containing proteins (Brand, 2005). The signalling pathway is terminated by the phosphodiesterases, metallohydrolases which degrade cAMP and/or cyclic GMP (cGMP) , and by the action of phosphatases, which turn-off the effects of PKA-mediated phosphorylation (Sim and Scott, 1999). Early studies by Mayer and colleagues in 1980 showed that, in cardiac myocytes, catecholamines and prostaglandins both resulted in a comparable increase of cAMP but had different functional effects; only the former having a positive inotropic effect (Hayes et al., 1980). These unexpected results indicated how a linear transduction between GPCR activation and effector activation through cAMP was too simplistic a model. Instead, it was proposed that cAMP is segregated in different subcellular compartments and this organisation is what allows the second messenger to orchestrate the complex array of stimulus-specific responses. Nearly 20 years later, cAMP compartmentalisation was directly visualised (Zaccolo et al., 2000; Nikolaev et al., 2006). This was achieved through employing new molecular tools for monitoring cAMP in real time (Nikolaev et al., 2004; Zaccolo et al., 2000; Ponsioen et al., 2004). The genetically encoded sensors utilise the phenomenon of fluorescence resonance energy transfer (FRET), and provide a real-time

readout of cAMP. The sensors are composed of a cAMP binding domain (CBD) from PKA (Zaccolo et al., 2000; Zaccolo and Pozzan, 2002) or EPAC (Nikolaev et al., 2004; Ponsioen et al., 2004) sandwiched between two spectral variants of the green fluorescent protein (GFP), commonly CFP (Cyan Fluorescent Protein) and YFP (Yellow Fluorescent Protein). Upon binding of cAMP, a conformational change occurs, altering the distance between the fluorophores, resulting in a change of FRET that can be detected by an optical microscope (Stangherlin et al., 2014). These sensors can be targeted to a specific subcellular site, which allows study of cAMP dynamics in a specific compartment (Surdo et al., 2017). In the next section of this introductory chapter, I will describe the elements of the cAMP cascade that contribute to its compartmentalisation.

1.3 cAMP compartmentalisation

Through the aid of FRET-targeted sensors, it was demonstrated that, upon β-adrenergic stimulation, cAMP does not equilibrate homogenously throughout the cardiac muscle cells, instead, it is distributed into compartments which can be as small as a few tens of nanometres (Surdo et al., 2017). Not only is the spatial distribution of cAMP tightly regulated, but its temporal dynamics also vary depending on the subcellular location. FRET-targeted sensors also revealed that the plasmalemma, sarcoplasmic reticulum, and the myofilaments, structures that are at most 300 nm apart, experience distinct amplitude and kinetics of the cAMP signal in response to catecholamine stimulation (Surdo et al., 2017; Zaccolo et al., 2021). This tight spatial temporal organisation is what allows for specificity of cAMP signalling, allowing it to fine-tune the extracellular stimuli with a myriad of different cellular functions. The subcellular localisation of the nanodomains is achieved by different components of the cAMP signalling cascade:

i) signal generators : G-protein coupled receptors and adenylyl cyclases

ii) signal effectors: PKA and EPAC, cyclic nucleotide-gated ion channels and Popeye domain containing POPDC proteins;

iii) tethering components: A-Kinase anchoring proteins (AKAPs).

iv) signal terminators: Phosphodiesterases (PDEs) and Phosphatases

1.3.1 G-protein-coupled receptors

cAMP signalling generally begins at the plasma membrane. When a seven transmembrane receptor that couples with GTP-binding proteins (GPCR) is activated by an extracellular cue, the membrane bound enzyme adenylyl cyclase (AC) converts adenosine triphosphate (ATP) into cAMP (Levitzki, 1988; Selbie and Hill, 1998; Mons et al., 1998). G proteins are trimeric α-β-γ complexes where the α subunit can dissociate and either stimulate the AC (G_{as}) or inhibit the AC (G_{ai}) enzymatic activity , inducing an increase or decrease in the level of cAMP, (Rodbell et al., 1971). The contribution of G proteins to cAMP compartmentalisation stems partially from their localisation within different domains in the plasma membrane. Here, GPCR and AC isoforms can physically couple, contributing to the precise cellular responses observed with specific cues (Emery et al., 2015). Disrupted pairing between GPCR and AC results in loss of compartmentalisation, as observed (Nikolaev et al., 2010). Another contributing element to cAMP compartmentalisation by GPCRs is the long-accepted paradigm of the internalisation of activated receptors which is thought to interrupt the signalling of the GPCR. This happens as part of a desensitisation process, which involves the receptor phosphorylation in some cases by GPCR kinases (GRKs) and recruitment of β-arrestin, followed up by GPCR endocytosis (Freedman and Lefkowitz, 1996; Dzimiri et al., 2004; Vinge et al., 2001; Suzuki et al., 2004). It has been demonstrated, however, that the internalised GPCR can continue signalling and generating cAMP, by coupling with the AC that is co-internalised (Lazar et al., 2020).

1.3.2 Adenylyl Cyclases

Once a GPCR is activated, the enzyme adenylyl cyclases generates cAMP from ATP (Levitzki, 1988). Two classes of AC exist: i) transmembrane AC (1 to 9) and ii) soluble AC10 (sAC). All membrane-bound AC share a similar architecture, apart from their transmembrane and catalytic domains (Sunahara et al., 1996), and can be regulated by different modulators, such as PKA, calcium or protein kinase C (PKC) (Dessauer et al.,

2017). The different AC isoforms localise at different subcellular sites and regulate distinct processes, placing them at the centre of highly organised microdomains, making them essential contributors of the compartmentalisation of cAMP (Cooper and Tabbasum, 2014). Supporting this notion, a number of AC have been found to participate in multiprotein complexes together with AKAPs (Bauman et al., 2006), GPCRs/G proteins (Dupré et al., 2007), PDEs and phosphatases (Crossthwaite et al., 2006). This organisation at the plasma membrane allows AC to undergo feedback inhibition or feedforward regulation through PKA (AC5,6, and 8) or PKC (AC2) dependent phosphorylation respectively (Bauman et al., 2006; Wills et al., 2012; Shen and Cooper, 2013).

1.3.3 Protein kinase A and PKA anchoring proteins

Of all cAMP effectors, Protein Kinase A (PKA) is the most studied (Walsh et al., 1968). Its inactive form is composed of a heterodimer with two regulatory (R) and two catalytic (C) subunits (Walsh et al., 1968; Corbin and Keely, 1977). PKA regulatory subunits include RI-α, RI-β, RII-α, RII-β; catalytic subunits include C-α, C-β and C-γ (Diskar et al., 2010). These subunits are highly dynamic signalling proteins; in the absence of cAMP, a dimer of R subunits binds to the catalytic ones, blocking their activity. RI-composed holoenzymes possess greater affinity for cAMP compared to RII ones which allows for a concentration-dependent regulatory mechanism (Dostmann et al., 1990). This different sensitivity to cAMP contributes to signalling compartmentalisation as it results in conditional PKA isoform activation based on the local cAMP concentration. This acts in conjunction with another fundamental aspect that mediates cAMP compartmentalisation, which is the action of A Kinase Anchoring Proteins (AKAP), which tether PKA at distinct subcellular location allowing its proximity with their specific substrates.

Upon cAMP binding to RI or RII, a conformational change occurs which leads to the release of the catalytic subunit resulting in two modes of regulation. The first is the cytosolic phosphorylation of adjacent protein targets (Taylor et al., 2013), mainly at a consensus motif [R/K][R/K/X]X[pS/pT] (Taylor et al., 1990). The second leads to the translocation of the active catalytic subunit to the nucleus where it primarily

phosphorylates proteins of the cAMP-response element binding protein (CREB) family, which in turn guides transcriptional regulation (London and Stratakis, 2022).
The free diffusion of the catalytic subunit would appear to go against the notion of cAMP compartmentalisation, as, in this model, PKA would also phosphorylate targets that are not within a nanodomain. However, a model has been proposed where PKA C subunits remain tethered to regulatory subunits during cAMP elevation and phosphorylate targets in the absence of the catalytic dissociation from the R subunit (Smith et al., 2017). Therefore, whether C subunit dissociation in necessary for phosphorylation is under debate.

Another essential player of cAMP compartmentalisation are A kinase Anchoring Proteins (AKAPs). By tethering PKA at specific subcellular sites, in proximity of the phosphorylation targets, they contribute to cAMP specificity and efficiency of signalling (Skroblin et al., 2010). The importance of AKAPs in the context of cAMP compartmentalisation is demonstrated, amongst others, by Gorshkov *et al.,* (Gorshkov et al., 2017). In this study, it was observed that a gradient of cAMP was present in developing hippocampal neurons, with higher levels of cAMP being generated in areas where AKAPs were anchoring PKA compared to other regions that did not have these. Disrupting PKA-AKAP interactions resulted in an increase of cAMP gradient, suggesting delocalisation of PKA (Gorshkov et al., 2017).

More than thirty AKAPs have been identified, all sharing the same motif responsible for binding PKA R subunits. These motifs contain a conserved dimerization-docking (D/D) domain at the N-terminal, which interacts with the AKAP amphipathic α-helix, encompassing 14-18 amino acid residues (Gold et al., 2006). In addition to the helix, which is conserved amongst family members, AKAPs also include interaction sites which are responsible for their subcellular targeting and bind to components of the cAMP signalling pathway, such as GPCRs (Malbon et al., 2004), phosphatases (Dodge-Kafka et al., 2010), PDEs (Dodge et al., 2001), kinases including PKC, extracellular signal-regulated kinases (ERK) 1 and 2, polycystic kidney disease (PKD), and others (Scott et al., 2013). Thus, AKAPs localise at different subcellular compartments (including the plasma membrane, nucleus, mitochondria, endo/sarcoplasmic reticulum, the primary cilium, and

other organelles) where they recruit different and/or multiple kinases (Torres-Quesada et al., 2017; Langeberg and Scott, 2015). Upon receptor stimulation, these will in turn phosphorylate protein targets in the vicinity of that compartment only. Thus, at a given site AKAPs bind different combinations of kinases, their substrates and cAMP effectors, greatly contributing to a large diversity of PKA-focused signalling complexes, named signalosomes (Greenwald and Saucerman, 2011).

Targeting of PKA to various subcellular loci is mediated by interaction of the R subunits with different AKAPs. PKA RI is mainly soluble, but has also been demonstrated to localize in proximity to membrane receptors (Burgers et al., 2012), where the targeting is achieved via binding mono or dual-specific AKAPs (Kovanich et al., 2010; Means et al., 2011). On the other hand, the particulate RII is known to bind specifically AKAPs that bind exclusively RII or both RII and RI (Kinderman et al., 2006).

Another good example of the contribution of AKAPs to cAMP compartmentalisation was demonstrated by Di Benedetto *et al.,*. Here, the authors employed Fluorescence Recovery After Photobleaching (FRAP) to show that PKA RI and RII are physically segregated in different compartments of the cardiac myocyte via binding endogenous AKAPs (Di Benedetto et al., 2008). This challenged the notion that PKA RI is primarily cytosolic and RII is associated with AKAPs. They demonstrated that the signalling in these compartments is regulated by specific stimuli. Through FRET-based reporters anchored to AKAPs binding either RI or RII they measured the levels of cAMP generated at these locations. They observed catecholaminergic stimulation through isoproterenol generates a cAMP response selectively confined to AKAP-anchored PKA RII, which in turn led to the phosphorylation of the adjacent Phospholamban (PLN) and troponin I and was sensitive to rolipram (PDE4 selective inhibitor), suggesting the presence of PDE4 in the same complexes.

On the other hand, PGE1 and GLP-1 stimulation generated a cAMP increase confined to AKAP-anchored PKA-RI compartments, where it was sensitive to PDE2A inhibition, and did not result in PLN or troponin I phosphorylation (Di Benedetto et al., 2008).

Further increasing the complexity of cAMP/PKA signalling, Smith *et al.,* reported that

AKAPs can translocate as response to specific stimuli, relocalising (Smith et al., 2006).

1.3.4 Exchange Protein directly Activated by cAMP

Small G proteins are classified into different families, one of which being the Ras family. This includes the Rap subfamily of proteins which cycle between an inactive GDP-bound state and an active GTP-bound state (Raaijmakers and Bos, 2009). Rap was first identified as a small Ras-like GTPase able to supress the Ras-mediated oncogenic transformation of cells (Kitayama et al., 1989). Rap is activated by several extracellular stimuli, resulting in several cellular effects: actin cytoskeleton dynamics, cell polarity, exocytosis, membrane protein recycling and cell differentiation, proliferation, and adhesion (Gloerich and Bos, 2010).

In 1988 de Rooij *et al.,* observed that cAMP-dependent activation of Rap1 was insensitive to inhibitors of PKA. They concluded that Rap1 is activated by cAMP independently of PKA. To explain this phenomenon, they conducted a database screening seeking potential activators of this protein leading to the identification of EPAC, exchange protein directly activated by cAMP (also known as cAMP-GEF or RAPGEF3) (de Rooij et al., 1998).

Two proteins were independently identified through this approach, EPAC1 and EPAC2, both containing a cyclic nucleotide-binding domain (CNB). They are multidomain proteins that include an N-terminal regulatory region and a C-terminal catalytic region. The amino-terminal regulatory region contains either one (EPAC1) or two (EPAC2) CNB, and is auto-inhibitory, blocking the GEF activity for Rap (Rehmann et al., 2006). This inhibition is relieved through a conformational change caused by binding of cAMP (de Rooij et al., 2000; Rehmann et al., 2008).

Like PKA, EPAC proteins are also spatially regulated through several anchoring mechanisms. Upon cAMP binding, EPAC1 is translocated to the plasma membrane (PM) through a mechanism involving its DEP domain (Consonni et al., 2012). Here, it tethers to phosphatidic acid or to phosphorylated cytoskeleton proteins to induce its downstream effectors (Gloerich and Bos, 2010; Ponsioen et al., 2009).

An additional targeting mechanism of EPAC1 occurs through its N-terminus interacting with members of the ezrin-radixin-moesin (ERM) family (Ponsioen et al., 2009). Radixin binds to EPAC1 and PKA simultaneously, bringing these two cAMP effectors together and creating a functional cAMP-sensing sub-plasma membrane compartment for efficient signal transduction (Hochbaum et al., 2011). EPAC1 and EPAC2 present distinct activation patterns in response to cAMP-raising stimuli. This suggests that various EPAC isoforms localise at different subcellular localisations, where they are regulated by distinct pools of cAMP. For example, in the cardiac myocyte, EPAC1 localises to the plasmalemma, sarcoplasm, and nuclear/perinuclear region (Cazorla et al., 2009; Pereira et al., 2015). Here, stimulation of β1-AR induces a β-arrestin-EPAC1 signalling complex which triggers a signalling cascade resulting in cardiomyocyte hypertrophy (Berthouze-Duquesnes et al., 2013).

On the other hand, EPAC2 has been found to localize at the T-tubules (Pereira et al., 2015). Its activation by cAMP in response to β1-AR stimulation leads to Ca^{2+} and calmodulin-dependent protein kinase II (CaMKII)-dependent diastolic sarcoplasmic reticulum (SR) calcium release and arrhythmias, via a pathway that involves EPAC-phosphoinositide 3-kinases (PI3K)-protein kinase B (Akt)-nitric oxide synthase (NOS1)(Pereira et al., 2013)

1.3.5 Phosphatases

By dephosphorylating PKA targets at specific cellular compartments (Virshup and Shenolikar, 2009), protein phosphatases (PPPs) are the last checkpoint of the cAMP/PKA signalling cascade (Heijman et al., 2013).

The three most abundant and extensively studied serine/threonine phosphatases are members of the protein phosphatase type 1 (PP1) and type 2 (PP2) family, including PP2A and PP2B (also known as Calcineurin or CaN), (Virshup and Shenolikar, 2009). These are multimeric enzymes in which the catalytic subunit is associated with numerous regulatory subunits. These regulators play a crucial role in determining PPP subcellular localization, substrate specificity, and enzymatic activity, adding significant complexity

to the phosphatase system and enabling highly specialized local functions. In cardiac myocytes, for example, PP1, PP2A, and CaN account for >90% of the total phosphatase activity (Heijman et al., 2013).

The notion of phosphatases contributing to cAMP compartmentalisation is relatively new. It stems from the demonstration that there are different concentrations of phosphatases in the bulk cytosol compared to the mitochondrial outer membrane (MOM) of cardiac myocytes (Burdyga et al., 2018). Burdyga *et al.* speculated that this differential localisation of phosphatases plays a role in the compartmentalization of cAMP/PKA signalling by suppression of accidental phosphorylation of PKA targets that may occur outside the designated signalling domain (Burdyga et al., 2018; Zaccolo et al., 2021).

1.3.6 Phosphodiesterases

Phosphodiesterases (PDE) are a super-family of metallohydrolases that encompasses 11 families (PDE 1-11), each including different isoforms, arising from a combination of multiple genes, alternative splicing sites, and multiple transcription starting points (Conti and Beavo, 2007). In the heart, 7 PDE families have been described: PDE1, PDE2, PDE3, PDE4, PDE5, PDE8, and PDE9. PDE1, PDE2, and PDE3 are dual-specificity enzymes that can hydrolyse both cAMP and cGMP; PDE4 and PDE8 selectively hydrolyse cAMP; and PDE5 and PDE9 selectively hydrolyse cGMP. Of the cAMP-hydrolysing PDEs expressed in the heart, cGMP inhibits PDE3 and possibly PDE1, whereas PDE2 is activated by cGMP (Zaccolo and Movsesian, 2007).

Each isoform has a specific tissue distribution, and each cell can express several PDE isoforms (Zaccolo et al., 2021). The overall structure between PDE members is similar, with the catalytic domain located at the C-terminal region being highly conserved. The function of each member, however, is distinct and unique (Conti and Beavo, 2007). The N-terminus of these enzymes differs and is responsible for targeting the PDEs to specific cellular locations (Bender and Beavo, 2006, Zaccolo, 2009). The PDE amino terminus is also responsible for unique regulatory properties and can carry post-translational modification sites. PDE3, PDE4 and PDE10 phosphorylation, for example, affects their enzymatic

activity and determines the ability of these enzymes to form macromolecular complexes with other proteins (Omori and Kotera, 2007; Azevedo et al., 2014).

cAMP specificity of signalling is regulated by its tight spatiotemporal organisation, achieved through the contribution of several components of the signalling pathway. In this synergistic organisation, however, it is the distribution and activity of different PDE isoforms that ultimately defines the topography of active subcellular cAMP nanodomains, by locally degrading cAMP at specific sites. Although the contribution of the phosphodiesterases to cAMP compartmentalisation has been demonstrated both experimentally (Jurevicius and Fischmeister, 1996; Zaccolo and Pozzan, 2002; Mongillo et al., 2004; Lefkimmiatis, 2014) and computationally (Lohse et al., 2017), how PDEs achieve this is still debated. This is because of the high diffusivity of cAMP. Several studies have shown the basal level of cAMP in various cells to be around 1 μM (Beavo et al., 1974; Börner et al., 2011; Koschinski and Zaccolo, 2017), and its diffusion coefficient to be around 40 μM/s (Nikolaev et al., 2004; Richards et al., 2016). Based on the reported Vmax (the maximum rate at which an enzyme can catalyse a reaction) and Km (the concentration of substrate which permits the enzyme to achieve half Vmax) values for PDEs, it may be challenging for the PDEs to maintain the concentration of cAMP below the activation threshold of PKA in specific compartments, especially after high concentrations of fast diffusing cAMP are generated as a result of hormonal stimulation (Koschinski and Zaccolo, 2017). A number of factors, however, may come into play in living cells, such as cAMP buffering, cytosol viscosity and physical barriers (Zaccolo et al., 2021).

A big advancement in the study of PDEs and their role in shaping the intracellular cAMP nanodomains was achieved with the development of FRET-based sensors. These allowed visualisation of the cAMP gradient and confirmation of the role of PDEs in shaping the different nanodomains in neonatal rat cardiac ventriculocytes (Zaccolo and Pozzan, 2002).

1.3.6.1 PDE2A

Phosphodiesterase 2 (PDE2A) is a one of the PDE able to hydrolase both cAMP and cGMP with similar affinity (Km of 30 and 10 μM, respectively) and efficacy (Vmax of 120 and 123 μmol min^{-1} mg^{-1}) (Francis et al., 2009). A unique feature of this family, however, is that its cAMP hydrolysing activity can be stimulated by high concentrations of cGMP, or inhibited by low cGMP concentrations. cGMP-mediated control of cAMP hydrolysis arises when cGMP binds allosterically to the GAF-B domain of PDE2A, resulting in a 10-fold higher rate of cAMP hydrolysis. This results in a negative cGMP-to-cAMP cross-talk. (Pavlaki and Nikolaev, 2018; Erneux et al., 1980). PDE2A is expressed in several tissues, including the heart, liver and adrenal gland (Lobo and Zaccolo, 2018).

1.3.6.2 PDE2A Structure

PDE2A holoenzyme is a homodimer of two 105 kDa subunits. These contain a N-terminal domain, a tandem of GAF domains (GAF A and GAF B; cGMP-stimulated PDE – Anabaena Adenylyl cyclase – E. coli FhlA transcription factor domain) and a C-terminal catalytic domain (Martins et al., 1982). The GAF-A domain is responsible for the dimerization of the holoenzyme. The GAF-B binds cGMP allosterically (1-5 μM), positively stimulating cAMP hydrolysis up to a 30-fold increase with Km values from 10-30 μM (Lugnier and Schini, 1990). In particular, cGMP binding at a flexible binding pocket within the GAF-B domain induces structural changes to enhance cGMP affinity. The GAF-A/GAF-B domains exist in parallel, as suggested by the crystal structure of the near full-length PDE2A (Pandit et al., 2009).

1.3.6.3 PDE2A Contribution to cAMP compartmentalisation

The contribution of PDE2A to cAMP compartmentalisation has been described in a number of studies. For example, the increase in cAMP due to PDE2A inhibition leads to the generation of a local pool of cAMP and activation of PKA RII, and consequently to the phosphorylation of the nuclear transcription factor of activated T cells (NFAT), which inhibits myocyte hypertrophy. This is not the case for PDE3 and PDE4, which inhibition

and consequent rise in cAMP results in a pro-hypertrophic effect (Zoccarato et al., 2015).

1.3.6.4 PDE2A Isoforms

The PDE2A family consists of a single gene that encodes three splice variants, each with different subcellular localisations: PDE2A1, at the cytosol (Lobo and Zaccolo, 2018) and the membrane bound PDE2A2 and PDE2A3 (Rosman et al., 1997). The C-terminal sequence (including GAF-A, GAF-B and catalytic domains) is conserved in all PDE2A isoforms, but they differ in their N-terminal sequences (Azevedo et al., 2014). Additionally, the N-terminal region of each PDE2A isoform differs in hydrophobicity, also influencing its localisation.

1.3.6.5 PDE2A2 at the mitochondria

PDE2A2 localises to the mitochondrial outer membrane (Acin-Perez et al., 2011; Monterisi et al., 2017; Lobo et al., 2020), where it regulates mitochondrial quality control through Parkin, a key coordinator of mitophagy. In particular, increased PDE2A2 acitivity results in reduced PKA-dependent phosphorylation of Parkin. This suppresses Parkin activation and hampers mitophagy, normally carried out by the PKA-phosphorylated protein. PDE2A2 inhibition on the other hand results in Parkin-mediated clearance of damaged mitochondria (Lobo et al., 2020).

Additionally, PDE2A2 regulates mitochondria morphology and apoptotic cell death via local modulation of cAMP/PKA signalling. Overexpression of PDE2A2 results in increased mitochondrial fragmentation, while its inhibition promoted mitochondrial elongation. This effect was linked to reduced phosphorylation of Drp1, a protein responsible for mitochondrial fission, indicating that PDE2A2 modulates mitochondrial morphology through PKA-mediated regulation of Drp1. Additionally, elevated PDE2A2 activity increased markers of apoptosis, such as Cytochrome c release, while inhibiting PDE2A2 protected against apoptosis by maintaining mitochondrial integrity. These findings highlight PDE2A2's role in regulating mitochondrial dynamics and cell survival via local modulation of cAMP/PKA signalling (Monterisi et al., 2017).

Therefore, even though some advances have been made in understanding this isoform's role and function at the mitochondria specifically, the exact biology of cAMP nanodomains regulated by PDE2A is yet to be fully characterised.

1.3.6.6 Pharmacology

For many years, the only PDE2A inhibitor available was EHNA (erythro-9-(2-hydroxy-3-nonyl)adenine). However, BAY 60-7550 is now the main inhibitor used, due to its superior potency and selectivity (Gomez and Breitenbucher, 2013).

BAY 60-7550 binds to the catalytic site of PDE2A and causes a conformational change of the H-loop, exposing a hydrophobic pocket which can accommodate the propylphenyl group of the compound (Zhu et al., 2013). Because BAY60-7550 binds to a conserved region between the isoforms, its effect is only family-selective, rather than isoform-selective. As each isoform localises at different sites in the cell where it controls specific biological functions, a drug which inhibits all the PDE2A at the same time presents severe drawbacks. The structure of PDE2 in complex with BAY 60-7550 identified a hydrophobic pocket consisting of Leu^{770}, Ile^{866}, and the hydrophobic side chains of The^{805} and Asp^{808}, this knowledge could help develop novel, PDE2-selective inhibitors in the future (Zhu et al., 2013).

1.3.6.7 Interplay with PDE3A and role in cAMP/cGMP crosstalk

cAMP and cGMP are key second messengers in the regulation of cardiac function. cAMP regulates force and frequency of contraction primarily by activating effectors such as PKA and EPAC (Zaccolo et al., 2021). cGMP, produced by guanylyl cyclases in response to nitric oxide (NO) or natriuretic peptides, modulates inotropy and metabolic responses via protein kinase G (PKG) and cyclic nucleotide-gated channels (Zaccolo and Movsesian, 2007). Although both pathways are involved in cardiac regulation, they often mediate opposing effects (Shah and MacCarthy, 2000).

The crosstalk between cAMP and cGMP is regulated partially by the phosphodiesterases, as cGMP is a regulator of some PDEs, so that the intracellular

concentration of cGMP can influence the intracellular concentration of cAMP. Different PDEs present different subcellular localization, affinity, and specificity for cAMP and cGMP. As a consequence, cAMP and cGMP signalling pathways are connected in a complex network with a precise spatial organization.

The interplay between these pathways is largely orchestrated by PDEs. cGMP can regulate several PDEs and thereby influence intracellular cAMP concentrations. This regulation is highly spatially organized, as different PDE isoforms exhibit distinct subcellular localizations and specificities for cAMP and cGMP (Zaccolo and Movsesian, 2007).

Among these, PDE2 and PDE3 play central roles in cAMP/cGMP crosstalk. PDE2 is activated by cGMP, enhancing cAMP hydrolysis and thereby exerting negative cGMP-to-cAMP crosstalk. This mechanism underlies, for example, cholinergic attenuation of β-adrenergic signalling in rabbit atrioventricular nodal cells (Han et al., 1996) and reduced β-adrenergic responses in rat ventricular myocytes (Mongillo et al., 2006). In the latter, cGMP activation of PDE2 led to a 50% decrease in the cAMP response to norepinephrine, resulting in attenuated intracellular Ca^{2+} transients and contractile responses.

In contrast, PDE3, while also capable of hydrolysing both cyclic nucleotides, is inhibited by cGMP, which competes with cAMP at its active site. This inhibition leads to positive cGMP-to-cAMP crosstalk, as cAMP degradation is suppressed, enhancing its signalling and supporting increased cardiac contractility (Zaccolo and Movsesian, 2007; Pavlaki and Nikolaev, 2018). Functionally, this dual regulatory role allows cardiomyocytes to fine-tune their responses: cGMP can suppress or enhance cAMP signalling depending on the relative activity of PDE2 and PDE3 within specific subcellular compartments.

Recent studies have shown that cGMP-induced changes in cAMP dynamics are highly localized, influencing discrete cAMP pools without significantly altering global cAMP levels. This spatial signalling enables selective activation of PKA-RI/PDE3- or PKA-RII/PDE2-associated nanodomains, leading to opposing effects on contractility (Di Benedetto et al., 2008). Live-cell FRET imaging has revealed that cardiac disease states can disrupt these microdomains, often enhancing PDE2 involvement in cAMP/cGMP breakdown and

shifting the balance of crosstalk compared to other PDEs (Pavlaki and Nikolaev, 2018).

1.4 cAMP signalling and energy metabolism

From the very beginning after its discovery, cAMP has been linked to metabolism, with Sutherland finding that breakdown of glycogen in the liver is hormone-induced and dependent on cAMP (Sutherland and Rall, 1958). This relationship has been mainly studied in the context of the liver, where cAMP is a mediator of glucose metabolism upon activation of glucagon-like peptide-1 (GLP) receptors (Ravnskjaer et al., 2016). In white adipose tissue, β-AR stimulation results in cAMP-dependent regulation of lipolysis, a process where triglycerides stored in adipocyte lipid droplets are hydrolysed to fatty acids. This occurs during instances of high energy demand, like fasting (Frayn, 2002). In skeletal muscle, glycogenolysis, which is critical for meeting energy demands of the muscle, is also promoted by cAMP (Ezrailson et al., 1983). Here, chronic activation of cAMP pathways promotes adaptive responses that include increased myofiber size, as well as metabolic transition to a more glycolytic fibre type (Chen et al., 2009b). Overall, cAMP serves as a crucial regulator of metabolic processes across various tissues, integrating hormonal and cellular signals to control energy balance. Its role in glycogen breakdown, lipolysis, and muscle adaptation highlights its importance in responding to energy demands, making it a key mediator of metabolic flexibility.

In the next section, I will describe how different elements of the cAMP signalling pathway contribute to different aspects of energy metabolism. I will focus on the role of adrenergic stimulation in the regulation of energy production in the cardiac myocyte.

1.4.1 GPCR in energy metabolism

It is well established that sustained β-adrenergic stimulation induces insulin resistance (Cipolletta et al., 2009), where the β_2-AR plays a role in glucose homeostasis by acting on pancreatic islet hormone secretion, and the metabolism of liver and muscle glucose transport (Usui et al., 2005). At cardiac level, several studies have raised the possibility of

using selective β2-agonists as potential modulators of cardiac muscle energy metabolism (Ciccarelli et al., 2013). Indeed, β_2 agonists induce a significant increase in glucose uptake with both acute treatment of myocytes *in vitro* or skeletal muscle *ex vivo*, reaching comparable levels to insulin stimulation (Nevzorova et al., 2006, 2002). A putative mechanism for this effect has been suggested to be mediated through phosphatidylinositol3 kinase (PI3K) and its downstream signalling pathway. In particular the phosphorylation and inactivation of TBC1D4 (also known as Akt substrate) by Akt. TBC1D4 inhibits the plasma membrane glucose transporter type 4 (GLUT4) translocation and consequently decreases glucose uptake (Sakamoto and Holman, 2008; Pérez-Schindler et al., 2011). Increased phosphorylation of TBC1D4 by Akt therefore would result in increased GLUT4 translocation and glucose uptake. TBC1D4 is also phosphorylated and inhibited by AMP kinase (AMPK) in response to energy stress, such as during exercise (Cartee and Wojtaszewski, 2007).

In line with the potential role of β2-AR in cardiac glucose metabolism, high levels of AMPK phosphorylation and activity in response to β2-AR stimulation have been observed in cardiomyocytes (Li et al., 2010).

On the other hand, *in vivo* studies have shown that carvedilol, a non-selective β-adrenergic receptor antagonist, is more effective than metoprolol, a β1-selective antagonist, in improving myocardial insulin sensitivity and glucose uptake in animal models of heart failure (Nikolaidis et al., 2006). This suggests that β2-AR signalling inhibition may have a beneficial impact on cardiac glucose metabolism under heart failure conditions. These conflicting findings may be attributed to variations in the experimental models used and/or differences between acute and chronic β2-AR stimulation. While acute activation of β2-AR can enhance glucose uptake by promoting GLUT4 translocation to the plasma membrane, chronic adrenergic stimulation, as observed in heart failure, may have detrimental effects due to the dysregulation of specific intracellular signalling pathways. This shift is associated with G-protein receptor kinase 2 (GRK2), which becomes upregulated in failing hearts and may mediate the transition from adaptive to maladaptive cardiac metabolism (Ciccarelli et al., 2011). GRK2 not only affects βAR signalling but may also modulate mitochondrial

function, with studies suggesting both protective (Fusco et al., 2012) and apoptotic roles (Chen et al., 2013), depending on the model and timing.

When considering βAR regulation of mitochondrial physiology and energetics in the cardiomyocytes, most studies have been conducted on rodent models (Sandroni et al., 2022). The effect of adrenergic stimulation on mitochondrial biogenesis in the cardiac muscle have been investigated mainly for βAR, and data appear conflicting (Sandroni et al., 2022). βAR agonists leads to increased mitochondrial DNA (mtDNA) and PGC1α (a master regulator of mitochondrial gene expression) in mice hearts (Wills et al., 2012). On the other hand, βAR stimulation through isoproterenol (non-selective βAR agonist), both *in vitro* and *in vivo* (Xu et al., 2016) and β2-selective agonist formoterol did not significantly affect mitochondrial biogenesis in cardiomyocytes, as indicated by unchanged PGC-1α expression (Vallorz et al., 2021).

Adrenergic stimulation also impacts cardiomyocyte oxidative phosphorylation (OXPHOS) in the developing heart (Sandroni et al., 2022). Adrenergic-deficient mouse embryos show reduced ATP content, extracellular acidification, and oxygen consumption rates, with an amelioration in this phenotype upon maternal isoproterenol treatment (Baker et al., 2015). In adult mice, acute βAR stimulation with isoproterenol enhanced mitochondrial OXPHOS in cardiomyocytes by increasing basal and maximal respiration, ATP-linked respiration, and ATP production. This mechanism involves DRP1-mediated mitochondrial fission (Coronado et al., 2018). On the other hand, chronic βAR stimulation shows detrimental effects, reducing mitochondrial membrane potential ($\Delta\Psi$m), increasing reactive oxygen species (ROS) (by-product of cellular metabolism) and impairing efficiency, particularly through calcium dysregulation and oxidative stress (Seydi et al., 2020). These opposing effects suggest time- and dose-dependent roles: short-term βAR activation boosts energy production, while prolonged exposure undermines mitochondrial function and contributes to pathology (Sandroni et al., 2022).

For β2-AR specifically, while β2-AR deletion reduces the activity of complex I and II (components of the electron transport chain) (Fajardo et al., 2011), moderate activation can enhance complex I expression and ATP synthase activation (Vallorz et al., 2021).

However, β2-AR overexpression decreased ATP production post-ischemia (Cross et al., 1999), suggesting that supraphysiological β2-AR activation may actually decrease OXPHOS. In line with this, β2-AR antagonism increased mitochondrial respiration compared to isoproterenol. However, this result is not replicated upon β2-AR genetic deletion (Coronado et al., 2018).

Although research on the effects of β1-AR on cardiac metabolism is limited, this receptor has been implicated in metabolic regulation in the heart. Tatman *et al.,* in fact, identified 430 genes related to metabolic processes that were either upregulated or downregulated as downstream effects of β1-AR signalling (Tatman et al., 2023).

Another GPCR involved in energy metabolism is the glucagon-like peptide-1 receptor (GLP-1R). GLP-1 is a peptide hormone secreted by pancreatic islets that targets the GLP-1 receptors (Zhong et al., 2024). The existence of GLP-1 receptors in myocardial cells highlights its cardiovascular involvement. GLP1 has gained broad public awareness because one of its agonist, semaglutide, was recently approved as a treatment for type 2 diabetes and obesity under the commercial names of Ozempic and Wegovy, respectively (Chao et al., 2023). In a cardiovascular context, treatment with a GLP-1 receptor agonist (GLP-1RA) reduces the occurrence of cardiovascular events in overweight or obese people without diabetes (Leite et al., 2022). A meta-analysis on over fifty thousand ambulatory patients has also revealed that people without a history of heart failure (HF) treated with GLP receptor agonists showed reduced cardiovascular risk and cardiovascular related mortality (Ferreira et al., 2023). GLP-1 RAs have a positive effect on cardiac metabolism by improving myocardial FA metabolism and stabilizing blood glucose levels. GLP-1 RAs increase myocardial glucose oxidation indirectly by elevating circulating insulin levels. This effect is associated with enhanced activity of pyruvate dehydrogenase, the rate-limiting enzyme of glucose oxidation (Almutairi et al., 2021). GLP-1 RAs also ameliorate mitochondrial dysfunction and oxidative stress in cardiomyocytes. They achieve this by enhancing endogenous antioxidant defences and inhibiting cardiomyocyte apoptosis (Saraiva and Sposito, 2014). Finally, GLP-1 RAs modulate myocardial fatty acid metabolism by reducing lipid accumulation and associated lipotoxicity. This contributes to improved

mitochondrial function and energy metabolism in the heart (Zhong et al., 2024).

1.4.2 Adenylyl cyclases in energy metabolism

Adenylyl cyclases convert ATP into cAMP (Levitzki, 1988). There are two classes of AC: I) transmembrane AC (1 to 9) and II) soluble AC10 (sAC). Because of its mitochondrial localisation, sAC is involved in different aspects of metabolism (Aslam and Ladilov, 2021). sAC is also localised in the cytoplasm and in various organelles, in the nucleus and in centrioles. Unlike many other ACs that are activated by GPCR, sAC is activated by bicarbonate and ATP, and stimulated by magnesium and calcium (Hindson, 2003).

The crystal structure of sAC revealed that, in addition to the shared architecture with the transmembrane AC, AC10 contains a small insertion in one of the catalytic domains that allows this enzyme to be activated by bicarbonate (Kamenetsky et al., 2006). Emerging research suggests that sAC is involved in metabolic regulation and energy homeostasis. Through cAMP signalling in particular, it influences insulin secretion as well as glucose and fatty acid metabolism in various tissues (Li et al., 2024). In the cardiac muscle, Complex I of the electron transport chain is regulated by a signalling axis involving sAC, cAMP and EPAC1 (Technikova-Dobrova et al., 2001; Papa, 2002). Specifically, electron transport is reduced upon sAC inhibition, driving a switch in metabolism from glucose to fatty acid oxidation (Chang et al., 2021). Additionally, sAC regulates mitochondrial ATP production by bicarbonate triggering, cAMP production and EPAC1 activation in ventricular cardiomyocytes (Greiser et al., 2023). In addition, Laudette *et al.* have demonstrated that sAC is palmitoylated in ventricular myocytes, leading to: i) increased intracellular cAMP, ii) greater EPAC1 activation, iii) lipid accumulation, and iv) mitochondrial dysfunction and cardiomyocyte death (Laudette et al., 2021).

1.4.3 Protein kinase A in energy metabolism

PKA regulates a series of functions in metabolism including glucose homeostasis, neural control of energy intake and expenditure, adipose tissue function and lipid trafficking (London and Stratakis, 2022). The regulation of lipid trafficking by PKA has primarily

been investigated in the context of the liver. Here PKA assists in the tight regulation of hepatic lipid trafficking and lipogenesis. One mechanism through which PKA achieves this is by regulating transcription factors involved in hepatic lipogenesis regulation (Kammoun et al., 2009; Kawaguchi et al., 2001; Nakagawa et al., 2014).

PKA is a key regulator of lipolysis, which is the process of sequential breakdown of triglycerides to liberate free fatty acids and glycerol (Grabner et al., 2021). Non-esterified fatty acids and glycerol are combined to generate triglycerides (TGA), and are stored into lipid droplets (LDs). These are encapsulated by layer of proteins called perilipins (PLINs). TAG and glycerol are liberated from LDs in order to be used as energy substrates in a process named lipolysis. In white adipose tissue, lipolysis is induced by an increase in cAMP, generated from the catecholaminergic stimulation of βARs. This activates PKA, resulting in the phosphorylation of perilipin 1 (PLIN1). This in turn allows the access of lipases to lipid droplets in a PKA phosphorylation-dependent fashion (Greenberg et al., 1991). The activation process of lipolysis may differ in oxidative tissues like the heart, because it express PLIN2 and PLIN5 instead of PLIN1. However, both represent a barrier for TAG hydrolysis as their cardiac-specific overexpression in mice causes lipid droplet accumulation and steatosis (Pollak et al., 2013; Ueno et al., 2017). However, the molecular mechanism underlying this observation remains unclear.

PLIN5 is one of the most extensively studied perilipins. It is expressed mainly in highly oxidative tissue like heart, brown adipose tissue, skeletal muscle and liver (Itabe et al., 2017). In the heart, PLIN5 inhibits TG breakdown by binding to and sequestering CGI-58, a co-activator of ATGL (adipose triglyceride lipase), the primary enzyme responsible for initiating triglyceride hydrolysis by converting stored TGs into free fatty acids and diglycerides. This lipolytic barrier created by PLIN5 is relieved through PKA-mediated phosphorylation at serine 155. Upon phosphorylation, CGI-58 is released from PLIN5, enabling it to activate ATGL and promote lipolysis. In contrast, PLIN2-enriched LDs do not rely on PKA signalling for lipolysis, highlighting a specific regulatory role for PLIN5 in controlling lipid breakdown in the heart. Additionally, PLIN5 overexpression affects mitochondrial function, likely by downregulating the mitochondrial FA transporter

carnitine palmitoyl transferase 1 (CPT 1), reducing fatty acid oxidation (FAO), and increasing glucose utilization. However, these metabolic changes do not impair cardiac function, suggesting that PKA signalling and mitochondrial adaptation help maintain energy balance (Pollak et al., 2015).

In the heart, PKA regulates the junction of glucose and fatty acid metabolism, also referred to as Randle cycle (Randle et al., 1963). This describes the reciprocal relationship between fatty acid and glucose utilisation, where a decrease in FAO causes an increase in glucose oxidation and vice-versa (Ng et al., 2024). This is particularly relevant in the cardiac muscle as the healthy heart is also metabolically flexible and even though it primarily uses fatty acid, it can readily shift between different energy substrates to maintain ATP production (Lopaschuk et al., 2021). In the Randal cycle, the impairment of glucose metabolism by fatty acid is dependent on the short-term inhibition of several glycolytic steps, namely i) glucose transport and phosphorylation, ii) 6-phosphofructo-1-kinase (PFK-1), and iii) pyruvate dehydrogenases (PDH) (Hue and Taegtmeyer, 2009). Phosphofructokinase (PFK) is a key regulator of glycolysis, catalysing the first irreversible and rate-limiting step. PFK1 is inhibited by cytosolic citrate and ATP levels, and is activated by fructose 2,6-bisphosphate (Fru-2,6-P2) and ADP (Mendez Garcia et al., 2023). Fru-2,6-P2 in turn is produced and degraded by the bifunctional enzyme phosphofructokinase-2/fructose bisphosphatase-2 (PFK-2). PKA modulates this reaction by phosphorylating PFK-2, leading to a decrease in Fru-2,6-P2. This diminishes PFK activity, thereby inhibiting glycolysis. Consequently, glucose is conserved, and fatty acid oxidation is promoted as an alternative energy source (Hue and Taegtmeyer, 2009).

A role that PKA plays in cardiac metabolism as a result of β adrenergic stimulation is on ATPase Inhibitory Factor 1 (IF1). Mitochondrial H^+-ATP synthase synthesizes most of cellular ATP requirements by OXPHOS (García-Bermúdez et al., 2015). The ATPase Inhibitory Factor 1 (IF1) is known to inhibit the hydrolase activity of the H^+-ATP synthase in situations that compromise OXPHOS. Mice treated with βAR agonist clenbuterol showed a significant increase in IF phosphorylation, as well as increase in the concentration of cAMP in isolated heart mitochondria. In line with this, incubation of

isolated mitochondria in the presence of the membrane-permeable db-cAMP triggered the rapid and complete phosphorylation of IF1. The authors suggest that under β-adrenergic activation, when the energy demand is enhanced, most of the IF1 reserve of the cell becomes inactivated to prevent its binding to the H^+-ATP synthase in order to favour a higher output of ATP. Consistent with this suggestion, upon β-adrenergic activation the ATP hydrolytic activity of the H^+-ATP synthase was significantly increased (García-Bermúdez et al., 2015).

1.4.4 A kinase anchoring proteins in energy metabolism

As mentioned earlier in the chapter, AKAPs are proteins that tether PKA at specific subcellular sites. They contribute greatly to cAMP compartmentalisation, by ensuring that the otherwise promiscuous PKA phosphorylates certain, local, targets. Optic atrophy 1 (OPA1) is an AKAP involved in lipid trafficking. In mouse fibroblasts (Pidoux et al., 2011) and human adipocytes (Rogne et al., 2018) it triggers lipolysis in response to adrenergic stimuli, anchoring a pool of PKA that phosphorylates the perilipins (Pidoux et al., 2011).

OPA-1 KO mice present cardiac dysfunction (Dorn et al., 2011), and OPA-1 protein expression is decreased in human and rat heart failure (Chen et al., 2009a), suggesting that the protein is involved in cardiac pathophysiology. OPA1 is crucial for mitochondrial inner membrane fusion. Piquereau *et al.,* utilized $OPA1^{+/-}$ mice, which exhibited a 50% reduction in OPA1 expression in cardiac tissue, presented no significant differences in cardiac function, but showed larger mitochondria with disrupted cristae structure. Even though the mitochondrial functional properties were maintained, direct energy channelling between mitochondria and myofilaments was weakened. Finally, when subjected to pressure overload, $OPA1^{+/-}$ mice exhibited compromised cardiac adaptation, suggesting that OPA1 is essential for maintaining mitochondrial integrity and function during cardiac stress (Piquereau et al., 2012).

1.4.5 EPAC in energy metabolism

EPAC is one of cAMP effectors and plays an important role in structure and function of the heart under physiological and pathological conditions (Fujita et al., 2017). EPAC1 signalosome is highly compartmentalized and occurs in several micro subcellular compartments, such as the plasma membrane, sarcoplasm, and the nuclear/perinuclear region of cardiomyocytes (Laudette et al., 2018). EPAC1 expresses at the mitochondria in vascular smooth muscle cells, where it regulates the dynamic phosphorylation of dynamin-1-like protein (DRP1), crucial for mitochondrial fission/fusion balance (Wang et al., 2016). Additionally, in cardiac ischemia, mitochondrial EPAC1 increases Ca^{2+} uptake and ROS production thereby promoting mitochondrial death signalling such as mitochondrial permeability transition pore (MPTP) opening and cytochrome c release, and ultimately cardiomyocyte death (Fazal et al., 2017).

A study by Laudette *et al.,* investigated a novel role of EPAC at the mitochondria in cardiac myocytes, where it was identified as a possible mediator of the cAMP regulation of mitochondrial metabolism. They show that cAMP-EPAC1 axis contributes to metabolic dysregulation and lipotoxicity in cardiomyocytes under lipid overload conditions (Laudette et al., 2021). Saturated fatty acids, like palmitate, trigger EPAC1 activation via palmitoylation of soluble adenylyl cyclase, increasing cAMP. EPAC1 enhances mitochondrial fatty acid uptake through CPT1, impairing fatty acid oxidation (FAO), leading to mitochondrial dysfunction, ROS generation, and cell death. EPAC1 also interacts with mitochondrial proteins (CPT1, ACADL, ATP5A) to regulate FA metabolism via CaMKII-mediated phosphorylation. Pharmacological inhibition of EPAC1 mitigates these detrimental effects by enhancing FAO, improving metabolic flexibility, and reducing glucotoxicity in lipid-overloaded cardiomyocytes. Furthermore, blocking EPAC1 prevents mitochondrial dysfunction and protects against cardiomyocyte death (Laudette et al., 2021).

1.4.6 Phosphatases in energy metabolism

Phosphatases dephosphorylate PKA targets and therefore can be considered the ultimate terminators of the cAMP signalling. Even though the role of phosphatases in the regulation of cardiac metabolism has not been extensively studied, some advancements have been achieved in pancreatic cells. In these, the leading hypothesis involving phosphatases in lipid metabolism is that PP1 activates acetyl-CoA carboxylase (ACC). ACC is the enzyme that catalyses the formation of malonyl-CoA, which in turn inhibits the enzyme CPT1. CPT1 is required for uptake of long-chain fatty acids into the mitochondria (Foster, 2012; Tong, 2005). The catalytic function of ACC is inactivated by AMP kinase phosphorylation (Saha and Ruderman, 2003). In pancreatic β-cell, ACC stimulation is markedly reduced by okadaic acid (OKA), a protein phosphatase 2A (PP2A) inhibitor. Pre-treatment of the cytosolic fraction with anti-PP2A serum attenuates the glutamate- and magnesium-mediated activation of ACC, thereby suggesting that ACC may be regulated by an OKA-sensitive PP2A-like enzyme (Kowluru et al., 2001).

1.5 Mitochondrial cAMP subcellular compartment

cAMP is responsible for a myriad of cellular responses. As described above, the specificity of signalling is obtained by the subcellular compartmentalisation of cAMP, achieved through the action of many players, most importantly by the phosphodiesterases. PDEs generate different concentrations of cAMP at different subcellular nanodomains, by hydrolysing cAMP locally. This avoids spillage of information amongst different pathways which occur independently but concurrently. Many cAMP nanodomains have been described, including at the plasma membrane, primary cilium, endoplasmic reticulum, Golgi apparatus and mitochondria (Zaccolo et al., 2021). The latter is described in the following section.

Mitochondria are organelles that produce the majority of cellular ATP in the eukaryotic cells through oxidative phosphorylation (OXPHOS) (Zhang et al., 2016). Structurally, they are enclosed by a two-layered membrane comprised of: i) the mitochondrial inner membrane (MIM), with highly dynamically folded in structures called cristae (Kondadi et al., 2020),

and ii) the mitochondrial outer membrane (MOM), that encircles the mitochondrial intermembrane space (MIS) (Jakobs et al., 2020). Mitochondria possess a dynamic nature and undergo three main processes. i) fusion and fission adjusts their shape and numbers in cells (Cerveny et al., 2007; Westermann, 2010). ii) motility, where they exploit the microtubule network to migrate to specific subcellular sites. iii) mitophagy, which eliminates dysfunctional mitochondria (Di Benedetto et al., 2021). These dynamics are highly plastic in response to the cell's energy demand, to developmental cues and to environmental stimuli (Zhang et al., 2016). Mitochondria have tightly regulated cAMP signalling. Each compartment in fact, including mitochondrial outer membrane, mitochondrial intermembrane space and mitochondrial matrix presents a spatially and functionally distinct cAMP signalosome. cAMP signalling at the mitochondria contributes to their adaptability as metabolic demands change (Carlucci et al., 2008). Several components of the cAMP signalling pathway have been identified in mitochondria (Zaccolo et al., 2021).

1.5.1 Mitochondrial Outer Membrane

A number of a AKAPs have been reported to tether PKA at the mitochondrial outer membrane, including AKAP1 (Ma and Taylor, 2002), AKAP2 (Wang et al., 2001), Rab32 (Alto et al., 2002), peripheral-type benzodiazepine receptor–associated protein 7 (PAP7) (Li et al., 2001), and Wiskott-Aldrich syndrome protein verprolin homologous (WAVE) (Danial et al., 2003). PKA R and C subunits were isolated from purified mitochondria over 30 years ago (Schwoch et al., 1990). A mass spectrometry analysis of the mitochondrial phosphopeptide pool has identified over 100 PKA targets, which suggests that the mitochondria may harbour additional cAMP signalosomes.

The best characterized mitochondrial functions modulated by the cAMP cascade hosted at the MOM are mitochondrial dynamics and apoptosis. cAMP regulates mitochondrial fission and fusion. PKA anchored at the MOM is activated by cytosolic cAMP and can phosphorylate Drp1 (dynamin-1-like protein), a large GTPase involved in the mitochondrial fission–fusion balance. Unphosphorylated Drp1 is recruited to the mitochondria where it polymerizes and promotes mitochondrial fission. PKA-dependent phosphorylation at

Ser^{637} inhibits the formation of Drp1 complexes and promotes mitochondrial fusion (Merrill et al., 2011; Lefkimmiatis, 2014). In addition, PTEN-induced putative kinase (PINK1) serves as a pro-fission signal by triggering PKA displacement from AKAP1. This results in fission of damaged mitochondria destined to mitophagy (Pryde et al., 2016).

Apoptosis is also regulated through the cAMP signalling pathway at the MOM. Here, AKAP1 overexpression enhances PKA-dependent phosphorylation of apoptotic regulators, including BCL2-associated agonist of cell death (BAD) (Affaitati et al., 2003), BCL2-associated X protein (BAX) (Srivastava et al., 1998), and BCL2-interacting mediator of cell death (BIM) (Moujalled et al., 2011). This has protein-specific outcomes: phosphorylation of BAD inhibits apoptosis, while phosphorylation of BAX and BIM promotes it. This highlights the complexity of cAMP/PKA signalling in mitochondria, suggesting the existence of distinct signalosomes with selective targeting mechanisms yet to be fully elucidated.

PDE2A2 is also present at the MOM. Here it regulates local cAMP levels and PKA-dependent phosphorylation of Drp1, affecting mitochondrial morphology and apoptosis. These effects were recapitulated in AC10-/- cells, confirming a role of PDE2A2 at the mitochondria outside the matrix (Monterisi et al., 2017). PDE2A2 at the MOM also interacts with the MINOS components MIC60 and coiled-coil-helix-coiled-coil-helix domain containing (ChChd) 3. Here, PDE2A2 regulates local levels of cAMP and controls Parkin recruitment to the mitochondria resulting in mitophagy (Lobo et al., 2020).

1.5.2 Mitochondrial Intermembrane Space

The MIS lies between the MOM and MIM (Jakobs et al., 2020). In the MIS, the level of cAMP is similar to that at the MOM (Zaccolo et al., 2021). The AKAP SKIP in the MIS interacts with the PKA RI subunit with high affinity (Kovanich et al., 2010). SKIP also interacts with several other proteins, including ChChd3, ChChd6, sorting and assembly machinery 50 (SAM50), metaxin 1 (MTX1), and MTX2. PKA phosphorylates ChChd3, and SKIP is required for this phosphorylation to take place (Means et al., 2011). ChChd3 and ChChd6 are components of the mitochondrial inner membrane organizing system

(MINOS), a multiprotein complex that is involved in the regulation of mitochondrial membrane architecture and formation of cristae junctions and contact sites between the outer and inner membranes (Pfanner et al., 2014). It is possible that the MIS contains a cAMP microdomain built around SKIP and relying on PKA type I.

1.5.3 Mitochondrial Matrix

Cytosolic cAMP cannot reach the mitochondrial matrix, as the membrane is not permeable to it (Acin-Perez et al., 2011). The matrix includes an independent pool of cAMP which is generated by the soluble adenylyl cyclase (AC10). This is activated by carbon dioxide/bicarbonate and regulated by Ca^{2+} (Acin-Perez et al., 2009). A Ca^{2+} dependent mechanism has been suggested to stimulate the matrix pool of cAMP that promotes mitochondrial ATP synthesis (Di Benedetto et al., 2013; Lefkimmiatis et al., 2013). It is currently uncertain if PKA regulates cAMP signalling in the matrix. On the one hand, PKA subunits lack any obvious mitochondrial targeting sequence, and this challenges the idea that they are present in the matrix (Valsecchi et al., 2014). This is supported by the failure of FRET-based sensors targeted to the matrix to detect any PKA enzymatic activity (Lefkimmiatis et al., 2013). On the other hand, large scale phosphoproteome analyses reveals that many enzymes in the TCA (Tricarboxylic Acid) cycle and ETC (electron transport chain) complex subunits are phosphorylated at the PKA consensus sites (Zhao et al., 2011).

1.6 Aims of the project

cAMP signalling is responsible for a myriad of cellular responses. cAMP is compartmentalised into nanodomains, which localisation is dictated by the hydrolysing action of the phosphodiesterases. Even though this is now an established concept, only a very limited number of nanodomains have been characterised. As it is the distribution and activity of different PDE isoforms that ultimately defines the topography of active subcellular cAMP nanodomains, they represent a valuable tool for discovering novel

nanodomains. It also offers the possibility to pharmacologically target phosphodiesterases individually, and consequently, modulate the nanodomains under their control, increasing the treatment efficacy and reducing its side effects for disease conditions linked to cAMP signalling disruption. This is particularly relevant as cAMP signalling is disrupted in cardiac disease (Kokkonen and Kass, 2017).

In the attempt to expand the knowledge on the cAMP signalling map, our laboratory conducted a phosphor-interactome study which unveiled a novel nuclear nanodomain under the control of PDE3A2 (Subramaniam et al., 2023). The experimental approach combined analysis of the PDE family-specific phosphoproteome with a study of the PDE isoform-specific interactomes. Here, adult rat ventricular myocytes (ARVM) were infected with adenoviral vectors encoding PDE2A2-RFP, PDE3A1-RFP or RFP. The RFP immunoprecipitations were analysed by MS which returned a list of possible interactors of the different PDEs. The interactors of each PDE were analysed in conjunction with the phosphopeptides upregulated on inhibition of the same PDE using STRING for network analysis (Subramaniam et al., 2023). The resulting subnetworks were organised by their known subcellular localisation by a previous member of the lab, Dr Kovanich. The resulting map projected onto the structure of a cardiac myocyte reveals several sub-networks at different sites where PDE-dependent cAMP nanodomains may be present.
Trough this approach the authors found that PDE3A2 is present in the nucleus, where it regulates a nuclear pool of cAMP in charge of gene expression. Inhibition of PDE3 results in enhanced PKA-depended phosphorylation on HDAC1, inhibiting its deacetylase activity. This, in turn, results in the de-repression of prohypertrophic gene transcription and cardiac myocyte hypertrophy (Subramaniam et al., 2023).

Eliciting the same approach, a map of the PDE2A2 interactors was generated. (Fig. 1.1). The connecting lines indicate proteins known to interact together.

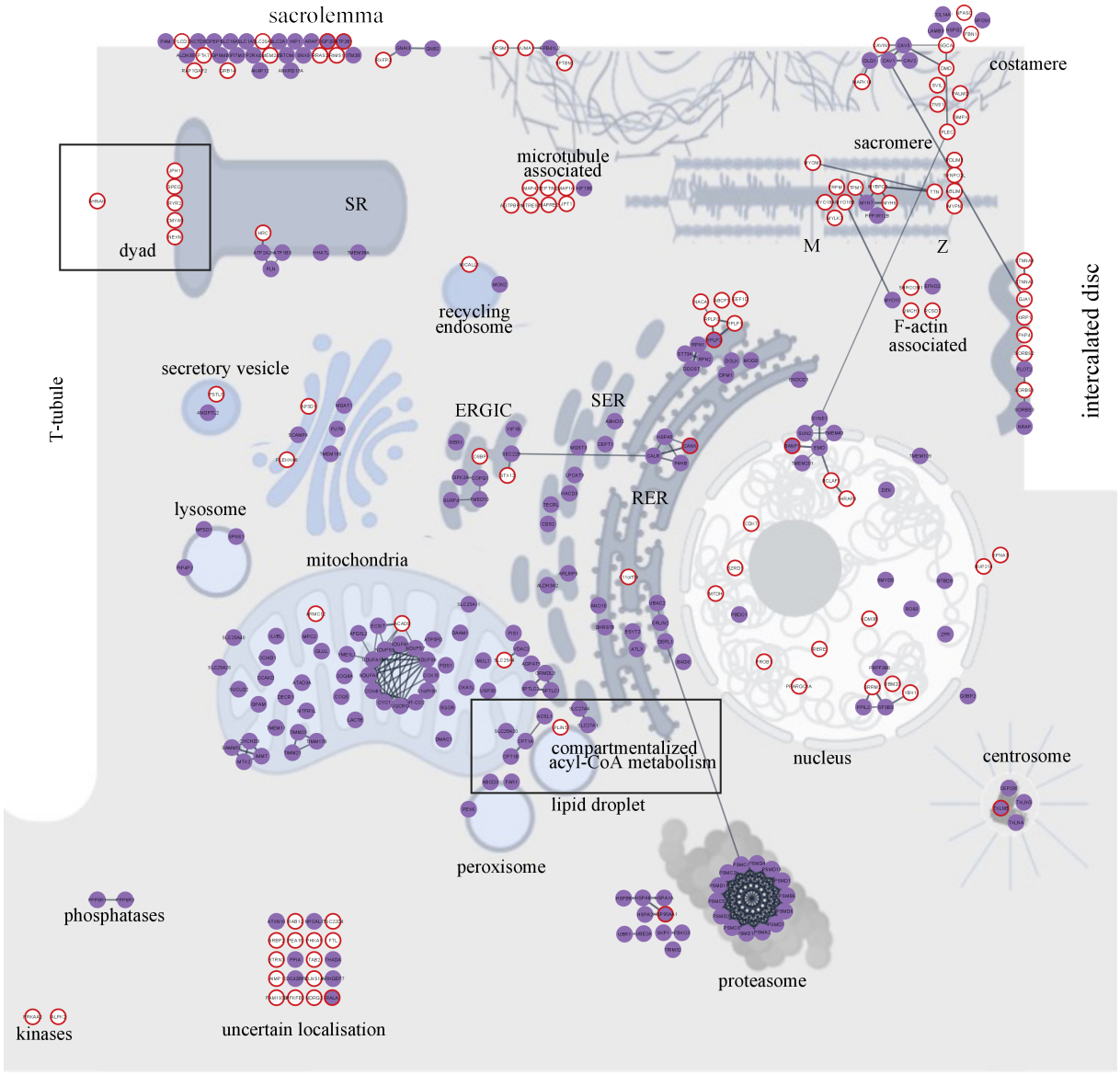


Figure 1.1. Mapping of PDE2A2 interactors organised by their subcellular localisation. PDE2A2 interactors arising from MS analysis are organised spatially based on their subcellular localisation. Interactions which have previously been described in the literature are indicated with a grey line. Purple circles indicate interactors, white circles with red rim indicate phosphotargets and purple circels with red rim indicate proteins identified both as interactors of PDE2A2 and phosphotargets on inhibition of PDE2A. Schematics generated by Dr Kovanich.

This proteomics analysis suggests multiple novel potential cAMP nanodomains under the control of PDE2A2 or PDE3A1 that may be involved in the regulation of energy substrate handling.

The overall aim of this thesis is to validate some of these nanodomains and to further

characterise their potential functional role.

Given the presence of PDE2A2 at the mitochondria (Acin-Perez et al., 2011; Rinaldi et al., 2018; Monterisi et al., 2017), and the roles this enzyme plays at this organelle (Zaccolo et al., 2021), I focused my study on the potential role of PDE2A2 in transporting energy substrates.

The specific aims are:

- **aim 1**: address whether PDE2A2 interacts with proteins which mediate the transport of metabolites for energy production. (Chapter 3)
- **aim 2**: address whether PDE3A1 interacts with proteins which mediate the transport of metabolites for energy production. (Chapter 4)
- **aim 3**: Explore the mechanism by which PDE2A2 regulates the uptake of fatty acid at the mitochondria (Chapter 5)

Chapter 2

Materials and methods

2.1 Antibodies

A list of the antibodies used in this thesis is included in the table 2.1.

Target	Species	Brand, Code	Dilution
ACSL1	rabbit	Cell Signaling, 4047	1:1000
CPT1A	rabbit	Proteintech, 15184-1-AP	1:1000
CPT1B	rabbit	Proteitech, 22170-1-AP	1:1000
MPC2	rabbit	Cell Signallins, 46141	1:1000
SLC25A20	rabbit	Proteitech, 19363-1-AP	1:1000
SLC25A20	rabbit	Abclonal, A23763	1:1000
SLC25A20	rabbit	Abcam ab244436	1:1000
VDAC1	mouse	Proteintech, 66345-1-Ig	1:1000
SLC27A4	rabbit	Abclonal, A21969	1:1000
SLC27A4	rabbit	Proteintech, 11013-1-AP	1:1000
SLC25A4	rabbit	Abclonal, A20842	1:1000
SLC25A4	rabbit	Proteintech, 15997-1-AP	1:1000

Target	Species	Brand, Code	Dilution
SLC2A1	Rabbit	Abclona, A11727	1:1000
SLC2A1	mouse	Proteintech, 66290-1-Ig	1:1000
SLC2A11	rabbit	Abclonal, A8163	1:1000
SLC16A1	rabbit	Cell Signalling, 85680	1:1000
pACC	rabbit	Cell Signaling, 3662	1:1000
ACC	rabbit	Cell Signaling, 3661	1:1000
DYKDDDDK	rabbit	Cell Signalling, 14793	1:1000
α-tubulin	rabbit	Abcam, ab729	1:2000
TOM20	mouse	Proteintech, 11802-1-AP	1:1000
TOM20	rabbit	Abclonal, A16896	1:1000
GFP	rabbit	Thermo Fisher, A-11122	1:1000
GAPDH	mouse	Cell signalling, 97166	1:2000
EIF3C	rabbit	Abclonal, A7022	1:1000
RBM39	rabbit	Abclonal, A15760	1:1000
YBX1	rabbit	Abclonal, A3534	1:1000
ILF2	rabbit	Abclonal, A13320	1:1000
SLC27A1	rabbit	Abclonal, A12847	1:1000
RFP	rabbit	Abcam, ab62341	1:1000
RFP	rabbit	Thermo Fisher, RF5R	1:1000
Phospho-Ser	rabbit	Abcam, ab9332	1:1000
Phospho-(Ser/Thr)	rabbit	Novus biological, NB100-1953	1:1000
Phospho-(Ser/Thr)	rabbit	Cell Signalling, 9621	1:1000

Table 2.1. List of antibodies used in this thesis. A list of the anitbodies used in this thesis is shown above. The columns indicate the name of the antibody, species, the brand and the dilution.

2.2 Cell culture

2.2.1 NRVM isolation and culture

Primary cardiac ventricular myocytes were isolated from 1 to 2-days old Sprague Dawley rats (Charles River Laboratories). After Schedule 1, hearts were removed and placed in ice cold ADS buffer containing (in mmol L^{-1}): 106 NaCl, 5.3 KCl, 20 HEPES, 0.8 NaH_2PO_4, 0.4 $MgSO_4$ and 5 glucose; pH adjusted to 7.40 with NaOH (all from Thermo Fisher Scientific). After the atria were removed and discarded, the ventricles were sliced longitudinally and placed in fresh ADS. The minced tissue was transferred into 50-ml falcon tubes and stirred at 37°C with 5% pancreatin (Thermo Fisher Scientific) and 0.32 mg/ml collagenase A (Roche) in ADS. 5 ml enzyme solution was used for the first step of digestion. The supernatant from the first digestion (5 minutes) was discarded. For each of the following four digestion, 9 ml of enzyme solutions were added, and the tissue stirred at 37°C for 20 minutes each. After each digestion, the tissue was allowed to sediment, the supernatant was collected and added to centrifuge tubes containing 10% newborn calf serum (NCS) (Thermo Fisher Scientific). The cell suspensions from the four digestions were pooled and sedimented at 2500 g for 5 minutes, and resuspended in 'M1' medium, composed of Dulbecco's modified Eagle's medium (DMEM) with 25mM HEPES, Medium 199 (M199), supplemented with 10% horse serum (HS), 5% newborn calf serum (NCS), 1% Glutamine and 0.1% Pen/Strep (all from Thermo Fisher Scientific). The cells were transferred into 100mm petri dishes incubated for 120 minutes at 37°C to allow selective adhesion of fibroblasts to the dishes. After the incubation, media containing unattached cardiomyocytes was resuspended in M1 medium and cells were plated accordingly for each experiment.

For imaging, $3x10^5$ cells were plated on laminin (Roche) coated 35 mm coverslips in 6-well plates. For biochemistry, $2.25x10^6$ cells were plated in 60mm petri dishes.

After 24 hours of culture, the medium was changed with 'M2' medium, containing Dulbecco's modified Eagle's medium (DMEM) with 25mM HEPES, Medium 199 (M199), supplemented with 5% horse serum (HS), 0.5% newborn calf serum (NCS), 1% Glutamine

and 0.1% Pen/Strep. The cardiomyocytes were infected with adenoviral vector suspension corresponding to multiplicity of infection (MOI) of 100. The vectors encoding PDE2A2-RFP, PDE3A1-RFP, or RFP only were acquired from Vector Biolabs. After 2 hours of infection, medium was replaced with fresh M2 medium. For plasmid transfection, the transfectin lipid reagent (Bio-Rad) was used following the manufacturer's instructions. Cells were left in incubation at 37°C and processed 18 to 24 hours after, depending on the expression level of the protein of interest.

Each biological replicate refers to a single preparation that includes 12 pups from 2 different mothers.

2.2.2 ARVM isolation and culture

Adult rat ventricular myocytes were isolated from Sprague-Dawley rats (Charles River Laboratories) through Langendorff perfusion system performed by either Dr Chao, Alexander Demby or Heeseung Jo as described previously (REF surdo 2017). Briefly, Adult rats were sacrificed via intraperitoneal injection of pentobarbital (3.5 mL) and heparin (1.5 mL, 5000 U) (Wockhardt UK), followed by cervical dislocation. The heart was excised, placed in ice-cold perfusion buffer, and perfused with oxygenated buffer via the aorta. Enzymatic digestion was initiated using trypsin and liberase (Sigma Aldrich) for 10-12 min, monitored for tissue dissociation. Digested ventricles were minced, filtered, and subjected to sequential calcium challenges to facilitate gradual calcium reintroduction. Cells were resuspended in ARVM medium containing M199 (Gibco), 5 mM creatine (Sigma Aldrich), 2mM L-carnitine (Sigma Aldrich), 5 mM taurine (Sigma Aldrich), 0.1% Insulin-transferrin-selenium-X (100X) (Gibco), 5% FBS (Gibco), 10μM Blebbistatin (Cayman chemical) and 1% Pen/Strep (Gibco). Cell viability was assessed microscopically.

Each biological replicate refers to a single heart.

2.2.3 Human Induced Pluripotent Stem Cell-Derived Cardiomyocytes

Human induced pluripotent stem cells were differentiated and cultured by Dr Koshinski. (hiPSCs M180 line, and M398 line (ref: Gosselin MRF, 2022)) were cultured as described previously. The cell lines were cultured in mTeSR Plus medium (Stemcell Technologies) on human embryonic stem cell (hESC)-qualified Matrigel (8 μg/cm^2; Corning-coated surfaces; cells were passaged twice a week using DPBS (Gibco) for rinsing and accutase (Sigma-Aldrich) for dissociation. The ROCK (Rho Kinase) inhibitor (StemMACS Y27632, 10 μmol/L; Miltenyi Biotech) was added for the first 24 hours after seeding. Differentiation into cardiomyocytes was induced in monolayer as described previously (ref:Campostrini, G 2021). Differentiated human inducible pluripotent stem cell-derived cardiac myocytes (hiPSC-CM) were maintained in RPMI 1640 medium with Glutamax and 25 mM HEPES (Gibco) plus B27 supplement (Gibco). Cells were seeded on Matrigel-coated 60 mm petri dishes at a density of 1.25x10^6 cell/dish. PDE2A2 overexpression experiments were performed at day 21 of differentiation by transducing hiPSC-CMs with PDE2A2-RFP or RFP only adenoviruses. The cells were harvested 24 hours post-transduction which is when they expressed the constructs.

2.2.4 Cell lines

Human Embryonic Kidney 293T cells (HEK293T) and Mouse Embryonic Fibroblasts (MEF) were grown in DMEM supplemented with 10% FBS, 1% Glutamine and 1% Pen/Strep. Cell lines were maintained in a humidified CO2 (5%) incubator at 37°C and were split every 2-3 days after reaching 80-90% confluency, after being washed and trypsinised (0.05% trypsin-EDTA, Thermo Fisher). All plasmids were transfected using jetPRIME (Polyplus transfection), according to manufacturer's instructions.

Each biological replicate refers to a single passage. Each passage is perfomed on a different day.

2.3 Biochemistry

2.3.1 Immunoprecipitation and western blot

Cells were washed three times with PBS and lysed by 30 minutes incubation in lysis buffer, being vortexed for 10 seconds every 10 minutes. Lysis buffer contained Tris HCL 50mM (Sigma-Aldrich), NaCl (Sigma-Aldrich), EDTA 1mM (Clbiochem), Triton 100x 0.5%(v/) (Promega), PBS (Gibco), complete EDTA-free protease inhibitor cocktail tablets (Roche) and PhosSTOP phosphatase inhibitor cocktail (Roche). Lysates were clarified by centrifugation at 13000 rpm for 15 min at 4°C. Protein concentrations were determined using the Bradford assay (Bio-Rad). 10 to 30 μg of protein per sample was used for whole cell lysates, whereas 200-500 μg protein was used for immunoprecipitation. The supernatant and incubated on an end-over-end shaker at 4°C for 2 h with 25 μL of anti-RFP/GFP antibody-linked beads (Chromotek) or anti-FLAG M2 beads (Sigma), respectively. The beads were pelleted by centrifugation for 1 min at 5000 g, washed 3-5x with wash buffer (Triton X-100 0.5% (v/v), in PBS) followed by elution by boiling the sample for 5 minutes at 96 °C and spin-down. The samples were resolved on 4% to 12% Bis-Tris polyacrylamide gels (Invitrogen) which were subsequently transferred onto a PVDF membranes (Millipore) through wet or dry transfer. After transfer, PVDF membranes were blocked for 1 h at room temperature in 5% skimmed milk TBS-T (Alfa Aesar). Next, the membranes were incubated with primary antibodies diluted in 5% skimmed milk TBS-T either for 1 hour at room temperature, or overnight at 4°C. The day after, the membranes were washed for 10 minutes 3 times with TBS-T and incubated at room temperature for 1 hour with a horseradish peroxidase (HRP)-conjugated secondary antibody. When membranes were stripped, stripping buffer (Restore Western Blot, Thermo Scientific) was added for 15 minutes, before re-blocking, antibody incubation and re-developing as described above. To reveal phosphoproteins, 5% phosphopblocker (Cell Biolabs, inc.) was used instead of skimmed milk to block membranes and to dilute primary antibodies. After 3 washes with TBS-T, chemiluminescent detection was performed using either SuperSignal Pico ECL western blot developing solution or SuperSignal West Atto solution (Thermo Fisher

Scientific). Chemiluminescent signal was detected using a ChemiDoc XRS+ (Bio-Rad) imaging system. Quantification of the obtained signal was performed using densitometry analysis with ImageJ V1.53K.

2.3.2 Mitochondrial fractionation

Cytosolic and mitochondrial fractions from HEK293T cells were generated using the Qproteome Mitochondria Isolation Kit (Qiagen), following the manufacturer's instructions. Briefly, cells were washed three times with ice cold PBS before being harvested. The pellet was resuspended in ice-cold kit Lysis Buffer and incubated for 10 minutes at 4°C on an end-over-end shaker. The lysate was centrifuged at 1000 x g for 10 minutes at 4°C. the supernatant was collected and the pellet, containing the cytosolic protein, was resuspended in 1.5 mL ice-cold kit Disruption Buffer. Cell disruption was completed by using a blunt-ended needle and a syringe, drawing the lysate slowly into the syringe and eject with one stroke for 10 times. The lysate was centrifuged at 1000 x g for 10 minutes at 4°C and transferred into a clean 1.5 mL tube. Centrifuge the supernatant at 6000 x g for 10 min at 4°C, this pellet contains mitochondria. The mitochondrial pellet was washed with 1 ml of the kit's Mitochondria Storage Buffer, and centrifuged 6000 x g for 20 min at 4°C. The cytosolic and mitochondrial pellets were resuspended in IP lysis buffer and immunoprecipitation from each fraction was performed.

2.3.3 Lipid droplets staining, imaging and analysis

Cells were seeded on 35 mm coverslips in 6-well plates at a density of $4x10^6$ cells/well in their culture medium. Cells were washed three times with PBS (Gibco) and fixed with 4% (w/v) paraformaldehyde (Thermo Fisher) in PBS, permeabilized with 0.1% (v/v) Triton X- 100 (TX) in PBS for 5 minutes and washed in PBS three times. Cells were stained with HCS LipidTOX™ Red neutral lipid stain (Thermo Fisher), diluted 1:200 in PBS for MEF and 1:100 for NRVM. A droplet of 50 μL was placed on a clean bench and the coverslip was placed on top and incubated at room temperature for 30 minutes for MEF and for 1 hour for NRVM. After the incubation period, the cells were washed twice by

gently submerging the coverslips in fresh PBS. The coverslips were then dried thoroughly by dabbing the edge on a paper towel and mounted on Superfrost Plus microscope slides (VWR) with Fluoroshield mounting media containing DAPI (Abcam) and sealed with nail varnish. Coverslips were imaged with the Olympus SpinSR10 spinning disc confocal system fitted with an Olympus IX-83 frame, a Yokogawa CSU-W1 SoRa superresolution spinning disc module, a Photometrics Prime BSI camera and a 60× objective (1.5 NA, UPLAPOHR60x), using Olympus cellSens Dimension software. Images were collected at 405nm and 567nm. 10 z-planes were acquired per site. Figures were processed and analyzed using ImageJ (FIJI, Schindelin et al 2012). Briefly, the 10 z-planes were projected to create a single image, segmentation was achieved by thresholding the image, and lipid droplet were detected and quantified through the 'analyze particle' command on ImageJ.

2.3.4 CPT1 activity assay

The assay was based on the original protocol with some modifications (Bieber et al., 1972). The assay measures the ability of CPT1 to efficiently shuttle fatty acids into the mitochondria. It is based on the knowledge that long chain fatty acids such as palmitoyl-CoA, require a shuttle system to be transported into the mitochondrial matrix. In the presence of carnitine, CPT1 converts LFCA into long-chain carnitines, releasing a CoA. CPT-1 activity was determined by spectrophotometry by measuring the amount of CoA released using the Ellman's reagent (5,5'-dithio-bis (2-nitrobenzoic acid (DTNB), Sigma-Aldrich) as previously described (ref: Bieber 1972). Briefly, DTNB has an oxidizing-disulfide-bond that is reduced in the presence of free thiols (CoA) forming a mixed-disulfide and releasing one molecule of 5-thio-2-nitrobenzoic acid (TNB). TNB can be spectrophotometrically read at 412 nm. (Fig. 2.1).

For experiments on MEF, cells were seeded in 100 mm petri dishes and cultured on DMEM until they reached 80% confluency. When comparing wildtype MEF and MEF$^{PDE2A-/-}$, cells were starved by replacing the medium with starvation medium (DMEM supplemented with 0.1% FBS and no added L-glutamine) for 24 hours before harvest, in order for the two lines to align metabolically (ref: Bhowmick T 2024). For experiments involving ARVM, cells

were processed right after isolation and treatment with the relevant inhibitors. One sample was treated with 40 μM etomoxir for 15 minutes as negative control. Cells were harvested via mechanical scraping with a sterile cell scraper and washed three times with PBS. The samples were lysed for 30 minutes in a buffer containing Tris HCL 50mM (Sigma-Aldrich), NaCl (Sigma-Aldrich), EDTA 1mM (Clbiochem), Triton 100x 0.5% (v/) (Promega), PBS (Gibco), complete EDTA-free protease inhibitor cocktail tablets (Roche) and PhosSTOP phosphatase inhibitor cocktail (Roche). Lysates were clarified by centrifugation at 13000 rpm for 15 min at 4°C. Protein concentrations were determined using the Bradford assay (Bio-Rad). 50 μg of protein were added a reaction buffer containing 40mM HEPES pH 7.4 (Sigma Aldrich), 440mM sucrose (Sigma Aldrich). 80mM KCl (Sigma Aldrich), 2mM EDTA (Santa Cruz Biotechnology), 80 μM palmitoyl-CoA (Santa Cruz Biotechnology) 0.2mM DTNB (Sigma Aldrich) and incubated for 30 minutes at room temperature. After one initial spectrophotometric reading 412nm to determine the basal concentration of CoA-SH, CPT1 enzymatic reaction was started by adding 5 mM L-carnitine, and the absorbance was measured every 30 seconds for 90 min at 412nm at 37°C. The concentration of CoA-SH released was calculated through Beer Lambert's law:

$$A = \varepsilon c l \tag{2.1}$$

CPT-1 activity was defined in nmol CoA-SH released/min/mg protein.

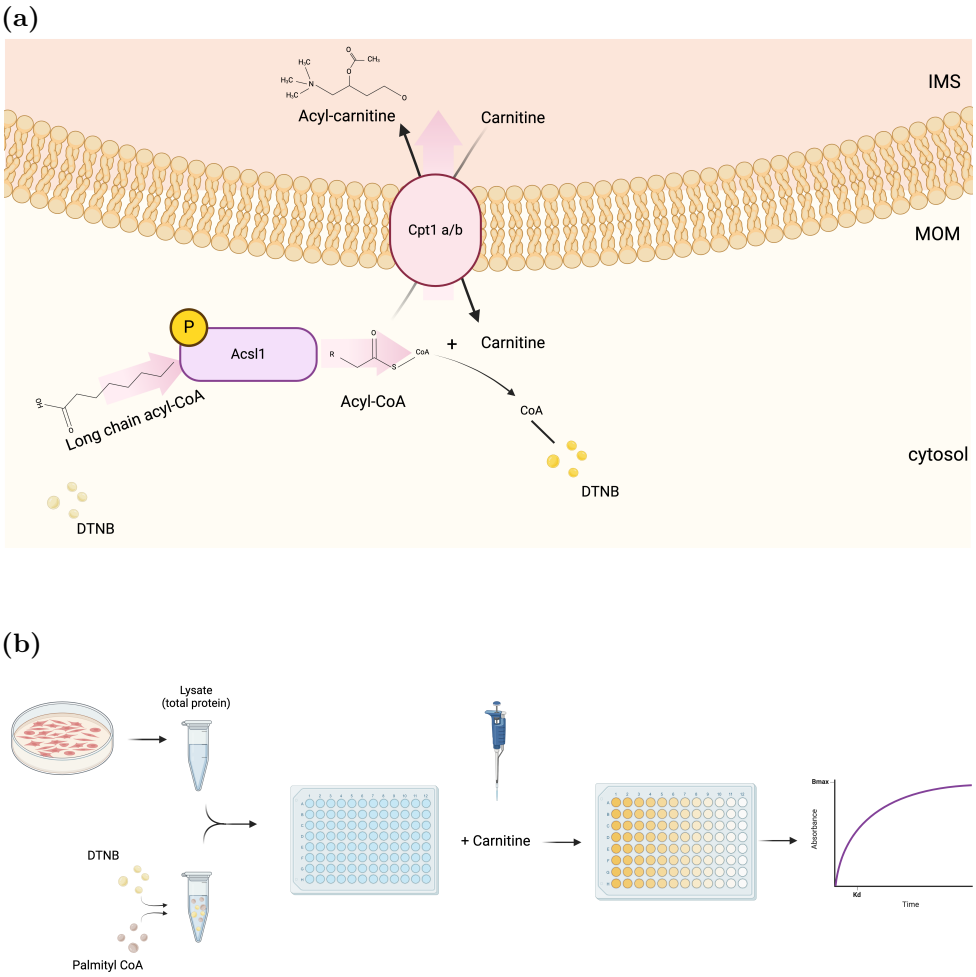


Figure 2.1. CPT1 assay. Schematic representation of the principle and sequence of the CPT1 assay.
a)at the MOM, LCFA are esterified and activated by the enzyme long-chain acyl-CoA synthetase 1, into Acyl CoAs. In the presence of carnitine, CPT1 shuttles Acyl CoAs through the MOM and in doing so CoAs are released. Free CoAs bind to DTNB, resulting in the release of TNB, which absorbance can be spectrophotometricall read at 412 nm.
b)Cells are plated and incubated before being lysed. The supernatant is kept in an eppendorf tube. In a different tube, DTNB is mixed with palmitoyl CoA. The lysate and the DTNB/palmitoyl CoA suspension are added onto a 96 well plate. After adding carnitine, TNB absorbance is read for 90 min at 412nm at 37°C. The concentration of CoA-SH released is calculated through Beer Lamber's law.

2.3.5 ^{3}H-Palmitate and ^{3}H-Oleate Oxidation

These experiments were run in collaboration with Dr Purnama from Professor Carr's group.

Fatty acid oxidation rates were determined by the production of $^{3}H_2O$ in the electron

transport chain as previously described (Barr RL, 2000; Lopaschuk and Barr, 1997). ARVM or MEF were seeded in laminin (Roche)-coated 24-well plates (5×10^4 cells/ well) and incubated in no-glucose DMEM (Gibco) medium that was supplemented with 12 mM glucose (Sigma Aldrich). For palmitate oxidation the medium was supplemented with 2% BSA, 0.3 mM palmitate (added to heated media for proper conjugation to BSA), and doped with 0.2 μCi/mL of Palmitic Acid (PA), [9,10-^{3}H(N):1mCi-37MBq] (PerkinElmer) per well. For oleate oxidation, the medium was supplemented with 2%BSA, 400 μM oleic acid (OA), and doped with 0.2 μCi/mL of oleate, [9,10-^{3}H(N): 1mCi-37MBq] (PerkinElmer). Cells were cultured in a normoxic incubator (5% CO_2 and 21% O_2) at 37°C for 6 hours. Palmitate and oleate oxidation rates were determined by the production of ^3H_2O released during this time into the incubation medium. After incubation, the supernatant was separated from the ^{3}H-palmitate or ^{3}H-OA via Folch extraction. 1.88 ml of chloroform:methanol (1:2 v/v) solution, 625 μl chloroform and 625 μl KCl-HCl solution (2 M KCl, 0.4 M HCl) were added to 0.5 ml of the perfusate sample. The solution was rotated on a laboratory Stuart rotator SB3 at 40 rpm for 1 hour before removing the top aqueous layer, while the organic layer was discarded. A solution of 1 ml choloform, 1 ml methanol and 0.9 ml KCl-HCl was added to the extracted aqueous solution, before further rotation for 1 h at 40 rpm. The top aqueous layer was retained and 0.5 mL (in duplicate) of this phase was added into a scintillation vial containing 10 mL of Ecolite liquid scintillation cocktail (MP Biomedicals, USA). The radioactivity (cpm) of the sample was counted using a Tri-Carb 2800TR Liquid Scintillation Analyzer (PerkinElmer) and rates of oxidation calculated as described in (Lopaschuk and Barr, 1997).

2.3.6 Seahorse assay

Cells were seeded at a density of 7×10^4 cells/well in XFe 96 microplates in the respective culturing medium. After 24 hours, the medium was replaced with Seahorse XF Base Medium (modified DMEM with Phenol Red, pH 7.4; Agilent), supplemented with glucose (10 mM, Sigma), glutamine (2 mM, Sigma), and sodium pyruvate (2 mM, Sigma), before being incubated at 37°C, at atmospheric CO_2 levels. Oxygen consumption rate (OCR)

were measured using the XFe 96 analyzer (Agilent). OCR measurements were taken followed by 3 measurements after sequential injection of the following compounds from the XF Cell Mito Stress Test Kit (Agilent): oligomycin (2 mM, injection port A), FCCP (2 mM, injection port B), and combined antimycin A (0.5 mM), and rotenone (0.5 mM) (injection port C).

2.3.7 Extracellular glucose measurements

The concentration of glucose in the culture media was detected using a miniaturization of a commercial kit (Merck; GAHK20). Culture media from either condition was diluted 1:3 in dH_2O. 50μl of each dilution were added per well on a F-bottom 96-well plate. Glucose solution from the kit was freshly made up and 100μl were added onto each sample. Plates were incubated at 35°C for 15 min inside a SpectraMax M5 plate reader. NADH absorbance was read at 340 nm wavelength. Glucose values from the samples were calculated by curve fitting to a known standard curve.The [glucose] values were subtracted from the [glucose] present in the medium.

2.3.8 Extracellular lactate measurements

Lactate from the culture media was calculated based on the NADH absorbance at 340 nm wavelength. Culture media from either condition was diluted 1:3 in dH_2O. 5μl of diluted sample were added per well well on a F-bottom 96-well plate and incubated with 100μl of freshly made running buffer solution (3.5 ml Glycine buffer pH 9.2 (per 100ml: 4.5g of glycine 99%, 1.3 ml hydrazine hydrate, 600 μl KOH 10M, ~95ml dH_2O), ~6.5ml dH_2O, 80μl Bovine L-lactate Dehydrogenase 2.5 KU, 10 mg NAD+) for 20 min at 37°C inside a SpectraMax M5 plate reader. NADH absorbance was read at 340 nm wavelength. Lactate values were calculated by curve fitting to a known standard curve using sodium L-lactate.

2.3.9 Mouse tissue homogenization

For some experiments, I utilized frozen heart tissue from wildtype mice and *pde2a*$^{-/-}$ previously harvested and genotyped by Dr Chao. The heart tissue which had been

stored in liquid nitrogen was minced on a pre-cooled porcelain mortar and pestle (Sigma Aldrich) until finely grinded. 70 μg of tissue were added to 700 μl of CellLytic Cell lysis Reagent (dialyzable mild detergent, bicine, and 150 mM NaCl) (Sigma Aldrich). The tissue underwent 3 rounds of mechanical homogenization ($\sim$10s) on ice with TissueRuptor II disposable probes (Qiagen). The samples were vortexed for 5-10 seconds every 10 minutes three times, and then centrifuged at 13000 rpm for 10 minutes at 4°C. Protein concentrations were determined using the Bradford assay (Bio-Rad).

2.4 Statistical analysis

Statistical significance tests were performed using Prism 9 (GraphPadPrism). Data are presented as mean$\pm$SEM. For n >10, normal distribution of the experimental data was tested with the Shapiro-Wilk test. For comparisons between 2 groups, Student t test was used for normally distributed data. For non-normally distributed data and n<10, a Mann-Whitney U test (unpaired data) or a Wilcoxon signed-rank test (paired data) was used. For comparison between >2 groups, Kruskal-Wallis test followed by a Dunn multiple comparison (non-normal distribution with nonpaired groups and n<10) was performed. Significance level for all tests was set at 95%. For experiments where values may be clustered, with a possibility of similarity within each cluster, a hierarchical analysis model in R using the lme4 package with clustering for individual data points followed by Bonferroni correction for multiple comparisons was applied (as previously described in the study by Sikkel *et al.*,. Here, the clustering is quantified by the intraclass correlation coefficient (ICC) (Sikkel et al., 2017). This measure represents the proportion of total variability in an outcome measure that is attributable to the isolation of origin.
P values of <0.05 were considered statistically significant. Representative images were chosen to closely match the average values of the respective groups.

Chapter 3

PDE2A2 metabolic interactors

3.1 Background

PDE2A hydrolyses both cAMP and cGMP with approximately equal affinity (Francis et al., 2009), and is expressed as three isoforms: PDE2A1, PDE2A2 and PDE2A3 (Francis et al., 2011). They all share the same C-terminal domain, which includes two GAF domains (GAF-A and GAF-B) but vary in their amino termini, which is responsible for their different subcellular localisation (Lugnier, 2006). GAF-A and GAF-B are responsible for the dimerization and cGMP binding (Martinez et al., 2002) (Fig. 3.1). In the heart, although PDE2A is only a small fraction of total PDE activity, it is a key player in the sympathetic regulation of cardiac function (Mongillo et al., 2006). This was demonstrated by measuring cAMP levels in live cells using fluorescent probes. In basal conditions, inhibition of PDE2 only generated a minimal increase in cAMP, however, this became significantly higher when the inhibition of PDE2 was preceded by β-adrenergic stimulation with norepinephrine, proving an effect of PDE2 in the catecholaminergic regulation of the heart. Additionally, global genetic ablation of PDE2A results in high embryonic lethality past E17.5–E18.5 dpc, indicating that this enzyme is involved in vital biological functions (Stephenson et al., 2009).

Even though the three isoforms show different subcellular localisation, their function is not redundant. Therefore, I sought to further characterise the specific function of one particular

isoform, PDE2A2. This isoform selectively localises to the outer mitochondrial membrane (MOM) (Monterisi et al., 2017), where it regulates some mitochondrial functions, such as mitochondrial dynamics and mitophagy (Lobo et al., 2020).

PDE2 activity and expression are increased in the failing human hearts both at RNA and protein level(Mehel et al., 2013; Kamel et al., 2023), in isoproterenol induced heart failure rat (Kaumann et al., 2009; Mehel et al., 2013) and in hypertrophied mouse myocytes after pressure overload and isoproterenol treatment, with a reversed effect on left ventricular (LV) hypertrophy, LV dilation, contractility and fibrosis observed with BAY 60-7550 treatment (Baliga et al., 2018). In line with these findings, PDE2 upregulation was shown have pro-hypertrophic effects, and PDE2 inhibition with BAY 60-7550 counteracted cardiomyocyte growth by inducing PKA-mediated phosphorylation of the nuclear factor of activated T cells (NFAT), thereby blocking the activation of the hypertrophic gene program (Zoccarato et al., 2015).

In paradox with these findings, PDE2A activation has also been suggested to have a cardioprotective effect. Increased PDE2A results in reduced β-adrenergic induced hypertrophic remodelling (Mehel et al., 2013). Additionally, cardiac PDE2-transgenic mice, in which chronically increased enzyme activity was shown to be protective against catecholamine-induced ventricular tachycardia and cardiac dysfunction following myocardial infarction (Vettel et al., 2017). In line with these findings, gene therapy with PDE2A overexpression leads to enhanced cardiac function and a reduction in arrhythmic events (Pavlaki et al., 2024). Another study employed gene therapy to acutely increase PDE2A activity which resulted in limited adverse left ventricular remodelling, reduced fibrosis, and decreased susceptibility to ventricular arrhythmias (Kamel et al., 2023). Whether inhibition of activation of PDE2A is beneficial in heart failure remains controversial. This paradox may be attributable to differences in the PDE2A isoforms expressed, and highlights the need to gain a more comprehensive knowledge of this enzyme. This highlights how, even though some advances have been made in understanding this isoform's role and function, the exact biology of cAMP nanodomains regulated by PDE2A2 is yet to be fully characterised.

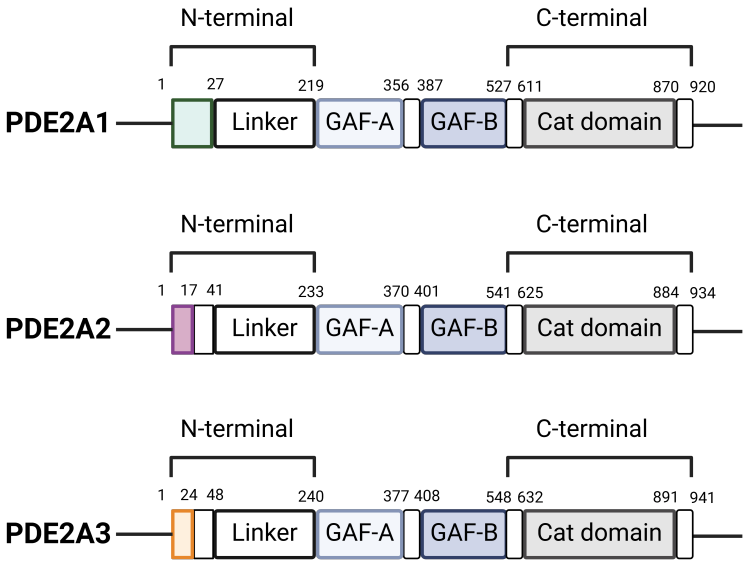


Figure 3.1. PDE2A isoforms. Schematic representation of PDE2A protein domains and differences among each isoform. Different colour at the N-terminal region represents a different aminoacidic sequence. Adapted from Dr Miguel Lobo's DPhil thesis, 2018.

3.2 Aims

The aim of this chapter is to identify and validate some of the putative interactions of PDE2A2 that arose from mass spectrometry analysis. Identification of proteins for validation is described in section 3.3; validation of interactions with proteins located at the mitochondria is described in section 3.4, while 3.5 focuses on validating interactions with proteins that do not localise at the mitochondria, but are still involved in cellular energy metabolism or substrate trafficking.

3.3 Identification of potential PDE2A2 interactors

In order to characterise the role of PDE2A2 dependent cAMP nanodomains, I used data generated by three independent mass spectrometry (MS) experiments from our lab (Subramaniam et al., 2023). Here, adult rat ventricular myocytes (ARVMs) were infected with adenoviral vectors encoding PDE2A2-RFP or RFP. The RFP immunoprecipitations

were analysed by MS which returned a list of possible interactors of the different PDEs. These interactors of PDE2A2 were analysed in conjunction with the phosphopeptides upregulated on inhibition of PDE2 using STRING for network analysis (Subramaniam et al., 2023). A map of PDE2A2 interactors projected onto the structure of a cardiac myocyte reveals several sub-networks at different sites where PDE2A2-dependent cAMP nanodomains may be present (Fig. 1.1).

Given the presence of PDE2A2 at the mitochondria (Acin-Perez et al., 2011; Rinaldi et al., 2018; Monterisi et al., 2017), and the high number of putative interactors from the MS analysis which are proteins involved in trafficking metabolic substrates, I hypothesised that PDE2A2 plays a role in transporting energy substrates. I initially concentrated on validating the interactions with proteins localised at the mitochondria. Due to the relevance of additional putative interactors involved in cellular energy production, I extended my work to include these as well. A list of the putative interactors is summarised in Table 3.1. The protein nomenclature is as defined by the human gene nomenclature (HGNC), mouse genome informatics (MGI) and rat genome (RGD) databases.

Protein Name	Alternative name	Statistical significance	Fold Change	No. of unique peptides	Sequence coverage [%]	Mol. Weight [kDa]
CPT1A	/	4.84	4.48	10	17.5	88
CPT1B	/	4.27	3.22	16	20.9	88
SLC25A20	CACT	5.68	7.38	1	3.7	33
SLC27A1	FATP1	3.58	6.27	11	24.6	71
SLC27A4	FATP4	6.11	9.91	6	13.4	72
SLC25A11	/	2.11	3.54	10	33.4	34
SLC25A4	ANT1, AAC1	5.15	4.62	2	6.2	38
SLC2A1	GLUT1	1.45	5.53	3	5.9	53
MPC2	SLC54A2	2.94	2.9	5	33.9	14
SLC16A1	MCT1	3.9	2.9	5	8.3	53

Table 3.1. PDE2A2 putative interactors identified through PDE2A2-RFP immunoprecipitation and MS analysis selected for further validation.
MS data for the indicated proteins from the PDE2A2 immunoprecipitate. The columns indicate:
Protein name: name defined by the human gene nomenclature (HGNC), mouse genome informatics (MGI) and rat genome (RGD) databases.
Alternative name: other common names used to refer to that protein.
Statistical Significance: -LOG(P value) from *t* test analysis (the higher the more significant) using RFP alone as control. Significance thresholds are [FDR] (false discovery rate) set at 0.05, and S-zero [S0](fold-change threshold) set at 1.3.
Fold change: fold change compared to the control, RFP IP.
Number of unique peptides: unique peptides (peptide whose amino acid sequence is specific to only one protein) identified by MS. The more unique peptides, the higher the confidence of interaction.
Sequence coverage: proportion of the protein's amino acid sequence identified through the detection of peptides in the MS. The higher the % the more sequence was detected.
Molecular weight: molecular weight of the protein.

3.4 Mitochondrial hits

I validated interactions by coimmunoprecipitation. Unless stated otherwise, human embryonic kidney 293T (HEK293T) cells were used. This cell line was chosen because

of its high efficiency of transduction, robustness and results reproducibility. Cells were infected with adenoviral vector encoding the fusion protein PDE2A2-RFP or RFP alone, or transfected with the respective plasmids. RFP alone and/or non-infected transfected cells were used as control. Protein complexes were immunoprecipitated with anti-RFP nanobody conjugated to agarose beads (RFP-Trap). The lysates were probed with an anti-RFP antibody to confirm the presence of the fusion proteins, and with a specific antibody to detect the endogenous interactors of interest.

3.4.1 The carnitine palmitoyl transferase shuttle

Under normoxic conditions, fatty acids are the main fuel of the heart, with 70%- 90% of the mitochondrial ATP being generated in the mitochondrial matrix through β-oxidation (Neely et al., 1972). In the cytosol, fatty acids are esterified by long-chain acyl Co-A synthetases (ACSL1) to produce acyl-CoAs (Lobo et al., 2009). Long-chain Acyl-CoAs are then converted into acyl-carnitine and shuttled into the mitochondria through the carnitine palmitoyl transferase shuttle. This consist of three elements, I)CPT1(Carnitine palmitoyl-transferase 1), II)SLC25A20, and III) CPT2 (Carnitine palmitoyl-transferase 2). These mediate the fatty acids translocation from cytosol to the matrix, where they enter the citric acid cycle to produce ATP, CO2 and the reducing equivalent NADH2 (Neely et al., 1972).

3.4.1.1 Carnitine palmitoyl-transferase 1 (CPT1)

CPT1 is located at the MOM and is expressed as three different isoforms with different tissue distribution. CPT1A is mainly expressed in the liver, CPT1B in the heart, and CPT1C in the brain (McGarry et al., 1978).

CPT1 topography consists of i) two transmembrane domains (TMD), a N- and a C-terminal, which both protrude on the cytosolic side of the mitochondrial outer membrane, and ii) a short loop region, connecting the two TMD, which protrudes into the mitochondrial intermembrane space (Fraser et al., 1997) (Fig. 3.2).

Since both CPT1A and CPT1B scored highly in the MS analysis, I performed

coimmunoprecipitation experiments to assess whether PDE2A2 interacts with both isoforms of CPT1.

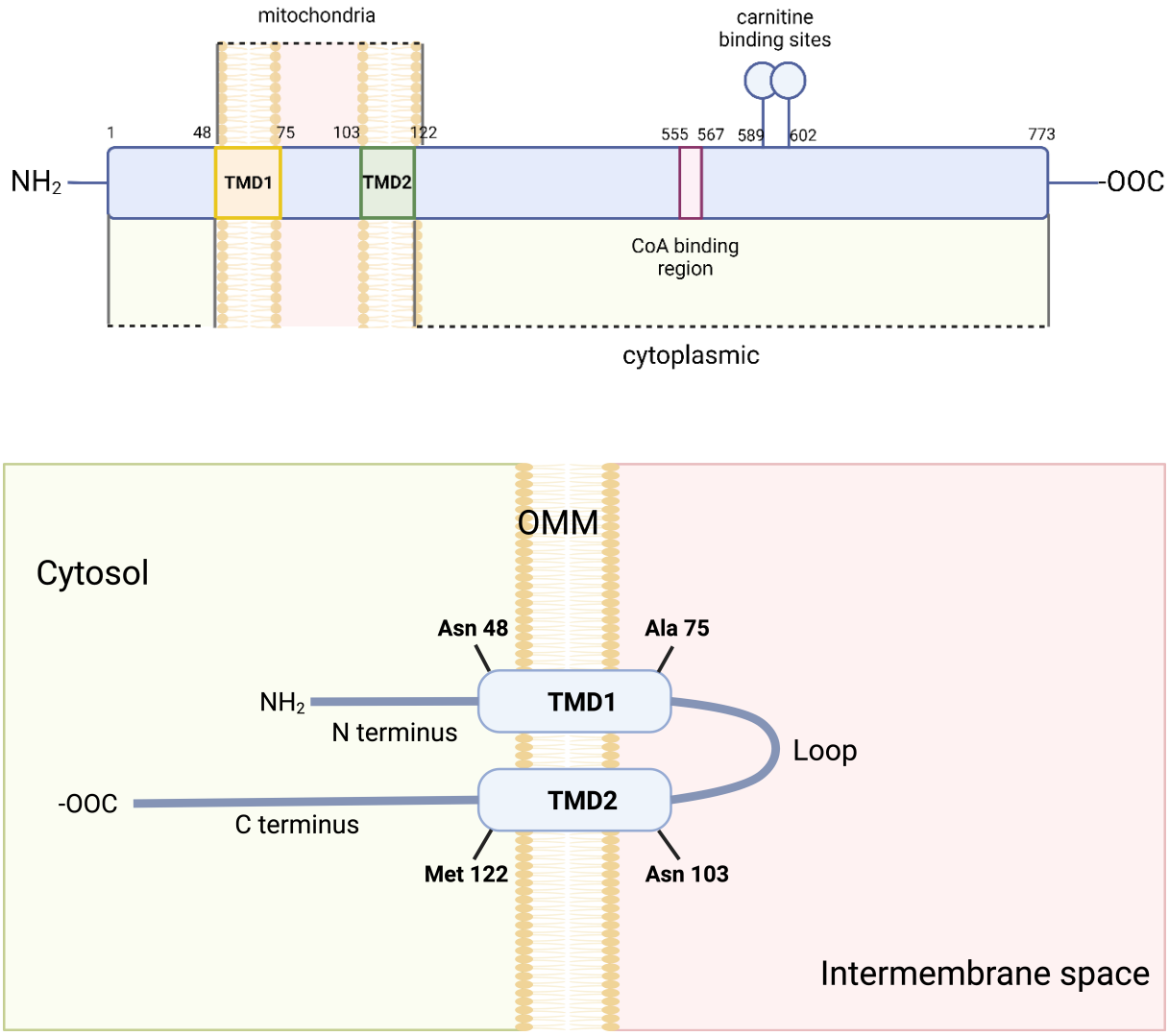


Figure 3.2. Schematic representation of CPT1 topology. The main features of the topology of CPT1 are two transmembrane domains (TM1 and TM2). One TMD with N_{cyto}-C_{MIS} orientation (cyto= cytosolic, MIS= inner mitochondrial space), and one with both the N- and C- termini of the protein are exposed on the cytosol. The loop region protrudes into the inner mitochondrial space. Adapted from Fraser et al. (1997) and from Liang (2023). Drawn with Biorender.

3.4.1.2 CPT1A

HEK293T cells were infected with adenoviral vector encoding either the fusion protein PDE2A2-RFP or RFP alone, used as control, as well as non-infected cells (NI). The specificity of the CPT1A antibody to detect endogenous protein was confirmed by western

blot with whole cell lysate (WCL), where a band of the expected size (86 kDa) was observed (Fig 3.3a). For this experiment, anti-RFP and anti-CPT1A antibodies probed the same membrane concomitantly. PDE2A2-RFP expression in infected cells was confirmed by western blot, as shown by the band at 150 kDa. The RFP control however is not detected in the WCL (Fig. 3.3a, left panel). This could be due to the strong signal of other nearby bands overcoming the RFP signal, or poor expression of the RFP protein. Protein complexes immunoprecipitated with RFP nanobody conjugated beads contained endogenous CPT1A (Fig. 3.3a, right panel). CPT1A also interacted strongly with the two other isoforms of PDE2A2 expressed in the heart: 2A1 and 2A3 (Fig. 3.3b). PDE2A1, 2A2 and 2A3 differ in their amino terminal region (Fig. 3.1); the fact that all PDE2A isoforms interact with CPT1A and CPT1B, suggests that the site of interaction does not involve the PDE2A N-terminus. It is worth noticing that the expression level of the different constructs varies.

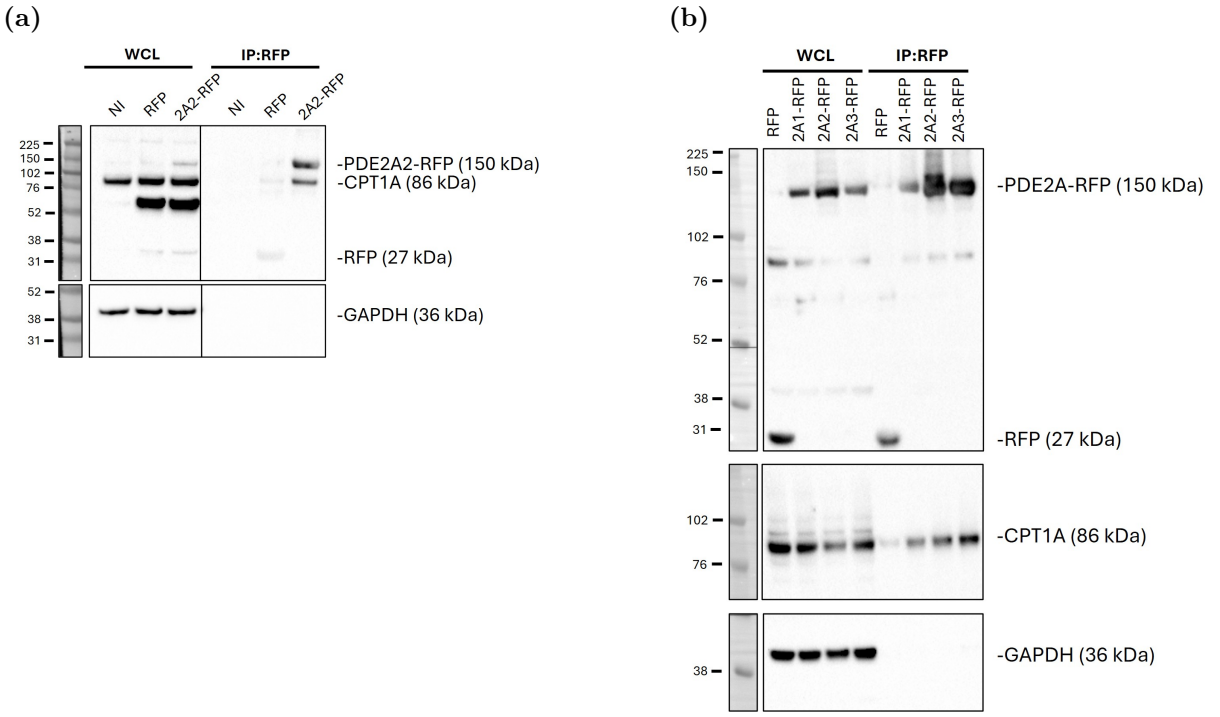


Figure 3.3. PDE2A2 interacts with CPT1A. Detection of endogenous CPT1A after PDE2A2-RFP or RFP immunoprecipitation in HEK293T cells infected with PDE2A2-RFP or RFP.
(a) Detection of endogenous CPT1A after PDE2A2-RFP immunoprecipitation in HEK293T cells infected with PDE2A2-RFP. RFP immunoprecipitation from RFP and non-infected cells used as controls. N=3.
(b) Detection of endogenous CPT1A after immunoprecipitation of each PDE2A isoform in HEK293T cells infected with PDE2A-RFP isoforms. N=3

3.4.1.3 CPT1B

Having validated CPT1A interaction, I moved to the cardiac specific isoform CPT1B. I validated the interaction in human induced pluripotent stem cell cardiomyocytes (hiPSC-CM), a more physiologically relevant model as I am primarily interested in investigating the role do PDE2A2 in the heart. hiPSC-CM were infected with PDE2A2-RFP or with RFP as a control. The specificity of the CPT1B antibody for the endogenous protein was tested by western blot on WCL, which revealed a band at the expected size (75-85 kDa). Immunoprecipitation of RFP confirms interaction of PDE2A2 with endogenous CPT1B (Fig. 3.4a). This interaction is recapitulated in neonatal rat ventricular myocytes (NRVM) (Fig. 3.4b).

As for CPT1A, CPT1B interacts with all the PDE2A isoforms, as shown by PDE2A-RFP pull-downs in NRVM (Fig. 3.4c). It is worth noticing that the expression level of the different constructs varies.

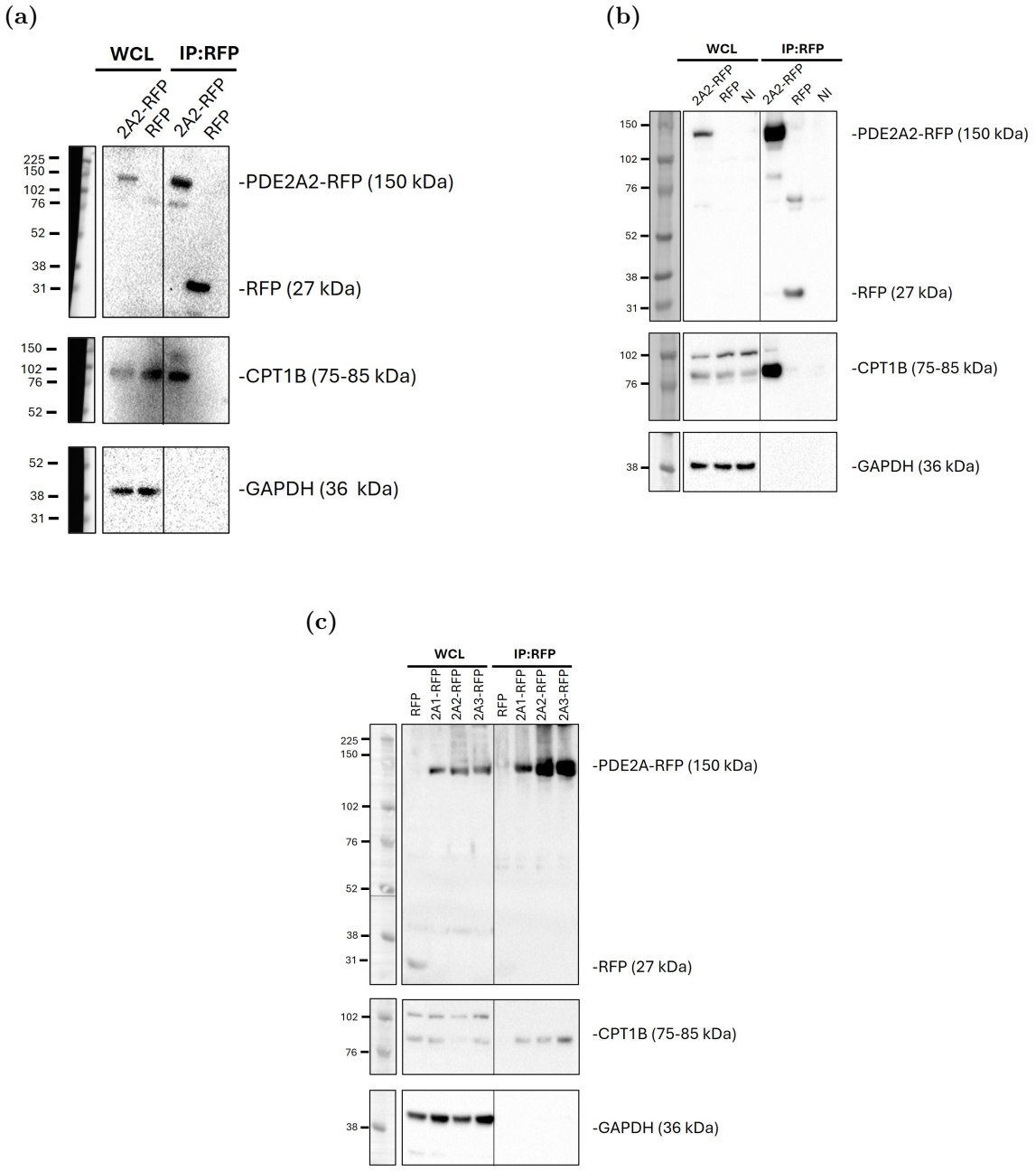
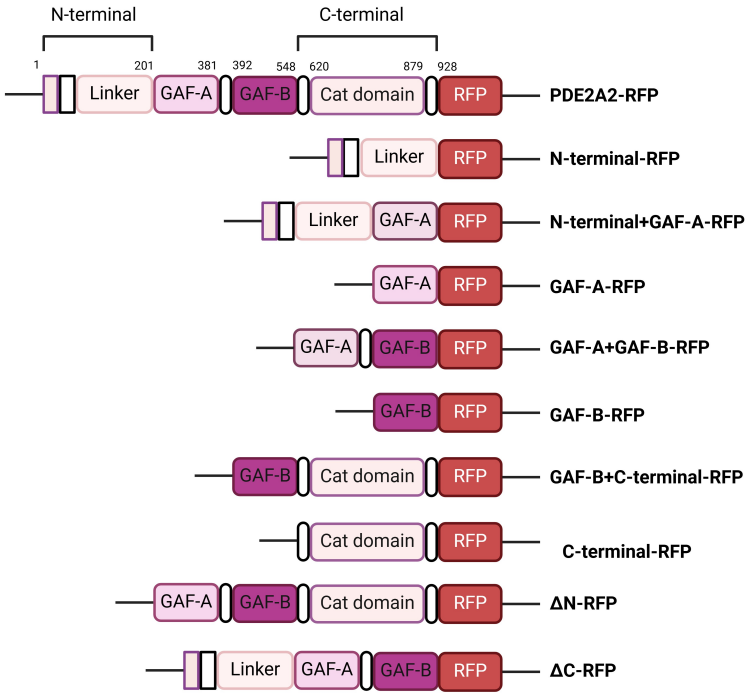


Figure 3.4. PDE2A2 interacts with CPT1B. Detection of endogenous CPT1B after PDE2A2-RFP or RFP immunoprecipitation.
(a) Detection of endogenous CPT1B after PDE2A2-RFP immunoprecipitation in hIPSC cells infected with PDE2A2-RFP. RFP immunoprecipitation from RFP cells used as controls. N=3 from 3 independent differentiations.
(b) Detection of endogenous CPT1B after PDE2A2-RFP immunoprecipitation in NRVM infected with PDE2A2-RFP. RFP immunoprecipitation from RFP or non-infected cells used as controls. N=3
(c) Detection of endogenous CPT1B after immunoprecipitation of each PDE2A isoform in NRVM infected with PDE2A-RFP isoforms. N=3

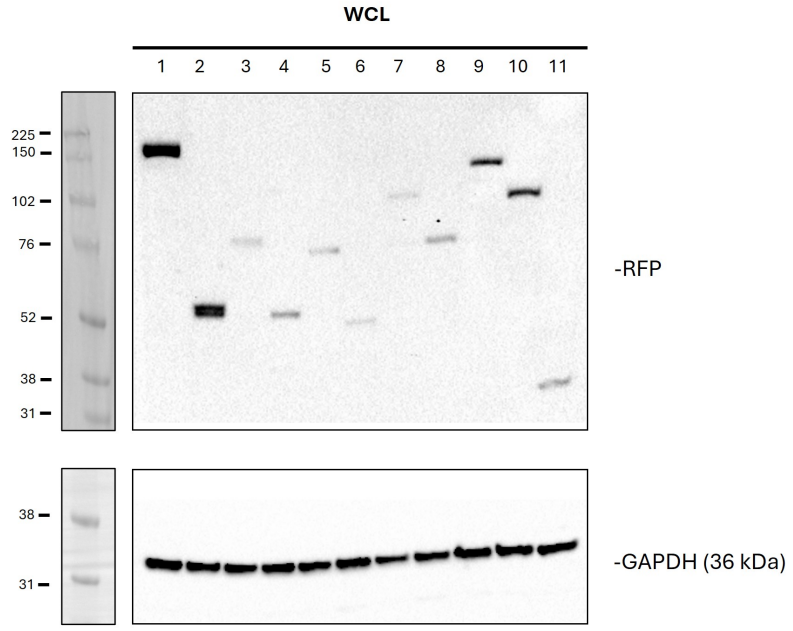
3.4.1.4 PDE2A2 interacts with CPT1B through the GAF domains

Coimmunoprecipitation experiments with the PDE2A isoforms suggested that the location of interaction with CPT1B does not involve the N-terminus of PDE2A2 (Fig. 3.4c). To characterise which PD2A2 domain is involved in the interaction, I co-overexpressed a construct encoding for CPT1B-FLAG fusion protein with plasmids expressing different fragments of PDE2A2-RFP, which had been previously generated in the lab (Fig. 3.5a)(Lobo et al., 2020). Expression of all fragments was confirmed by western blot analysis of HEK 293T cell lysate probed with anti-RFP antibodies (Fig. 3.5b). Subsequently, I performed western blot analysis of protein complexes immunoprecipitated with anti-RFP conjugated beads from cell lysates obtained from HEK293T cells co-expressing PDE2A2-RFP fragments with CPT1B-FLAG and probed with either anti-RFP or anti-FLAG antibodies. The results in Fig. 3.6 show that CPT1B does not interact with the N-terminal, the catalytic domain nor the C-terminal of PDE2A2. The strongest interaction is observed with the GAF-A domain, followed by the GAF-B domain. This suggest that both GAF domains are involved in CPT1B/PDE2A2 interaction, and that GAF-A is the minimal requirement for the interaction to take place. It is worth noticing that the expression level of the different constructs varies.

(a)



(b)



1. PDE2A2-RFP
2. N-terminal-RFP
3. N-terminal+GAF-A-RFP
4. GAF-A-RFP
5. GAF-A+GAF-B-RFP
6. GAF-B-RFP
7. GAF-B+C-terminal-RFP
8. C-terminal-RFP
9. ΔC-terminal-RFP
10. ΔN-terminal-RFP
11. mRFP

Figure 3.5. GAF-A domain is required for the interaction between PDE2A2 and CPT1B.
(a) Illustration of the PDE2A2-RFP constructs generated in the lab.
(b) Detection of PDE2A2-RFP fragments expressed in HEK293T cells. N=3

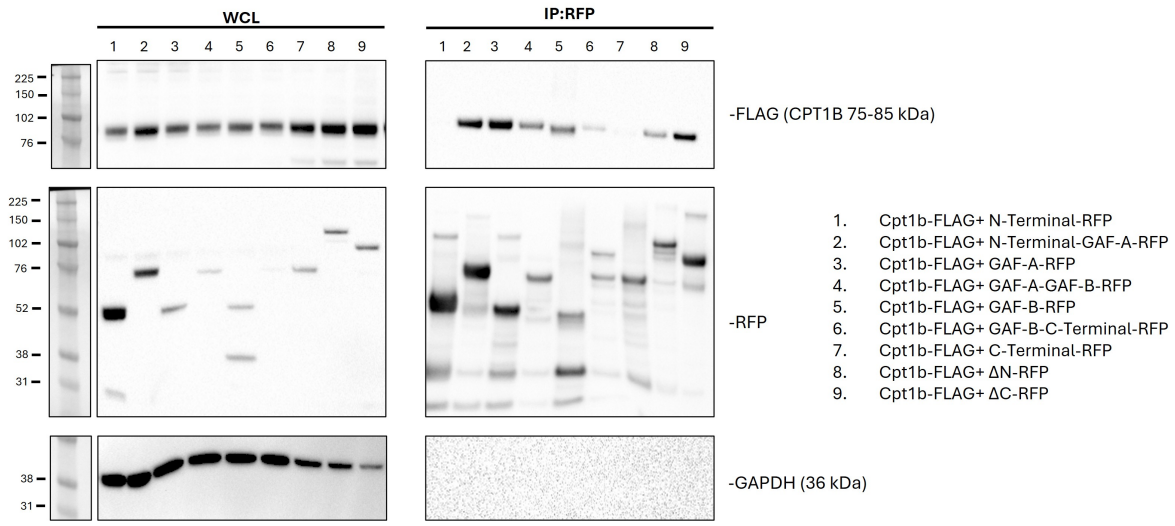


Figure 3.6. Detection of CPT1B-FLAG after PDE2A2-RFP fragment immunoprecipitation in HEK 293T cells transfected with PDE2A2-RFP constructs and CPT1B-FLAG. RFP immunoprecipitation of mRFP was used as a negative control. N=4

3.4.2 SLC25A20

SLC25A20, or carnitine-acylcarnitine translocase, transports long-chain acylcarnitine across the mitochondrial inner membrane towards CPT2, for them to then enter the citric acid cycle (Kodde et al., 2007).

To confirm the putative interaction between PDE2A2 and SLC25A20 suggested by MS analysis, I performed coimmunoprecipitation experiments. Firstly, I attempted to detect endogenous SLC25A20 in RFP immunoprecipitation from HEK293T cells infected with PDE2A2-RFP (Fig. 3.7 a). I was not able to detect any SLC25A20 in either the RFP immunoprecipitation or in the input, which suggests that the endogenous level of the protein was below the antibody detection limit. Since SLC25A20 shows high protein expression in heart muscle (*human protein atlas*, 2025), I repeated the experiment in NRVM, overexpressing the three different PDE2A isoforms, 2A1, 2A2 and 2A3. Even in this model, I failed to detect endogenous SLC25A20 (Fig. 3.7 b). It is worth noticing that the expression level of the different constructs varies.

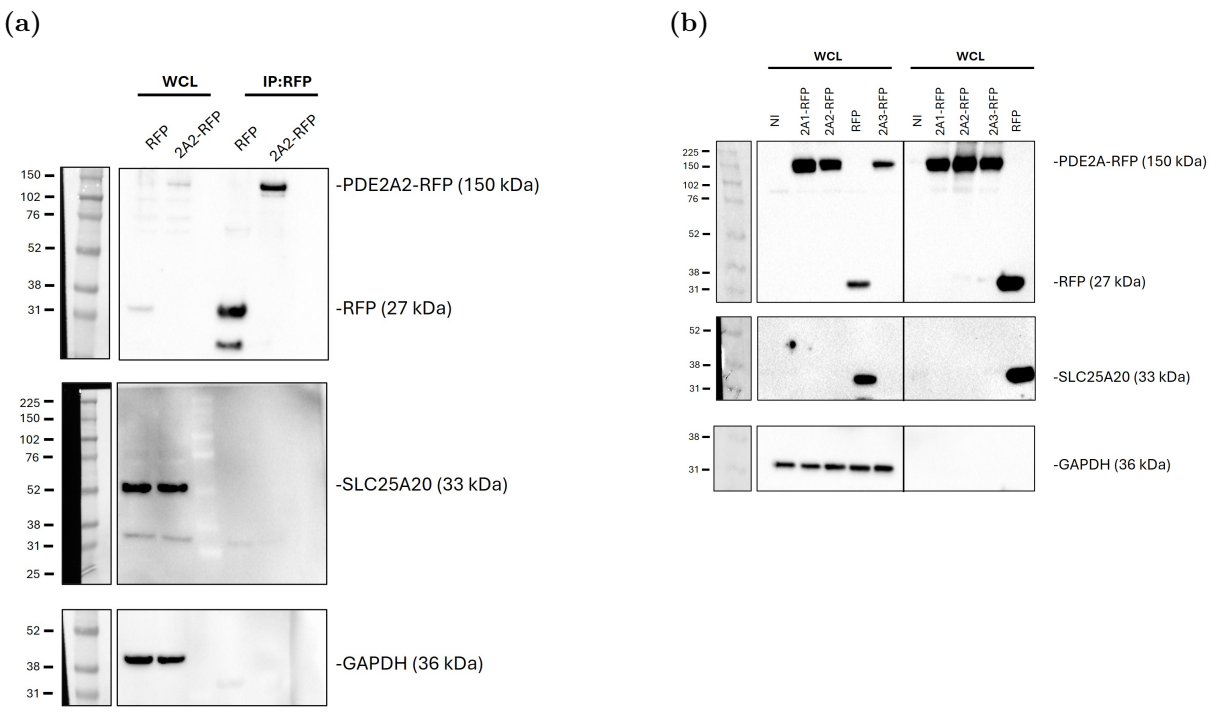


Figure 3.7. Antibodies fail to detect endogenous SLC25A20. PDE2A2-RFP or RFP immunoprecipitation was probed with SLC25A20 antibodies to attempt the endogenous protein. These fail to reveal a band at the expected molecular weight (33 kDa) in both (a) HEK293T, N=3 and (b) NRVM. N=1

Since SLC25A20 localises at the inner mitochondrial membrane, I performed coimmunoprecipitation experiments from a mitochondrial fraction rather than the whole cell lysate. I performed protein fractionation followed by coimmunoprecipitation of PDE2A2-RFP in HEK293 cells infected with PDE2A2-RFP (Fig. 3.8). To confirm the purity of the fractions, I probed the membranes for cytosolic and mitochondrial proteins respectively. The cytosolic protein GAPDH was detected only in the cytosolic fraction, and the mitochondrial protein TOM20 was detected only in the mitochondrial fraction (Fig. 3.8). α-tubulin was detected both in the cytosolic and the mitochondrial fraction, which suggests that the mitochondrial fraction might not be completely clean. As expected, endogenous SLC25A20 is observed in the mitochondrial fraction input (proving that the antibody is able to detect the endogenous protein), and not in the cytosolic one. PDE2A2-RFP is present in the mitochondrial fraction, confirming PDE2A2 mitochondrial localisation as previously published (Acin-Perez et al., 2011; Monterisi et al., 2017; Rinaldi

et al., 2018), however, RFP immunoprecipitation still fails to confirm PDE2A2 and SLC25A20 interaction (Fig. 3.8).

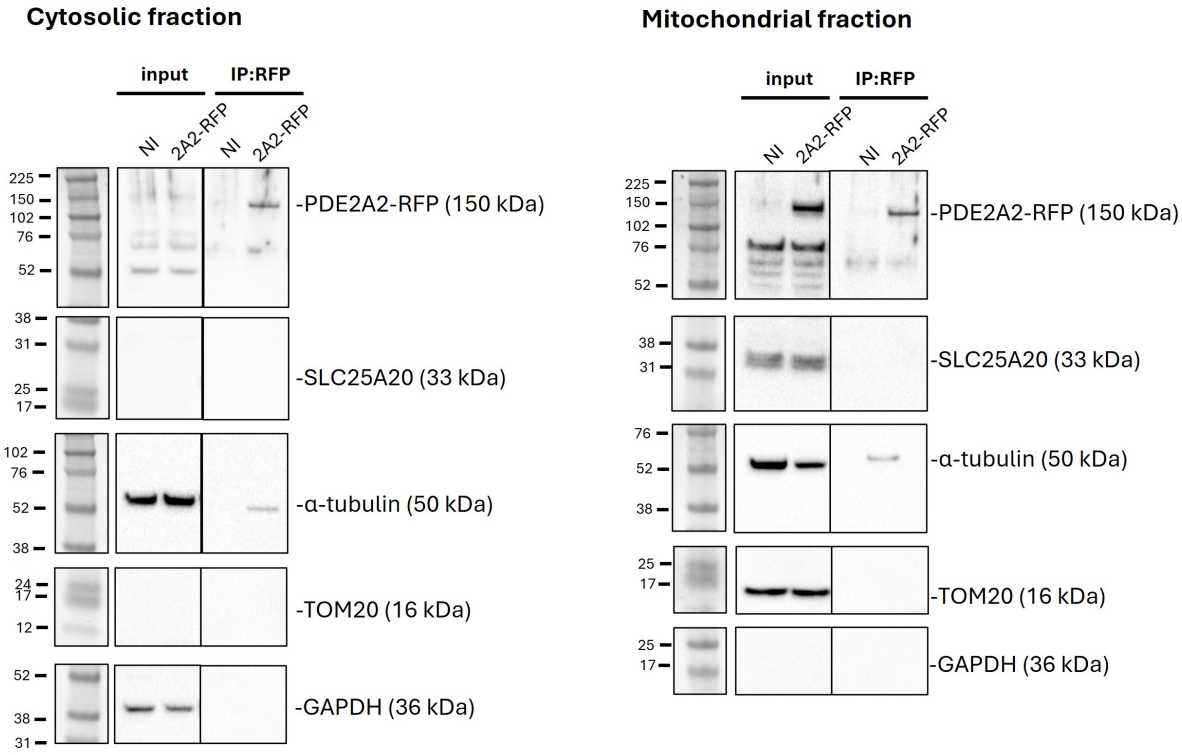


Figure 3.8. Endogenous SLC25A20 is detected in mitochondrial fractions. (left panel) Cytosolic fraction of HEK293T cells transfected with PDE2A2-RFP does not show endogenous SLC25A20. α -tubulin is detected, as well as GAPDH, used as cytosolic markers. (right panel) Endogenous SLC25A20 is detected in the mitochondrial fraction in the input, however it is not present in the RFP immunoprecipitation. TOM20, used as mitochondrial marker, is detected in the mitochondrial fraction. GAPDH is not revealed, but α -tubulin is, indicating the fractionation might not be completely clean. N=1

HEK293T cells were therefore co-transduced with PDE2A2-RFP and SLC25A20-FLAG. As Fig. 3.9 shows, both proteins are detected in the RFP immunoprecipitation, validating the interaction between PDE2A2 and SLC25A20. It is important to note that co-overexpressing both proteins may force the interaction to occur, suggesting that this may not happen *in vivo*.

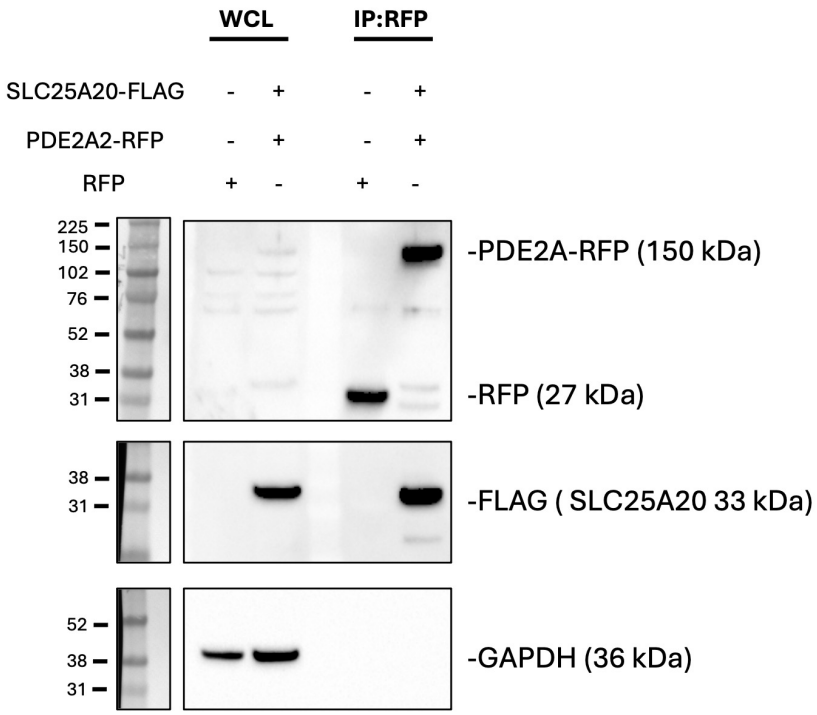


Figure 3.9. SLC25A20 and PDE2A2 interact when both overexpressed. HEK293T cells transduced with SLC25A20-FLAG and PDE2A2-RFP show presence of both proteins in RFP immunoprecipitate, indicating the proteins are able to interact. N=3

3.4.3 SLC25A

The SLC25 family of proteins is also referred to as the mitochondrial soluble carrier protein family. As the name suggests, it includes the transport proteins localised at the mitochondrial membranes. They transport the molecules and ions required for mitochondrial metabolism to occur, linking cytosolic and mitochondrial metabolism (Kunji et al., 2020). The SLC25 family includes 53 proteins, most of which localise to the inner mitochondrial membrane. The mass spectrometry analysis identified SLC25A4 and SLC25A11, two isoforms of this family, as possible interactors of PDE2A2. I performed co-immunoprecipitation experiments to validate this data.

3.4.3.1 SLC25A4

Solute carrier family 25 member 4 is also known as ANT1. At the inner mitochondrial membrane, it imports ADP into the mitochondrion and exports ATP into the intermembrane space, which is confluent with the cytosol (Klingenberg, 2008). The

myocardial energy utilizing processes require rapid and unlimited exchange of adenine nucleotides by SLC25A4 (LaNoue et al., 1986). Because SLC25A4 limits the rate of ADP supplied to the mitochondria and ATP to the cytosol, is possible that this transporter functions as a regulatory site for oxidative phosphorylation (Portman, 2002). To validate the potential interaction between PDE2A2 and SLC25A4, coimmunoprecipitation experiments in HEK293T cells overexpressing PDE2A2-RFP were performed. I confirmed the specificity of SLC25A4 antibody to detect endogenous protein by western blot on WCL, which revealed a band at the expected size (33 kDa) (Fig. 3.10). Results show that SLC25A4 interacts with PDE2A2, as both PDE2A2-RFP and endogenous SLC25A4 are detected in the RFP immunoprecipitation (Fig. 3.10). RFP only infected cells and non-infected cells (NI) were used as controls.

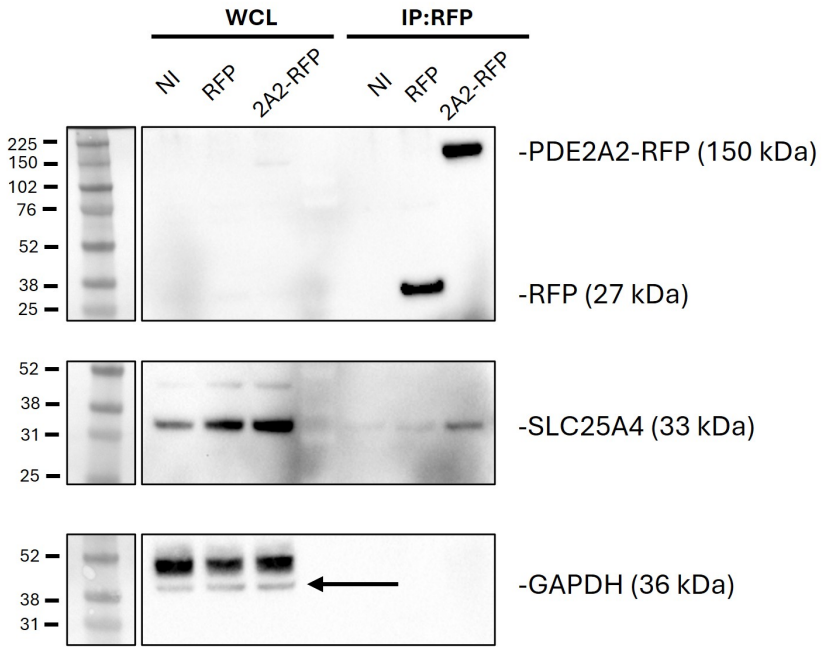


Figure 3.10. PDE2A2 interacts with SLC25A4. Detection of endogenous SLC25A4 after RFP immunoprecipitation in HEK293T cells infected with PDE2A2-RFP, RFP only or non-infected. N=3

3.4.3.2 SLC25A11

The mitochondrial oxoglutarate carrier SLC25A11 (or OGC) exchanges cytosolic malate for 2-oxoglutarate from the mitochondrial matrix. It plays an important role in the malate-aspartate shuttle, the oxoglutarate-isocitrate shuttle, and glucogenesis (Kunji

et al., 2020). To assess the interaction between SLC25A11 and PDE2A2, I performed coimmunoprecipitation experiments in HEK293T cells overexpressing PDE2A2-RFP. Initially, I failed to detect endogenous SLC25A11 in the whole cell lysate (Fig. 3.11 a). It is worth noticing that the expression level of the different constructs varies. Because SLC25A11 expression level in this cell line is very high (Thul et al., 2017), I suspected that the antibody I was using was not performing efficiently. A new antibody efficiently detected endogenous SLC25A11 in the whole cell lysate of HEK293T cells (Fig. 3.11 b). RFP immunoprecipitation of RFP from HEK293T cells overexpressing PDE2A2-RFP, however, failed to validate the interaction between PDE2A2 and endogenous SLC25A11 (Fig. 3.11 c). Due to lack of time, I was unable to attempt coimmunoprecipitation experiments where both proteins are overexpressed.

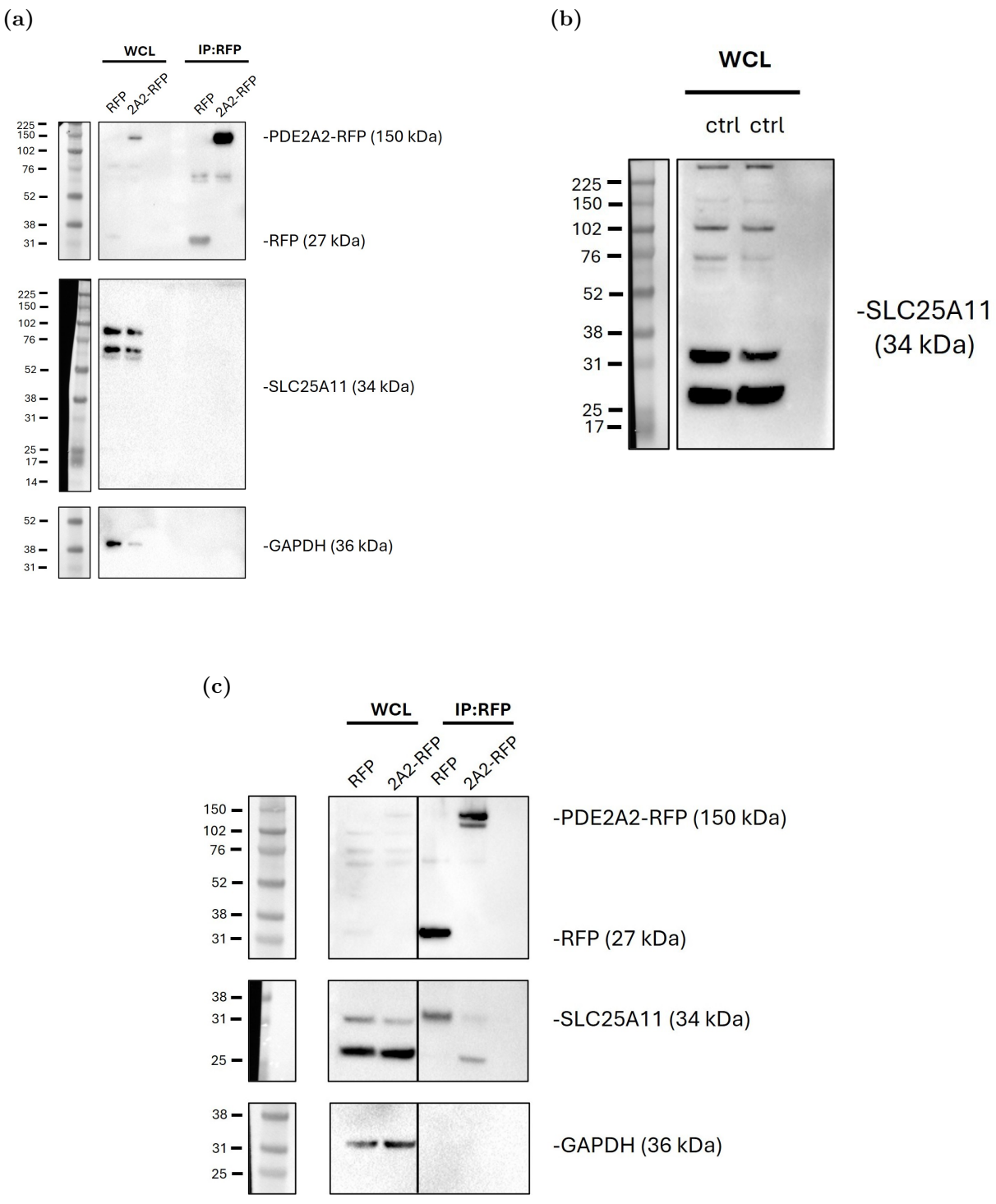


Figure 3.11. Attempt to validate the interaction between PDE2A2 and SLC25A11.
(a) Input and RFP immunoprecipitate probed SLC25A11 fail to reveal a band at the expected molecular weight. Detection of endogenous CPT1B after PDE2A2-RFP or RFP immunoprecipitation. N=3
(b) WCL from HEK293T cells probed with a different antibody detects endogenous SLC25A11. N=1
(c) No specific interaction is detected in RFP immunoprecipitate by SCL25A11 antibody. N=3

3.4.4 MPC2

Even though it relies mainly of fatty acids to satisfy the enormous ATP demand, the heart is metabolically flexible and can switch between different substrates based on their availability (Smith et al., 2018). As a product of glycolysis in the cytosol, pyruvate needs to be transported into the mitochondrial matrix to be fully harnessed to generate ATP (McCommis and Finck, 2023). At the mitochondrial inner membrane, pyruvate is transported by the mitochondrial pyruvate carrier (MPC). Two different groups have identified two proteins, MPC1 and MPC2, as two paralogous subunits composing the heteromeric complex of MPC in mammals (Bricker et al., 2012; Herzig et al., 2012). Recently however, it has been demonstrated that human MPC2 functions independently of MPC1 to induce pyruvate transport (Nagampalli et al., 2018).

MPC2 was identified as a putative interactor of PDE2A2 by the MS analysis. I performed coimmunoprecipitation experiments to confirm this potential interaction.

hiPSC-CM were infected with either PDE2A2-RFP or RFP as a control. The specificity of the MPC2 antibody was confirmed by western blot, with the detection of a band at the expected size (14 kDa) on the WCL (Fig. 3.12 a). Immunoprecipitation of RFP contains both PDE2A2-RFP and endogenous MPC2, confirming the interaction between the two proteins (Fig. 3.12 a). This result is confirmed in NRVM, infected with either PDE2A2-RFP or not infected (NI) (Fig. 3.12 b).

When different PDE2A isoforms were overexpressed in NRVM (2A1-RFP, 2A2-RFP, 2A3-RFP) and RFP was pulled-down, a weaker interaction between 2A1 and 2A3 was detected compared to 2A2 (Fig. 3.12 c). It is worth noticing that the expression level of the different constructs varies.

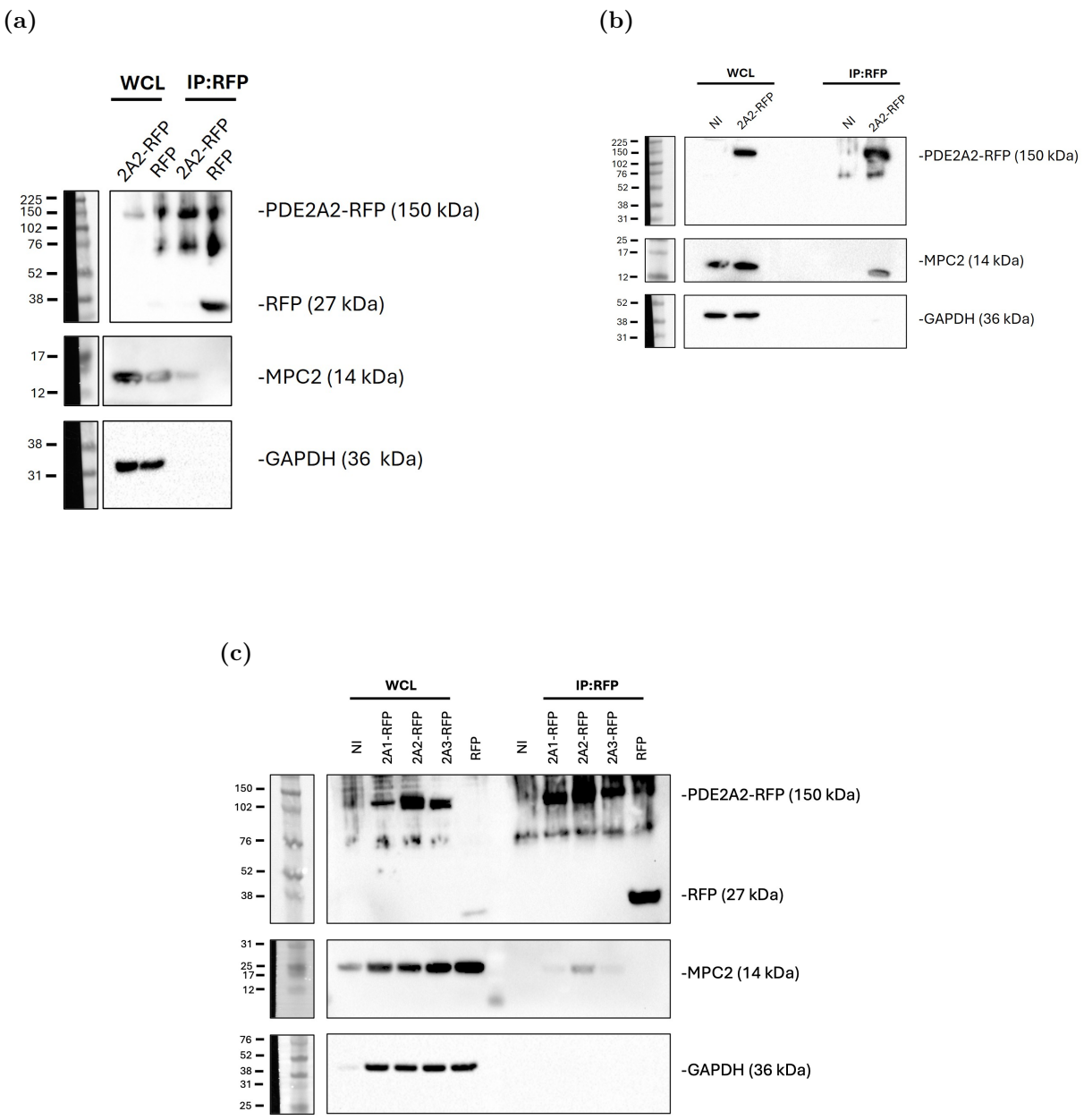


Figure 3.12. PDE2A2 interacts with MPC2. Detection of endogenous MPC2 after RFP immunoprecipitation.
(a) Detection of endogenous MPC2 after PDE2A2-RFP immunoprecipitation in hIPSC cells infected with PDE2A2-RFP. RFP immunoprecipitation from RFP cells used as controls. N=3 from 3 independent differentiations.
(b) Detection of endogenous MPC2 after PDE2A2-RFP immunoprecipitation in NRVM infected with PDE2A2-RFP. RFP immunoprecipitation from RFP or non-infected cells used as controls. N=3
(c) Detection of endogenous MPC2 after immunoprecipitation of each PDE2A isoform in NRVM infected with PDE2A-RFP isoforms. N=3

3.5 Other putative interactors

3.5.1 SLC27A

Long chain fatty acids are an essential source of energy in cardiac metabolism. The journey from substrate in the circulation to ATP released by the mitochondria relies on the action of several transporters along the way (Anderson and Stahl, 2013). Fatty acid transporter proteins (FATPs) are a family of six transporters responsible for the transport of fatty acids from the extracellular space to the cytoplasm (SLC27, solute carrier family 27). The different isoforms have sequence similarities, but differ in tissue expression (Anderson and Stahl, 2013). SLC27A1 and SLC27A4 were identified as possible PDE2A2 interactors by the mass spectrometry analysis (Table 3.1).

3.5.1.1 SLC27A1

SLC27A1 has been reported to localise at the plasma membrane (Schaffer and Lodish, 1994), is present in a variety of tissues, and has been directly linked to long-chain fatty acid transport (Wu et al., 2006). SLC27A1 interacts with ACSL-1, a member of the acyl-CoA synthetase long-chain family, to form a complex (Richards et al., 2006; Zou et al., 2003). I attempted to confirm the interaction between SLC27A1 and PDE2A2. In order to do so, I infected HEK293T cells with a virus encoding PDE2A2-RFP. Probing the whole cell lysate failed to show a specific band at the molecular weight of SLC27A1 (71 kDa), and instead revealed several non-specific bands (Fig. 3.13 a). SLC27A1 antibody also failed to detect the expected band in the RFP (Fig. 3.13 a). I repeated the experiment in NRVM, using the same antibody and observed the same results (Fig. 3.13 b). Therefore, the putative interaction between PDE2A2 and SLC27A1 could not be validated.

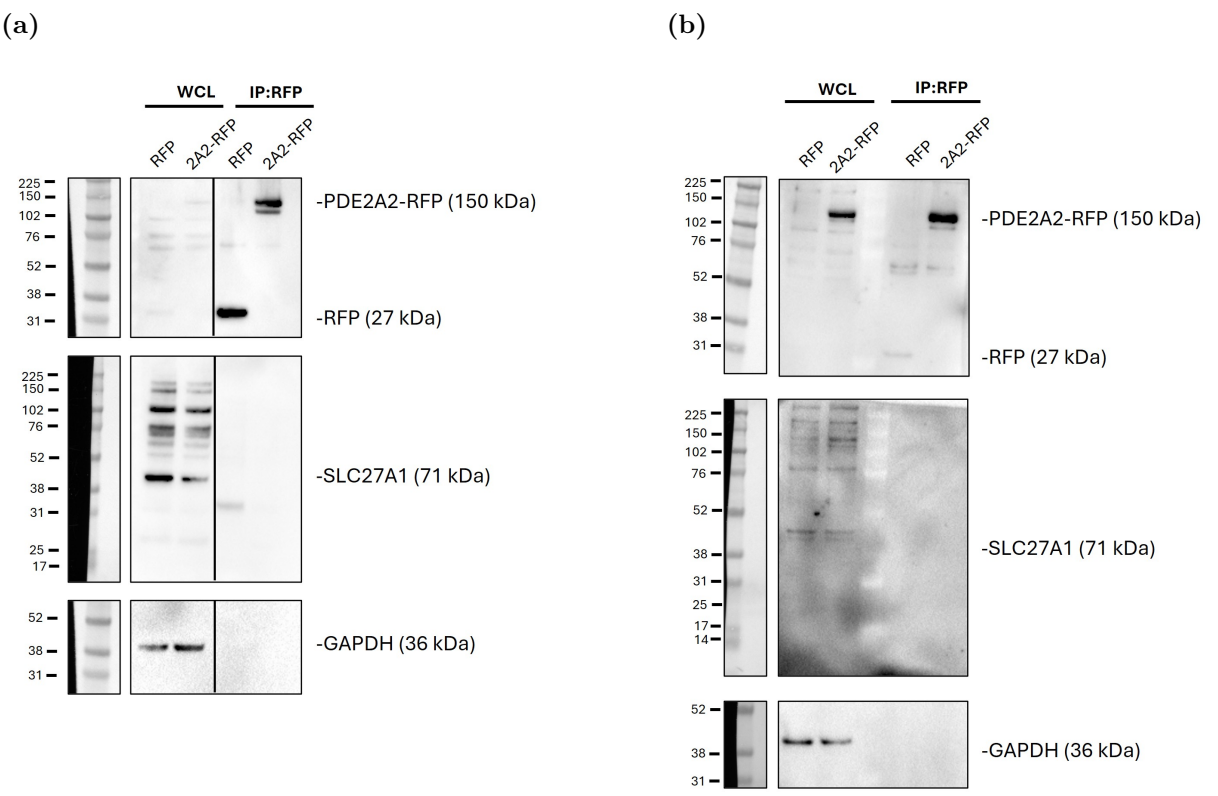


Figure 3.13. Attempt to validate the interaction between PDE2A2 and SLC27A1. Cells infected with PDE2A2-RFP or RFP only. Input and RFP immunoprecipitate probed SLC27A1 fail to reveal a band at the expected molecular weight (71 kDa) in (a) HEK293T and (b) NRVM. N=3

3.5.1.2 SLC27A4

SLC27A4 is not a direct fatty acid transporter but plays a predominant function as a fatty acyl-CoA synthetase (ACS) (Stahl et al., 1999). Unlike the other proteins in the SLC27 family, SLC27A4 has an ER localisation domain (Milger et al., 2006), however, it has also been located at the plasma membrane in intestinal enterocytes (Stahl et al., 1999). This discrepancy has been attributed to the capability of SLC27A4 to translocate, similarly to other solute carrier transporter families (SLC2A) (Stahl et al., 1999). SLC27A4 plays a role in FA transport via ACS-activated vectorial acylation, (Milger et al., 2006) which occurs when exogenous fatty acids are transported across the plasma membrane concomitant with activation to CoA thioesters (Arias-Barrau et al., 2010).

SLC27A4 interacts with PDE2A2-RFP, as demonstrated by coimmunoprecipitation

experiments (Fig. 3.14). HEK293T cells were infected with PDE2A2-RFP or RFP as a control. SLC27A4 antibody specificity to detect endogenous protein was verified by western blot analysis on the WCL, where a band at the expected size (72 kDa) was detected (Fig. 3.14). RFP immunoprecipitation was probed for SLC27A4, and the endogenous protein was detected. Anti-RFP probing confirmed that PDE2A2 is also present in the pull-down, validating the interaction between PDE2A2 and SLC27A4. It is worth noticing that the expression level of the different constructs varies.

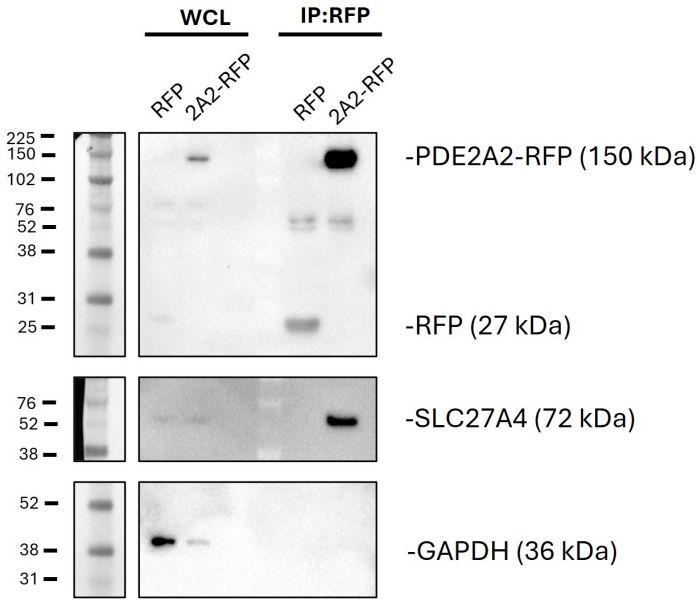


Figure 3.14. PDE2A2 interacts with SLC27A4. Detection of endogenous SLC25A4 in PDE2A2-RFP immunoprecipitation from HEK293T cells infected with PDE2A2-RFP or RFP only. N=3

3.5.2 SLC2A1

Solute carrier protein family 2 member 1, SLC2A1 (also known as GLUT1), is the main transporter involved in cellular uptake of glucose into the cell. It catalyses passive movement of glucose down concentration gradients (Holman, 2020). SLC2A1 availability at the plasma membrane can be regulated by member protein translocation (Holman et al., 1990). SLC2A1 is proposed as a putative interactor of PDE2A2 by the mass spectrometry analysis.

To validate this interaction, coimmunoprecipitation experiments were performed (Fig.

3.15). HEK293T cells were infected with PDE2A2-RFP or RFP only (used as a control) together with lysates from non-infected cells. I confirmed the specificity of SLC2A1 antibody in detecting endogenous protein by western blot on the WCL, which revealed a band at the expected size (40 kDa) (Fig. 3.15). RFP was coimmunoprecipitated with anti-RFP antibody conjugated beads, and it was then probed for PDE2A2 with anti-RFP antibody and for endogenous SLC2A1 with the respective antibody. Both proteins were detected concurrently in the same pull-down, confirming the interaction between PDE2A2 and SLC2A1.

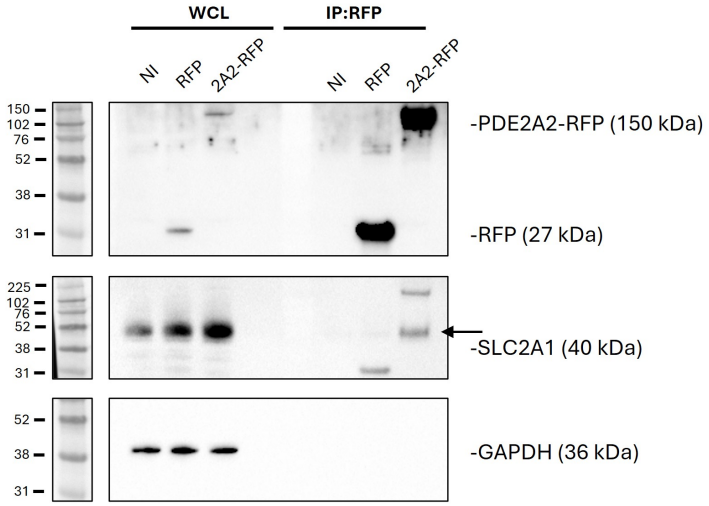


Figure 3.15. PDE2A2 interacts with SLC2A1. Detection of endogenous SLC2A1 in PDE2A2-RFP immunoprecipitation from HEK293T cells infected with PDE2A2-RFP or RFP only. N=3

3.5.3 SLC16A1

Monocarboxylates such as lactate, pyruvate and ketone bodies are trafficked at the plasma membrane by SLC16A1 (also known as MCT1) which transports them into the cytosol (Halestrap, 2013). SLC16A1 catalyses either net transport of one monocarboxylate (i.e. lactate, pyruvate or ketone body) with one proton, or by exchanging one carboxylate for another (Deuticke, 1982). As a transporter of monocarboxylates, SLCA16 plays an important role in cell metabolism, such as aerobic glycolysis and pH homeostasis (Yu et al., 2020). To confirm the putative interaction between this transporter and PDE2A2,

which had been highlighted by MS analysis, coimmunoprecipitation were performed (Fig. 3.16). SLC16A1 ability to detect endogenous protein was tested on WCL through western blot, where a band of the expected molecular weight (43 kDa) was detected (Fig. 3.16). HEK293T cells infected with PDE2A2-RFP or with RFP only (control) were used to derive RFP pull-down. The RFP immunoprecipitation contained PDE2A2 and endogenous SLC16A1. This confirmed the interaction between the two proteins.

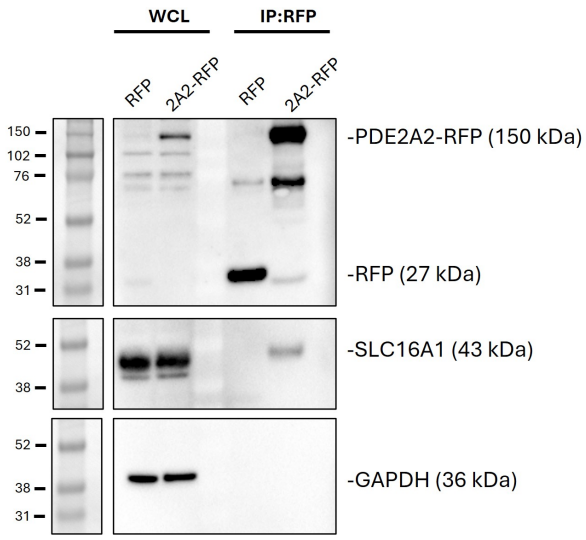


Figure 3.16. PDE2A2 interacts with SLC16A1. Detection of endogenous SLC16A1 in PDE2A2-RFP immunoprecipitation from HEK293T cells infected with PDE2A2-RFP or RFP only. N=3

3.6 A metabolon at the mitochondrial outer membrane

In 1985 Srere coined the word 'metabolon' (Srere, 1985). He defined it as a group of enzymes that organise spatially to form transient protein-protein interactions, creating a supramolecular complex aid at channelling metabolites among the component enzymes. Metabolons mediate 'substrate channelling', so that the reaction intermediates are isolated from the bulk environment surrounding them (Degenring et al., 2004). The postulated advantages of the existence of metabolons include i) local enrichment of metabolite to achieve higher reaction rates, ii) protection of unstable intermediates and

iii) sequestration of cytotoxic metabolites (Laursen et al., 2015; Spivey and Merz, 1989; Rickey and Weilch, 1995). Proposed metabolons for substrate channelling include the tryptophan synthase (Miles, 2001), the glycolytic enzyme metabolon (including enzymes like phosphofructokinase, aldolase, and glyceraldehyde-3-phosphate dehydrogenase (GAPDH) (Menard et al., 2014), and the fatty acid synthase complex (Smith, 1994).

The validation work in this chapter so far corroborates interactions between PDE2A2 and several enzymes involved in substrate trafficking. These proteins are not known to interact with each other, and belong to different pathways: the fatty acid, glucose and pyruvate one respectively.

This raised the question on whether these may form a metabolon-like supramolecular complex wherein enzymes of several metabolic pathways regulate different substrates transport into the mitochondria. I initially concentrated on CPT1A and CPT1B, as these showed the highest statistical significance in addition to high scores for number of unique peptides identified by the MS analysis and sequence coverage (3.

In order to test this hypothesis, I over expressed a construct encoding for CPT1B-FLAG fusion protein in HEK293T cells and immunoprecipitated CPT1B-FLAG. I then probed for proteins that I have demonstrated interact with PDE2A2, and that are known to be part of different metabolic pathways. It has recently been demonstrated that different sub-populations of mitochondria exist, which localise either deep in the cytoplasm or closer to the plasma membrane. It is possible that the metabolon-like complex would form at the latter (Porat-Shliom et al., 2019). Since there are no available antibodies able to detect endogenous PDE2A, HEK293T cells were also transfected with a construct encoding the PDE2A2-GFP or -RFP fusion proteins. Protein complexes were immunoprecipitated with FLAG antibody conjugated beads, then probed with FLAG and RFP antibodies to confirm the presence of the fusion proteins, and with antibodies for the interactor of interest.

Both CPT1B and PDE2A2 were successfully co-expressed and immunoprecipitated (Fig. 3.17 a). SLC27A4 was also detected, albeit weakly, in the FLAG immunoprecipitate, suggesting it interacts with CPT1B when PDE2A2 is overexpressed. Endogenous SLC25A20 is not detected in either the input or the immunoprecipitate (Fig. 3.17

a). Endogenous MPC2 (Fig. 3.17 b) is not detected in the FLAG pull-down samples, suggesting that this protein does not interact. In the same FLAG immunoprecipitation, SLC2A1 and SLC16A1 are detected (Fig. 3.17 b), indicating that CPT1B may interact in the presence of PDE2A2 with these two proteins respectively.

Preliminary data show that SLC25A4 is also present in the FLAG immunoprecipitation from the lysate of HEK293T cells co-transduced with PDE2A2-RFP and CPT1B-FLAG (Fig. 3.17 c). However, this experiment needs to be repeated, as, even though the presence of the PDE2A2-GFP was initially assessed optically on an epifluorescence microscope, the GFP antibody failed to show the respective band at the correct molecular weight (150 kDa).

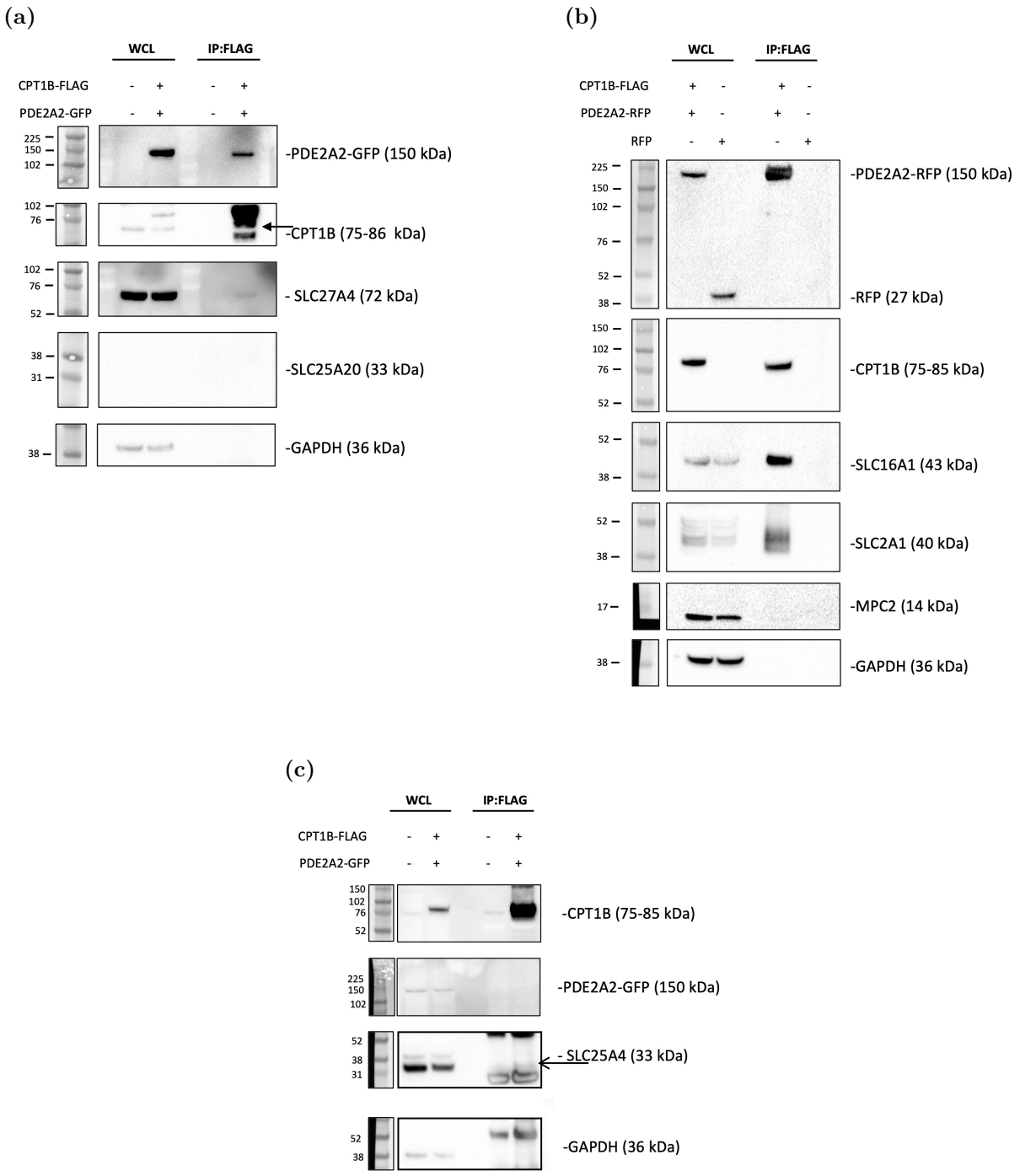


Figure 3.17. CPT1B interacts with proteins involved in the trafficking of different substrates with overexpression of PDE2A2. Detection of endogenous proteins in FLAG immunoprecipitate from HEK293T cells expressing CPT1B-FLAG and PDE2A2.
(a) Detection of endogenous SLC27A4 and attempt to detect SLC25A20. N=3
(b) Detection of endogenous SLC16A1, SLC2A1. MPC2 is not detected in the pull-down. N=3
(c) Detection of endogenous SLC25A4

In order to understand whether these proteins interact with CPT1B only in the

overexpression of PDE2A2, I performed coimmunoprecipitation experiments in HEK283T cells overexpressing CPT1B-FLAG only. In this FLAG immunoprecipitation (Fig. 3.18 a), SLC2A1 is detected, albeit weakly, indicating that its interaction with CPT1B does not require PDE2A2 overepression. This is also true for SLC25A4 (Fig. 3.18 a) as well as for SLC16A1 (Fig. 3.18 b). MPC2 is not detected (Fig. 3.18 b), indicating that this protein is not part of the proposed multiprotein complex.

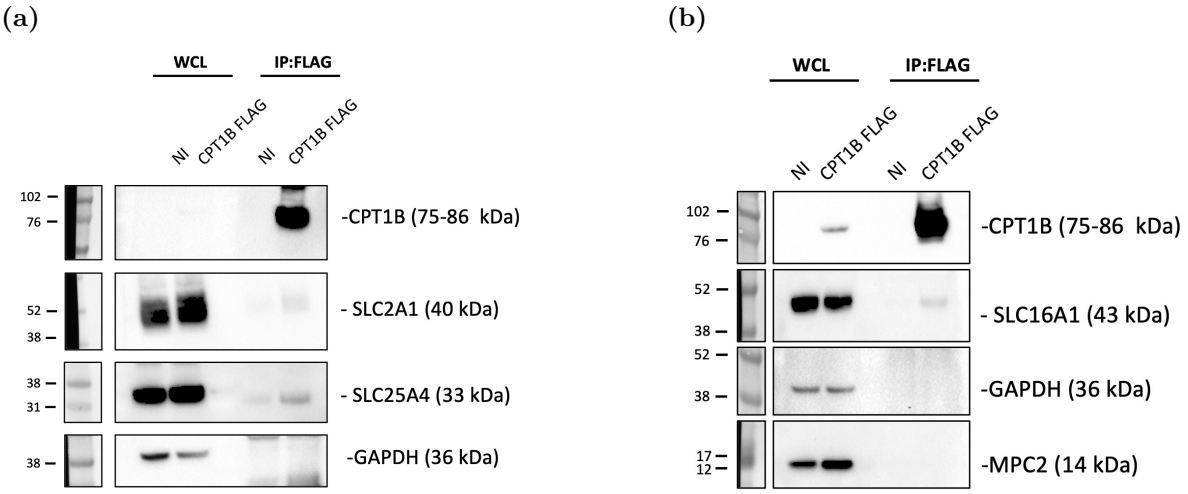


Figure 3.18. CPT1B interacts with proteins involved in the trafficking of different substrates. Detection of endogenous proteins in FLAG immunoprecipitate from HEK293T cells expressing CPT1B-FLAG.
(a) Detection of endogenous SLC2A1 and SLC25A4. N=2
(b) Detection of endogenous SLC16A1. MPC2 is not detected in the pull-down. N=2

3.7 Summary of results and discussion

A summary of all the PDE2A2 interactors tested is shown in Table 3.2. PDE2A2-RFP or PDE2A2-GFP was always overexpressed. A schematic representation of the confirmed interactions is shown in Fig. 3.19.

Protein Name	Result	Validation type	Model
CPT1A	Confirmed	Endogenous	HEK293T
CPT1B	Confirmed	Endogenous	hIPSC, NRVM
CPT1B-PDE2A2 GAF-A/-B	Overexpressed	HEK293T	
SLC25A20	Confirmed	Overexpressed	NRVM, HEK293T
SLC27A1	Not confirmed	Endogenous	NRVM, HEK293T
SLC27A4	Confirmed	Endogenous	HEK293T
SLC25A11	Not confirmed	Endogenous	HEK293T
SLC25A4	Confirmed	Endogenous	HEK293T
SLC2A1	Confirmed	Endogenous	HEK293T
MPC2	Confirmed	Endogenous	hIPSC, NRVM
SLC16A1	Confirmed	Endogenous	HEK293T

Table 3.2. Summary of the PDE2A2 interactors tested.
The table shows a summary of the validation work from this chapter. The name of each protein is included, together with the outcome of the validation; whether the proteins were endogeous or overexpressed; and the model the interaction was tested in.

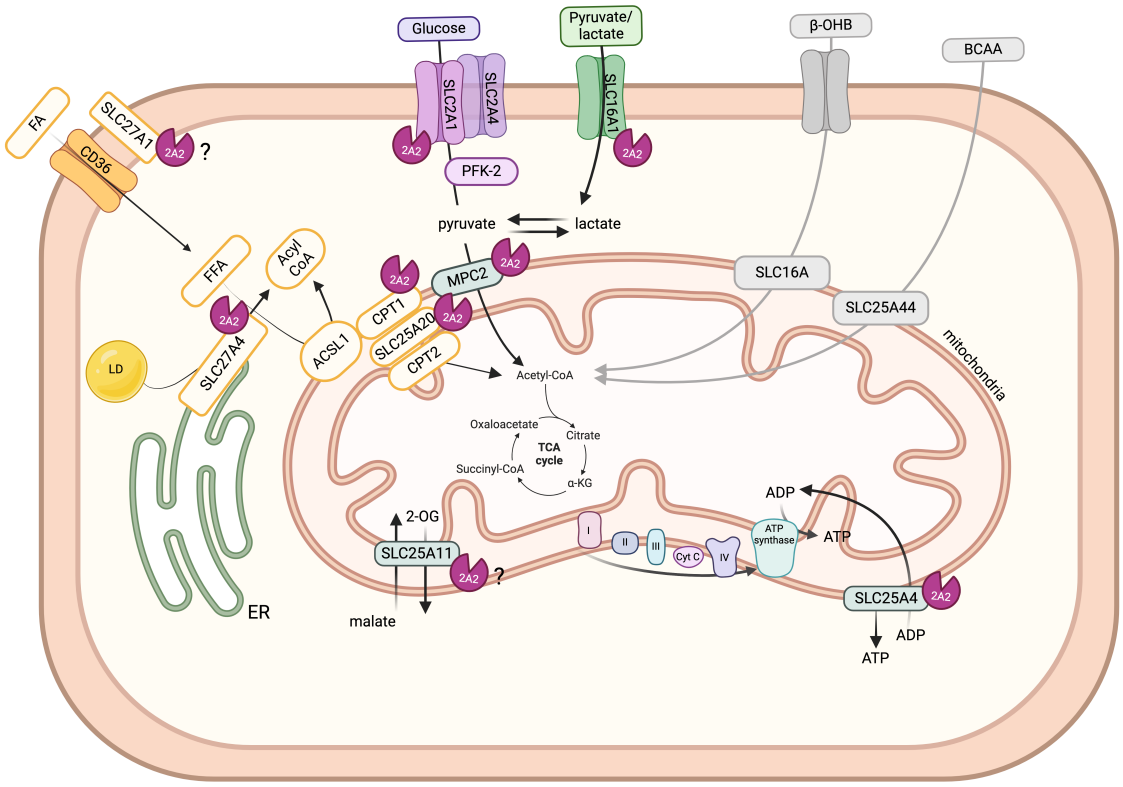


Figure 3.19. PDE2A2 interacts with a number of proteins involved in the trafficking of substrates aid at energy production. Schematic representation of the interactions validated in this chapter. A question mark next to the protein indicates the interaction was not validated experimentally. Drawn with Biorender.

The relationship between cAMP and cellular metabolism has been studied for many years (Ravnskjaer et al., 2016). However, there are aspects of it that are yet to be elucidated. One of them is the regulation by cAMP of the uptake of substrates used for energy production. In this section, I started addressing the question of whether cAMP might regulate the transport of different metabolic substrates into the cell and the mitochondria.

As PDE2A2 localises at the mitochondria, I hypothesise that PDE2A2 may be one of the players in the cAMP dependent regulation metabolites trafficking.

The mass spectrometry analysis performed by the lab on ARVM overexpressing PDE2A2-RFP produced a significant amount of data on putative interactors with the 2A2 isoform. Organising these spatially based on their subcellular localisation outlines potential cAMP domains under the control of PDE2A2 (Fig. 1.1). I initially validated targets localised at

the mitochondria and then ones with elements involved in substrate trafficking.
Validating the interaction between PDE2A2 and these substrate-trafficking proteins could identify a new role of PDE2A2, where it regulates the journey of metabolites aimed at energy production. Additionally, it may provide an avenue for selective displacement, and therefore specific ablation, of PDE2A2 activity at those sites -something that cannot be achieved by pharmacological inhibition, since current inhibitors bind the catalytic site and all PDE2A isoforms share the same catalytic domain. In some experiments the level of expression of the over-expressed constructs appears to vary. As my initial validation was assessing whether an interaction was occurring, the analysis was qualitative only, with a binary outcome of yes/no. However, when quantifying the interaction these data should be taken into consideration, as they can be informative on several aspects of the interaction.

3.7.1 PDE2A2 interacts with elements involved in trafficking FA

The journey of FA from the circulation to the mitochondria relies on the activity of a series of enzymes. Two of these are SLC27A4 and SLC27A1, different isoforms of the SLC27A family. I validated the interaction between PDE2A2 and SLC27A4 (Fig. 3.14). I was not able to validate the interaction of PDE2A2 with SLC27A1. This was due to the inability of the antibodies to detect endogenous proteins in the samples (Fig. 3.13). SLC27A4 localises to the endoplasmic reticulum, where it functions as a fatty acyl-CoA synthetase (ACS), enabling the transport of FA via ACS-activated acylation (Milger et al., 2006).

I also demonstrated that PDE2A2 interacts with elements of the carnitine palmitoyl transferase shuttle, an essential machinery that allows long chain fatty acids to enter the mitochondria. CPT1, located at the MOM, converts acyl-CoA into acyl-carnitines, and shuttles them into the intermembrane space, where they are translocated by SLC25A20 into the matrix.
My data shows that PDE2A2 interacts with both CPT1 isoforms: I) the predominantly hepatic CPT1A (Fig. 3.3) and II) the predominantly cardiac CPT1B (Fig. 3.4). I

demonstrate that the interaction involves the GAF-A domain (Fig. 3.5). GAF domains are responsible for the dimerization of the PDE2A holoenzyme and docking of cGMP, so it would not be expected for them to be the domain involved with binding of other proteins as this could interfere with the dimerization/docking. However, my results were clear and reproducible. Furthermore, interaction between PDE2A2 and the GAF domains has been shown for other proteins, like Parkin (Lobo et al., 2020).

Knowledge of the specific location of the PDE2A2-CPT1 interaction could lead to the development of ways to disrupt it. Selective displacement could affect the role of either protein, and therefore modulate the biological functions controlled by them. Displacing PDE2A2 would alter the local concentration of cAMP around CPT1B, affecting the signalling pathway at this localisation.

From my data, PDE2A2 interaction with SLC25A20 was only experimentally demonstrated upon overexpression of both proteins (Fig. 3.9). This suggests that the two proteins are able to interact, but the interaction may not happen *in vivo*. PDE2A2 has been reported to localise at the mitochondria inner membrane (MIM) through protein fractionation, electron microscopy, and super-resolution imaging (Monterisi et al., 2017). Therefore, it is possible that the proteins do interact at the MIM, and that the negative result may be due to a weak interaction that is lost upon treatment with a harsh lysis protocol. More optimisation is required to demonstrate PDE2A2 and SLC25A20 interact in physiology. Further work could investigate whether CPT1 and SLC25A20 are part of the same macro-molecular complex, which includes PDE2A2.

3.7.2 PDE2A2 interactions with elements involved in alternative energy production pathways

Other PDE2A2-interactors revealed by the MS analysis performed on ARVM samples by Subramaniam et al. (2023) are part of pathways that traffic different metabolic substrates, such as glucose and pyruvate.

Only a small portion of the ATP required by the heart is provided by the hydrolysis

of glucose. This glucose is either exogenously sourced from the circulation or extracted from glycogen stores. The transport of glucose into the cytosol is facilitated by the glucose transporters (SLC2A, or GLUTs), and once it has entered the cell it is rapidly phosphorylated to glucose 6-phosphate (G6P). G6P enters many metabolic pathways, resulting in the generation of pyruvate, NADH and a small amount of substrate-level ATP. Pyruvate enters the cytosol through the transporter SLC16A1 (also known as MCT1). Here, it can be converted to lactic acid or enter the mitochondria to undergo oxidation. Pyruvate enters into the mitochondrial matrix through the transporter MPC2, localised at the MIM. In the matrix, it is converted into acetyl-CoA, and can enter the citric acid cycle to produce ATP, CO_2 and the reducing equivalents $NADH_2$ and $FADH_2$.

I validated the interaction between PDE2A2 and the plasma membrane transporter for glucose (SLC2A1) (Fig. 3.15), plasma membrane transporter of pyruvate (SLC16A1) (Fig. 3.16) and mitochondrial transporter of pyruvate (MPC2) (Fig. 3.12). Moreover, I demonstrated that PDE2A2 interacts with SLC25A4 (Fig. 3.10), which, at the MIM, imports ADP into the mitochondrion and exports ATP into the MIS, which is confluent with the cytosol (Klingenberg, 2008). Finally, I attempted to validate the putative interaction between PDE2A2 and the mitochondrial oxoglutarate carrier SLC25A11 (Fig. 3.11). SLC25A11 plays a role in the malate-aspartate shuttle, the oxoglutarate-isocitrate shuttle, and gluconeogenesis (Kunji et al., 2020). I was not successful in demonstrating this interaction experimentally. This could be due to the location of SLC25A11 at the MIS meaning it may require more delicate lysis procedures, or because of a weak interaction between the two proteins.

These findings suggest that PDE2A2 may be functionally integrated with key nodes of cardiac metabolic flux, potentially acting as a spatial regulator of energy substrate handling. Its interactions with SLC2A1, SLC16A1, MPC2, and SLC25A4 indicate a possible role in coordinating metabolic signaling between the plasma membrane and mitochondria. Given PDE2A2's known role in cAMP/cGMP hydrolysis, this spatial organization may enable fine-tuning of cyclic nucleotide signaling in response to changes in substrate availability or energy demand. Overall, these findings open the possibility that PDE2A2 modulates

cardiac energetics, potentially linking second messenger signalling to metabolic control.

3.7.3 A metabolon-like complex at the mitochondrial outer membrane

PDE2A2 interacts with elements from different energy production pathways. I hypothesised that these proteins are all concurrently present in a metabolon-like complex. The complex would regulate the transport of the different substrates into the mitochondria. A metabolon is a group of enzymes that organise spatially to form transient protein-protein interactions, creating a supramolecular complex aimed at channelling metabolites among the component enzymes (Srere, 1985). My results show that SLC16A1, SLC2A1 and SLC25A4 are all present simultaneously in CPT1B-FLAG immunoprecipitate, with and without PDE2A2 overexpression (Fig. 3.17, Fig. 3.18). As they interact in the presence of PDE2A2 suggests that these enzymes, canonically considered to be part of different metabolic pathways, may come together to form a supramolecular complex.

It is possible that the functional effect of these interaction is the regulation of import of different substrates. For example, it may be speculated that such a complex may coordinate the utilisation of glucose and fatty acid as energetic substrates.

It should be noted that these results do not prove whether PDE2A2 presence is necessary for these elements to interact, or for the metabolon-like complex to form. This is because PDE2A2 was over-expressed in all the experiments. A way to investigate whether PDE2A2 mediates the interaction between these enzymes is to perform a CPT1B co-immunoprecipitation experiemnt on lysate from PDE2A$^{-/-}$ cells. If SLC16A1, SLC2A1 and SLC25A4 are still present in the CPT1B pull-down, then PDE2A2 presence is not required for their interaction.

The possibility of a metabolon-like complex is particularly relevant as the heart is metabolically flexible. Even though fatty acids represent the dominant source of energy substrates, the heart can switch between oxidising FA and different energetic substrates such as glucose and lactate, as well as small amounts of ketone bodies and amino acids

(Lopaschuk et al., 2021). The reason for the heart's adaptability to different fuels is relative to which substrate is more advantageous in any given situation. Energy stored in high-energy phosphate bonds in glucose requires relatively less oxygen than does an equivalent energy storage from metabolism of fatty acids. In particular, for each mole of O_2 consumed, there is a 53.7% higher energy production (in the form of high-energy phosphate bonds) from the metabolism of glucose than from the metabolism of a fatty acid. Therefore, one gram of FA produces significantly more high-energy bonds than a gram of glucose, but at a greater relative cost in oxygen (Kessler and Friedman, 1998). Hence, when oxygen is abundant and food is scarce, there is an advantage in utilizing fatty acids for fuel as opposed to using glucose. However, when oxygen is scarce, usually the case in cardiac pathology, it would be more advantageous to oxidise glucose rather that fatty acids.

An ability to target the switch between different substrates would provide an incredibly powerful tool to treat and prevent metabolic-dependent heart conditions.

This is interesting as in heart failure the heart loses this metabolic flexibility and becomes energy deficient because of its inability to produce ATP. (Actis Dato et al., 2024). Hallmarks of the metabolic changes that characterise the failing heart also include a decrease in fatty acid β-oxidation (Dávila-Román et al., 2002), a rise in glucose uptake and lipotoxicity (Diakos et al., 2016). However, this paradigm has recently been challenged in a study which showed 20 patients with nonischaemic heart failure with reduced ejection fraction (HFrEF) retained significant cardiac metabolic flexibility (Watson et al., 2023). This new data highlights the lack of complete understanding of heart metabolism during heart failure and underscores the importance of further study.

Additionally, increasing evidence suggests that the heart not only is able to switch between substrates but operates optimally when it uses a mixture of them, especially with respect to fatty acids and glucose (Glatz et al., 2006). Indeed, tilting the balance towards the predominant use of one of those substrates, is associated with impaired cardiac contractile function (Glatz et al., 2020).

The mechanisms underlying the heart's metabolic flexibility are not yet fully understood, and elucidation on them could provide effective new therapeutic strategies. Some elements that contribute to the flexibility of include: I) substrate uptake into cardiomyocytes by facilitated diffusion through specific membrane-associated proteins (Glatz and Luiken, 2018) and II) mitochondrial oxidation (whereby substrate preference is determined by mechanisms such as the Randle cycle) (Hue and Taegtmeyer, 2009). The latter, first described by Philip Randle in 1963, describes the competition for oxidation between glucose and fatty acids (Randle et al., 1963). Additional control is exerted by subcellular localization of metabolites; for instance, allosteric inhibition of CPT-1 by malonyl-CoA limits the entry of acyl-CoA esters into the mitochondrial matrix, thus attenuating β-oxidation (Glatz et al., 2020).

Even though there have been efforts to understand the relationship between different metabolic pathways, these fail to elucidate the exact mechanisms of interplay between them. Therefore, the possibility of a multiprotein, metabolon-like complex which includes elements of both the glucose and fatty acid pathways is an interesting starting point to study the coordination of the utilisation of glucose and fatty acid as energetic substrates. In conclusion, it would be reasonable to postulate that two or more pathways that: i) are closely dependent on each other, and ii) whose interplay is vital for the heart muscle to survive, would be in physical proximity where their interplay can be tightly regulated through cAMP signalling. Additionally, the presence of PDE2A2 could mean that the regulation of the interplay between different substrates is mediated by cAMP.

Fig.3.20 shows a possible spatial organisation of the metabolon-like complex at the MOM which includes elements of different metabolic pathways. These include CPT1, SLC27A4, SLC25A4, SLC2A1, SLC16A1 and PDE2A2. The gray lines indicate interaction between CPT and the respective proteins. Presence of PDE2A2 adjacent to a protein indicates a validated interaction between the two.

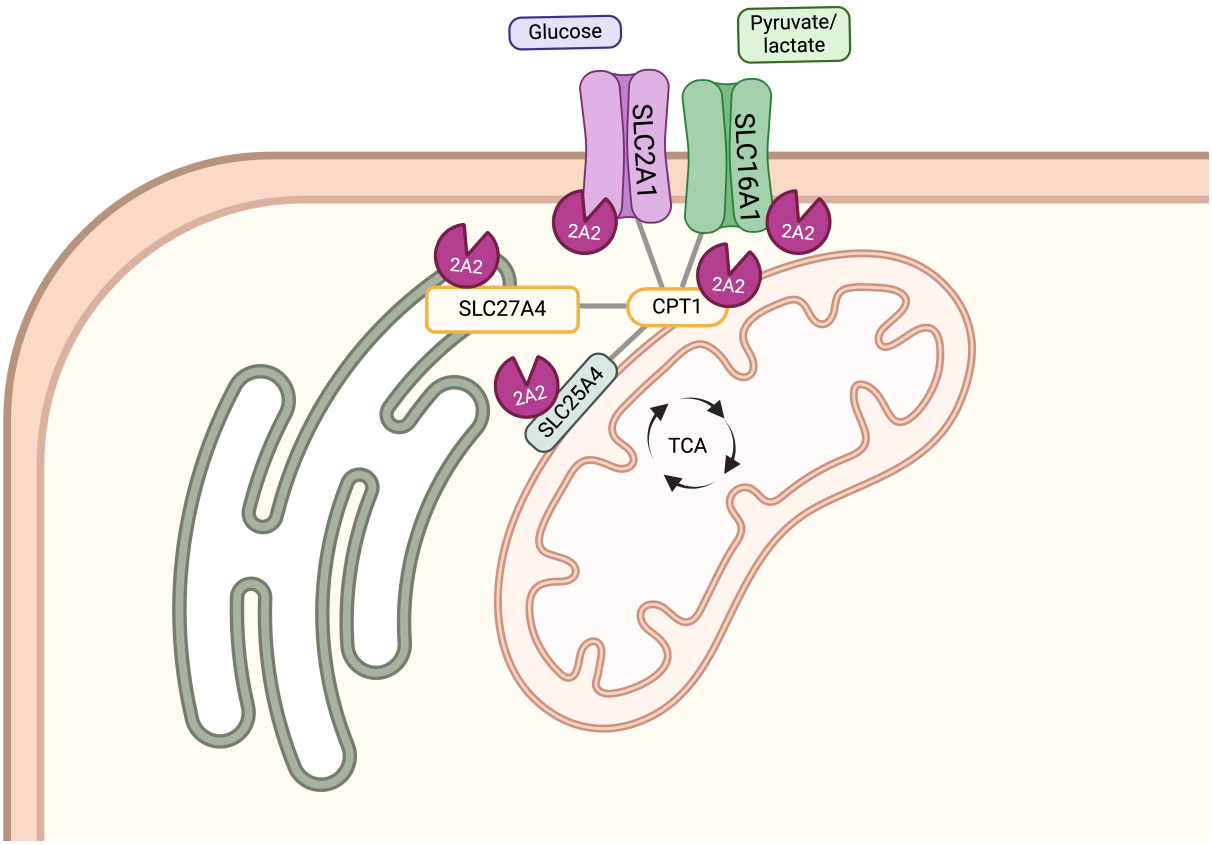


Figure 3.20. Schematic representation of a metabolon-like complex at the MOM. Elements involved in the trafficking of different subtartes interact with PDE2A2 and with CPT1B, suggesting the presence of a metabolon-linke complex at the MOM which could play a role in the intercplay between different substrates utilisation. The gray line between CPT1 and other proteins indicates a validated interaction. Presence of PDE2A2 adjacent to a protein indicates interaction between the two. Drawn with Biorender

In chapter 5, I study the functional relevance of some of the interactions validated in this chapter, and the mechanisms through which PDE2A2 may regulate cardiac metabolism.

Chapter 4

PDE3A1 interactors

4.1 Background

Similarly to PDE2, PDE3 can bind to and hydrolyse both cAMP and cGMP with high affinity (Wechsler et al., 2002). Two PDE3 genes have been described: *PDE3A* is primarily expressed in cardiac myocytes; and *PDE3B* is mainly present in adipocytes (Reinhardt et al., 1995). PDE3A has two isoforms with different subcellular localisations: PDE3A1 is present at internal membranes, whereas PDE3A2 is present both in the cytosol and at membranes, and PDE3A3 is found mainly in the cytosol (Wechsler et al., 2002).

PDE3 is a critical regulator of cardiac contractility by modulating cAMP/PKA concentrations at different sites (Yan et al., 2007). PDE3 activity results in decreased PKA-dependent phosphorylation of Phospholamban (PLB), reducing the reuptake of calcium by the sarcoplasmic reticulum, and therefore slowing relaxation (Ghigo and Mika, 2019). Additionally, elevation of cAMP via PDE3 inhibition activates PKA, which results in increase in the trans-sarcolemmal influx of Ca^{2+}, via phosphorylation of Rad, a protein that associates with L-type Ca^{2+} channels and reduces their open probability (Papa et al., 2022). This, in turn, triggers a much larger Ca^{2+} mobilization from sarcoplasmic reticulum store via RyR2 (Yan et al., 2007).

PDE3 is particularly relevant in the cardiovascular system, as inhibitors show inotropic and vasodilatory effects attributable to an elevation in cAMP (Movsesian, 1999). Drugs

like milrinone and enoximone, which inhibit PDE3, have been used in the clinic to augment contractility and reduce afterload in patients with dilated cardiomyopathy. However, long-term use increased mortality, makes them suitable only for short-term treatment in case of acute, refractory heart failure (Brecker et al., 1993).

4.1.1 PDE3A1 in cAMP/cGMP cross-talk

PDE3 regulates cAMP/cGMP cross-talk (Lugnier et al., 1999), as its regulation involves the interconnection between the two cyclic nucleotides signalling (Lugnier et al., 1999). This enzyme has dual-specificity and binds with high affinity both cAMP and cGMP, however, the Vmax for cAMP hydrolysis is 10-fold higher than for cGMP hydrolysis. Thus, cGMP behaves as a competitive inhibitor of cAMP hydrolysis because of the high affinity to cAMP and the low rate of cGMP hydrolysis (Lugnier, 2006). Consequently, the levels of cGMP can alter the availability of PDE3 to degrade cAMP, thus regulating cAMP concentration. cAMP-hydrolysing activity of PDE3 by cGMP presents several physiological consequences. In cardiac sinoatrial cells, inhibition of cAMP hydrolysis by PDE3 appears to contribute to the potentiation of delayed rectifier K+ currents by cGMP (Feinstein et al., 2012). In frog ventricular myocytes, agents that raise intracellular cGMP content by stimulating soluble guanylyl cyclase potentiate L-type Ca^{2+} currents via inhibition of PDE3 (Diebold et al., 2009; Seybold et al., 2005; Surapisitchat et al., 2007).

The differential sensitivity of PDE isoforms to cGMP concentrations defines the cross-talk between cAMP and cGMP (Zaccolo and Movsesian, 2007). PDE2 and PDE3 in particular exhibit varying affinities for cGMP. At low cGMP concentrations (~50 nM), PDE3 is selectively inhibited, increasing cAMP and enhancing contractility (Hambleton et al., 2005). Intermediate cGMP levels (~200–500 nM) activate PDE2, which promotes cAMP degradation and reduces contractility (Beavo et al., 1971). Experimental evidence in human atrial myocytes supports these concentration-dependent effects, demonstrating bidirectional regulation of calcium currents via PDE3 inhibition at low cGMP and PDE2 activation at high cGMP (Méry et al., 1993). Additionally, the effects of cGMP on PDE3 and PDE2 may depend on intracellular cAMP and Ca^{2+} levels. It is possible that inhibition

of PDE3 activity by cGMP may be more important at low concentrations of cAMP and Ca^{2+}, whereas effects of cGMP on PDE2 may be more important under other conditions (Hambleton et al., 2005).

Therefore, the balance between PDE2 and PDE3 activities allows for fine-tuned regulation of cardiac responses through cAMP/cGMP crosstalk. In summary, elevated cGMP levels can simultaneously activate PDE2 and inhibit PDE3. Activation of PDE2 reduces cAMP levels, leading to decreased contractility, while inhibition of PDE3 increases cAMP levels, enhancing contractility. The net effect on cardiac function depends on the relative activities of these enzymes and the specific physiological context.

This intricate interplay ensures that cardiac function is precisely regulated, allowing the heart to respond appropriately to varying physiological demands and protecting against potential overstimulation. Because of this tight relation between PDE2 and PDE3, it is not inconceivable that these two enzymes co-regulate a cAMP/cGMP nanodomain.

Mass spectrometry (MS) analysis on PDE2A2 and PDE3A1 immunoprecipitates from adult rat ventricular myocytes revealed a number of proteins which interact with the two phosphodiesterases. These putative interactors can be spatially organised by the known subcellular localisation of the proteins interacting with each PDE isoform, to generate a map of sub-networks at different sites where PDE-family dependent cAMP nanodomains may be present, as described in chapter 3 (Fig. 1.1). Whilst most interactors are unique to either PDE2A2 (210) or PDE3A1 (464), 134 appear to be shared between the two (Subramaniam et al., 2023). It is possible that PDE2A2 and PD3A1 co-regulate a number of cAMP nanodomains. As many of the shared interactors play a role in the transport of metabolic substrates, it is possible that the cAMP under the shared control of PDE2A2 and PDE3A1 regulates the transport of metabolites aimed at energy production.

4.1.2 PDE3 and RNA binding proteins

The contribution of PDE3 to cardiac contractility has been extensively explored, however a novel potential role of this phosphodiesterase has recently emerged (De Waal et al.,

2016; Lee et al., 2023; Zhai et al., 2016). This entails PDE3 acting in conjunction with RNA binding proteins (RBP) to mediate several cellular responses. RNA binding proteins regulate much of the post transcriptional regulation (PTR) of gene expression, which represent the regulatory layer responsible for the fine-tuning protein synthesis that allows to achieve specific cellular phenotypes (Gerstberger et al., 2014). RBPs associate with nascent mRNA to form ribonucleoprotein complexes exported into the cytoplasm to regulate gene expression post-transcriptionally, (Singh et al., 2015) and associate with tRNA and rRNA to form ribosomes (Catalanotto et al., 2023). Abnormal RBP function may lead to change or loss of protein function, and is associated with an array of diseases from neurodegenerative ones (Huang et al., 2020) to different types of cancer (Hoyos and Abdel-Wahab, 2018). It can also contribute to cancer treatment resistance by modulating several RNA-related mechanisms (Tao et al., 2024; Pereira et al., 2017). Recently, RBP have been reported to play a role in cardiac disease too (Völkers et al., 2024). Several RBPs in vascular endothelial cells, smooth muscle cells and inflammatory immune cells have been identified as central regulators of genes related to the progression of vascular inflammation and subsequent atherosclerosis (Völkers et al., 2024), the most common manifestation of cardiovascular disease (Libby, 2021). Additionally, RPBs have been linked to heart failure, where aberrant splicing patterns caused by variants in RBPs contribute to severe cardiac dysfunction and ventricular dilatation in animal models of dilated cardiomyopathy (Schneider et al., 2020; Fenix et al., 2021). Additionally, RBPs are crucially involved in dysregulated mRNA translation and protein synthesis in the failing heart, where this is dramatically increased during pathological cardiac hypertrophy or reperfusion damage (Gudbjarnason et al., 1964). Given the role of RBP in cardiac disease, and that the RNA-based therapeutic approaches are under intense investigation in cardiac disease, targeting RBP–RNA interactions as therapeutic intervention for cardiovascular pathologies is particularly interesting.

Fo example, PDE3 has been demonstrated to interact with the RBP SLFN12, which plays an important role in cancer-cell apoptosis (Lee et al., 2023). Velcrins are compounds that include a subset of PDE3A inhibitors (De Waal et al., 2016), they kill cancer cells

expressing high levels of PDE3A and RBP Schlafen family member 12 (SLFN12). Velcrins induce the formation of PDE3A-SLFN12 complexes, resulting in the death of the cancer cell (Lee et al., 2023). The mechanism of this is not completely understood, however it has been hypothesised that it may involve the upregulation of SLFN12 ribonuclease activity by velcrin-induced PDE3A–SLFN12 complex formation, resulting in specific cleavage of tRNALeu(TAA), causing ribosomal stalling, global inhibition of protein synthesis and cell death (Lee et al., 2023).

Another example of a PDE3 binding RBPs is the complex formed between PDE3B and CUG-binding protein 1 (CUGBP1). This is a multifunctional RNA-binding protein which has been associated with both cardiovascular (Giudice et al., 2014) and metabolic disorders (Sen et al., 2009), insulin resistance (Savkur et al., 2001), obesity (Hinney et al., 2014) and diabetes (Verma et al., 2013). CUGBP regulates insulin secretion through binding and activating PDE3B (Zhai et al., 2016). Zhai *et al.* demonstrate that CUGBP is present in rodent islets and in β-cell lines, and it is overexpressed in the islets of diabetic mice. Overexpression of CUGBP in mice results in a decreased insulin secretion, significant decrease in cAMP, and increase in mRNA levels of *PDE3B*. CUGBP1 was found to directly bind a specific ATTTGTT sequence residing in the 3$\backsim$ UTR of PDE3B and to stabilise *PDE3B* mRNA. Insulin secretion was no longer reduced upon CUGBP1 overexpression in the presence of PDE3 inhibitor cilostamide (Zhai et al., 2016).

4.2 Aims

The MS analysis from Subramaniam et al. (2023) revealed a number of potential interactors of PDE2A2 and PDE3A1, some exclusively interacting with one phosphodiesterase, and some that are shared between two. Proteins involved in metabolic substrate trafficking that interact with PDE2A2 were validated in Chapter 3. Chapter 4 first validates interactions between PDE3A1 and proteins which interact with PDE2A2 (4.3) and then validates the interaction between PDE3A1 and the RBP EIF3C, RBM39, YBX and ILF2 (4.4).

A list of the putative interactors is summarised in Table 4.1. The protein nomenclature

is as defined by the human gene nomenclature (HGNC) , mouse genome informatics (MGI) and rat genome (RGD) databases.

Protein Name	Alternative name	Statistical significance	Fold Change	No. of unique peptides	Sequence coverage [%]	Mol. Weight [kDa]
CPT1A	/	2.86	1.26	11	17.5	88
CPT1B	/	2.95	1.38	17	20.9	88
SLC27A4	FATP4	5.04	6.34	7	6	72
SLC16A1	MCT1	1.96	1.85	5	8.3	53
EIF3C	/	1.45	2.25	3	4	110
RBM39	/	1.90	1.79	2	7.6	70
YBX1	/	1.75	1.81	12	63.7	49
ILF2	/	2.57	1.17	5	17.3	43

Table 4.1. PDE3A1 putative interactors identified through PDE3A1-RFP immunoprecipitation and MS analysis selected for further validation. MS data for the indicated proteins from the PDE3A1 IP. Statistical Significance (the higher the more significant) refers to t-test analysis using RFP alone as control. This yielded 464 interaction partners for PDE3A1, significance thresholds are false discovery rate [FDR], 0.03 and S-zero is the fold-change threshold [S0], $\sim$ 1.3. (the higher the more significant), Fold Change (compared to RFP IP), number of unique peptides identified by MS, % of sequence coverage and molecular weight are shown.

I validated interactions by coimmunoprecipitation. Unless stated otherwise, Human embryonic kidney 293T (HEK293T) cells were used. This cell line was chosen because of its high efficiency of transduction, robustness and results reproducibility. Cells were infected with adenoviral vector encoding the fusion protein PDE3A1-RFP or RFP alone or transfected with the respective plasmids. RFP alone and/or non-infected/transfected cells were used as control. Protein complexes were immunoprecipitated with anti-RFP nanobody conjugated to agarose beads (RFP-Trap). The lysates were probed with an anti-RFP antibody to confirm the presence of the fusion proteins, and with a specific antibody to detect the endogenous interactors of interest.

4.3 Metabolic proteins

4.3.1 Carnitine palmitoyl-transferase 1 (CPT1)

As described in more detail in Chapter 3 (section 3.4.1), CPT1 catalyses the rate limiting step in long-chain fatty acid oxidation (Neely et al., 1972). It is localised at the mitochondrial outer membrane (MOM), where it shuttles long-chain Acyl-CoAs in the form of Acyl-carnitine into the mitochondrial intermembrane space. CPT1 is expressed as three different isoforms with different tissue distribution. CPT1A is mainly expressed in the liver, CPT1B in the heart, and CPT1C in the brain (McGarry et al., 1978). Structurally, CPT1 includes two transmembrane domains (TMD); N- and a C- terminal domains, which both protrude on the cytosolic side of the mitochondrial outer membrane; and a short loop region, connecting the two TMD, which protrudes into the mitochondrial intermembrane space (Fraser et al., 1997) (Fig. 3.2). CPT1 structure is largely conserved across the different isoforms. They share the same catalytic domains, necessary for their function, but have different regulatory sites, which means they possess different sensitivity to malonyl-CoA, with CPT1A being moderately sensitive to the enzyme, CPT1B highly sensitive and CPT1C relatively insensitive (McGarry and Brown, 1997; Wolfgang and Lane, 2006). Both CPT1A and CPT1B emerge as putative interactors of PDE3A1 from the MS analysis performed on PDE3A1-RFP immunoprecipitate (Subramaniam et al., 2023).

4.3.1.1 CPT1A

To validate CPT1A interaction with PDE3A1, coimmunoprecipitation experiments were performed. HEK293T were cells infected with adenoviral vector encoding either the fusion protein PDE3A1-RFP or RFP alone, used as control. The specificity of the CPT1A antibody to detect endogenous protein was confirmed by western blot with whole cell lysate (WCL). A band at the expected molecular weight (86 kDa) was detected, confirming the specificity and efficacy of the antibody (Fig.4.1). PDE3A1-RFP expression in infected cells was also confirmed by western blot, as shown by the band at 137 kDa. Protein complexes

immunoprecipitated with RFP nanobody conjugated beads contained endogenous CPT1A (Fig.4.1). The interaction between CPT1A and PDE3A1 appears to be much weaker than CPT1A and PDE2A2 (Fig.4.1).

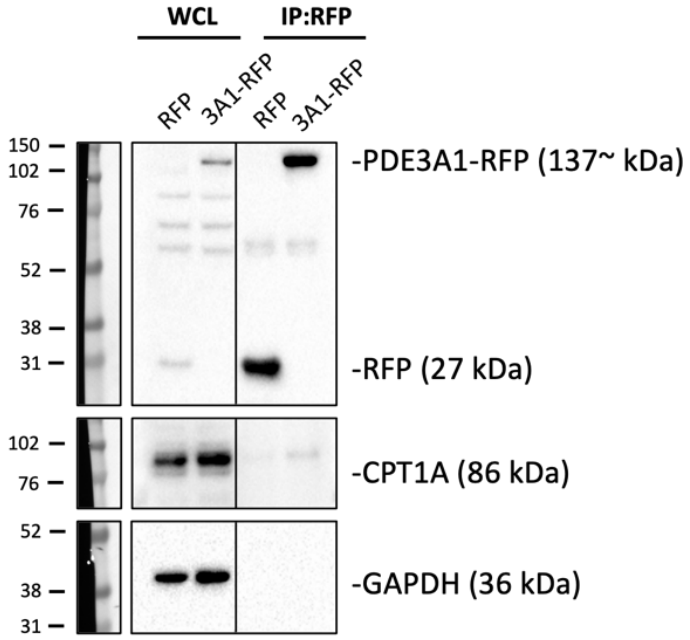


Figure 4.1. PDE3A1 interacts with CPT1A. Detection of endogenous CPT1A after PDE3A1-RFP or RFP immunoprecipitation in HEK293T cells infected with PDE3A1-RFP or RFP. N=3.

4.3.1.2 CPT1B

After having validated the interaction between CPT1A and PDE3A1, the interaction between the heart isoform, CPT1B, and PDE3A1 was confirmed. To assess this, coimmunoprecipitation experiments were performed in neonatal rat ventricular myocytes (NRVM) infected with PDE3A1-RFP or RFP as a control. NRVM were chosen because they present a higher expression level of CPT1B, compared to HEK293T, which predominantly express CPT1A. The specificity of CPT1B antibody for the endogenous protein was tested by western blot on WCL, which revealed a band at the expected size (75-85 kDa). RFP immunoprecipitation of RFP confirms interaction of PDE3A1-RFP with endogenous CPT1B (Fig. 4.2). Similarly to CPT1A, CPT1B-PDE3A1 interaction appears to be weaker than observed for CPT1B-PDE2A2 (Fig. 3.4b). A faint band in the RFP lane

appears at the molecular weight of CPT1B. This happens in two out of three experiments on average, and may be either non-specific interaction between the antibody and the RFP-conjugated nanobeads, or spill over from the adjacent well due to a loading error.

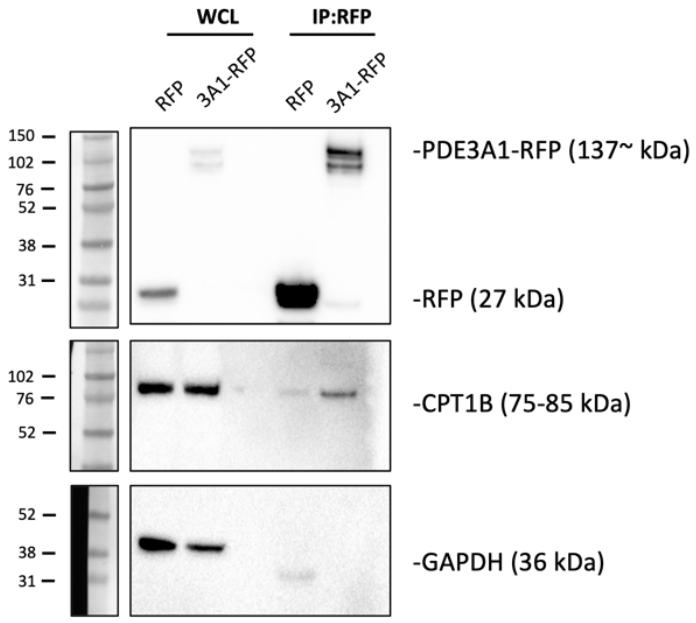


Figure 4.2. PDE3A1 interacts with CPT1B. Detection of endogenous CPT1B from NRVM after PDE3A1-RFP or RFP immunoprecipitation. RFP immunoprecipitation from RFP cells used as controls. N=3

4.3.2 SLC27A4

In general, fatty acid transporter proteins (FATPs, also known as solute carrier family 27 (SLC27) family members) transport fatty acids from the extracellular space to the cytoplasm (Anderson and Stahl, 2013). However, SLC27A4 is not a fatty acid transporter, but is a fatty acyl-CoA synthetase (ACS) (Stahl et al., 1999). MS analysis on PDE3A1-RFP immunoprecipitate indicates 3A1 and SLC27A4 to interact (Subramaniam et al., 2023). Coimmunoprecipitation experiments on HEK293T cells were performed to confirm the interaction. Cells were infected with adenoviral vector encoding PDR3A1-RFP or RFP, as a control. SLC27A4 antibody specificity to detect endogenous protein was verified by western blot on WCL, where a band at the expected size (72 kDa) was detected (Fig. 4.3) RFP immunoprecipitation was probed for SLC27A4, and the endogenous protein was

detected. Anti-RFP probing confirmed presence of PDE3A1-RFP in the same pull-down, validating the interaction between the two proteins. PDE3A1-RFP is not detected in the whole cell lysate from cells infected with the fusion protein. This may be because the cells did not express the protein very strongly.

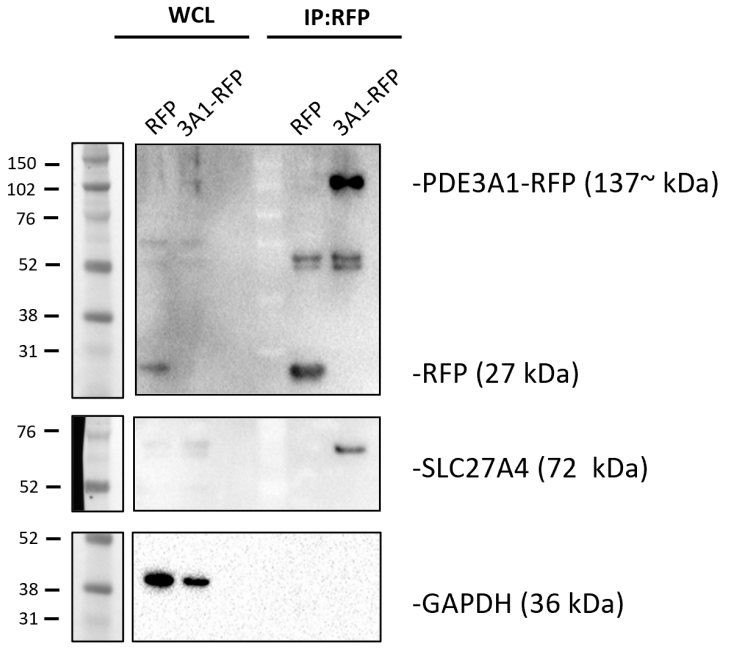


Figure 4.3. PDE3A1 interacts with SLC27A4. Detection of endogenous SLC27A4 in PDE3A1-RFP immunoprecipitation from HEK293T cells infected with PDE3A1-RFP or RFP only. N=3

4.3.3 SLC16A1

Situated at the plasma membrane, SLC16A1 traffics monocarboxylates such as lactate, pyruvate and ketone bodies into the cell (Halestrap, 2013). As a transporter of monocarboxylates, SLCA16 plays an important role in multiple metabolic processes, including aerobic glycolysis and pH homeostasis (Yu et al., 2020). SLC16A1 is another of the proteins which interact with PDE2A2, to also be identified as a putative interactor of PDE3A1 by the MS analysis (Subramaniam et al., 2023). Coimmunoprecipitation experiments were performed to confirm PDE3A1-SLC16A1 interaction. HEK293T cells were infected with PD3A1-RFP or RFP only, used as a control. SLC16A1 ability to detect endogenous protein was tested on WCL through western blot, where a band of the

expected molecular weight (43 kDa) was detected (Fig. 4.4). The presence of PDE3A1-RFP is confirmed through western blot. RFP immunoprecipitation contained PDE3A1 and endogenous SLC16A1, confirming the interaction between the two (Fig. 4.4).

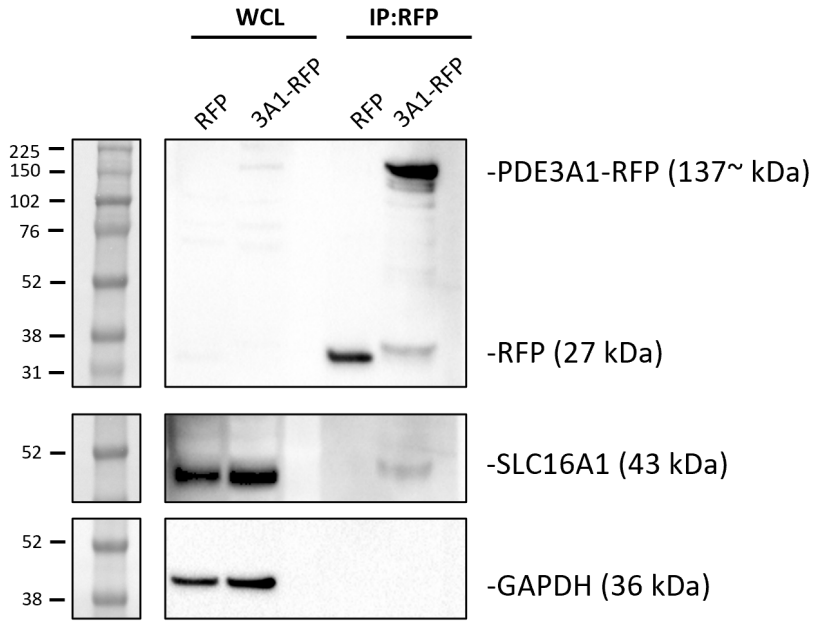


Figure 4.4. PDE3A1 interacts with SLC16A1. Detection of endogenous SLC16A1 in PDE3A1-RFP immunoprecipitation from HEK293T cells infected with PDE3A1-RFP or RFP only. N=3

4.4 RNA-binding proteins

While a significant amount of the gene expression that controls the distinct functional properties of each cell is achieved at the level of gene-specific transcription, many post-transcriptional modifications are essential to cell-specific expression patterns, which dictate function (Corbett, 2018). Much of the post-transcriptional regulation of gene expression occurs through the action of RBPs, which are responsible for the fine-tuning of protein synthesis (Gerstberger et al., 2014). A number of RBP have been reported to interact with PDE3, resulting in altered protein function (Lee et al., 2023; Zhai et al., 2016). The interactome analysis in Subramaniam et al. (2023) revealed a series of RBP as potential interactors of PDE3A1,the validation of which is attempted in this chapter. In table 4.1 are listed the putative RBP emerged from the MS analysis (Subramaniam et al., 2023).

4.4.1 EIF3C

EIF3C (eukaryotic translation initiator factor 3 subunit C) is an RNA binding protein that binds ribosomes and recruits gate-keeper proteins to the decoding centre, contributing to initiating translation (Obayashi et al., 2017). EIF3C was indicated as one of potential interactors of PDE3A1 from the MS analysis (Subramaniam et al., 2023). To validate this, coimmunoprecipitation experiment were performed. HEK293T cells were infected with adenovirus encoding PDE3A1-RFP, RFP only, or not infected. Both lysates from RFP only infected cells and non-infected cells were used as controls. EIF3C antibody was tested for its specificity to detect endogenous protein by western blot, where a band at the expected molecular weight was visible (110 kDa). RFP immunoprecipitate was probed with anti-RFP antibodies to confirm the presence of PDE3A1-RFP fusion protein (Figure 5.7 a). A band at the right molecular weight is detected in the RFP pull-down. However, the lanes containing lysates from the non-infected and RFP control also show a weak band at the molecular weight of EIF3C (Fig. 4.5a). Therefore, I was not able to unequivocally confirm the interaction between these two proteins. This experiment was repeated by another member of the lab, Dr Rahul Yadav, who performed the immunoprecipitation by spinning down the beads at a lower speed (1300 rpm) for 2 minutes, compared to my protocol for which I span the sample at 6000 rpm for 5 minutes. Dr Yadav was able to detect clear signal between PDE3A1 and EIF3C (Fig. 4.5b). In this experiment, Dr Yadav confirmed interaction of EIF3C with PDE2A2 as well (Fig. 4.5b).

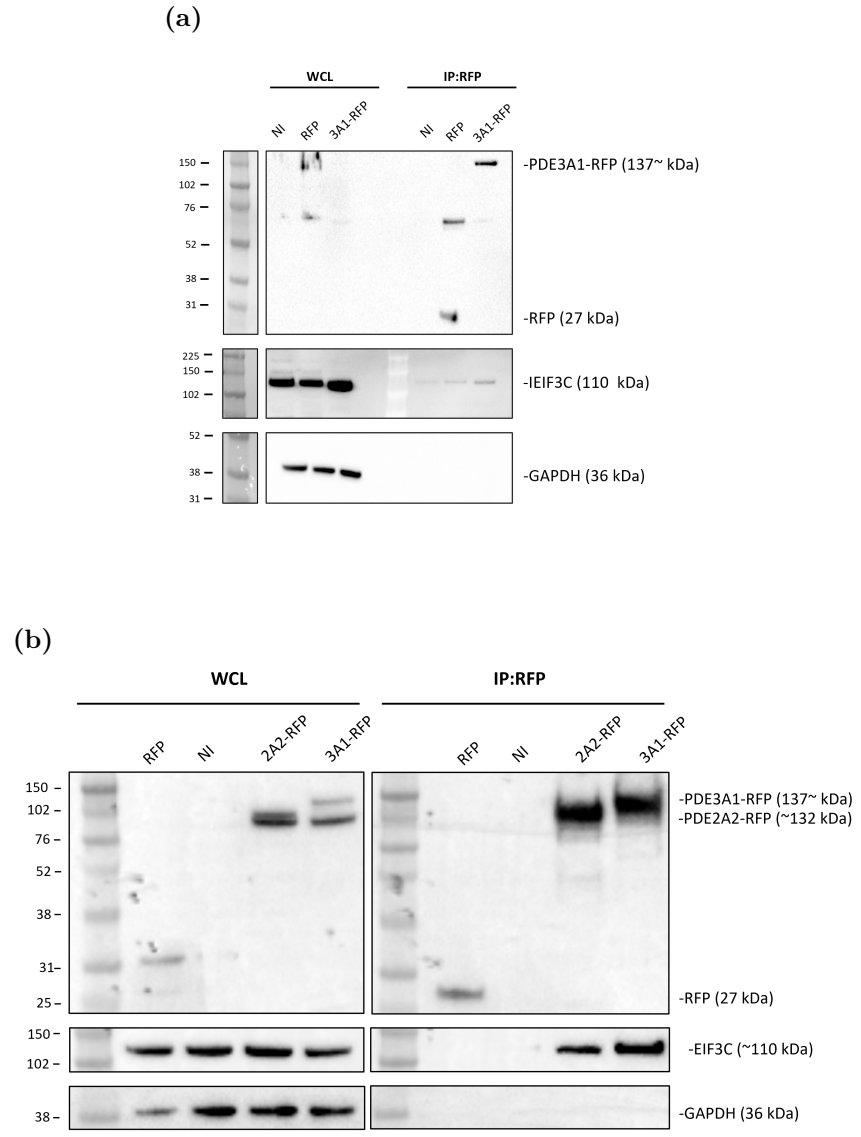


Figure 4.5. PDE3A1 interacts with EIF3C. Detection of endogenous EIF3C in PDE3A1-RFP immunoprecipitation from HEK293T cells infected with PDE3A1-RFP, RFP only, or non-infected (NI).
a) Unsuccessful attempt to detect endogenous EIF3C from HEK293T. N=1
b) Detection of endogenous EIF3C in PDE2A2-RFP and in PDE3A1-RFP immunoprecipitates. Experiment performed by Dr Rahul Yadav. 2A2=PDE2A2-RFP, 3A1=PDE3A1-RFP. N=3

4.4.2 RBM39

Some RBPs are crucial regulators of alternative splicing (AS), a common aspect of gene regulation which engenders transcript diversity and leads to modifications of protein structure and function (Ule and Blencowe, 2019). In pathological conditions, defects in AS

and RBP have been associated with numerous diseases and types of cancer (Gerstberger et al., 2014; Singh et al., 2015).

RMB39 is extensively involved in AS, either by directly binding to RNA or by recruiting other splicing factors (Xu et al., 2022). RMB39 has been gaining significant interest as a drug target for cancer (Xu et al., 2022) due to an anti-tumour effect for which the dominant explanation has focused on the disruption of RNA splicing (Uehara et al., 2017; Han et al., 2017). RBM39 was revealed as a putative interactor of PDE3A1 from the mass spectrometry analysis from ARVM (Subramaniam et al., 2023). To validate the interaction, coimmunoprecipitation experiments in HEK293T cells overexpressing PDE3A1-RFP were performed. The efficacy of RBM39 antibody to detect endogenous protein was confirmed by western blot, where a band at the expected molecular weight (70 kDa,), was observed (Fig. 4.6a). RFP immunoprecipitate, however, fails to show a band at this molecular weight, suggesting the interaction does not occur in this system. Anti-RFP probing of the immunoprecipitate confirms the presence of PDE3A1-RFP in the pull down (Fig. 4.6b). This experiment was repeated by another member of the lab, Dr Rahul Yadav, with a different RBM39 antibody (Protein Tech, number 21339-1-AP). In HEK293T cells, this antibody is able to detect endogenous RBM39 (Fig. 4.6b). In RFP immunoprecipitate, it reveals the presence of PDE3A1 and of RBM29, confirming the interaction between the two (Fig. 4.6b).

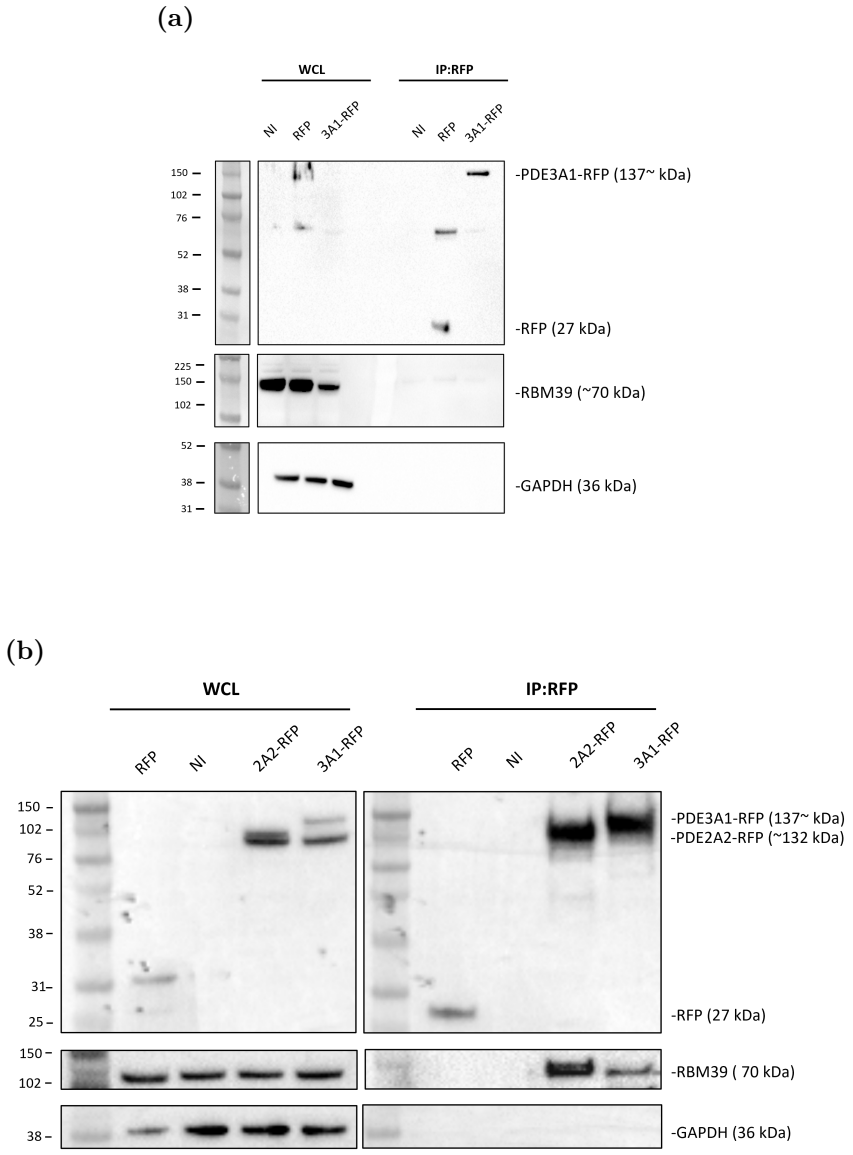


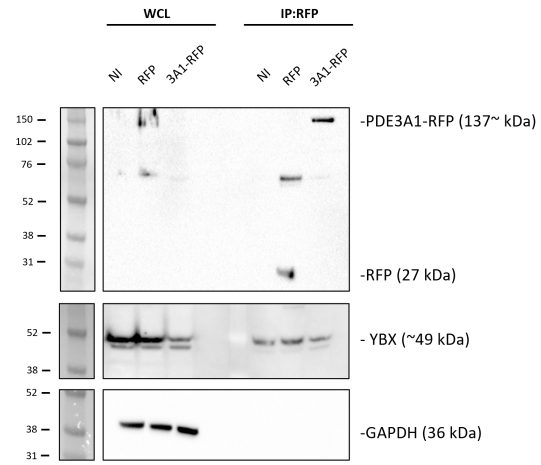
Figure 4.6. PDE3A1 interacts with RBM39. Detection of endogenous RBM39 in PDE3A1-RFP immunoprecipitation from HEK293T cells infected with PDE3A1-RFP, RFP only or non-infected (NI).
a) Unsuccessful attempt to detect endogenous RBM39 from HEK293T. N=1
b) Detection of endogenous RBM39 by Dr Rahul Yadav. 2A2=PDE2A2-RFP N=3

4.4.3 YBX and AKT

YBX1, or Y-box-binding protein-1, is a member of the cold-shock domain protein superfamily. It binds both DNA and RNA (Eliseeva et al., 2011), regulating both DNA repair as well as RNA transcription, translation and mRNA packaging (Kohno et al., 2003). YBX-1 is phosphorylated by AKT (or PKB, protein kinase B), and that this post

translational modification is particularly relevant in cancer as it promotes the expression of genes related to cell growth and drug resistance (Maier et al., 2019; Bader and Vogt, 2008; Li et al., 2017; Basaki et al., 2007). Both YBX and AKT have been identified as putative interactors of PDE3A1 by the interatomic study on ARVM (Subramaniam et al., 2023). The efficacy of the antibody to detect endogenous YBX was assessed by western blot analysis. This showed a band at the correct molecular weight of YBX (49 kDa) (Fig. 4.7a). YBX is not detected in the RFP immunoprecipitate, suggesting the interaction may not occur in this system (Fig. 4.7a). Presence of PDR3A1 is confirmed by western blot, where anti-RFP antibody probing reveals the presence of the fusion protein both in the WCL and in the immunoprecipitate. On the other hand, the antibody for AKT was did not detect a specific band at the expected molecular weight in the whole cell lysate at 60 kDa (Fig. 4.7b), or in the RFP immunoprecipitate either (Fig. 4.7b).

(a)



(b)

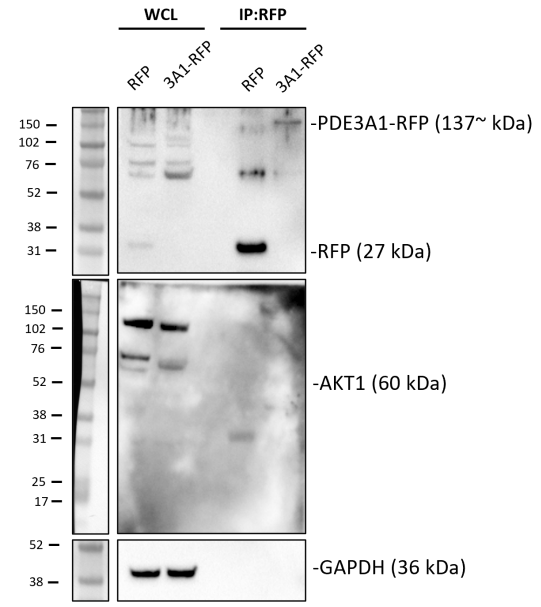


Figure 4.7. Attempt to validate PDE3A1-YBX interaction, and PDE3A1-AKT interaction. a) YBX antibody detects endogenous protein in the whole cell lysate of HEK293T infected with PDE3A1-RFP, RFP only, or non-infected (NI). No band is detected in the RFP immunoprecipitate. N=1. b) AKT antibody fails to detect endogenous protein in the whole cell lysate of HEK293T infected with PDE3A1-RFP and RFP only. N=1

4.4.4 ILF2

The *Interleukin enhancer-binding factor 2* (*ILF2*) gene encodes NF45, the regulatory subunit of NF90/NF110 complexes that are involved in various aspects of RNA metabolism (Barber, 2009). ILF2 forms a complex with interleukin enhancer-binding factor 3 (ILF3) which affects the redistribution of nuclear mRNA to the cytoplasm. ILF2 is another RBP which emerges as interactor of PDE3A1 from the MS analysis on PDR3A1-RFP immunoprecipitate. Coimmunoprecipitation experiments were performed to confirm this potential interaction. The specificity of the ILF2 antibody was confirmed by western blot, with the detection of a band at the expected size (43 kDa) on the WCL (Fig. 4.8). Immunoprecipitation of RFP contains both PDE3A1-RFP and endogenous ILF2, confirming the interaction between the two proteins (Fig. 4.8).

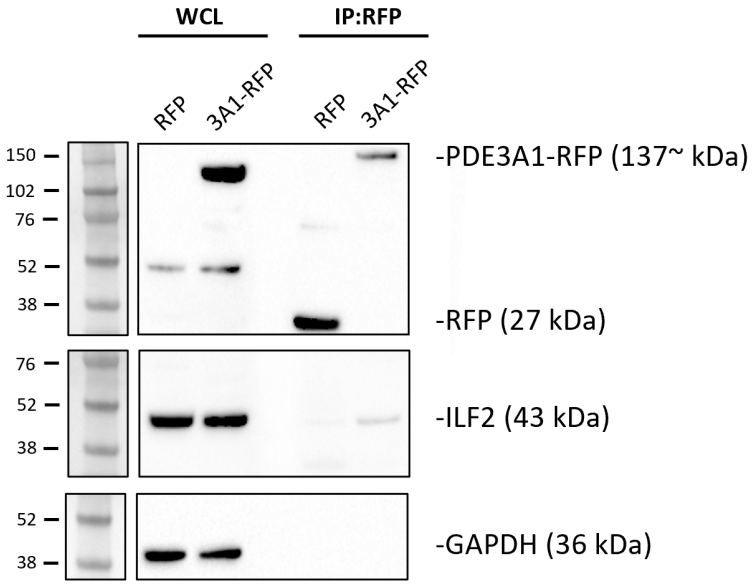


Figure 4.8. PDE3A1 interacts with ILF2. Detection of endogenous ILF2 in PDE3A1-RFP immunoprecipitation from HEK293T cells infected with PDE3A1-RFP or RFP only. N=3

4.5 Summary of results and discussion

A summary of all the PDE3A1 interactors tested is shown in Table 4.2. PDE3A1-RFP was always overexpressed. A schematic representation of the confirmed interactions is shown in Fig. 4.9.

Protein Name	Result	Validation Type	Model
CPT1A	Confirmed	Endogenous	HEK293T
CPT1B	Confirmed	Endogenous	NRVM
SLC27A4	Confirmed	Endogenous	HEK293T
SLC16A1	Confirmed	Endogenous	HEK293T
EIF3C	Confirmed	Endogenous	HEK293T
RBM39	Confirmed	Endogenous	HEK293T
YBX1	Not confirmed	Endogenous	HEK293T
ILF2	Confirmed	Endogenous	HEK293T

Table 4.2. Summary of the PDE3A1 interactors tested.
The table shows a summary of the validation work from this chapter. The name of each protein is included, together with the outcome of the validation; whether the proteins were endogeous or overexpressed; and the model the interaction was tested in.

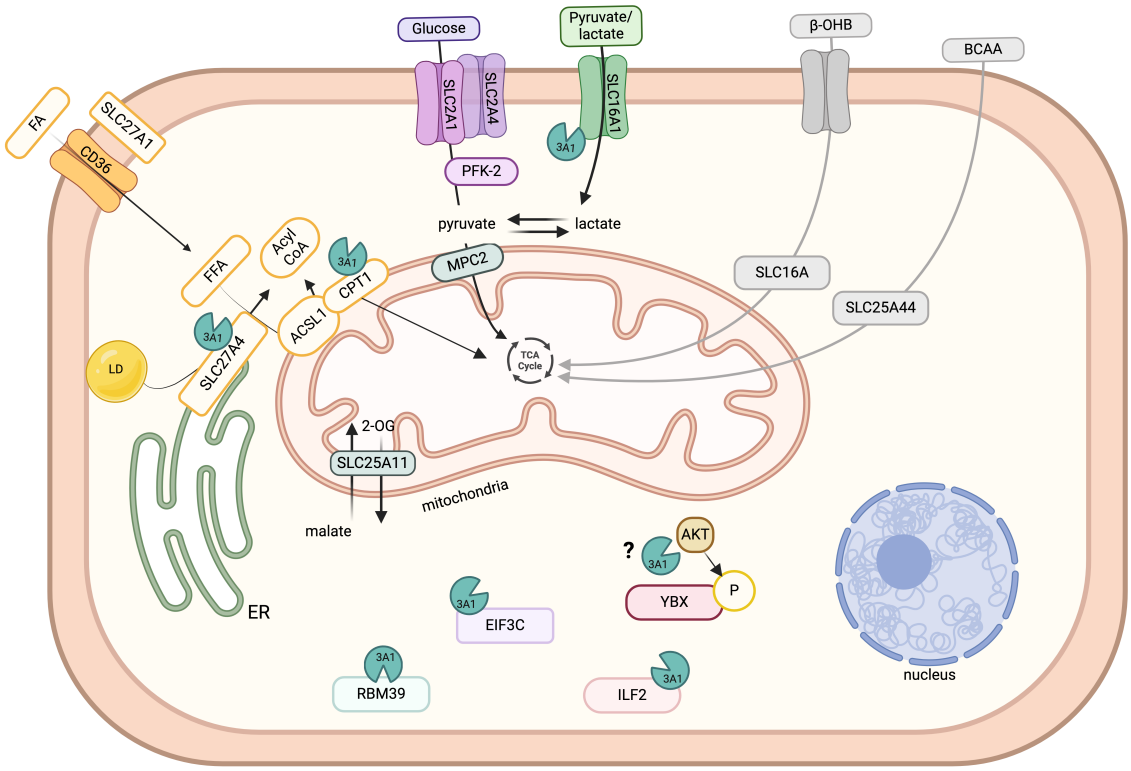


Figure 4.9. PDE3A1 interacts with a number of proteins. Schematic representation of the interactions validated in this chapter. Some are involved in the trafficking of substrates aid at energy production, others are RNA binding proteins. A question mark next to the protein indicates the interaction was not validated experimentally. Drawn with Biorender.

As the most abundant PDE in the heart, PDE3 is one of the best characterised phosphodiesterases in the cardiac muscle (Osadchii, 2007). PDE3 is a well-known regulator of cardiac contractility, and consequently, inhibitors of this enzyme have been used as therapeutic agents in the treatment of heart failure for more than 2 decades (Zaccolo and Movsesian, 2007). Inhibitors such as milrinone have positive inotropic effects, attributable to the elevation of cAMP and/or cGMP in myocytes. The inhibitors are family-specific only, and therefore the increase in second messengers will reach similar levels in all the domains controlled by different PDE3 isoforms. Thanks to their positive inotropic effect, PDE3 inhibitors are used to augment contractility and reduce afterload in patients with dilated cardiomyopathy (Movsesian, 1999). However, even though they present hemodynamic benefits in the treatment of acute heart failure, long-term use increase mortality (Fukuta et al., 2021). These biphasic effects could be due to diverse cellular responses elicited by

increasing cAMP in all domains controlled by the PDE3 isoforms. This highlights the importance of developing therapeutic strategies with less severe side effects. One strategy could be targeting the specific isoforms, therefore modulating only the nanodomains under their control.

Even though PDE3 has been studied mainly in the context of cardiac contractility, some studies have linked it to metabolism. Inhibition of PDE3 promotes lipolysis, glucose production, and insulin secretion. (Cheung et al., 2003). *Pde3b* knock-out (KO) mice present alterations in the energy homeostasis, which can be beneficial (decreased white adipose tissue and increased lean mass)or detrimental (insulin resistance) (Choi et al., 2006). In obese patients, total cAMP-hydrolyzing PDE, PDE3 and PDE4 activities were significantly reduced in adipose tissue depots compared to non-obese patients (Degerman et al., 2011)

Therefore, even though some advances have been made in understanding what part PDE3 plays in the regulation of glucose and fatty acid metabolism, the exact role of this enzyme in this cotext is yet to be understood.

4.5.1 PDE3A1 interacts with elements involved in trafficking different metabolites

MS analysis of PDE3A1 immunoprecipitate from ARVM reveals a series of putative interactions in ventriculocytes (Subramaniam et al., 2023). A number of these interactions are involved in the transport of metabolic substrates. My results from this chapter showed that PDE3A1 interacts with the FA transporters CPT1A/B (Fig. 4.1 and Fig. 4.2) and SLC27A4 (Fig. 4.3). Additionally, I validated the interaction between PDE3A1 with the pyruvate transporter at the plasma membrane SLC16A1 (Fig. 4.4). It is possible that PDE3A1 plays a role in the trafficking of metabolites aimed at being consumed for energy production. This hypothesis could be testing by investigating the activity of these transporters upon PDE3 inhibition.

As both PDE3A1 and PDE2A2 (Chapter 3) interact with these transporters (CPT1A/B, SLC27A4 and SLC16A1), it is possible that these two phosphodiesterases are co-regulating the same pool of cAMP. This would be in charge of modulating the transport of different substrates across the cell destined to be consumed for energy production. To test this hypothesis, the first step would be to address whether PDE2A2 and PDE3A1 are simultaneously present in the same complex. To do this, immunoprecipitate of either CPT1, SLC27A4 or SLC16A1 could be tested by western blot, probing for both PDE2A2 and PDE3A1.

The coordinated regulation of multiple PDEs towards the same nanodomain is not a novel concept. Different phosphodiesterases have been shown to collectively modulate a shared nanodomain, highlighting their interplay in fine-tuning localized signalling. For example, PDE3 and PDE4 co-regulate a cAMP nanodomain at the plasma membrane, in proximity of β-adrenergic receptors and L-type calcium channels, directly modulating excitation-contraction coupling (Beltejar et al., 2017). The authors demonstrate that the two PDEs work in a complementary manner. Inhibition of PDE3 alone leads to modest increases in cAMP levels, primarily due to PDE3's role in baseline degradation. Blocking PDE4 causes a much sharper cAMP increases, particularly in response to receptor stimulation. When both PDE3 and PDE4 are inhibited simultaneously, cAMP levels rise drastically, leading to uncontrolled signalling. PDE3 inhibition by cGMP indirectly boosts cAMP levels by reducing PDE3 activity. However, PDE4 remains active, acting as a backup mechanism to prevent excessive cAMP accumulation when PDE3 is suppressed (Beltejar et al., 2017). In a similar way, PDE2 and PDE3 could co-regulate a shared pool of cAMP in charge of trafficking substrates belonging to different metabolic pathways.

Another hypothesis is that the co-regulation of the transport of metabolic substrates by PDE2 and PDE3 may involve cross talk between cAMP and cGMP. As described earlier in the chapter, PDE3 is a dual-specificity phosphodiesterase that preferentially hydrolyzes cAMP, but is inhibited by cGMP, making it a key mediator of cAMP/cGMP cross-talk. In contrast, PDE2 also targets both nucleotides but is activated by cGMP, highlighting opposing regulatory roles between the two enzymes.Therefore, the balance

between PDE2 and PDE3 activities allows for fine-tuned regulation of cardiac responses through cAMP/cGMP cross talk. It is possible that PDE2 and PDE3 regulate the trafficking of metabolites from different metabolic pathways through cross talk of cAMP and cGMP.

A tight regulation of delivery of metabolites would be logical when it comes to energy production. This is because even though fatty acids are the preferred metabolic nutrient, the heart is substrate-omnivore and consumes the most advantageous substrates. Understanding the mechanisms underlying the heart's metabolic flexibility is particularly important as, even though historically the failing heart has been described to lose its flexibility, recent data has demonstrated how some flexibility is retained for patients with HFrEF (Watson et al., 2023).

4.5.2 PDE3A1 interacts with RNA binding proteins

I was able to validate the interaction between PDE3A1 and ILF2 (Fig. 4.8), whereas I was not able to unequivocally demonstrate interaction with EIF3C (eukaryotic translation initiator factor 3 subunit C) (Fig. 4.5a), YBX (Fig. 4.7) and RBM39 (Fig. 4.6a). PDE3A1-EIF3C and PDE3A1-RBM39 interactions were later corroborated by another member of the laboratory, Dr Rahul Yadav (Fig. 4.5b and Fig. 4.6b).

Whilst the role of PDE3 in cardiac contractility has been extensively explored, a novel potential role of this enzyme has emerged (De Waal et al., 2016; Lee et al., 2023; Zhai et al., 2016). PDE3 has been shown to act in conjunction with RBP to mediate a series of cellular responses. Normally, RBPs regulate much of the post transcriptional regulation of gene expression. Abnormal RBP function may lead to change or loss of protein function and is associated with an array of diseases, including cardiac pathologies. Several RBPs have been recognized as key regulators of genes involved in vascular inflammation and the development of atherosclerosis (Völkers et al., 2024), the most common manifestation

of cardiovascular disease (Libby, 2021). RNA binding protein 20 (RBM20) in particular is one of the best characterised RBP with a pathological role in heart. Mutations in RBM20 are linked to dilated cardiomyopathy, likely due to aberrant splicing of key cardiac genes like *titin* (TTN), which regulates myocardial passive stiffness and stretch sensing (Völkers et al., 2024). Additionally, RBM20 mislocalization and the formation of RNP granules in the cytosol caused by variants in the arginine–serine-rich region in RBM20 have also been suggested as a potential cause of dilated cardiomyopathy (Völkers et al., 2024). Additionally, RBP involvement in dysregulated mRNA translation results in increased protein synthesis during cardiac hypertrophy (Gudbjarnason et al., 1964).

The interaction between PDE3A1 and RBPs is particularly interesting for several reasons. It is possible that by interacting with RBP, PDE3A1 acts as a scaffold in multiprotein complexes, providing stability and ensuring the downstream activity of those specific RBPs. This is the case for the RNA binding protein SLFN12 (Lee et al., 2023; Wu et al., 2020), as described above. Another possibility is that, by interacting with the PDE and binding to RNA, RBPs ensure targeted localisation of PDE3A1 around RNA. This would allow hydrolysing of the local cAMP and formation of another cAMP nanodomain. This concept is not completely novel. Referred to as "moonlighting", it indicates hitherto-unknown connections between seemingly disparate cellular processes and unexpected "moonlighting" activities that proteins carry out in a highly compartmentalized cellular environment (Liao et al., 2016). For example, enzymes can moonlight to regulate mRNA utilization in response to co-factor or metabolite levels (Muckenthaler et al., 2008). An example of a dual-function protein moonlighting as an RNA-binding protein (RBP) is aconitase, which normally catalyzes the conversion of citrate to isocitrate. Under normal iron levels, aconitase functions as an iron–sulfur enzyme; however, in iron-deficient conditions, the disintegration of its iron–sulfur cluster disrupts enzymatic activity and induces a conformational change that enables RNA binding. In this state, cytoplasmic aconitase (encoded by ACO1) acts as iron regulatory protein 1 (IRP1), binding to the UTRs of transcripts such as ferritin and transferrin to regulate iron homeostasis (Balcerak

et al., 2019).

Conversely, RNA could affect enzyme activity, and, collectively, these interactions could form regulatory RNA-enzyme-metabolite networks. An example is yeast mitochondrial enzyme NAD^+-specific isocitrate dehydrogenase (IDH), which binds specifically to the 5' leader sequences of several mitochondrial mRNAs. Binding of these mRNAs to IDH inhibits its enzymatic activity (Hentze and Preiss, 2010). In particular, the hypothesis of a cAMP nanodomain in the proximity of RBP seems particularly likely as some RBP phosphorylation is affected upon inhibition of PDE, indicating that RBP phosphorylation state is regulated by a downstream effector of local cAMP under the control of PDE3 (Beltejar et al., 2017).

The importance of studying the interplay between PDEs and RBP is highlighted not only by their emerging role in cardiovascular disease, but also by their attractive therapeutic potential.

A summary of all the interactors that have been tested in this chapter is shown in Table 4.1. Figure 4.9 shows a schematic representation of the confirmed interactions with PDE2A2 and PDE3A1.

Chapter 5

PDE2A2 regulation of the fatty acid uptake machinery

5.1 Background

In Chapter 3, the interactions between PDE2A2 and several proteins that are involved in trafficking metabolic substrates were validated. In this chapter, the physiological significance of these interactions is investigated. I propose that PDE2A2 modulates the level of cAMP where the PDE2A2 interactors localise, which in turn regulates the trafficking of different metabolic substrates.

In particular, this chapter investigates whether PDE2A2 regulates the uptake of fatty acids (FA) by the mitochondria. FAs are the main fuel for the heart. (Opie, 2004). At the plasma membrane, long chain fatty acids (LCFA) are transported into the cytoplasm mainly by the fatty acid translocase CD36 (Fig. 5.1)(Coburn et al., 2001) and by the fatty acid transporter proteins (FATPs, or SLC27A) (Schaffer and Lodish, 1994). Here, SLC27A facilitates the efficiency of uptake by allowing LCFA to actively diffuse into the cell and by coupling with acyl-CoA-synthases (ACSL) (Richards et al., 2006). ACSLs esterify long-chain fatty acids, producing the less toxic acyl-CoAs. Some SLC27A isoforms can also localise at internal membranes. For example, SLC27A4 localizes to the endoplasmic reticulum and catalyses the esterification of FAs with CoA (Zhan et al., 2012).

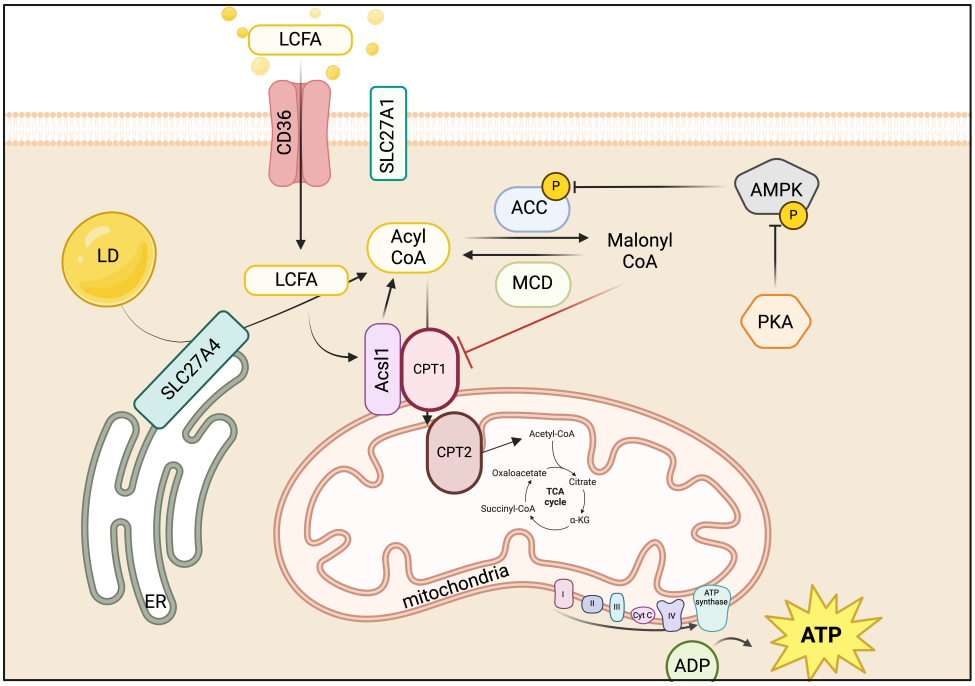


Figure 5.1. Schematic representation of FA uptake.
At the plasma membrane, long-chain fatty acids (LCFA) are transported into the cytoplasm by the translocase CD36 and SLC27A1. SLC27A4, localised at the endoplasmic reticulum (ER), facilitates uptake by coupling with ACSL (acyl-CoA synthases), which esterify LCFA into acyl-CoAs. CPT1 shuffles acyl-CoA into the mitochondria as acyl-carnitines. Acyl-carnitines are re-converted to acyl-CoAs by CPT2. LD=lipid droplet. CPT1 is inhibited by malonyl-CoA, synthesized from acetyl-CoA by ACC (acetyl-CoA carboxylase). AMPK (AMP-activated protein kinase) phosphorylates and inhibits ACC. AMPK is phosphorylated and inhibited by PKA (protein kinase A). Malonyl-CoA decarboxylase (MCD) catalyses the conversion of malonyl-CoA to acetyl-CoA. LCFA are stored into lipid droplets (LD);

As they cannot freely diffuse into the mitochondrial membrane, acyl-CoAs are translocated into the mitochondria via the carnitine shuttle. This consist of three elements: I) CPT1 (Carnitine palmitoyl-transferase 1); II) SLC25A20 (carnitine-acylcarnitine translocase, CACT); and III) CPT2 (Carnitine palmitoyl-transferase 2). In the first step, at the mitochondrial outer membrane, CPT1 catalyses the transfer of the acyl group from coenzyme A to carnitine to form palmitoyl carnitine which it shuttles into the inter mitochondrial space (MIS). Here, the carnitine acyl-carnitine translocase (CACT, or SLC25A20) carries them through the IMS in exchange for free carnitine. Finally, at the mitochondria inner membrane (MIM), carnitine palmitoyltransferase 2 (CPT2), converts the acyl-carnitines back to long-chain acyl-CoAs, where they enter the citric acid cycle (Fig. 5.2).

CPT1 catalyses the rate limiting step for the import of FA into the mitochondria. It is inhibited by Malonyl-CoA (Foster, 2012), which is produced from acetyl-CoA by acetyl-CoA carboxylase (ACC) (Tong, 2005). Phosphorylation of ACC by AMP Kinase (AMPK) inhibits the enzyme, ultimately resulting in decreased Malonyl-CoA production, increased CPT1 activity, and therefore increased FA oxidation (Saha and Ruderman, 2003) (Fig. 5.1).

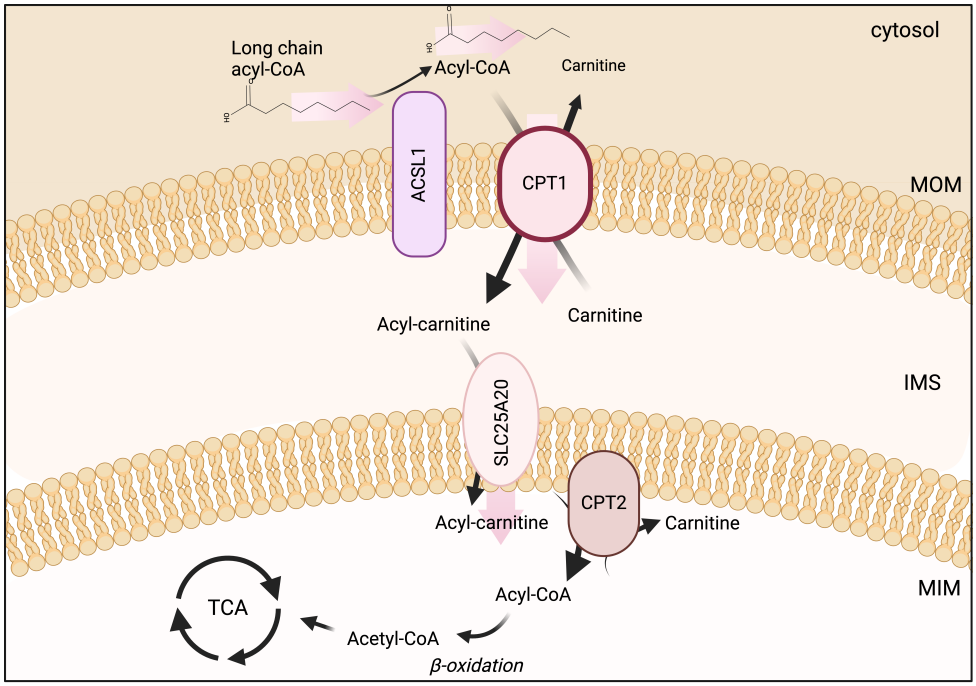


Figure 5.2. Schematic representation of FA uptake.
Acyl-CoAs are transported into the mitochondria via the carnitine shuttle, comprising. CPT1 (carnitine palmitoyl-transferase 1) transfers acyl groups to carnitine at the mitochondrial outer membrane (MOM), forming palmitoyl carnitine. SLC25A20 (CACT, carnitine acyl-carnitine translocase) shuttles acyl-carnitine across the inner mitochondrial membrane (IMM) in exchange for free carnitine. CPT2 (carnitine palmitoyl-transferase 2) converts acyl-carnitines back to acyl-CoAs at the IMM, enabling their entry into the citric acid cycle.

5.2 Aims

The aim of this chapter is to investigate whether PDE2A2 regulates the trafficking of FA destined for use as fuel for ATP production. In particular, by exerting its hydrolysing function on cAMP, PDE2A2 may define a nanodomain in control of the transport of FAs into the mitochondria.

This hypothesis is explored through a series of experiments that sequentially follow the mechanism of FAs transport through various steps. This is done in physiological conditions and upon modulating *PDE2A* expression and PDE2A activity:

i) At the outer mitochondrial membrane, the ability of CPT1 to shuffle FA into the mitochondria is measured.

ii) The capability of mitochondria to perform oxidative phosphorylation is quantified.

iii) In the cytosol, lipid droplets are quantified as a measure of FA accumulation.

iv) Whether the phosphorylation state of several targets of the FA import chain is modified is studied.

v) The effect on cellular respiration is investigated.

5.3 Does PDE2A modulate CPT1 activity?

Mass spectrometry (MS) analysis previously performed by the lab revealed CPT1A and CPT1B as a putative interactors of PDE2A2 (Subramaniam et al., 2023). In chapter 4, these interactions were verified by coimmunoprecipitation experiments in hiPSC-derived cardiac myocytes, as well as in neonatal cardiac myocytes and in HEK293T cells (Chapter 3: Fig. 3.3 and Fig. 3.4).

I hypothesised that the functional effect of these interactions relies on PDE2A2 regulating a pool of cAMP where CPT1 localises, in charge of modulating the mitochondrial trafficking of FAs. In order to investigate this hypothesis, the activity of CPT1 was measured upon manipulation of *PDE2A* expression and on PDE2A activity.

I assessed the activity of CPT1 by colorimetric assay (Chapter 2). This spectrophotometrically measures the change in colour of DTNB (5,5'-dithio-bis-(2-nitrobenzoic acid)) over time, which, in the presence of free thiols, is converted into TNB. For these experiments, DTNB and palmitate are added to cell lysates. Upon the addition of carnitine, CPT1 in the lysate converts acyl-palmitates into acyl-carnitines, releasing CoA (containing free thiols), resulting in DTNB being converted into TBN. The

increase of TNB, read at 412 nm, is measured over time, from which the rate of reaction of CPT1 can be deducted. As CPT1 is the only enzyme that converts acyl-palmitates into acyl-carnitine, it can be assumed that the rate of reaction reflects the activity of CPT1. First, the activity of CPT1 was measured in tissue from a mouse heart which presented a cardiac specific knock out (KO) for *PDE2A*. In the *PDE2AKO* tissue CPT1 activity is reduced (Fig. 5.3) compared to tissue from mice without the mutation (wildtype, WT). Each data point represents the activity of CPT1. This is obtained from a serious of steps. First, the absorbance of TNB is read over time. These value are then converted in data points representing the concentration of TNB through Beer Lambert's law (see chapter 2). The concentration values are plotted and one-phase association curve is fitted for each curve. This provides several values, including the span and the association rate constant (K). The activity of CPT1 is obtained by timing the span and K. An example of the concentration curve is shown in Fig.5.4, which originates from one of the data points from the graph in Fig. 5.3.

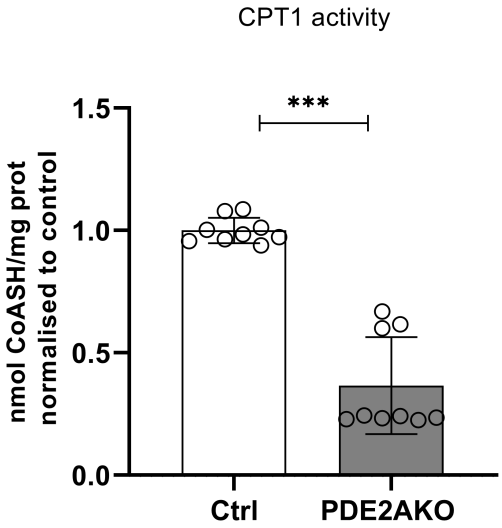


Figure 5.3. CPT1 activity was reduced in PDE2AKO mouse heart tissue.
CPT1 colorimetric assay detected a decrease in CPT1 activity in heart tissue from mice with a cardiac specific knock out for *PDE2A* compared to wildtype heart tissue. n=3 different hearts. Each data point represents a technical repeat. Hierarchical analysis model in R using Ime4 package with Bonferroni correction, Tukey p value $p<0.005$ ($p= 0.00000000313$).

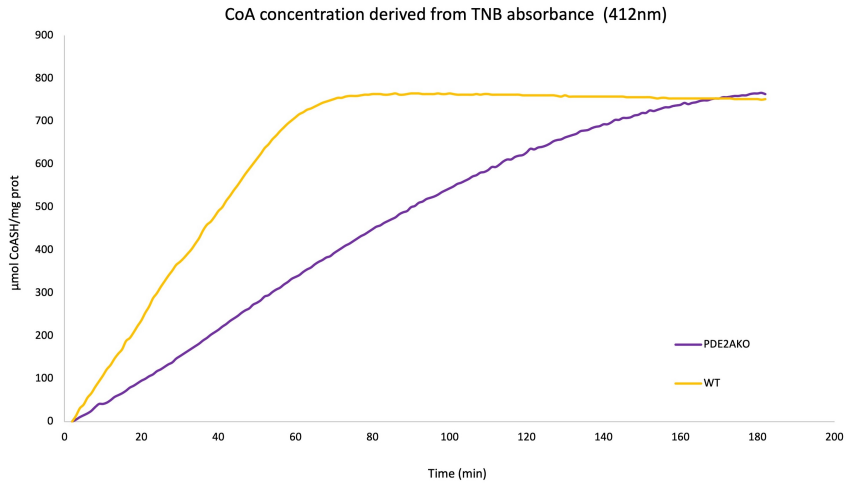


Figure 5.4. Representative curve of CoA concentration curve used in the CPT1 activity assay.
Absorbance values of TNB were recorded over time and converted to concentration values using Beer-Lambert's law and plotted. The curves displayed are fitted with a one-phase association model, yielding span and association rate constant, used to calculate CPT1 activity.

The reduction in CPT1 activity suggests that PDE2A may play a role in regulating the uptake of FA. Based on these results it is possible that the regulation of CPT1 is dependent on the physical presence of PDE2A or on the PDE hydrolysing activity. To elucidate on this, I used a pharmacological approach to specifically inhibit PDE2A enzymatic activity with BAY 60-7550. BAY 60-7550 was applied at a concentration of 10 nM, which specifically inhibits PDE2A without also inhibiting other PDEs (PDE1 and PDE5) (Boess et al., 2004). CPT1 activity was measured in adult rat ventricular myocytes (ARVM). CPT1 activity is reduced upon BAY 60-7550 treatment in ARVM, to a similar level to etomoxir treatment, a pharmacological inhibitor of CPT1 (An et al., 2022) (Fig. 5.5a). Etomoxir concentration was fixed at 40 μM, a concentration used in the literature to inhibit CPT1 (Laudette et al., 2021). The decreased in CPT1 activity observed in ARVM is recapitulated in mouse embryonic fibroblasts lacking *PDE2A* (MEF$^{Pde2a-/-}$) compared to wildtype MEF (Fig. 5.5b). The employment of MEF is due to the fact that they were the only available cell line with the *PDE2A KO*.

Inhibiting PDE2A pharmacologically will only affect the enzymatic activity of the PDE, but will not displace it. Therefore, the decrease in CPT1 activity observed upon PDE2A inhibition suggests that CPT1 function is dependent on PDE2A hydrolysing activity rather

than PDE2A presence at the MOM.

Having established that PDE2A enzymatic activity has an impact on CPT1 activity, it was important to understand whether this PDE is active at baseline level, keeping homeostasis, or if it modulates levels of cAMP generated as a result of hormonal stimulation, for example, β-adrenergic stimulation.

In order to investigate this, the CPT1 assay performed in ARVM upon addition of 0.1 nM of isoproterenol, a β-adrenergic agonist which results in the generation of cAMP. Here, a decrease in CPT1 activity is observed (Fig. 5.5a), to a similar level to etomoxir and BAY 60-7550 treatment. This suggests that PDE2A hydrolysing activity at the MOM is a result of catecholaminergic stimulation.

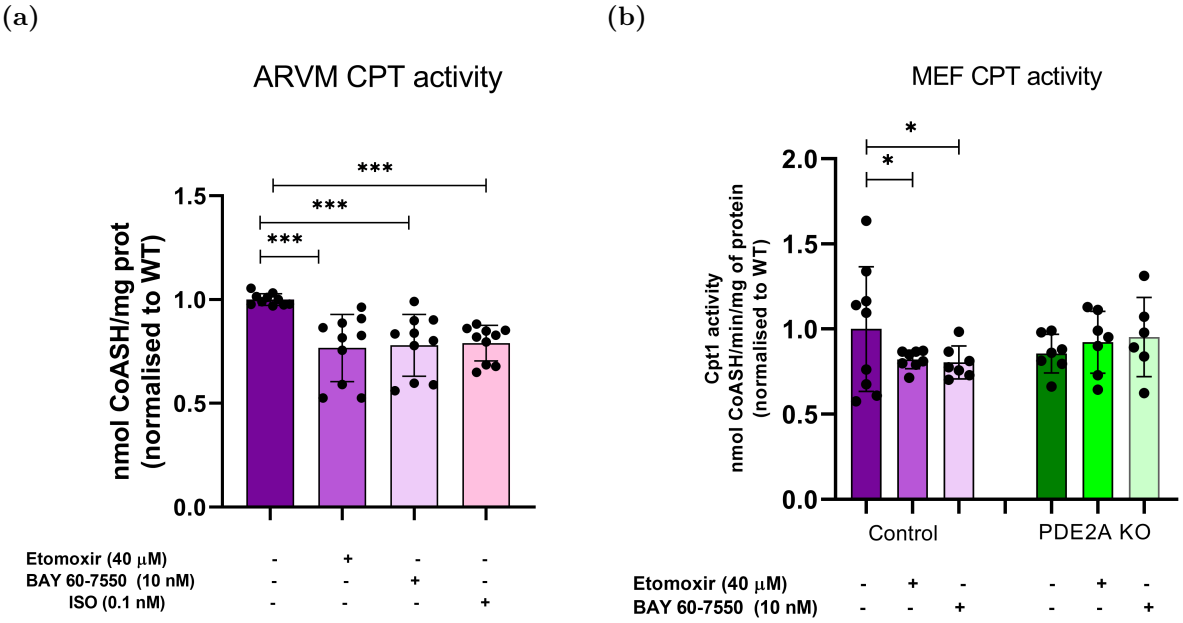


Figure 5.5. CPT1 activity was reduced upon PDE2A absence and inhibition, and upon catecholaminergic stimulation.
a) ARVM: CPT1 activity was decreased upon PDE2A inhibition with BAY 60-7550 10 nM for 30 minutes. CPT1 activity was also decreased upon β adrenergic stimulation obtained with 0.1 nM isoproterenol for 10 minutes. Etomoxir treatment of 40 uM for 30 minutes. n=3 different hearts. Each data point represents a technical repeat. Hierarchical analysis model in R using Ime4 package with Bonferroni correction. Tukeys p-values for ***<0.005
b) MEF: CPT1 activity was decreased in PDE2A KO mouse embryonic fibroblasts and in fibroblasts treated with BAY 60-7550 10 nM for 24 hours. $n \geq 6$. Each data point represents an experiment. Two-way-ANOVA. P-values ctrl vs etomoxir p=0.048, ctrl vs BAY 60-7550 p=0.02

PDE2A is a cyclic GMP-stimulated phosphodiesterase that hydrolyses both cAMP and cGMP, albeit with low affinity (Lobo and Zaccolo, 2018). Therefore, the decreased activity observed upon absence or inhibition of PDE2A could be due to the action of either second messenger. In order to assess whether CPT1 action is dependent on the cAMP or cGMP signalling pathway, CPT1 activity was measured upon PKA inhibition by PKI (PKA Inhibitor 14-22 Amide, myristoylated). PKA is an effector of the cAMP pathway, but not of the cGMP pathway. Therefore, if a change on CPT1 activity is observed upon PKA inhibition, this suggests that the effect observed above is PKA dependent, and consequenlty, cAMP (rather than cGMP) dependent. As there was a significant increase in CPT1 activity in ARVM (Fig. 5.6a), it is likely that it is cAMP signalling regulating the activity of CPT1 through the activity of PKA. The decrease in CPT1 activity is lost when BAY 60-7550 is applied together with PKI. The activity of CPT1 in fact, is comparable to PKI treatment alone (Fig 5.6b).

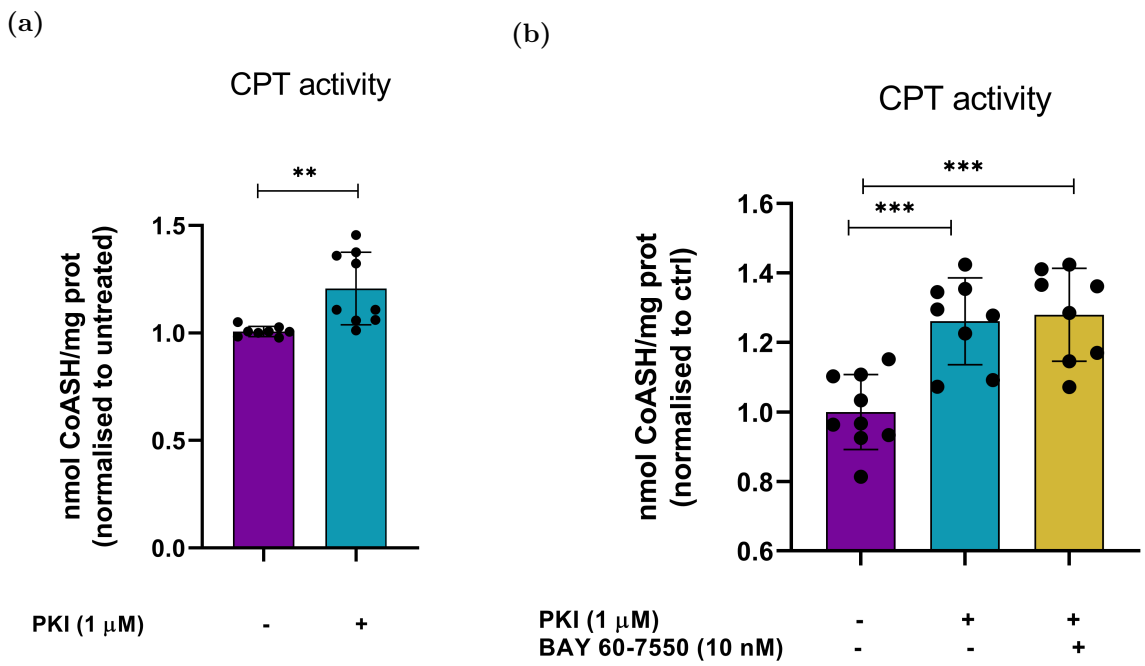


Figure 5.6. CPT1 activity is increased upon PKA inhibition.
a) CPT1 activity was increased in ARVM upon PKA inhibition with PKI 1 uM for 30 minutes. n=3 different hearts. Each data point represents a technical repeat. Hierarchical analysis model in R using Ime4 package with Bonferroni correction. Tukeys p-values <0.005
b) The effect of PDE2A inhibition on CPT1 activity is lost upon joint BAY 60-7550 and PKI treatment. n=3 different hearts. Each data point represents a technical repeat. Hierarchical analysis model in R using Ime4 package with Bonferroni correction. Tukeys p-values <0.005. P-values ctrl vs PKI=0.0002463; ctrl vs PKI+BAY=0.00008212; PKI vs PKI+BAY=0.8974467

5.4 Does PDE2A affect CPT1 activity through a malonyl CoA/acetyl-CoA carboxylase axis?

CPT1 catalyses the rate limiting step for the import of FA into the mitochondria. It is inhibited by malonyl-CoA (Foster, 2012), which is produced from acetyl-CoA by acetyl-CoA carboxylase (ACC) (Tong, 2005). Phosphorylation of ACC by AMP Kinase (AMPK) inhibits the enzyme, ultimately resulting in decreased Malonyl-CoA production, increased CPT1 activity, and thus, increased FA oxidation (Saha and Ruderman, 2003). PKA in turn phosphorylates AMPK, inhibiting its activity (Djouder et al., 2010).

From my results, PDE2A absence or inhibition results in decreased activity of CPT1. I

hypothesised that this effect may be a result of an alteration of the malonyl CoA/ACC axis. In particular, a reduction in PDE2A results in an increase in cAMP and consequently increased PKA activity. AMPK phosphorylation by PKA should therefore increase as well, resulting in decreased phosphorylation of ACC. ACC activity should increase, and augment the production of malonyl CoA, ultimately inhibiting the activity of CPT1 (Fig. 5.7a). To test this hypothesis, the level of ACC phosphorylation was tested. It is expected that a reduction of ACC phosphorylation is observed upon cAMP increase (Fig. 5.7b).

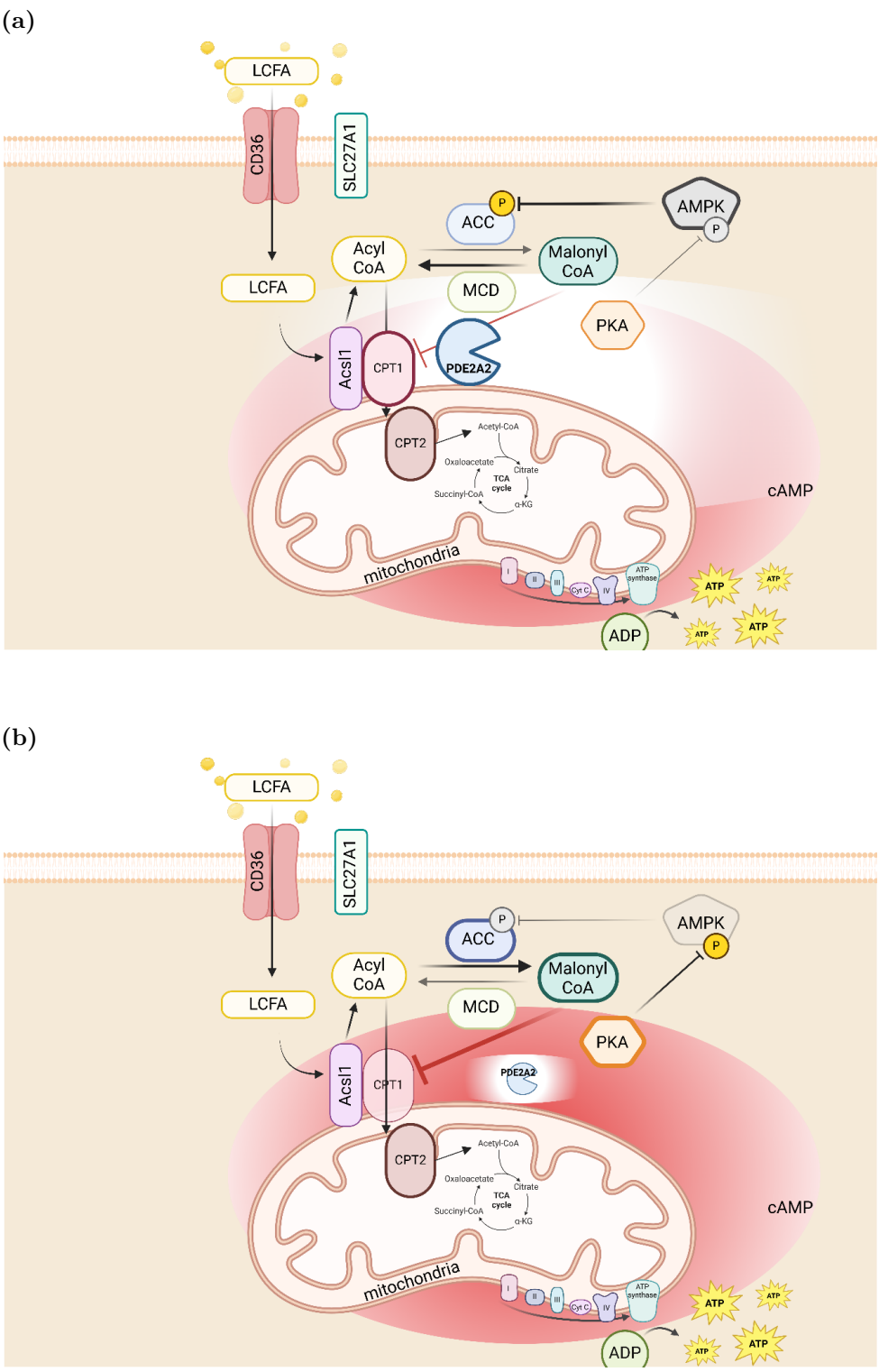


Figure 5.7. Schematic representation of the proposed mechanism of CPT modulation by PDE2A.

a) PDE2A is present and active, keeping the level of cAMP at bay. PKA activity is reduced, and the inhibitory PKA-dependent phosphorylation of AMPK is lower. AMPK phosphorylates ACC, inhibiting its catalysis of malonyl CoA. Lower malonyl CoA concentrations result in higher CPT1 activity.

b) PDE2A is absent or inhibited, and the levels of cAMP rise accordingly. PKA activity is high, phosphorylating and inhibiting AMPK. The inhibitory AMPK-dependent phosphorylation of ACC is reduced. ACC catalyses the production of malonyl CoA, resulting in decreased CPT1 activity.

The phosphorylation on ACC was tested on lysate from neonatal rat ventricular myocytes (NRVM). These cells were used as the they were the closest model available in the lab at the time of the experiment. The specificity of the ACC and phosphorylated-ACC (p-ACC) antibody was tested by western blot, which revealed a band at the expected molecular weight of 280 kDa (Fig. 5.8b). NRVM were treated with 25 μM forskolin, an adenylyl cyclase activator, for 10 minutes, to increase the level of intracellular cAMP (this is the cAMP saturating concentration) (Fig. 5.8b). No change in the level of phosphorylation is observed between treatment and control (non-treated cells) (Fig. 5.8). It may not be simple to experimentally detect a decrease in phosphorylation if the effect is either very small, or the baseline phosphorylation already low. Therefore, NRVM were treated with AICAR (100μM), an AMPK activator, for 24 hours. After AICAR treatment alone, ACC phosphorylation increased. However, upon simultaneous activation of AMPK and cAMP, a decrease in ACC phosphorylation was observed. This result suggests that the change in ACC phosphorylation is regulated by cAMP.

(a)

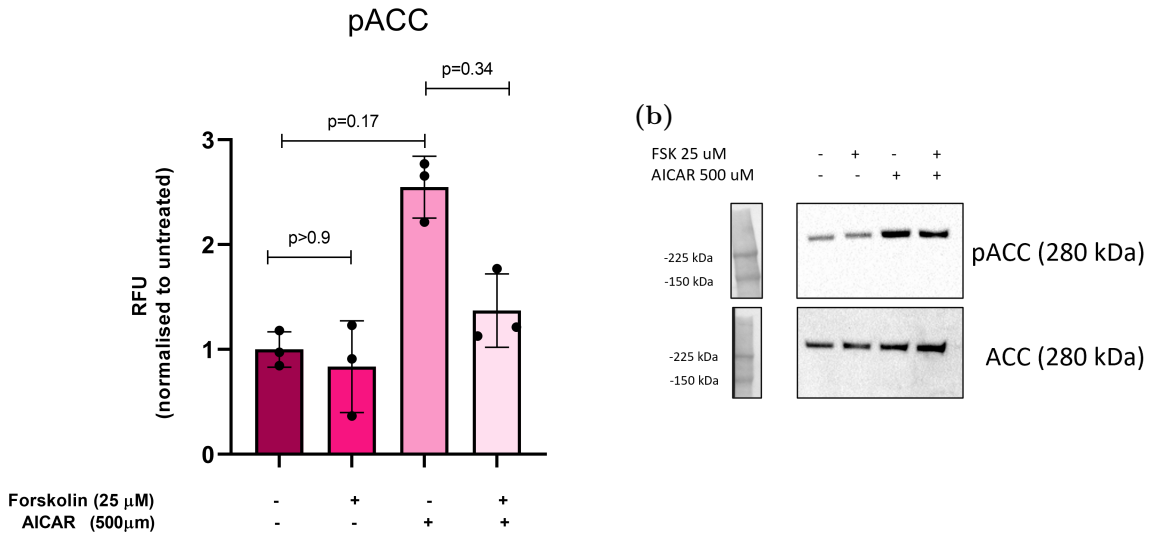


Figure 5.8. An increase in cAMP paired with AMPK activation results in decreased ACC phosphorylation.
a)Densitometric quantification of the western blots. NRVM lysate shows no change in ACC phosphorylation upon cAMP increased (with 25 μM forskolin) in basal conditions. AMPK activation through AICAR (100μM) results in increased ACC phosphorylation. Joint AICAR and forskolin treatment results in decreased ACC phosphorylation compered to AICAR treatment only.
b) Representative western blot.
n=3 independent isolations. Each isolation included 12 pups from 2 different mothers. Frideman test with Dunn's correction(matched, non parametric One-way-ANOVA).

In order to assess whether the reduced phosphorylation of ACC is modulated by PDE2A hydrolysing activity, the phosphorylation level of ACC was measured upon BAY 60-7550 treatment (10 nM for 30 minutes). Indeed, ACC phosphorylation is decreased upon PDE2A inhibition (Fig. 5.9). Surprisingly, inhibiting PKA (PKI 1 μM for 30 minutes) as well as PDE2A simultaneously results in decreased ACC phosphorylation, to a comparable level to PDE2A inhibition alone (Fig. 5.9). Follow up experiments could elucidate on these contrasting results.

(a)

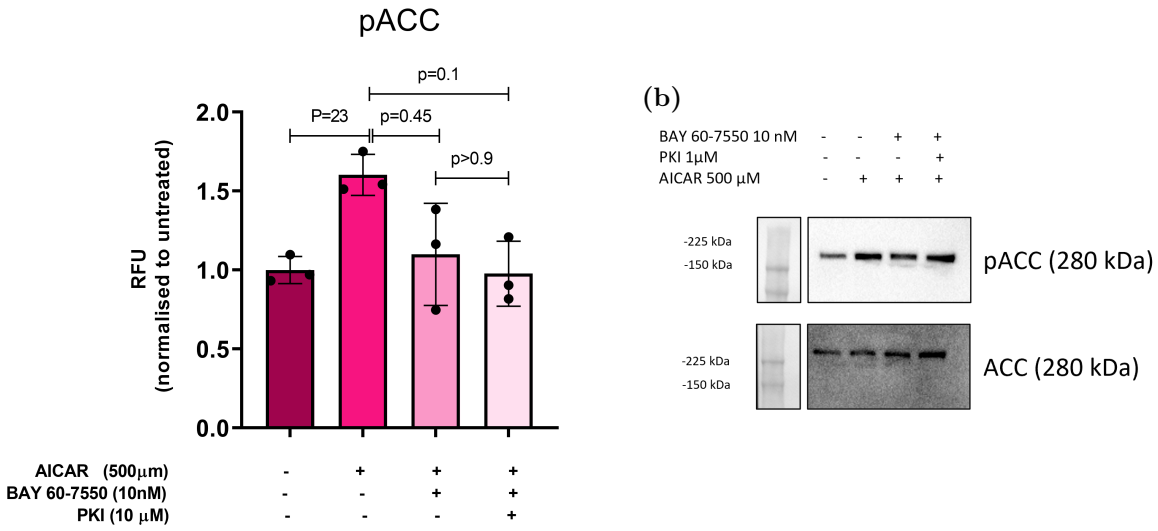


Figure 5.9. ACC phosphorylation is decreased upon cAMP increase.
a) Densitometric quantification of the western blots. NRVM lysate reveals that the phosphorylation of ACC decreases upon joint treatment of AICAR (100μM) and BAY 60-7550 (10 nM). The level of ACC phosphorylation is decreased upon simultaneous treatment of AICAR (100μM M), BAY 60-7550 (10 nM) and PKI (1μM) compared to AICAR treatment alone.
b)Representative western blot.
n=3 independent isolations. Each isolation included 12 pups from 2 different mothers. Frideman test with Dunn's correction(matched, non parametric One-way-ANOVA).

Overall, this data supports the hypothesis that the decrease in CPT1 activity upon PDE2A inhibition could result from an alteration of ACC phosphorylation, and consequently, activity.

5.5 Is PDE2A required for CPT1A expression?

Having observed a reduction in the activity of CPT1 with either an absence or inhibition of PDE2A, it can be hypothesised that this effect is due to different levels of CPT1 expression. To test this, absolute CPT1A protein levels were measured by western blot. MEF from animals with a cardiac specific knockout of the *pde2a* gene (MEF$^{Pde2a-/-}$) were compared to fibroblasts from wildtype mice (MEF^{WT}). The ability of the CPT1A antibody to detect the endogenous protein was confirmed by western blot on whole cell lysate (WCL),

where a band of the expected size (86 kDa) was observed (Fig. 5.10b). The level of CPT1A was normalised to the expression levels of GAPDH, used as a loading control (Fig. 5.10a). CPT1A expression was lower in the MEF$^{pde2a-/-}$, even if the mitochondria level were unchanged, measured by probing for the voltage-dependent anion channel (VDAC) (Fig. 5.10). This is a protein localised at the MOM, used to quantify the mitochondria present in the two cell lines. VDAC antibody specificity was also tested on whole cell lysate, revealing a band at the expected molecular weight (35-37 kDa) (Fig. 5.10b). These results indicate that the expression of CPT1 may be modulated by PDE2A, where absence of PDE2A results in dysregulation of CPT1 expression. The mechanism through which this may happen was not investigated further because of time constrains.

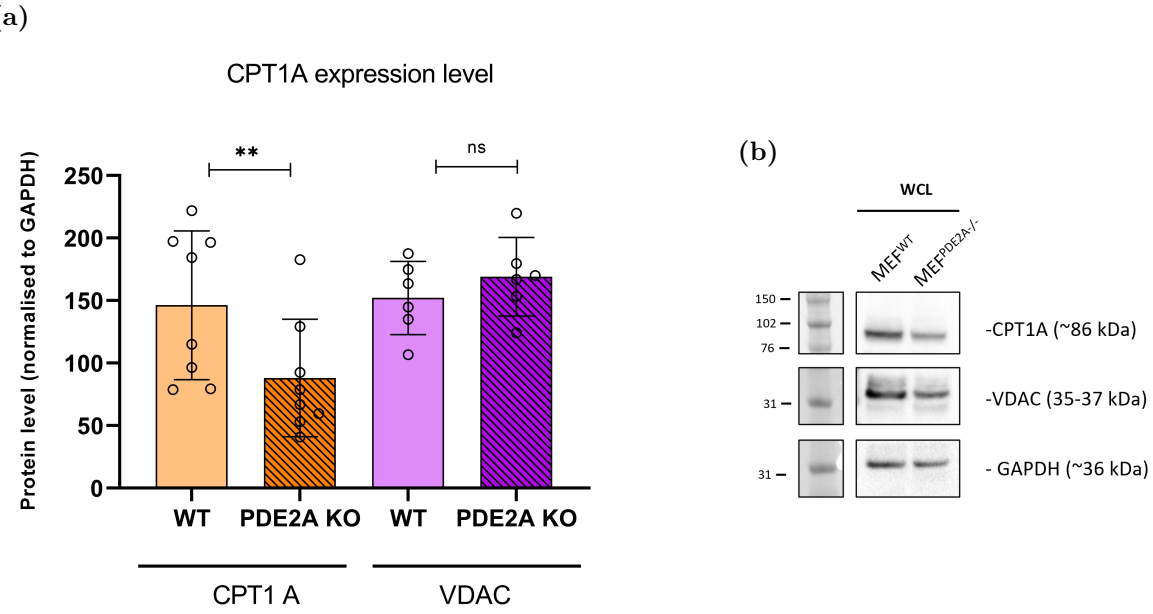


Figure 5.10. CPT1A protein expression in downregulated in MEF$^{pde2a-/-}$.
a)Densitometric quantification of the western blots. CPT1A protein level was downregulated in MEF$^{pde2a-/-}$ when normalised to total protein content (GAPDH). No change is detected between WT and PDE2AKO VDAC. Wilcoxon matched-pairs test (non-parametric t-test). p values CPT1A: WT vs PDE2AKO p=0.007; VDAC: WT vs PDE2AKO p=0.56 levels, indicating unchanged mitochondrial content.
b) Representative image of a western blot experiment used for the quantification.
$n \geq 6$.

5.6 Does PDE2A regulate fatty acid oxidation?

CPT1 activity diminishes when cAMP is increased, upon PDE2A inhibition or absence. This should result in less FA being imported into the mitochondria, and a decrease in FA oxidation (FAO). To test this hypothesis, a radiolabelled FA assay was performed (Fig. 5.11). These experiments were developed in collaboration with Dr Ujang Purnama from the group of Associate Professor Carolyn Carr. The assay measures oxidative phosphorylation based on the supplementation and extraction of radiolabelled FA. It provides measures of either oleic acid (OA) or palmitic acid (PA). Both were tested in ARVM and MEF to establish which substrate would be a better candidate for this experiment. In ARVM, palmitic acid showed a higher mitochondrial oxidation compared to oleic acid (Fig. 5.11a), and therefore was used for the following experiments. On the other hand, palmitic acid and oleic acid oxidation did not differ in fibroblasts (Fig. 5.11b), and oleic acid was used instead as this was the FA mainly used by the lab at the time. ARVM$^{pde2a\text{-}/\text{-}}$ show a significantly reduced FAO compared to wildtype (Fig. 5.11c). The same finding is confirmed in MEF (Fig. 5.11d). This confirms that absence of PDE2A impairs FA oxidation. The magnitude of the change appears to be much more significant in ARVM than in MEF. This could be because myocytes rely heavily on FAO as their primary energy source under normal conditions. Therefore, the disruption of the FAO pathway would have a much more pronounced effect in cardiomyocytes, as their baseline metabolic dependency on this pathway is higher compared to fibroblasts which rely more on glycolysis for energy production.

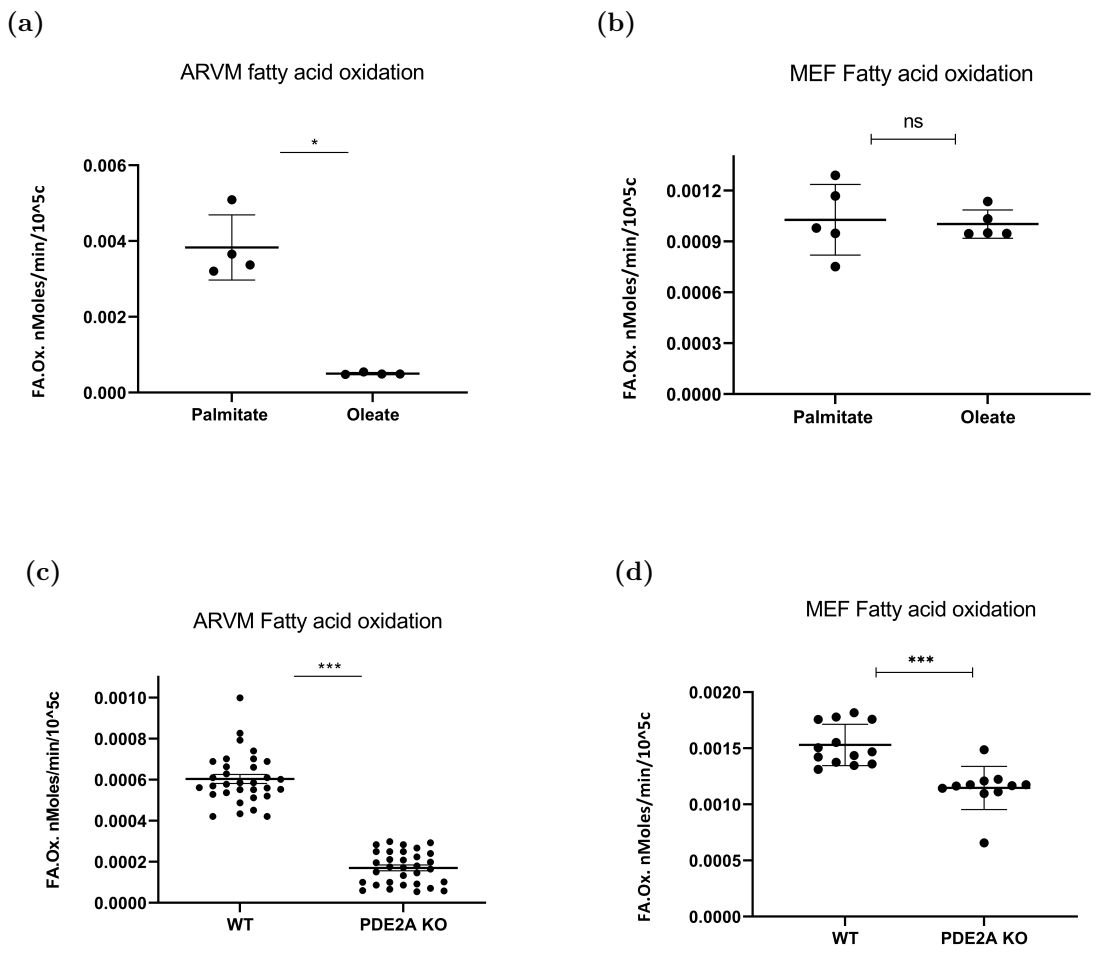


Figure 5.11. Mitochondrial FA oxidation in reduced in the absence of PDE2A.
a) PA showed a higher mitochondrial oxidation compared to OA in adult rat ventricular myocytes (ARVM). Mann-Whitney test (non-parametric *t*-test) p=0.02 n=1
b) PA and OA mitochondrial oxidation was not significantly different in mouse embryonic fibroblasts (MEF). n=1.
d) ARVM$^{pde2a\text{-}/\text{-}}$ showed reduced PA mitochondrial oxidation compared to WT. n=3 different hearts Mann-Whitney test (non-parametric *t*-test) p=0.0001 . P<0.005
e) MEF$^{pde2a\text{-}/\text{-}}$ showed reduced OA mitochondrial oxidation compared to WT. n=3 Wilcoxon matched-pairs test (non-parametric *t*-test). P<0.005

5.7 Does impaired mitochondrial FA oxidation result in FA accumulation in the cytosol?

Previous work in this chapter demonstrated that cAMP regulates the uptake of FA into the mitochondria. I hypothesised that the reduced FA oxidation efficiency observed upon

absence of PDE2A (Fig. 5.11) may result in accumulation of FA in the cytosol, which would be stored in lipid droplets (LD). Measuring LDs therefore, can be a readout of accumulation of FA in the cytosol. Therefore, I measured LD in MEF$^{pde2a\text{-}/\text{-}}$ by staining them with the lipid dye LipidTox. An increase in both LD number and total LD area is observed in MEF$^{pde2a\text{-}/\text{-}}$ compared to the MEF$^{\mathrm{WT}}$(Fig. 5.12).

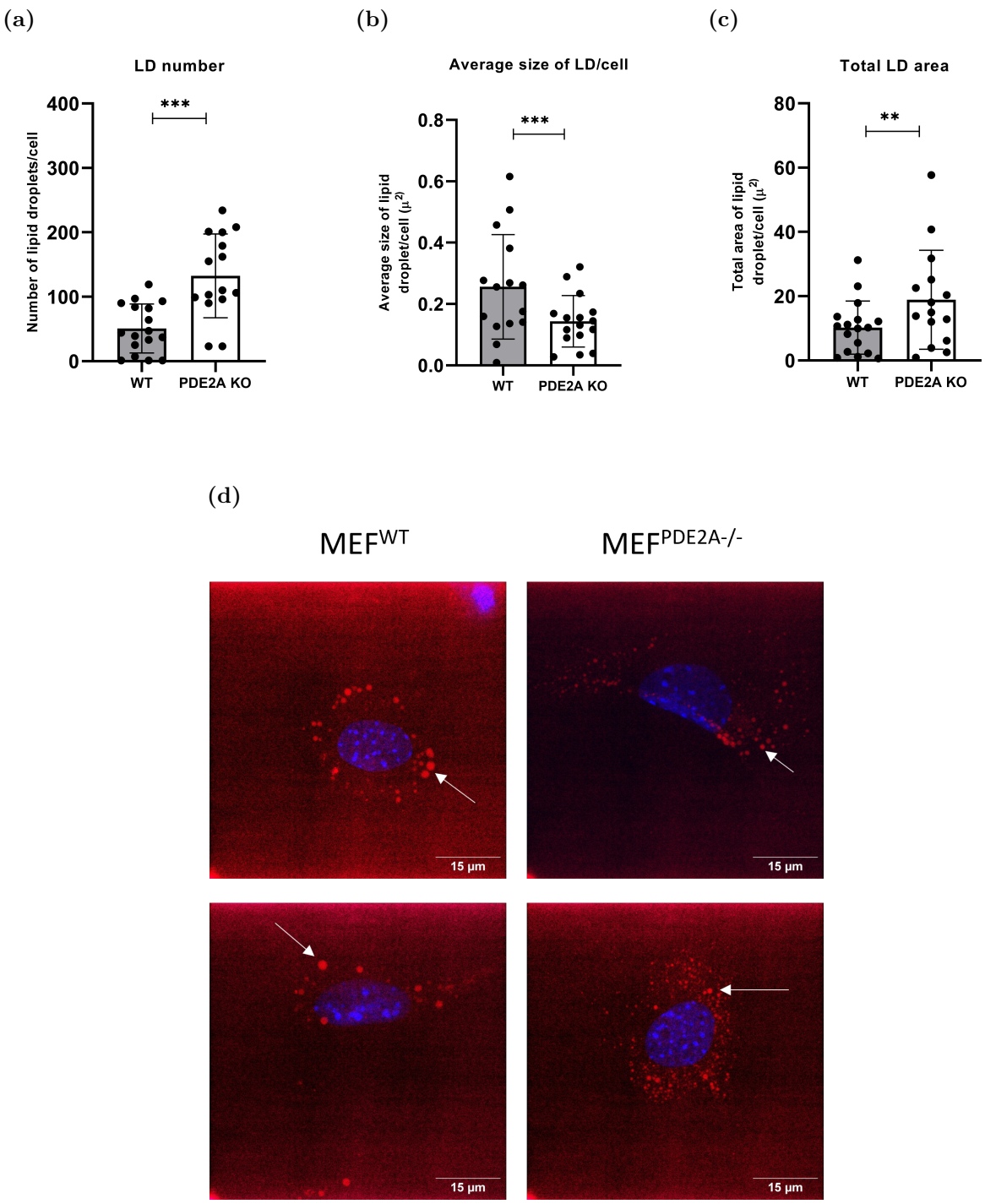


Figure 5.12. Absence of PDE2A results in accumulation of LD in the cytosol of MEF.

a) Lipid droplet number p=0.002 and b) total lipid droplet area is increased in MEF$^{pde2a-/-}$ compared to MEF^{WT}. p=0.017

c) The average lipid droplet size is decreased in MEF$^{pde2a-/-}$. p=0.02

d) Representative images of MEF^{WT} and MEF$^{pde2a-/-}$. White arrows indicate LDs. LipidTox 1:200 staining in red for the lipid droplets, and DAPI in blue staining the nucleus. Hierarchical analysis model in R using lme4 package with Bonferroni correction. n=2 Each dot represents a measurement per cell.

Droplet staining on NRVM, used as a more physiologically relevant model, also show an increase in LD number and total LD area in cells treated with 10 nM BAY 60-7550 for 6 hours (Fig. 5.13). Sodium oleate (NaOl) is used as a control, as treatment of NaOl at 200 μM for 6 hours induces LD biogenesis (Zadoorian et al., 2023). The effect of PDE2A inhibition in NRVM on LD biogenesis is much more severe than the effect of PDE2A absence on MEF.

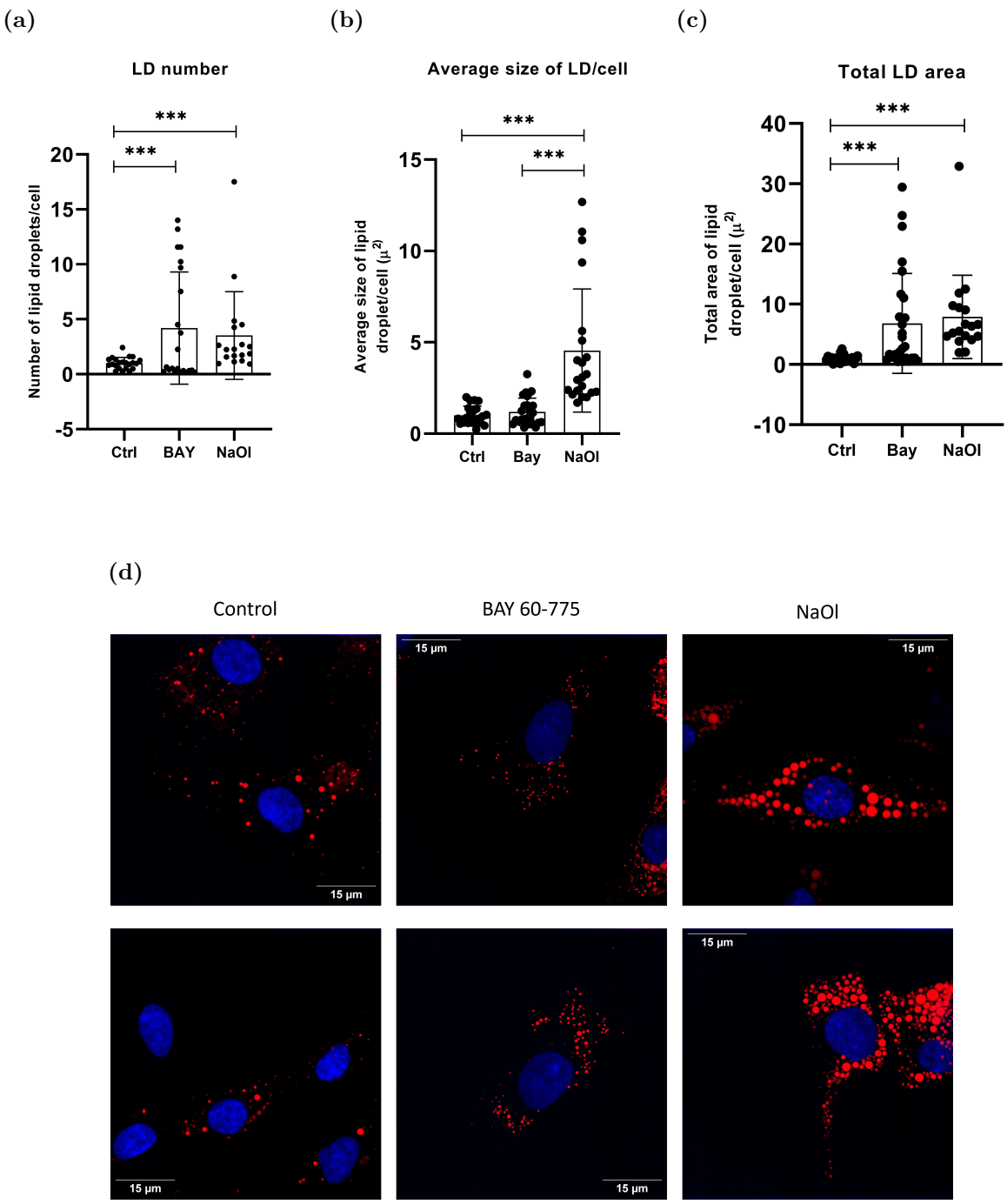


Figure 5.13. Inhibition of PDE2A results in accumulation of LD in the cytosol of NRVM.

a) Lipid droplet number and b) total lipid droplet area is increased in NRVM treated with 10 nM BAY 60-7550.

c)The average size of the LD is unchanged.

d)Representative images of NRVM. White arrows indicate LDs. LipidTox 1:100 staining in red the lipid droplets, and DAPI in blue staining the nucleus. n=3 independent isolations. Each isolation included 12 pups from 2 different mothers. Hierarchical analysis model in R using Ime4 package with Bonferroni correction p value <0.005.

5.8 Could the PDE2A-dependent cAMP nanodomain regulate PLIN 5 activity through PLIN 5 phosphorylation?

FA are essential players in cardiac metabolism, as they are the main fuel of the heart, with 70%- 90% of the mitochondrial ATP being generated in the mitochondrial matrix through β-oxidation (Neely et al., 1972). In the cytoplasm, they are stored in lipid droplets. Perceived only as fat reservoirs for a long time (Fawcett, 1966), LD have emerged in recent years as fully entitled organelles with key functions in lipid and energy homeostasis (Farese and Walther, 2009). LD play a central role in lipid metabolism by regulating the balance between lipid storage and mobilisation (Olzmann and Carvalho, 2019). Perilipins (PLIN) are a family of proteins that coat LD and serve many functions, including regulation of lipolysis and controlling lipotoxicity (Itabe et al., 2017). Perilipin 5 (PLIN5) is the isoform mainly expressed in muscle and heart tissue and, upon phosphorylation by PKA at serine 155, is responsible for tethering LD to mitochondria (Miner et al., 2023). PLIN5 interacts with SLC27A4, promoting efficient channelling of FAs from LDs to mitochondria (Miner et al., 2023). This is relevant to my study for two reasons. Firstly, I have shown that SLC27A4 interacts with PDE2A2 (Chapter 3, Fig. 3.14). Secondly, the phosphoproteomic analysis in the study by Subramaniam *et al.*, identifies a series of proteins whose phosphorylation was upregulated upon inhibition of PDE2A by BAY 60-7550, and found PLIN5 to be one of them (Subramaniam et al., 2023). Interestingly, the phosphorylation site upregulated upon on BAY 60-7550 treatment is at serine S17 which was not previously known to be phosphorylated. The amino acid sequence adjacent to S17 identified by the MS analysis was DQRGKDTTLALHSRMSGDQTAQDPGSSLGEL, which is suspected to contain a non-canonical PKA substrate motif. I hypothesised that S17 of PLIN5 is phosphorylated by PKA. It is possible that this phosphorylation regulates some aspects of LD anchoring or biogenesis, as PKA phosphorylation at a different site (S155) affects LD-mitochondria anchoring. I next sought to confirm this by investigating PLIN5 phosphorylation at S17 by PKA (Miner et al., 2023).

Ideally, these experiments would entail lysing the cells and detect the phosphorylation of a protein with an antibody that recognises the phosphorylated protein. As there is no commercially available antibody for phosphorylated-PLIN5, HEK293T cells were transfected with a plasmid encoding the fusion protein PLIN5-GFP, then immunoprecipitated with anti-GFP nanobody conjugated to agarose beads (GFP-Trap). The immunoprecipitate was probed with an anti-phospho-PKA substrate antibody which detects proteins phosphorylated by PKA at a serine (S) or threonine (T) [P(S/T)PKA]. Confirmation of the fusion protein presence was achieved by western blot, where an anti-GFP antibody reveals a band at the expected molecular weight (79 kDa) (Fig. 5.14b). The MS analysis revealed an increase in phosphorylation of PLIN5 upon inhibition of PDE2A by BAY 60-7550 at a concentration of 1μM. I treated the cells expressing PLIN5-GFP with BAY 60-7550, however using the lower concentration of 10 nM. This is because it is now known that concentrations of BAY 60-7550 higher than 10 nM inhibit not only PDE2A, but also PDE1 and PDE5 (Boess et al., 2004). This was then compared the phosphorylation of PLIN5 in basal condition (DMSO cells), or upon cAMP increase dependent on I) adenylyl cyclase activation (forskolin treatment), or II) non-specific PDE inhibition (3-isobutyl-1-methylxanthine (IBMX) treatment, a non-selective phosphodiesterase inhibitor).

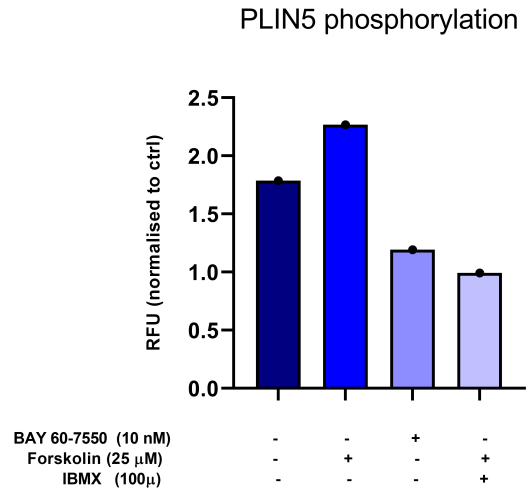
GFP antibody efficiency was tested by western blot on the whole cell lysate, where a band at the expected molecular weight was revealed (Fig. 5.14b). GFP immunoprecipitate probed with the same antibody confirms the presence of PLIN5-GFP fusion protein in the pull-down (Fig. 5.14b).

Probing the immunoprecipitate with P(S/T)PKA antibody reveals a band at the correct molecular weight of PLIN5, suggesting that PKA does phosphorylate the protein. The signal is increased upon BAY 60-7550 treatment, confirming the results from the phosphoproteomic study. However, when controlling for the amount of PLIN5 expressed by the cells, detected by probing the membrane with an anti-GFP antibody, the difference between treatment groups is lost. Interestingly, the P(S/T)PKA antibody reveals another band at a different molecular weight (around 31 kDa)(Fig. 5.14b), where the signal in

the BAY 60-7550 lane appears to be stronger. It is possible that BAY 60-7550 at a concentration of 10 nM is not enough to elicit an effect on PLIN5 phosphorylation. It is also likely that the detection of the changes in phosphorylation was not successful, since no change in PLIN5 phosphorylation is detected upon addition of forskolin 25 μM and IBMX 100 μM, which should result in saturating concentration of cAMP and therefore maximal PKA dependent phosphorylation. This experiment would need to be repeated as it was only attempted once.

The phosphorylation effect on PLIN5 was not studied further due to time constraints.

(a)



(b)

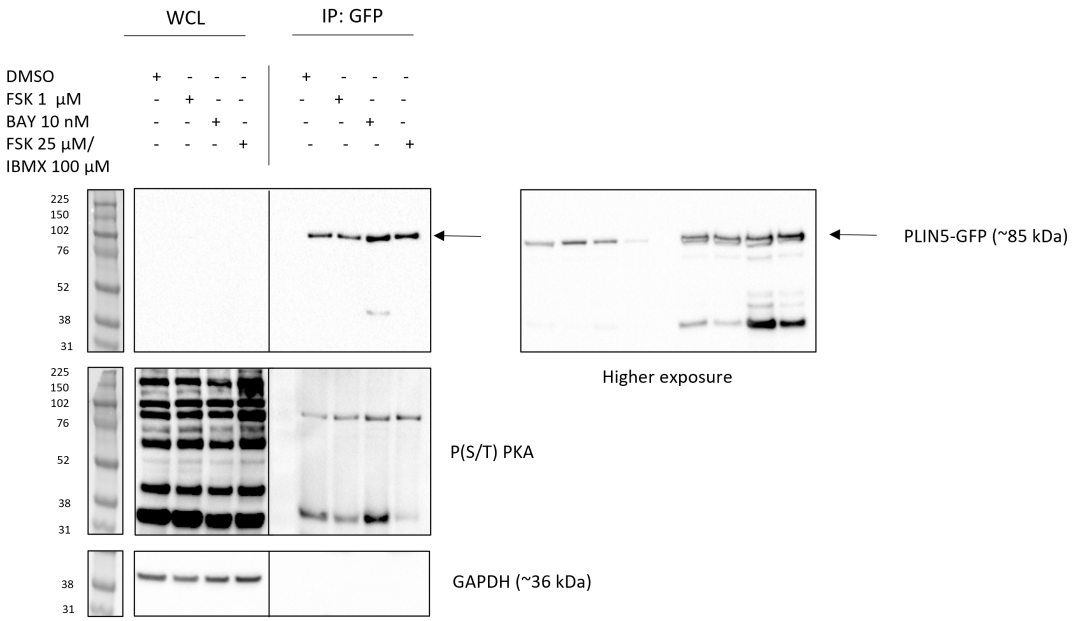


Figure 5.14. Western blot analysis of Perilipin 5 phosphorylation upon cAMP increase.
a) Densitometric quantification of the western blot.
b)PLIN5-GFP immunoprecipitate from HEK293T probed with P(S/T) antibody fails to show an increased in PLIN5 phosphorylation. The arrow indicates the band which corresponds to PLIN5-GFP molecular weight of (~85 kDa). n=1 The image on the right hand side is the same membrane exposed for a longer period of time in order to reveal the bands at PLIN5-GFP in the whole cell lysate. (~85 kDa). n=1

5.9 Does inhibition of PDE2A increases ACSL1 phosphorylation?

Upon intracellular translocation, FA are activated to long-chain acyl-CoAs (LCACoAs) by ACSLs, which catalyse the ATP-dependent ligation of FA to coenzyme A (Mashek and Coleman, 2006). LCACoAs are substrate for the downstream pathway that metabolises FA and produces the necessary ATP for the heart to perform its pump activity (Li et al., n.d.). There are five different isoforms of ACSL, with ACSL1 being the predominant isoenzyme, expressed mainly in adipose tissue, liver, and heart; (Mashek and Coleman, 2006). ACSL1 localises at the MOM (Cooper et al., 2015), where it interacts with CPT1 to direct the FA towards β-oxidation (Lee et al., 2011). MS has been used to analyse ACSL1 posttranslational modifications. Overexpression of ACSL1 in hepatocytes, brown adipocytes, and differentiated 3T3-L1 adipocytes treated with hormones and drug activators of PKA or AMPK reveal several novel acetylation and phosphorylation sites (Frahm et al., 2011). This includes a phosphorylation site at serine 230, which we previously identified in the phosphoproteomic study on ARVM upon PDE2A inhibition (Subramaniam et al., 2023). The amino acid sequence around the phosphorylation site is ENKLTPCLKIIVIMDSYDNDLVERGQKCGVE which contains a β-Adrenergic Receptor kinase (β -ARK) substrate motif. It is possible ACLS1 phosphorylation is indirectly dependent on PKA. Inhibition of PDE2A would in fact result in cAMP increase, and consequently increase in PKA activity. Amongst the different targets, PKA would phosphorylate also other kinases, including perhaps β ARK. β-ARK would in turn phosphorylate and regulate ACSL1.

I therefore investigated the change in phosphorylation level of ACSL1 upon PDE2A inhibition, in order to determine whether this regulates its activity in trafficking FA.

Similarly to PLIN5, there is no commercially available antibody for phosphorylated-ACSL1, and in this case, no antibody for phospho β-ARK substrate either. Therefore, HEK293T cells were transfected with a plasmid encoding the ACSL1-FLAG fusion protein. This was immunoprecipitated with anti-FLAG antibody conjugated to agarose beads (ANTI-FLAG

M2). Detection of phosphorylation was achieved by western blot, probing with an antibody that detects any protein containing a phosphorylation site at a serine or a threonine P(S/T). Western blot analysis on the immunoprecipitate confirmed the presence of the fusion protein, as FLAG antibody detects a band at the expected molecular weight (78 kDa) (Fig. 5.15).

As the MS analysis revealed an increase in phosphorylation of ACSL1 upon inhibition of PDE2A, the cells expressing ACSL1-FLAG were treated with BAY 60-7550. This was compared to the phosphorylation of ACSL1 under basal conditions (DMSO treated cells), or upon cAMP increase dependent on I) moderate adenylyl cyclase activation (forskolin treatment), II) PDE3 inhibition (cilostamide treatment) or III) FSK and non-specific PDE inhibition (3-isobutyl-1-methylxanthine (IBMX) treatment, a non-selective phosphodiesterase inhibitor) to generate a saturating concentration of cAMP.

The phospho-S/T antibody was initially successful at detecting some signal in the ACSL1-FLAG immunoprecipitate (Fig. 5.15). However, the result was not replicated in the further experiments. This was also the case with two more P-S/T antibodies, suggesting that these antibodies lack the efficacy required to detect signal from proteins which contain phosphorylated serine or threonine in western blot analysis. In the whole cell lysate, they only reveal a few bands, a surprising result, since WCL, unlike the immunoprecipitate, contains all proteins from the lysate, many of which will contain phosphorylated serine and threonine. Thus, the phosphorylation of ACSL1 dependent on PDE2A inhibition remains to be characterised.

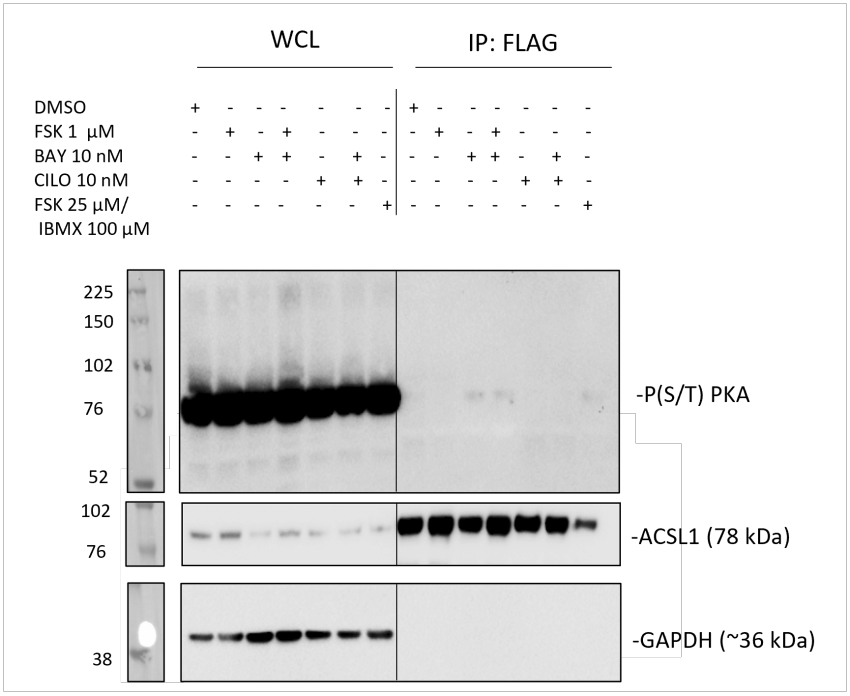


Figure 5.15. Western blot analysis of ACSL1 phosphorylation upon cAMP increase. ACSL1-FLAG immunoprecipitate from HEK293T probed with P(S/T) PKA substrate antibody fails to show an increased in ACSL1 phosphorylation. n=5

5.10 Does PDE2A affect mitochondrial respiration?

PDE2A2 interacts with elements involved in trafficking different substrates in the cell and in the mitochondria for ATP production, like glucose, pyruvate and FA (Chapter 3). In this chapter, I demonstrated that PDE2A modulates the import of FA through its hydrolytic activity on cAMP. This raised the question on whether the effect on FA transport and oxidation would impact the overall mitochondrial respiration of the cell. In order to establish this, mitochondrial respiration was measured using the Seahorse Mito-Stress assay. This assay quantifies the oxygen consumption rate (OCR), an indicator of oxidative phosphorylation (OXPHOS), and the extracellular acidification rate (ECAR), a measure of glycolytic activity, under baseline conditions and after the addition of metabolic inhibitors.

A pilot experiment showed the MEF$^{pde2a-/-}$ to have lower respiratory capacity compared to MEF^{WT} (Fig. 5.16). However, due to different growth rates between MEF^{WT} and MEF$^{pde2a-/-}$, there was a high variability in the cell density across the wells, and four of repeated experiments did not show the same result. From this preliminary experiment,

it appears that the baseline OCR is slightly reduced in the MEF$^{pde2a-/-}$. After the basal respiration is recorded, oligomycin is injected. This inhibits ATP synthase, reducing OCR by blocking ATP production. The MEF$^{pde2a-/-}$ post-oligomycin drop appears to be the same as MEF^{WT} suggesting ATP synthesis is not impaired. Carbonyl cyanide p-trifluoromethoxy phenylhydrazone (FCCP) is then added. This is an uncoupler that collapses the proton gradient, driving maximal electron transport and OCR increase. The MEF^{WT} show a sharp OCR rise, indicating their adaptability to energy demands. On the other hand, the MEF$^{pde2a-/-}$ OCR remains lower, indicating a lower reserve capacity, suggesting changes in the capacity or substrate uptake or oxidation. This finding is in line with the results showing that MEF$^{pde2a-/-}$ present a reduced ability to import FA into the mitochondria, as well as showing dysregulated FAO (Fig. 5.5 and Fig. 5.11). Finally, rotenone and antimycin A are injected. These inhibitors block Complex I and III, shutting down mitochondrial respiration. The remaining OCR represents non-mitochondrial oxygen consumption (e.g., ROS production or alternative oxidases). As both the MEF^{WT} and MEF$^{pde2a-/-}$ reach the same low level, it suggests that mitochondrial respiration is the major contributor to OCR in both cases. This also indicates that the cell number is comparable amongst the two conditions. Increased ECAR indicates a higher rate of glycolysis and lactate production in MEF$^{pde2a-/-}$ compared to MEF^{WT}, suggesting increased cellular reliance on this metabolic pathway casued by absence of *pde2a*(Fig. 5.17). Overall, this results suggests that the ability to perform OXPHOS is compromised in MEF$^{pde2a-/-}$, and it is possible that these cells are relying more on glycolysis. This is a preliminary result, and more experiments are needed to confirm these findings.

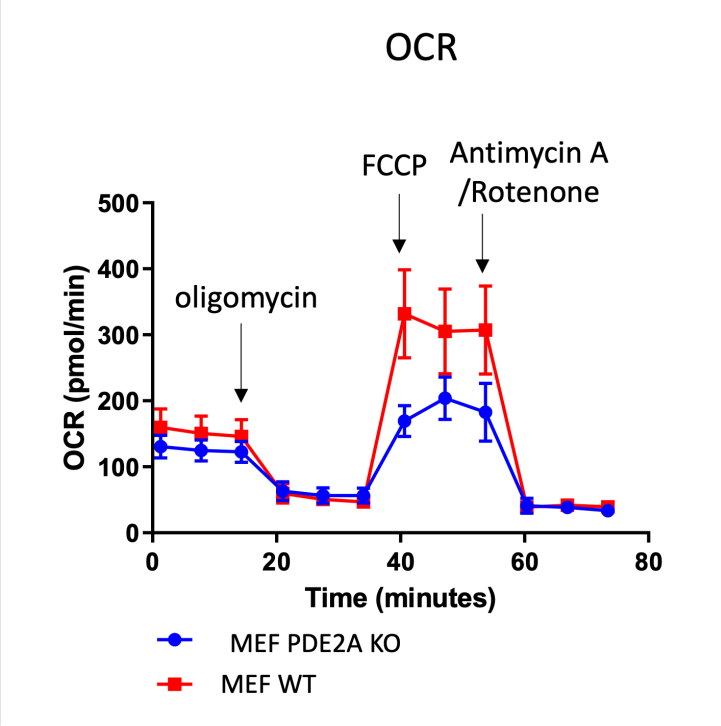


Figure 5.16. Absence of PDE2A results in decreased oxygen consumption.
Seahorse assay reveals a decreased oxygen consumption rate in MEF$^{pde2a-/-}$ compared to WT. n=1 (one biological repeat i.e. one passage, mean data relates to different technical replicates)

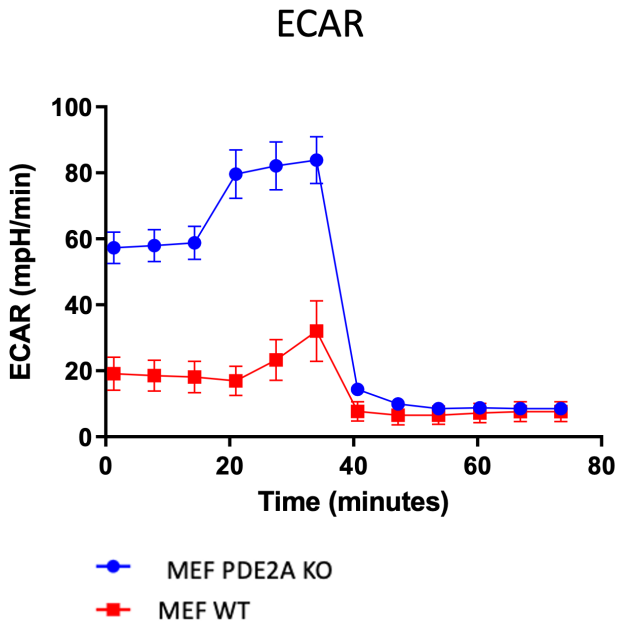


Figure 5.17. Absence of PDE2A results in increased Extracellular Acidification Rate.
Seahorse assay reveals an increased ECAR in MEF$^{pde2a-/-}$ compared to WT. n=1 (one biological repeat i.e. one passage, mean data relates to different technical replicates)

To gain an insight into the effect of PDE2A on the metabolic state of cells, I measured the extracellular concentration of glucose and lactate in culture media from both MEF^{WT} and MEF$^{pde2a\text{-}/\text{-}}$. These preliminary results (Fig. 5.18) indicate that MEF$^{pde2a\text{-}/\text{-}}$ produce higher levels of lactate compared to MEF^{WT} (Fig. 5.18a), suggesting an increased reliance on glycolysis. Additionally, glucose consumption (determined based on extracellular glucose levels subtracted to the initial amount of glucose in the media) is elevated in MEF$^{pde2a\text{-}/\text{-}}$ (Fig. 5.18b). This further supports a shift towards glycolytic metabolism, potentially to meet their energy demands. These findings suggest that the two cell lines have distinct metabolic profiles. However, as these results are preliminary, further replicates and validation are necessary to confirm these observations.

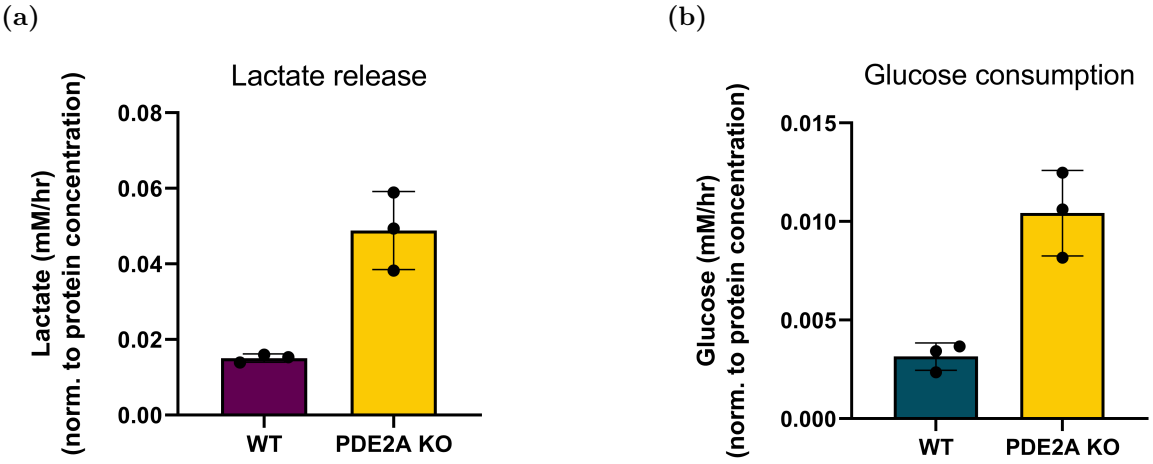


Figure 5.18. Absence of PDE2A results in increase lactate release and glucose consumption.
Calculated glucose consumption and lactate release from media of MEF^{WT} and MEF$^{pde2a\text{-}/\text{-}}$. Each data point represents a technical repeat. the n=1

5.11 Summary of results and discussion

The heart teeters on a knife edge between its enormous energy demand and the amount of ATP it produces to meet this demand. Most energy production derives from the β-oxidation of FAs (FAO). FAs represent more than 70% of all substrates utilised for ATP production, with the remaining sources being glucose, lactate, ketone bodies and amino acids (Neely et al., 1972). A number of pathological processes that affect heart function (including ischemia, sepsis, and heart failure) are associated with a combination of a reduction in FAO, relative increase in anaerobic glycolysis and, in some cases, accumulation of lipids, named lipotoxicity (Schulze et al., 2016). Indeed, the failing human heart is associated with severe metabolic dysregulation, characterized by intramyocardial triacylglycerol (TAG) accumulation and a transcriptional profile similar to that of an animal model of lipotoxicity and contractile dysfunction (Sharma et al., 2004). Diabetes and metabolic syndrome are also characterised by early diastolic changes and lipid accumulation (Peterson, 2006). A dysregulation of the FA consumption pathway and/or accumulation is therefore considered one of the causes or exacerbating factors in heart dysfunction.

Despite extensive study of the relationship between cAMP and metabolism, there are aspects that are still not fully characterised (Ravnskjaer et al., 2016; Frayn, 2002; Ezrailson et al., 1983), such as the interplay between cAMP and lipid trafficking. PDE2A2 localises at the mitochondrial outer membrane (Monterisi et al., 2017; Acin-Perez et al., 2011), where it degrades cAMP, regulating a pool of second messengers responsible for some aspects of mitochondrial dynamics. These include regulation of fission and fusion through PKA-dependent phosphorylation of DRP (Monterisi et al., 2017) and mitophagy, mediated by PKA-dependent phosphorylation of Parkin (Lobo et al., 2020).
MS analysis revealed a series of putative interactors of PDE2A2, many of which are proteins involved in trafficking FA to ensure their utilisation as energy substrates. Chapter 3 validated the interactions between PDE2A2 and enzymes/transporters involved in trafficking different substrates for ATP production, including glucose, pyruvate and FAs. In this chapter, the functional effect of some of these interactions was investigated.

I hypothesised that functional effect of PDE2A2 interaction with CPT1 is through PDE2A2 hydrolysing activity.

5.11.1 Characterisation of PDE2A2 and CPT1 interaction

I hypothesised that functional effect of PDE2A2 interaction with CPT1 is through PDE2A2 hydrolysing activity. In particular, I theorise that PDE2A2 regulates a pool of cAMP where CPT1 localises, and here it modulates mitochondrial trafficking of fatty acid.

I have shown that absence of PDE2A or pharmacological inhibition of PDE2A decreases CPT activity , as shown by a colorimetric assay from heart tissue of mice with a deletion of the *pde2a* gene (Fig. 5.3). PDE2A pharmacological inhibition, through BAY 607550, in ARVM and in MEF recapitulated the observed result (Fig. 5.5a and Fig. 5.5b). When bound to PDE2A, BAY-60-7550 induces a conformational change of the enzyme revealing a hydrophobic pocket which can accommodate the propylphenyl group of the compounds (Zhu et al., 2013). Binding to BAY-60-7550 does not affect PDE2A presence at the MOM, and therefore, it can be assumed that the functional effect of PDE2A2 on CPT1 is dependent on the PDE hydrolysing activity rather that its presence at the MOM, however, an additinal way to test this hypothesis is by measuring the activity of CPT1 in cells overexpressing the dominant negative version of PDE2A2-RFP (DN-PDE2A2-RFP). This is a catalytically dead version of PDE2A2 (and therefore does not perform any hydrolytic activity on cAMP), which displaces the endogenous protein. If the contribution of PDE2A2 to CPT1 role was structural, then CPT1 activity upon DN-PDE2A2-RFP overexpression would not be affected. Even though from my data a structural role of PDE2A2 in relation to CPT1 cannot be excluded, my results indicate that CPT1 activity is, at least partially, regulated by PDE2A hydrolysing activity at the MOM.

It can be argued that absence or inhibition of PDE2A will impact all the family's isoforms (PDE2A1, 2A2 and 2A3), and therefore, it may not be possible to conclude

that the effects observed are specific to PDE2A2. Although it is true that modulation of PDE2A will result in all its isoforms being affected, it is also true that the three PDE2A localise at different subcellular compartments. PDE2A1 localises at the cytosol (Lobo and Zaccolo, 2018), PDE2A3 to the plasma membrane, and PDE2A2 to the mitochondria (Monterisi et al., 2017). Therefore, the effect observed on CPT1, which only localises at the MOM, would be a result of PDE2A2 hydrolysing activity around the same location. From my data, β-adrenergic stimulation with isoproterenol resulted in reduced CPT1 activity to a comparable level to etomoxir treatment, a commercially available CPT1 inhibitor (Fig. 5.5a). These data suggest that PDE2A regulation of CPT1 may be downstream of catecholaminergic stimulation. Finally, inhibiting PKA with protein kinase inhibitor (PKI) resulted in an increase of CPT1 activity, demonstrating the effects observed upon PDE2A inhibition and absence are dependent on PKA activity and consequently on cAMP, rather than cGMP signalling pathway (Fig. 5.6a). This is because PKA is only an effector of cAMP, and inhibiting it should produce the same effect as a decrease in cAMP concentration, mimicking high PDE activity. Since absence of PDE2A, and therefore increase in cAMP, resulted in a decrease in CPT1 activity, a decrease in PKA activity should result in the opposite effect, i.e. in an increase in CPT1 activity. Since this is what was observed upon PKA inhibition, it suggests that the change in CPT1 activity upon PDE2A inhibition is PKA dependent and therefore cAMP dependent too. Additionally, the effect of PDE2A inhibition on CPT1 activity was lost when by PKA and PDE2A were simultaneously inhibited. CPT1 activity in fact, was comparable to the level with PKI treatment alone (Fig. 5.6b). PKI acts by interacting with and blocking the catalytic pocket in the calytic subunit of PKA. The fact that PDE2A inhibition (which alone had decreased CPT1 activity) is lost when PKA is inhibited, suggests that, if the C subunit of PKA is blocked by PKI, it cannot phosphorylate its targets, independently of what level of cAMP is (provided there is enough PKI in the cell).

Alternatively, PKA may act on another component of this signalling cascade to increase CPT1 activity in a way that overrides the effect that a local increase in cAMP around CPT1 due to the effect that PDE2A2 inhibition has. For example, it is possible that

PKA phosphorylates and inhibits a phosphatase that dephosphorylates ACC. Then PKI would inhibit this inactivation and ACC phosphorylation would remain low even in the presence of BAY 60-7550, if the effect on the phosphatase overrides the effect of PKA on AMPK. This mechanism would also explain the lack of effect on the ACC phosphorylation observed upon PKI treatment (Fig 5.9).

A way to orthogonally check that the effect on CPT1 activity is not dependent on cGMP, would be to assess the enzyme activity upon cGMP stimulation. This can be achieved by treating the samples with the nitric oxide donor SNAP (S-Nitroso-N-Acetylpenicillamine) Kots and Bian (2024). Inhibiting a cGMP-dependent PDE (like PDE5, PDE6, and PDE9) would also increase [cGMP]. This approach could be paired with AC inhibitors, which would result in a decrease of [cAMP].

The role of CPT1 in FAO is critical, and dysregulation of this enzyme characterises several pathologies. Absence of CPT1B is lethal in mice (Abozguia et al., 2010) and CPT1B deficiency causes cardiac lipotoxicity and increases pressure overload-induced cardiac hypertrophy (Schulze et al., 2016). Alterations in FA metabolism in hypoxic and ischemic hearts is characterized by reduced rates of oxidation and uptake, higher levels of fatty acyl-CoA and increased conversion of FA to tissue lipids. Higher levels of FA and their fatty acyl-CoA esters are reported to be detrimental to myocardial structure and function (Neely and Morgan, 1974). Because of its fundamental involvement in the transport of FA allowing for their subsequent oxidation, CPT1 has been a desirable target for heart failure treatment (Mengi and Dhalla, 2004). The treatment therapies involve inhibiting CPT1 to shift the fuel metabolism of the heart towards glucose oxidation (Rupp and Jacob, 1992). Rats with constriction of the ascending aorta, (performed to induce hypertrophy and heart failure) and treated with etomoxir for twelve weeks had improved left ventricular, as well as myocardial, performance without inducing a significant additional left ventricular hypertrophy (Turcani and Rupp, 1997). Thus, inhibition of CPT1 helped prevent a pathological phenotype developing. Additionally, the CTP1 inhibitor perhexiline has limited use in hypertrophic cardiomyopathies and is believed to work by modulating the cardiac metabolism, switching it from FA to carbohydrate consumption (Abozguia

et al., 2010). However, this drug has severe side effects (Ren et al., 2021). As CPT1 is already being studied as a therapeutic avenue for cardiac pathology, its modulation by PDE2A offers an additional possibility to target it.

5.11.2 PDE2A2 as a modulator of CPT1 through an ACC/Malonyl-CoA axis

I hypothesise that the regulation of PDE2A2 on CPT1 is dependent on a malonyl CoA/acetyl-CoA Carboxylase axis. CPT1 catalyses the rate limiting step for the import of FA into the mitochondria. It is inhibited by malonyl-CoA (Foster, 2012), which is produced from acetyl-CoA by acetyl-CoA carboxylase (ACC) (Tong, 2005). Phosphorylation of ACC by AMPK inhibits the enzyme, ultimately resulting in decreased malonyl-CoA production, increased CPT1 activity, and thus increased FA oxidation (Saha and Ruderman, 2003).
From the above results, it can be appreciated that CPT1 activity decreased upon absence or inhibition of PDE2A. Blocking or deleting PDE2A resulted in an increase of cAMP. Theoretically, higher cAMP would result in higher PKA activation, which in turn would result in increased PKA-dependent phosphorylation of AMPK, which has an inhibitory effect. Reduced phosphorylation of AMPK would result in reduced phosphorylation (and therefore inhibition) of ACC, which would then convert more acyl-CoAs into the CPT1 inhibitor malonyl-CoA (Fig. 5.7).
I experimentally tested whether a decrease in ACC phosphorylation occurs upon PDE2A inhibition. From my results, western blot analysis on NRVM showed that ACC phosphorylation is indeed decreased upon PDE2A-dependent increase in cAMP increase (Fig. 5.8). However, the difference in phosphorylation levels only becomes detectable when cAMP generation is paired with AMPK activation. This may be due to the fact that it is not simple to experimentally detect a decrease in phosphorylation if the effect is either very small, or the baseline phosphorylation is already low. By activating AMPK pharmacologically, the baseline phosphorylation level of ACC is increased, and the decrease upon forskolin treatment becomes measurable. Even though the difference between the

sample treated with AICAR (which increases ACC phosphorylation) and the one treated with AICAR and forskolin (which increases cAMP concentration) are not statistically significant, a trend can be observed, which suggests the decrease in ACC phosphorylation upon cAMP increase (Fig. 5.8.) A trend in decrease of ACC phosphorylation can also be observed upon PDE2A inhibition. The non-significance can be atribuited to the low n number of experiments and the statistical criteria I applied to the analysis of my results. These results are therefore compatible with the hypothesis that the increase in cAMP which has an effect on ACC phosphorylation is indeed modulated by PDE2A (Fig. 5.9). Surprisingly, inhibiting PKA as well as PDE2A simultaneously results in decreased ACC phosphorylation, to a comparable level to PDE2A inhibition alone (Fig. 5.9). This could be due to several reasons. PKI, the drug used to inhibit PKA, may not have worked efficiently. Alternatively, it is possible that the phosphorylation of ACC is dependent on a different kinase. Follow up experiments could elucidate on these contrasting results.
A interesting next step to investigate the hypothesis of PDE2A regulating a ACC/malonyl CoA axis would be to quantify malonyl CoA in the absence and inhibition of PDE2A. Additionally, measuring CPT1 activity upon ACC inhibition could provide an orthogal way to corroborate this hypothesis.

5.11.3 PDE2A2 affects CPT1A expression

As absence or inhibition of PDE2A resulted in a decrease in CPT activity, it can be hypothesised that this effect is due to different levels of CPT1 expression in the wildtype and knockout line. From my findings, western blot analysis of absolute levels of CPT1A in MEF$^{Pde2a\text{-}/\text{-}}$ and MEF$^{\mathrm{WT}}$ indeed showed a reduction of CPT1A in the in MEF$^{Pde2a\text{-}/\text{-}}$ (Fig. 5.10). This variation is independent of mitochondrial protein content, which remained unvaried between the two lines, as shown by western blot analysis of absolute protein level of VDAC (Fig. 5.10), often used as mitochondrial marker. This result suggests that PDE2A may modulate CPT1A protein expression, however, the mechanism through which this happen is not explored. It is possible that either the synthesis of CPT1A is reduced by a mechanism under the control of PDE2A, or that the absence of PDE2A results in

the accelerated degradation of CPT1A.

5.11.4 PDE2A regulates FAO

I show that CPT1 transport of FA into the mitochondria is reduced upon PDE2A-dependent increase of cAMP, and that FAO is reduced in the absence of *Pde2a* (Fig. 5.11). The magnitude of the change appears to be much more significant in ARVM than in MEF. This could be because myocytes rely heavily on FAO as their primary energy source under normal conditions. Therefore, the disruption of the FAO pathway would have a much more pronounced effect in cardiomyocytes, as their baseline metabolic dependency on this pathway is higher compared to fibroblasts which rely more on glycolysis for energy production.

5.11.5 PDE2A absence or inhibition results in cytosolic lipid accumulation, and may affect PLIN5 phosphorylation

In mammals, cytosolic FA are synthesised into triglycerides by the esterification of diacylglycerol through diacylglycerol acyltransferases (DGAT1 and DGAT2). Once the newly synthesized neutral lipids accumulate beyond a critical concentration, they are stored into cytoplasmic lipid droplets (LD) (Zadoorian et al., 2023). Dysregulated accumulation in cells and mutations in genes associated with lipid droplets have been linked with a number of pathologies, including obesity and type 2 diabetes (Daemen et al., 2018), cancer (Cruz et al., 2020) and cardiovascular disease, where excessive accumulation and enlargement of cardiac lipid droplets may promote disease progression for pathologies such as cardiomyopathy and heart failure (Zadoorian et al., 2023).

I hypothesised that a reduction in FA uptake by the mitochondria upon PDE2A absence results in accumulation of FA in the cytosol, and consequently LD biogenesis. I tested this experimentally, by staining MEF$^{pde2a-/-}$ for lipid droplets (Fig. 5.12). The readout of LD can inform on accumulation of FA in the cytosol, as they are not able to be shuffled into the mitochondria and would instead be stored in LD. Indeed, the number of

cytosolic LD increased significantly, together with the total LD area (Fig. 5.12a and Fig. 5.12c). The size of the individual droplets, on the other hand, decreased (Fig. 5.12b). It has been suggested that LD size could be reflective of different metabolic states of these organelles. For example, smaller LDs could be ready to be consumed releasing FA aimed at β-oxidation (Rambold et al., 2015). As my results show a decrease in LD size, it may be the case that increased lipolysis is occurring. This could be the result of increased PKA-dependent phosphorylation of hormone-sensitive lipase (HSL) and perilipin proteins. It is also possible that the difference in size of LD is an adaptation of the knockout cells to other pathways which regulate LD biology.

Pharmacological inhibition of PDE2A with BAY 607550 in NRVM also results in LD number and total area increase to a similar level to sodium oleate treatment, which is known to induce LD biogenesis (Zadoorian et al., 2023) (Fig. 5.13a and Fig. 5.13c). In contrast with the data from the MEF$^{pde2a-/-}$,the size of LD in NRVM is unvaried (Fig. 5.13b). Unlike the MEF$^{pde2a-/-}$, NRVM only had temporary inhibition of PDE2A instead of chronic absence. The phenotypical difference between the LDs could be attributed to a change in LD biology which only occurs upon long term absence of PDE2A.

LDs are coated by proteins named perilipins (PLIN), which play a number of roles including regulating lipolysis and controlling lipotoxicity (Itabe et al., 2017). Perilipin 5 localises at the mitochondria where, upon PKA-dependent phosphorylation at serine 155, it promotes the channelling of FA from the lipid droplet to the mitochondria (Miner et al., 2023). MS analysis from Subramaniam et al. (2023) revealed PLIN5 phosphorylation to be upregulated upon inhibition of PDE2A by BAY 60-7550 at serine 17, with the consensus sequence DQRGKDTTLALHSRMSGDQTAQDPGSSLGEL, a non-canonical PKA site. I investigated whether PKA phosphorylates PLIN5. Even though the experiments trying to clarify phosphorylation of PLIN5 were inconclusive (Fig. 5.14), it is still possible that PKA phosphorylates PLIN5 at S17. It is likely that that this modification has an effect on the LD binding the mitochondria, as S17 is located at the C-terminal of PLIN5, which is the mitochondria tethering domain of the

protein (Miner et al., 2023). Phosphorylation of PLIN5 at S17 was reported in another study (Kolleritsch et al., 2020), and its phosphorylation was found to be increased upon mutation of the S155 site to a phospho-null one. This modification results in decreased DRP1 recruitment and consequently decreased mitochondrial fission. The authors did not investigate the PLIN5 S17 phosphorylation pattern any further but speculated that its increase in phosphorylation may be an adaptation to the lack of S155 phosphorylation. Additionally, even though PLIN5 is not indicated as a putative binding partner of PDE2A2, from the interactomic analysis performed on PDE2A2-RFP immunoprecipitate, it does interact with SLC27A4 (Miner et al., 2023). This binding promotes efficient channelling of FA from LD into the mitochondria. I demonstrated an interaction between SLC27A4 and PD2A2 (Chapter 3, Fig. 3.14). Therefore, it is possible that the three proteins are present in the same macromolecular complex, where the channelling of FA in under the control of PKA-dependent phosphorylation of PLIN5 at different sites. The development of phosphorylated-PLIN5 antibodies could help elucidate this mechanism in future work.

5.11.6 PDE2A inhibition may result in an increase in ACSL1 phosphorylation

ACSL1 esterifies and activates LCFA, in order for them to be shuffled into the mitochondria. ACSL1 localises at the MOM (Cooper et al., 2015), where it interacts with CPT1 to direct FA towards β-oxidation (Lee et al., 2011). ACSL1 has been linked to the development of cardiac hypertrophy and heart failure; ACSL1 was found to be reduced in failing human myocardium, and when overexpressed, ACSL1 delayed progressive cardiac remodelling and failure (Goldenberg et al., 2019). Additionally, mice lacking ACSL1 show decreased FAO, increased glucose and pyruvate oxidation, and developed cardiac hypertrophy (Ellis et al., 2011). ACSL1 may be regulated post-transcriptionally. In mice that were fasted or fasted and then refed, mRNA and protein expression levels of ACSL1 were measured, and discrepancies observed. *Acsl1* RNA levels were decreased in gastrocnemius, inguinal adipose, and liver. ACSL1 protein levels were increased in gastrocnemius but decreased in inguinal adipose and liver (Mashek and Coleman, 2006). In addition, ACSL1 activity was

downregulated in rat adipocytes incubated with the membrane-permeable cAMP analogue, dibutyryl-cAMP (Hall and Saggerson, 1985). These data suggests that posttranscriptional or posttranslational modification may contribute to the regulation of ACSL.

MS has been used to analyse ACSL1 posttranslational modifications. Overexpression of ACSL1 in hepatocytes, brown adipocytes, and differentiated 3T3-L1 adipocytes treated with hormones and drug activators of PKA or AMPK reveal several novel acetylation and phosphorylation sites (Frahm et al., 2011). This includes a phosphorylation site at serine 230, which the laboratory previously identified in a phosphoproteomic study on ARVM upon PDE2A inhibition (Subramaniam et al., 2023). The amino acid sequence around the phosphorylation site contains a β-Adrenergic Receptor kinase substrate motif. Since there are no commercially available antibodies that detect a phosphorylated β-Adrenergic Receptor kinase (β-ARK) substrate, I studied the phosphorylation of ACSL1 with an antibody which detects any protein which contains a phosphorylated serine or threonine. The results, however, were inconclusive, as, even though the phosphorylation of ACSL1 appeared to be increased upon PDE2A inhibition in my first attempt (Fig. 5.15), I was not able to replicate this finding. More optimisation is required for this experiment. Thus, phosphorylation of ACSL1 dependent on PDE2A inhibition remains to be characterised. With reference to the data published in the literature, it can be postulated that PDE2A's effect on ACSL1 phosphorylation could have an inhibitory effect on ACSL1. This can be surmised as a direct increase in cAMP reveals a phosphorylated site of ACSL1 at S230 (Frahm et al., 2011). Additionally, *Acsl1*$^{-/-}$ mice exhibit reduced FAO (Ellis et al., 2011). At the same time, of PDE2A-dependent increase in cAMP also results in phosphorylation of ACSL1 at S230 (Subramaniam et al., 2023). In conjunction with this, my results show that *Pde2a*$^{-/-}$ rats display reduced FAO. Therefore, it is possible that the increase in cAMP would lead to a rise PKA activity, which could phosphorylate and regulate other kinases, including β-Adrenergic Receptor kinase. β-ARK could phosphorylate and inhibit ACSL1, resulting in decreased FA transport and FAO, therefore recapitulating the *Acsl1*$^{-/-}$ phenotype. Future work could test this hypothesis.

s

5.11.7 PDE2A effect on mitochondrial respiration

Given the effect of PDE2A absence and inhibition on FA import and FAO, I was interested in investigating how PDE2A affects mitochondrial respiration. It is possible that the cells would rely more on glucose oxidation rather than FA oxidation. Alternatively, they could switch to a more glycolytic metabolism. To elucidate on how the cells compensate for the reduced FAO, I performed the Seahorse mito-stress assay, which measures the oxygen consumption rate (OCR) as an indicator of mitochondrial respiration.

The Seahorse mito-stress assay results from a preliminary experiment indicate that MEF$^{pde2a-/-}$ exhibit lower baseline OCR, suggesting reduced mitochondrial respiration (Fig. 5.16). A blunted FCCP-induced OCR increase indicates limited reserve capacity and possible deficits in substrate uptake or oxidation. These observation would align with the observed defects in FA import and FAO (Fig. 5.5 and Fig. 5.11). The observed reduction in OCR suggests that PDE2A plays a crucial role in maintaining mitochondrial energy metabolism. The reduced response to FCCP indicates a limited capacity to meet increased energy demands, which may stem from compromised FA import and FAO. Given that non-mitochondrial oxygen consumption remains unchanged, the primary defect likely lies in oxidative phosphorylation rather than alternative metabolic pathways. In line with this, higher ECAR values for MEF$^{pde2a-/-}$ indicate a potential reliance on glycolysis in the absence of PDE2A.

A key limitation of this experiment arises from the different growth rates of the two cell lines, leading to disparities in cell number at the end of the assay. This variability introduces significant noise into the data, complicating the interpretation of cellular respiration measurements and limiting the robustness of any conclusions drawn.

Supporting the hypothesis of a shift toward glycolysis as an adaptive response, the results in figure 5.18) indicate that MEF$^{pde2a-/-}$ consume more glucose and produce more lactate than the respective control line.

Overall, these findings suggest that PDE2A2 modulates a specific pool of cAMP that regulates FA import into mitochondria by controlling CPT1 activity. PDE2A inhibition increases cAMP, activating PKA, which inhibits AMPK. This reduces ACC phosphorylation, leading to increased malonyl CoA levels, which in turn suppress CPT1 activity. Consequently, FAO is impaired, causing FA accumulation and altered mitochondrial respiration. These effects were observed in *pde2a* knockout models and in cells presenting PDE2A inhibition. Additionally, PDE2A inhibition may ACSL1 and PLIN5 phosphorylation, though their functional impact remains unclear.

In chapter 6, I delineate the overall findings in this thesis, discussing strength, weaknesses and future experiments.

Chapter 6

Conclusions

6.1 Background

The cAMP/PKA signalling pathway plays a crucial role in cell physiology and pathophysiology. It regulates various cellular processes, including hormone secretion, gene expression, cell metabolism, survival, and death. cAMP signalling is disrupted in various cardiac diseases; dysregulation is linked with cancer, hormonal disorders, pulmonary hypertension and cardiovascular, neurological and psychiatric conditions (Maurice et al., 2014).

cAMP signalling is compartmentalised, with each of the players in the signalling pathway (from GPCRs to phosphatases) contributing to the formation of different cAMP nanodomains. In this spatially organised signal transduction, it is the effect of the phosphodiesterases that ultimately defines the topography of cAMP signalling. By degrading the second messenger locally, PDEs allow cAMP to achieve different levels at different sites in the cell (Zaccolo et al., 2021). Eleven families of PDEs give rise to several isoforms within the same family. These can localise at specific subcellular sites, where they regulate cAMP pools in charge of specific cellular functions. The contribution of PDE activity allows for fine tuning of cAMP signalling, avoiding spillage of information across different pathways. This is crucial because these pathways are independent to the

β-adrenergic regulation of cardiac myocyte contraction and relaxation but happen at the same time.

cAMP has been studied extensively within the context of metabolism. Prior studies have elucidated its role on glucose metabolism in the liver (Ravnskjaer et al., 2016), regulation of lipolysis in white adipose tissue (Frayn, 2002) and of glycogenolysis in skeletal muscle (Ezrailson et al., 1983). The regulation of metabolism by cAMP in the heart, however, has not been fully elucidated. In particular, the role of cAMP in the trafficking of substrates aimed at being used for energy production.

Amongst the different PDEs, PDE2A is a cyclic GMP-stimulated phosphodiesterase that hydrolyses both cAMP and cGMP, and is involved in shaping some of the mitochondrial cAMP compartments. The PDE2A2 isoform localises at the mitochondrial outer membrane (MOM), where it regulates mitochondrial quality control through PKA-dependent phosphorylation of Parkin (Lobo et al., 2020). Also at the MOM , PDE2A2 regulates mitochondrial dynamics of fission and fusion, and cell survival via local modulation of cAMP/PKA signalling (Monterisi et al., 2017).

6.2 Aims of the project

This thesis aims to expand our understanding of cAMP signaling in energy metabolism, specifically exploring how cAMP modulates the transport of energy substrates within localized nanodomains regulated by PDEs. The findings support the hypothesis cAMP pools under the control of specific PDEs influence metabolic substrate transport, with key insights gained through the following investigations:

1. Validation of PDE2A2 interactions with proteins involved in metabolite transport for energy production (**Chapter 3**).

2. Validation of PDE3A1 interactions with proteins mediating metabolite transport

(**Chapter 4**).

3. Exploration of how PDE2A2 regulates fatty acid uptake at the mitochondria (**Chapter 5**)

These findings provide new perspectives on the spatial regulation of cAMP in metabolism and open avenues for future research into PDE-targeted metabolic interventions.

6.3 Summary of Results, limitations and future work

6.3.1 Chapter 3, PDE2A2 metabolic interactors

Mass spectrometry analysis revealed PDE2A2 to interact with several proteins involved in the transport of energy substrates. In Chapter 3, I validate some of these. In particular, I demonstrate that PDE2A2 interacts with elements involved in trafficking FA. These include components of the carnitine palmitoyl transferase shuttle,which allows FA to enter the mitochondria; these include: i) CPT1A, ii) CPT1B and iii) SLC25A20;. Additionally, I validated PDE2A2 interaction with SLC27A4, which contributes to the transport of FA across the cell. I demonstrated that PDE2A2 also interacts with elements involved in trafficking different metabolic subtracts, such as the plasma membrane transporter for glucose (SLC2A1) and the pyruvate (SLC16A1), as well as the mitochondrial transporter of pyruvate (MPC2). Furthermore, I demonstrate that PDE2A2 is part of a macromolecular complex which includes elements involved in trafficking different substrates into the cell or the mitochondria, namely fatty acids, glucose and pyruvate. This is a particularly exciting finding as these elements are not known to come together into a single complex. These findings could pave the way to understanding the molecular mechanisms behind the heart's flexibility and provide a therapeutic target to address the loss of flexibility which occurs in heart failure. Future work could expand on the metabolon-like complex, for example, by investigating whether other interactors described in Chapter 3 are part of this multiprotein complex. Studying the exact location of the interaction between

the proteins could also allow to develop strategies to manipulate the interactions. An advantage of disrupting these interactions could be forcing the cells to shift to a different metabolic pathway. One limitation in this chapter is the low expression of PDE2A2, as well as the lack of a PDE2A antibody. As a result, in all the coimmunoprecipitation experiments the fusion protein PDE2A2-RFP or PDE2A2-GFP was overexpressed. On the other hand, the great majority of interactors were endogenous proteins, which reduces the likelihood of artefactual interactions and supports the physiological relevance of the identified protein–protein interactions. A way to further corroborate the interactions validated by co-immunoprecipitation experiments would be to employ a proximity ligation assay, which confirms the adjacency between two proteins of interest. Another limitation of the validation work is that for some of the interactors, the antibodies were not efficient at detecting the endogenous level of the protein, like for SLC27A1.

6.3.2 Chapter 4, PDE3A1 interactors

I demonstrated that PDE3A1 interacts with some of the same elements involved in the trafficking of metabolic substrates which interact with PDE2A2. In particular with proteins involved in the transport of FA including CPT1A/B and SLC27A4. I also demonstrated that PDE3A1 interacts with the pyruvate transporter at the plasma membrane SLC16A1. This opens the possibility that the regulation of the trafficking of metabolites across the cells is dependent on a pool of cAMP under the shared regulation of PDE2 and PDE3, and potentially through cAMP/cGMP cross-talk, although the exact mechanism remains to be established. Future work could elucidate on whether other players in the trafficking of metabolites interact with PDE3A1. Another interesting possibility is that PDE3A1 is also part of the metabolon-like structure which PDE2A2 is involved in. Additionally, future studies could expland on the functional effect of PDE3A1 interactions with these metabolic proteins. Similarly to PDE2A2, the study could concentrate on the effect on uptake of FA, FAO, lipid accumulation and mitochondrial respiration. Modulating the levels of cAMP and cGMP could help elucidate on whether PDE2A2 and PDE3A1 regulation of FA transport relies on cAMP/cGMP cross-talk. Additionally, I validated the interaction

between PDE3A1 and several RNA-binding proteins (RBPs). These include ILF2, EIF3C and RBM39. Studying RBPs is particularly interesting given the emerging pivotal role of the latter in cardiovascular disease. Interaction of RBPs with PDEs could serve several purposes, from complex stability to regulation of post translational modifications. Future work could investigate these hypotheses. Unlike for PDE2A2, PDE3A1 expression is higher, and efficient antibodies exist for this protein. One limitation of the validation work in this chapter is the overexpression of PDE3A1 in all the coimmunoprecipitation experiments. Future work could focus on confirming the interactions between the interactors and endogenous PDE3A1. On the other hand, all the PDE3A1 interactors are endogenous proteins.

6.3.3 Chapter 5, PDE2A2 regulation of the fatty acid uptake machinery

PDE2A2 localises at the MOM, where it interacts with some elements involved trafficking metabolites. I hypothesise that here PDE2A2 controls a pool of cAMP responsible for regulating the import of fatty acids into the mitochondria. I demonstrated that PDE2A inhibition results in decreased AMPK-dependent phosphorylation of Acetyl carboxylase (ACC). This is the enzyme that catalyses the formation of malonyl CoA, which inhibits CPT1. As the phosphorylation on ACC has an inhibitory effect, decreased pACC would result in higher production of malonyl CoA. Even though future work could confirm this hypothesis further, by quantifying the malonyl CoA in the various conditions, a limitation is posed by the lack of kits and protocols to do so in a quick, accessible way.

In line with the reduced pACC upon PDE2A-dependent increase in cAMP, CPT1 activity to import FA into the mitochondria was decreased upon PDE2A inhibition or absence. Consequently, FAO was also decreased upon PDE2A absence. The dysregulation in FA uptake resulted in the accumulation on lipid droplets. Preliminary data indicate that, ultimately, the mitochondrial respiration of the cells lacking *pde2a* gene was decreased, and the metabolism was shifted towards glycolysis. An clear limitation of this experiment is the high variability of the data, resulted by the different growing rates between cell lines,

which leads to different cell numbers in the measuring wells.

Future work could consolidate how PDE2A affect mitochondrial respiration. In particular, the seahorse assay could help investigate the cellular response to fatty acid oxidation specifically (Palmitate Oxidation Assay). It could also assess whether PDE modulation alters fuel usage preferences (Mito Fuel Flex Test) and investigate the relative contribution of glycolysis vs. OXPHOS to ATP production (ATP rate assay).

Additionally, a way to study the effect of dynamic metabolic changes such as a switch in metabolites consumption is to use stable isotopologue-resolved metabolomics. This uses stable isotope tracers, like 13^{C} in conjunction with mass spectrometry and/or nuclear magnetic resonance (NMR) spectroscopy to trace the fate of individual atoms within metabolic pathways. Therefore, glucose/FA/pyruvate tracers could be a valuable tool to study metabolic dynamics under the control of PDE2A2.

Additionally, more research could attempt to rescue the phenotype observed upon PDE2A inhibition and absence, and test whether the metabolic state of myocytes can be pushed towards the consumption of a specific substrate/glycolysis.

To test whether the ATP production by mitochondria is also affected by PDE2A2, the newly developed fluorescent sensor for monitoring intracellular ATP (iATPSnFR2) can be employed (Marvin et al., 2024). Future work can also elucidate on whether PDE2A plays a scaffolding role at the MOM as well as an enzymatic function. This can be tested by coimmunorepcipitaing the any of the interactors of chapter 3 from *pde2a* KO cells, and checking whether the other components of the metabolon-like structure are still present. If they are still detectable, that would mean that PDE2A2 is not necessary for their interaction; if they are not present, that would suggest PDE2A2 needs to be present in order for the multiprotein complex to come together. One limitation of this chapter is the absence of *Pde2a* knockout animals, which necessitated the use of a previously isolated mouse embryonic fibroblast line and frozen heart tissue, rather than freshly isolated cardiac myocytes.

Another limitation of this chapter is the lack of human-derived samples. While the heart tissue and MEFs from genetically modified mice provided valuable mechanistic insights, the

absence of human data limits the direct translatability of the findings to clinical contexts. Validation in human models would be necessary to confirm the physiological relevance of the observed interactions.

6.3.4 Concluding remarks

cAMP organisation in different compartments offers the possibility to pharmacologically target phosphodiesterases individually. Consequently, it can be possible to modulate only the nanodomains under their control, increasing the treatment efficacy and reducing its side effects. An extensive map of β-adrenergic stimulated cAMP nanodomains and their control by different PDEs would represent a valuable tool to gain a more comprehensive understanding of the landscape of its signalling pathway and provide a rationale to develop novel targeted therapeutic strategies. In particular, investigating the role of PDEs in the regulation of metabolism is particularly relevant as a growing body of literature links metabolic disorders like obesity and diabetes to dysregulation of adrenergic receptor signalling (Boyda et al., 2013; Yasuda et al., 2006; Ziegler et al., 2012).

As a dysregulation in FA metabolism is a common denominator in cardiac physiology, being able to target FA dynamics represents a valuable therapeutic target. By modulating trafficking of fatty acids, and potentially other energy substrates, PDE2A2 is a promising avenue which could help address the dysregulation of FA dynamics that occur in cardiac pathology.

Overall, PDE2A2 emerges as a modulator of metabolite trafficking, and an attractive therapeutic target for modulating lipid metabolism.

Bibliography

Abozguia, K., Elliott, P., McKenna, W., Phan, T. T., Nallur-Shivu, G., Ahmed, I., Maher, A. R., Kaur, K., Taylor, J., Henning, A., Ashrafian, H., Watkins, H. and Frenneaux, M. **'Metabolic modulator perhexiline corrects energy deficiency and improves exercise capacity in symptomatic hypertrophic cardiomyopathy**', *Circulation* **122**(16), 1562–9. 2010.

Acin-Perez, R., Russwurm, M., Gunnewig, K., Gertz, M., Zoidl, G., Ramos, L., Buck, J., Levin, L. R., Rassow, J., Manfredi, G. and Steegborn, C. **'A phosphodiesterase 2A isoform localized to mitochondria regulates respiration**', *J Biol Chem* **286**(35), 30423–30432. 2011.

Acin-Perez, R., Salazar, E., Kamenetsky, M., Buck, J., Levin, L. R. and Manfredi, G. **'Cyclic AMP produced inside mitochondria regulates oxidative phosphorylation**', *Cell metabolism* **9**(3), 265–276. 2009.

Actis Dato, V., Lange, S. and Cho, Y. **'Metabolic Flexibility of the Heart: The Role of Fatty Acid Metabolism in Health, Heart Failure, and Cardiometabolic Diseases**', *Int J Mol Sci* **25**(2). 2024.

Affaitati, A., Cardone, L., de Cristofaro, T., Carlucci, A., Ginsberg, M. D., Varrone, S., Gottesman, M. E., Avvedimento, E. V. and Feliciello, A. **'Essential role of A-kinase anchor protein 121 for cAMP signaling to mitochondria**', *Journal of Biological Chemistry* **278**(6), 4286–4294. 2003.

Almutairi, M., Gopal, K., Greenwell, A. A., Young, A., Gill, R., Aburasayn, H., Al Batran, R., Chahade, J. J., Gandhi, M., Eaton, F., Mailloux, R. J. and Ussher, J. R. **'The GLP-1 Receptor Agonist Liraglutide Increases Myocardial Glucose Oxidation Rates via Indirect Mechanisms and Mitigates Experimental Diabetic Cardiomyopathy**', *Can J Cardiol* **37**(1), 140–150. 2021.

Alto, N. M., Soderling, J. and Scott, J. D. **'Rab32 is an A-kinase anchoring protein and participates in mitochondrial dynamics**', *The Journal of cell biology* **158**(4), 659–668. 2002.

An, Q., Lin, R., Wang, D. and Wang, C. **'Emerging roles of fatty acid metabolism in cancer and their targeted drug development**', *European Journal of Medicinal Chemistry* **240**, 114613. 2022.

Anderson, C. M. and Stahl, A. **'SLC27 fatty acid transport proteins**', *Mol Aspects Med* **34**(2-3), 516–28. 2013.

Arias-Barrau, E., DiRusso, C. C. and Black, P. N. (2010), *Methods to Monitor Fatty Acid Transport Proceeding Through Vectorial Acylation*, Humana Press, Totowa, NJ, pp. 233–249.

Aslam, M. and Ladilov, Y. **'Regulation of Mitochondrial Homeostasis by sAC-Derived cAMP Pool: Basic and Translational Aspects**', *Cells* **10**(2). 2021.

Azevedo, M. F., Faucz, F. R., Bimpaki, E., Horvath, A., Levy, I., de Alexandre, R. B., Ahmad, F., Manganiello, V. and Stratakis, C. A. **'Clinical and molecular genetics of the phosphodiesterases (PDEs)**', *Endocr Rev* **35**(2), 195–233. 2014.

Bader, A. G. and Vogt, P. K. **'Phosphorylation by Akt disables the anti-oncogenic activity of YB-1**', *Oncogene* **27**(8), 1179–1182. 2008.

Baker, C. N., Gidus, S. A., Price, G. F., Peoples, J. N. and Ebert, S. N. **'Impaired cardiac energy metabolism in embryos lacking adrenergic stimulation**', *Am J Physiol Endocrinol Metab* **308**(5), E402–13. 2015.

Balcerak, A., Trebinska-Stryjewska, A., Konopinski, R., Wakula, M. and Grzybowska, E. A. **'RNA–protein interactions: disorder, moonlighting and junk contribute to eukaryotic complexity**', *Open Biology* **9**(6), 190096. 2019.

Baliga, R. S., Preedy, M. E. J., Dukinfield, M. S., Chu, S. M., Aubdool, A. A., Bubb, K. J., Moyes, A. J., Tones, M. A. and Hobbs, A. J. **'Phosphodiesterase 2 inhibition preferentially promotes NO/guanylyl cyclase/cGMP signaling to reverse the development of heart failure**', *Proc Natl Acad Sci U S A* **115**(31), E7428–e7437. 2018.

Barber, G. N. **'The NFAR's (nuclear factors associated with dsRNA): evolutionarily conserved members of the dsRNA binding protein family**', *RNA Biol* **6**(1), 35–9. 2009.

Basaki, Y., Hosoi, F., Oda, Y., Fotovati, A., Maruyama, Y., Oie, S., Ono, M., Izumi, H., Kohno, K., Sakai, K., Shimoyama, T., Nishio, K. and Kuwano, M. **'Akt-dependent nuclear localization of Y-box-binding protein 1 in acquisition of malignant characteristics by human ovarian cancer cells**', *Oncogene* **26**(19), 2736–46. 2007.

Bauman, A. L., Soughayer, J., Nguyen, B. T., Willoughby, D., Carnegie, G. K., Wong, W., Hoshi, N., Langeberg, L. K., Cooper, D. M., Dessauer, C. W. and Scott, J. D. **'Dynamic regulation of cAMP synthesis through anchored PKA-adenylyl cyclase V/VI complexes**', *Mol Cell* **23**(6), 925–31. 2006.

Beavo, J. A., Hardman, J. G. and Sutherland, E. W. **'Stimulation of adenosine 3',5'-monophosphate hydrolysis by guanosine 3',5'-monophosphate**', *J Biol Chem*

246(12), 3841–6. 1971.

Beavo, J., Bechtel, P. and Krebs, E. **'Activation of protein kinase by physiological concentrations of cyclic AMP**', *Proceedings of the National Academy of Sciences* **71**(9), 3580–3583. 1974.

Beltejar, M.-C. G., Lau, H.-T., Golkowski, M. G., Ong, S.-E. and Beavo, J. A. **'Analyses of PDE-regulated phosphoproteomes reveal unique and specific cAMP-signaling modules in T cells**', *Proceedings of the National Academy of Sciences* **114**(30), E6240–E6249. 2017.

Berthouze-Duquesnes, M., Lucas, A., Saulière, A., Sin, Y. Y., Laurent, A. C., Galés, C., Baillie, G. and Lezoualc'h, F. **'Specific interactions between Epac1, β-arrestin2 and PDE4D5 regulate β-adrenergic receptor subtype differential effects on cardiac hypertrophic signaling**', *Cell Signal* **25**(4), 970–80. 2013.

Bieber, L. L., Abraham, T. and Helmrath, T. **'A rapid spectrophotometric assay for carnitine palmitoyltransferase**', *Analytical Biochemistry* **50**(2), 509–518. 1972.

Boess, F. G., Hendrix, M., van der Staay, F.-J., Erb, C., Schreiber, R., van Staveren, W., de Vente, J., Prickaerts, J., Blokland, A. and Koenig, G. **'Inhibition of phosphodiesterase 2 increases neuronal cGMP, synaptic plasticity and memory performance**', *Neuropharmacology* **47**(7), 1081–1092. 2004.

Boyda, H. N., Procyshyn, R. M., Pang, C. C. and Barr, A. M. **'Peripheral adrenoceptors: the impetus behind glucose dysregulation and insulin resistance**', *J Neuroendocrinol* **25**(3), 217–28. 2013.

Brand, T. **'The Popeye domain-containing gene family**', *Cell Biochem Biophys* **43**(1), 95–103. 2005.

Brecker, S. J. D., Xiao, H. B., Mbaissouroum, M. and Gibson, D. G. **'Effects of intravenous milrinone on left ventricular function in ischemic and idiopathic dilated cardiomyopathy**', *The American Journal of Cardiology* **71**(2), 203–209. 1993.

Bricker, D. K., Taylor, E. B., Schell, J. C., Orsak, T., Boutron, A., Chen, Y.-C., Cox, J. E., Cardon, C. M., Van Vranken, J. G., Dephoure, N., Redin, C., Boudina, S., Gygi, S. P., Brivet, M., Thummel, C. S. and Rutter, J. **'A Mitochondrial Pyruvate Carrier Required for Pyruvate Uptake in Yeast, Drosophila, and Humans**', *Science* **337**(6090), 96–100. 2012.

Brisson, G. R., Malaisse-Lagae, F. and Malaisse, W. J. **'The stimulus-secretion coupling of glucose-induced insulin release. VII. A proposed site of action for adenosine-3',5'-cyclic monophosphate**', *J Clin Invest* **51**(2), 232–41. 1972.

Burdyga, A., Surdo, N. C., Monterisi, S., Di Benedetto, G., Grisan, F., Penna, E., Pellegrini, L., Zaccolo, M., Bortolozzi, M. and Swietach, P. **'Phosphatases control PKA-dependent functional microdomains at the outer mitochondrial membrane**', *Proceedings of the National Academy of Sciences* **115**(28), E6497–E6506. 2018.

Burgers, P. P., Ma, Y., Margarucci, L., Mackey, M., van der Heyden, M. A., Ellisman, M., Scholten, A., Taylor, S. S. and Heck, A. J. **'A small novel A-kinase anchoring protein (AKAP) that localizes specifically protein kinase A-regulatory subunit I (PKA-RI) to the plasma membrane**', *J Biol Chem* **287**(52), 43789–97. 2012.

Börner, S., Schwede, F., Schlipp, A., Berisha, F., Calebiro, D., Lohse, M. J. and Nikolaev, V. O. **'FRET measurements of intracellular cAMP concentrations and cAMP analog permeability in intact cells**', *Nat Protoc* **6**(4), 427–38. 2011.

Carlucci, A., Lignitto, L. and Feliciello, A. **'Control of mitochondria dynamics and**

oxidative metabolism by cAMP, AKAPs and the proteasome', *Trends in Cell Biology* **18**(12), 604–613. 2008.

Cartee, G. D. and Wojtaszewski, J. F. **'Role of Akt substrate of 160 kDa in insulin-stimulated and contraction-stimulated glucose transport**', *Appl Physiol Nutr Metab* **32**(3), 557–66. 2007.

Catalanotto, C., Barbato, C., Cogoni, C. and Benelli, D. **'The RNA-Binding Function of Ribosomal Proteins and Ribosome Biogenesis Factors in Human Health and Disease**', *Biomedicines* **11**(11). 2023.

Cazorla, O., Lucas, A., Poirier, F., Lacampagne, A. and Lezoualc'h, F. **'The cAMP binding protein Epac regulates cardiac myofilament function**', *Proc Natl Acad Sci U S A* **106**(33), 14144–9. 2009.

Cerveny, K. L., Tamura, Y., Zhang, Z., Jensen, R. E. and Sesaki, H. **'Regulation of mitochondrial fusion and division**', *Trends in cell biology* **17**(11), 563–569. 2007.

Chang, J.-C., Go, S., Gilglioni, E. H., Duijst, S., Panneman, D. M., Rodenburg, R. J., Li, H. L., Huang, H.-L., Levin, L. R. and Buck, J. **'Soluble adenylyl cyclase regulates the cytosolic NADH/NAD+ redox state and the bioenergetic switch between glycolysis and oxidative phosphorylation**', *Biochimica et Biophysica Acta (BBA)-Bioenergetics* **1862**(4), 148367. 2021.

Chao, A. M., Tronieri, J. S., Amaro, A. and Wadden, T. A. **'Semaglutide for the treatment of obesity**', *Trends Cardiovasc Med* **33**(3), 159–166. 2023.

Chen, M., Sato, P. Y., Chuprun, J. K., Peroutka, R. J., Otis, N. J., Ibetti, J., Pan, S., Sheu, S. S., Gao, E. and Koch, W. J. **'Prodeath signaling of G protein-coupled receptor kinase 2 in cardiac myocytes after ischemic stress occurs**

via extracellular signal-regulated kinase-dependent heat shock protein 90-mediated mitochondrial targeting', *Circ Res* **112**(8), 1121–34. 2013.

Cheung, P., Yang, G. and Boden, G. **'Milrinone, a selective phosphodiesterase 3 inhibitor, stimulatesl lipolysis, endogenous glucose production, and insulin secretion**', *Metabolism* **52**(11), 1496–1500. 2003.

Choi, Y. H., Park, S., Hockman, S., Zmuda-Trzebiatowska, E., Svennelid, F., Haluzik, M., Gavrilova, O., Ahmad, F., Pepin, L., Napolitano, M., Taira, M., Sundler, F., Stenson Holst, L., Degerman, E. and Manganiello, V. C. **'Alterations in regulation of energy homeostasis in cyclic nucleotide phosphodiesterase 3B-null mice**', *J Clin Invest* **116**(12), 3240–51. 2006.

Ciccarelli, M., Chuprun, J. K., Rengo, G., Gao, E., Wei, Z., Peroutka, R. J., Gold, J. I., Gumpert, A., Chen, M., Otis, N. J., Dorn, G. W., n., Trimarco, B., Iaccarino, G. and Koch, W. J. **'G protein-coupled receptor kinase 2 activity impairs cardiac glucose uptake and promotes insulin resistance after myocardial ischemia**', *Circulation* **123**(18), 1953–62. 2011.

Ciccarelli, M., Santulli, G., Pascale, V., Trimarco, B. and Iaccarino, G. **'Adrenergic receptors and metabolism: role in development of cardiovascular disease**', *Frontiers in Physiology* **Volume 4 - 2013**. 2013.

Cipolletta, E., Campanile, A., Santulli, G., Sanzari, E., Leosco, D., Campiglia, P., Trimarco, B. and Iaccarino, G. **'The G protein coupled receptor kinase 2 plays an essential role in beta-adrenergic receptor-induced insulin resistance**', *Cardiovascular Research* **84**(3), 407–415. 2009.

Coburn, C. T., Hajri, T., Ibrahimi, A. and Abumrad, N. A. **'Role of CD36 in membrane transport and utilization of long-chain fatty acids by different tissues**', *J Mol*

Neurosci **16**(2-3), 117–21; discussion 151–7. 2001.

Consonni, S. V., Gloerich, M., Spanjaard, E. and Bos, J. L. **'cAMP regulates DEP domain-mediated binding of the guanine nucleotide exchange factor Epac1 to phosphatidic acid at the plasma membrane**', *Proceedings of the National Academy of Sciences* **109**(10), 3814–3819. 2012.

Conti, M. and Beavo, J. **'Biochemistry and physiology of cyclic nucleotide phosphodiesterases: essential components in cyclic nucleotide signaling**', *Annu. Rev. Biochem.* **76**(1), 481–511. 2007.

Cooper, D. E., Young, P. A., Klett, E. L. and Coleman, R. A. **'Physiological consequences of compartmentalized acyl-CoA metabolism**', *Journal of Biological Chemistry* **290**(33), 20023–20031. 2015.

Cooper, D. M. and Tabbasum, V. G. **'Adenylate cyclase-centred microdomains**', *Biochem J* **462**(2), 199–213. 2014.

Corbett, A. H. **'Post-transcriptional regulation of gene expression and human disease**', *Curr Opin Cell Biol* **52**, 96–104. 2018.

Corbin, J. and Keely, S. **'Characterization and regulation of heart adenosine 3': 5'-monophosphate-dependent protein kinase isozymes**', *Journal of Biological Chemistry* **252**(3), 910–918. 1977.

Coronado, M., Fajardo, G., Nguyen, K., Zhao, M., Kooiker, K., Jung, G., Hu, D. Q., Reddy, S., Sandoval, E., Stotland, A., Gottlieb, R. A. and Bernstein, D. **'Physiological Mitochondrial Fragmentation Is a Normal Cardiac Adaptation to Increased Energy Demand**', *Circ Res* **122**(2), 282–295. 2018.

Cross, H. R., Steenbergen, C., Lefkowitz, R. J., Koch, W. J. and Murphy, E.

'Overexpression of the cardiac β2-adrenergic receptor and expression of a β-adrenergic receptor kinase-1 (βARK1) inhibitor both increase myocardial contractility but have differential effects on susceptibility to ischemic injury', *Circulation research* **85**(11), 1077–1084. 1999.

Crossthwaite, A. J., Ciruela, A., Rayner, T. F. and Cooper, D. M. **'A direct interaction between the N terminus of adenylyl cyclase AC8 and the catalytic subunit of protein phosphatase 2A**', *Mol Pharmacol* **69**(2), 608–17. 2006.

Cruz, A. L., Barreto, E. d. A., Fazolini, N. P., Viola, J. P. and Bozza, P. T. **'Lipid droplets: platforms with multiple functions in cancer hallmarks**', *Cell death & disease* **11**(2), 105. 2020.

Daemen, S., Gemmink, A., Brouwers, B., Meex, R. C., Huntjens, P. R., Schaart, G., Moonen-Kornips, E., Jörgensen, J., Hoeks, J. and Schrauwen, P. **'Distinct lipid droplet characteristics and distribution unmask the apparent contradiction of the athlete's paradox**', *Molecular metabolism* **17**, 71–81. 2018.

Danial, N. N., Gramm, C. F., Scorrano, L., Zhang, C.-Y., Krauss, S., Ranger, A. M., Robert Datta, S., Greenberg, M. E., Licklider, L. J. and Lowell, B. B. **'BAD and glucokinase reside in a mitochondrial complex that integrates glycolysis and apoptosis**', *Nature* **424**(6951), 952–956. 2003.

de Rooij, J., Rehmann, H., van Triest, M., Cool, R. H., Wittinghofer, A. and Bos, J. L. **'Mechanism of Regulation of the Epac Family of cAMP-dependent RapGEFs *'**, *Journal of Biological Chemistry* **275**(27), 20829–20836. 2000.

de Rooij, J., Zwartkruis, F. J., Verheijen, M. H., Cool, R. H., Nijman, S. M., Wittinghofer, A. and Bos, J. L. **'Epac is a Rap1 guanine-nucleotide-exchange factor directly activated by cyclic AMP**', *Nature* **396**(6710), 474–7. 1998.

De Waal, L., Lewis, T. A., Rees, M. G., Tsherniak, A., Wu, X., Choi, P. S., Gechijian, L., Hartigan, C., Faloon, P. W. and Hickey, M. J. **'Identification of cancer-cytotoxic modulators of PDE3A by predictive chemogenomics**', *Nature chemical biology* **12**(2), 102–108. 2016.

Degenring, D., Röhl, M. and Uhrmacher, A. M. **'Discrete event, multi-level simulation of metabolite channeling**', *Biosystems* **75**(1), 29–41. 2004.

Degerman, E., Ahmad, F., Chung, Y. W., Guirguis, E., Omar, B., Stenson, L. and Manganiello, V. **'From PDE3B to the regulation of energy homeostasis**', *Curr Opin Pharmacol* **11**(6), 676–82. 2011.

Dessauer, C. W., Watts, V. J., Ostrom, R. S., Conti, M., Dove, S. and Seifert, R. **'International Union of Basic and Clinical Pharmacology. CI. Structures and Small Molecule Modulators of Mammalian Adenylyl Cyclases**', *Pharmacol Rev* **69**(2), 93–139. 2017.

Deuticke, B. **'Monocarboxylate transport in erythrocytes**', *J Membr Biol* **70**(2), 89–103. 1982.

Di Benedetto, G., Lefkimmiatis, K. and Pozzan, T. **'The basics of mitochondrial cAMP signalling: Where, when, why**', *Cell Calcium* **93**, 102320. 2021.

Di Benedetto, G., Scalzotto, E., Mongillo, M. and Pozzan, T. **'Mitochondrial Ca2+ uptake induces cyclic AMP generation in the matrix and modulates organelle ATP levels**', *Cell metabolism* **17**(6), 965–975. 2013.

Di Benedetto, G., Zoccarato, A., Lissandron, V., Terrin, A., Li, X., Houslay, M. D., Baillie, G. S. and Zaccolo, M. **'Protein kinase A type I and type II define distinct intracellular signaling compartments**', *Circulation research* **103**(8), 836–844. 2008.

Diakos, N. A., Navankasattusas, S., Abel, E. D., Rutter, J., McCreath, L., Ferrin, P., McKellar, S. H., Miller, D. V., Park, S. Y. and Richardson, R. S. **'Evidence of glycolysis up-regulation and pyruvate mitochondrial oxidation mismatch during mechanical unloading of the failing human heart: implications for cardiac reloading and conditioning**', *JACC: Basic to Translational Science* **1**(6), 432–444. 2016.

Diebold, I., Djordjevic, T., Petry, A., Hatzelmann, A., Tenor, H., Hess, J. and Görlach, A. **'Phosphodiesterase 2 mediates redox-sensitive endothelial cell proliferation and angiogenesis by thrombin via Rac1 and NADPH oxidase 2**', *Circ Res* **104**(10), 1169–77. 2009.

Diskar, M., Zenn, H.-M., Kaupisch, A., Kaufholz, M., Brockmeyer, S., Sohmen, D., Berrera, M., Zaccolo, M., Boshart, M. and Herberg, F. W. **'Regulation of cAMP-dependent protein kinases: the human protein kinase X (PrKX) reveals the role of the catalytic subunit αH-αI loop**', *Journal of biological chemistry* **285**(46), 35910–35918. 2010.

Djouder, N., Tuerk, R. D., Suter, M., Salvioni, P., Thali, R. F., Scholz, R., Vaahtomeri, K., Auchli, Y., Rechsteiner, H., Brunisholz, R. A., Viollet, B., Mäkelä, T. P., Wallimann, T., Neumann, D. and Krek, W. **'PKA phosphorylates and inactivates AMPKalpha to promote efficient lipolysis**', *Embo j* **29**(2), 469–81. 2010.

Dodge, K. L., Khouangsathiene, S., Kapiloff, M. S., Mouton, R., Hill, E. V., Houslay, M. D., Langeberg, L. K. and Scott, J. D. **'mAKAP assembles a protein kinase A/PDE4 phosphodiesterase cAMP signaling module**', *The EMBO journal* . 2001.

Dodge-Kafka, K. L., Bauman, A., Mayer, N., Henson, E., Heredia, L., Ahn, J., McAvoy, T., Nairn, A. C. and Kapiloff, M. S. **'cAMP-stimulated protein phosphatase 2A activity associated with muscle A kinase-anchoring protein (mAKAP)**

signaling complexes inhibits the phosphorylation and activity of the cAMP-specific phosphodiesterase PDE4D3', *Journal of Biological Chemistry* **285**(15), 11078–11086. 2010.

Dorn, G. W., Clark, C. F., Eschenbacher, W. H., Kang, M.-Y., Engelhard, J. T., Warner, S. J., Matkovich, S. J. and Jowdy, C. C. **'MARF and Opa1 control mitochondrial and cardiac function in Drosophila**', *Circulation research* **108**(1), 12–17. 2011.

Dostmann, W., Taylor, S. S., Genieser, H., Jastorff, B., Døskeland, S. and Ogreid, D. **'Probing the cyclic nucleotide binding sites of cAMP-dependent protein kinases I and II with analogs of adenosine 3', 5'-cyclic phosphorothioates**', *Journal of Biological Chemistry* **265**(18), 10484–10491. 1990.

Dupré, D. J., Baragli, A., Rebois, R. V., Ethier, N. and Hébert, T. E. **'Signalling complexes associated with adenylyl cyclase II are assembled during their biosynthesis**', *Cell Signal* **19**(3), 481–9. 2007.

Dzimiri, N., Muiya, P., Andres, E. and Al-Halees, Z. **'Differential functional expression of human myocardial G protein receptor kinases in left ventricular cardiac diseases**', *Eur J Pharmacol* **489**(3), 167–77. 2004.

Dávila-Román, V. G., Vedala, G., Herrero, P., De Las Fuentes, L., Rogers, J. G., Kelly, D. P. and Gropler, R. J. **'Altered myocardial fatty acid and glucose metabolism in idiopathic dilated cardiomyopathy**', *Journal of the American College of Cardiology* **40**(2), 271–277. 2002.

Eliseeva, I. A., Kim, E. R., Guryanov, S. G., Ovchinnikov, L. P. and Lyabin, D. N. **'Y-box-binding protein 1 (YB-1) and its functions**', *Biochemistry (Mosc)* **76**(13), 1402–33. 2011.

Ellis, J. M., Mentock, S. M., Depetrillo, M. A., Koves, T. R., Sen, S., Watkins, S. M., Muoio, D. M., Cline, G. W., Taegtmeyer, H., Shulman, G. I., Willis, M. S. and Coleman, R. A. **'Mouse cardiac acyl coenzyme a synthetase 1 deficiency impairs Fatty Acid oxidation and induces cardiac hypertrophy**', *Mol Cell Biol* **31**(6), 1252–62. 2011.

Emery, A. C., Liu, X. H., Xu, W., Eiden, M. V. and Eiden, L. E. **'Cyclic Adenosine 3',5'-Monophosphate Elevation and Biological Signaling through a Secretin Family Gs-Coupled G Protein-Coupled Receptor Are Restricted to a Single Adenylate Cyclase Isoform**', *Mol Pharmacol* **87**(6), 928–35. 2015.

Erneux, C., Couchie, D. and Dumont, J. E. **'Characterization of horse thyroid cyclic nucleotide phosphodiesterases**', *Eur J Biochem* **104**(1), 297–304. 1980.

Ezrailson, E. G., Entman, M. and Garber, A. **'Adrenergic and serotonergic regulation of skeletal muscle metabolism in rat. I. The effects of adrenergic and serotonergic antagonists on the regulation of muscle amino acid release, glycogenolysis, and cyclic nucleotide levels**', *Journal of Biological Chemistry* **258**(20), 12494–12498. 1983.

Fajardo, G., Zhao, M., Berry, G., Wong, L. J., Mochly-Rosen, D. and Bernstein, D. **'β2-adrenergic receptors mediate cardioprotection through crosstalk with mitochondrial cell death pathways**', *J Mol Cell Cardiol* **51**(5), 781–9. 2011.

Farese, R. V. and Walther, T. C. **'Lipid droplets finally get a little RESPECT**', *Cell* **139**(5), 855–860. 2009.

Fawcett, D. (1966), *An Atlas of Fine Structure: the Cell, Its Organelles, and Inclusions*, W. B. Saunders Company.

Fazal, L., Laudette, M., Paula-Gomes, S., Pons, S., Conte, C., Tortosa, F., Sicard, P., Sainte-Marie, Y., Bisserier, M. and Lairez, O. **'Multifunctional mitochondrial Epac1 controls myocardial cell death**', *Circulation research* **120**(4), 645–657. 2017.

Feinstein, W. P., Zhu, B., Leavesley, S. J., Sayner, S. L. and Rich, T. C. **'Assessment of cellular mechanisms contributing to cAMP compartmentalization in pulmonary microvascular endothelial cells**', *Am J Physiol Cell Physiol* **302**(6), C839–52. 2012.

Fenix, A. M., Miyaoka, Y., Bertero, A., Blue, S. M., Spindler, M. J., Tan, K. K. B., Perez-Bermejo, J. A., Chan, A. H., Mayerl, S. J., Nguyen, T. D., Russell, C. R., Lizarraga, P. P., Truong, A., So, P.-L., Kulkarni, A., Chetal, K., Sathe, S., Sniadecki, N. J., Yeo, G. W., Murry, C. E., Conklin, B. R. and Salomonis, N. **'Gain-of-function cardiomyopathic mutations in RBM20 rewire splicing regulation and re-distribute ribonucleoprotein granules within processing bodies**', *Nature Communications* **12**(1), 6324. 2021.

Ferreira, J. P., Saraiva, F., Sharma, A., Vasques-Nóvoa, F., Angélico-Gonçalves, A., Leite, A. R., Borges-Canha, M., Carvalho, D., Packer, M., Zannad, F., Leite-Moreira, A. and Neves, J. S. **'Glucagon-like peptide 1 receptor agonists in patients with type 2 diabetes with and without chronic heart failure: A meta-analysis of randomized placebo-controlled outcome trials**', *Diabetes, Obesity and Metabolism* **25**(6), 1495–1502. 2023.

Fesenko, E. E., Kolesnikov, S. S. and Lyubarsky, A. L. **'Induction by cyclic GMP of cationic conductance in plasma membrane of retinal rod outer segment**', *Nature* **313**(6000), 310–3. 1985.

Foster, D. W. **'Malonyl-CoA: the regulator of fatty acid synthesis and oxidation**', *J Clin Invest* **122**(6), 1958–9. 2012.

Frahm, J. L., Li, L. O., Grevengoed, T. J. and Coleman, R. A. **'Phosphorylation and Acetylation of Acyl-CoA Synthetase- I**', *J Proteomics Bioinform* **4**(7), 129–137. 2011.

Francis, S. H., Blount, M. A. and Corbin, J. D. **'Mammalian cyclic nucleotide phosphodiesterases: molecular mechanisms and physiological functions**', *Physiol Rev* **91**(2), 651–90. 2011.

Francis, S. H., Corbin, J. D. and Bischoff, E. (2009), *Cyclic GMP-Hydrolyzing Phosphodiesterases*, Springer Berlin Heidelberg, Berlin, Heidelberg, pp. 367–408.

Fraser, F., Corstorphine, C. G. and Zammit, V. A. **'Topology of carnitine palmitoyltransferase I in the mitochondrial outer membrane**', *Biochem J* **323 (Pt 3)**(Pt 3), 711–8. 1997.

Frayn, K. **'Adipose tissue as a buffer for daily lipid flux**', *Diabetologia* **45**, 1201–1210. 2002.

Freedman, N. J. and Lefkowitz, R. J. **'Desensitization of G protein-coupled receptors**', *Recent Prog Horm Res* **51**, 319–51; discussion 352–3. 1996.

Fujita, T., Umemura, M., Yokoyama, U., Okumura, S. and Ishikawa, Y. **'The role of Epac in the heart**', *Cell Mol Life Sci* **74**(4), 591–606. 2017.

Fukuta, H., Goto, T., Wakami, K., Kamiya, T. and Ohte, N. **'Effect of beta-blockers on heart failure severity in patients with heart failure with preserved ejection fraction: a meta-analysis of randomized controlled trials**', *Heart Failure Reviews* **26**(1), 165–171. 2021.

Fusco, A., Santulli, G., Sorriento, D., Cipolletta, E., Garbi, C., Dorn, G. W., n., Trimarco,

B., Feliciello, A. and Iaccarino, G. **'Mitochondrial localization unveils a novel role for GRK2 in organelle biogenesis**', *Cell Signal* **24**(2), 468–475. 2012.

García-Bermúdez, J., Sánchez-Aragó, M., Soldevilla, B., del Arco, A., Nuevo-Tapioles, C. and Cuezva, J. M. **'PKA Phosphorylates the ATPase Inhibitory Factor 1 and Inactivates Its Capacity to Bind and Inhibit the Mitochondrial H⁺-ATP Synthase**', *Cell Reports* **12**(12), 2143–2155. 2015.

Geelen, M. J. and Vaartjes, W. J. **'Levels of cyclic 3'-5' -adenosine monophosphate (cAMP) in maintenance cultures of rat hepatocytes in response to insulin and glucagon**', *Lipids* **12**(7), 577–80. 1977.

Gerstberger, S., Hafner, M. and Tuschl, T. **'A census of human RNA-binding proteins**', *Nature Reviews Genetics* **15**(12), 829–845. 2014.

Ghigo, A. and Mika, D. **'cAMP/PKA signaling compartmentalization in cardiomyocytes: Lessons from FRET-based biosensors**', *J Mol Cell Cardiol* **131**, 112–121. 2019.

Giudice, J., Xia, Z., Wang, E. T., Scavuzzo, M. A., Ward, A. J., Kalsotra, A., Wang, W., Wehrens, X. H., Burge, C. B. and Li, W. **'Alternative splicing regulates vesicular trafficking genes in cardiomyocytes during postnatal heart development**', *Nature communications* **5**(1), 3603. 2014.

Glatz, J. C. and Luiken, J. F. **'Dynamic role of the transmembrane glycoprotein CD36 (SR-B2) in cellular fatty acid uptake and utilization**', *Journal of lipid research* **59**(7), 1084–1093. 2018.

Glatz, J. F., Bonen, A., Ouwens, D. M. and Luiken, J. J. **'Regulation of sarcolemmal transport of substrates in the healthy and diseased heart**', *Cardiovasc Drugs*

Ther **20**(6), 471–6. 2006.

Glatz, J. F. C., Nabben, M., Young, M. E., Schulze, P. C., Taegtmeyer, H. and Luiken, J. **'Re-balancing cellular energy substrate metabolism to mend the failing heart'**, *Biochim Biophys Acta Mol Basis Dis* **1866**(5), 165579. 2020.

Gloerich, M. and Bos, J. L. **'Epac: defining a new mechanism for cAMP action'**, *Annu Rev Pharmacol Toxicol* **50**, 355–75. 2010.

Gold, M. G., Lygren, B., Dokurno, P., Hoshi, N., McConnachie, G., Taskén, K., Carlson, C. R., Scott, J. D. and Barford, D. **'Molecular basis of AKAP specificity for PKA regulatory subunits'**, *Molecular cell* **24**(3), 383–395. 2006.

Goldenberg, J. R., Carley, A. N., Ji, R., Zhang, X., Fasano, M., Schulze, P. C. and Lewandowski, E. D. **'Preservation of Acyl Coenzyme A Attenuates Pathological and Metabolic Cardiac Remodeling Through Selective Lipid Trafficking'**, *Circulation* **139**(24), 2765–2777. 2019.

Gorshkov, K., Mehta, S., Ramamurthy, S., Ronnett, G. V., Zhou, F. Q. and Zhang, J. **'AKAP-mediated feedback control of cAMP gradients in developing hippocampal neurons'**, *Nat Chem Biol* **13**(4), 425–431. 2017.

Grabner, G. F., Xie, H., Schweiger, M. and Zechner, R. **'Lipolysis: cellular mechanisms for lipid mobilization from fat stores'**, *Nature Metabolism* **3**(11), 1445–1465. 2021.

Greenberg, A. S., Egan, J. J., Wek, S. A., Garty, N. B., Blanchette-Mackie, E. J. and Londos, C. **'Perilipin, a major hormonally regulated adipocyte-specific phosphoprotein associated with the periphery of lipid storage droplets'**, *Journal of Biological Chemistry* **266**(17), 11341–11346. 1991.

Greenwald, E. C. and Saucerman, J. J. **'Bigger, better, faster: principles and models**

of AKAP anchoring protein signaling', *Journal of cardiovascular pharmacology* **58**(5), 462–469. 2011.

Greiser, M., Karbowski, M., Kaplan, A. D., Coleman, A. K., Verhoeven, N., Mannella, C. A., Lederer, W. J. and Boyman, L. **'Calcium and bicarbonate signaling pathways have pivotal, resonating roles in matching ATP production to demand**', *Elife* **12**, e84204. 2023.

Gudbjarnason, S., Telerman, M., Chiba, C., Wolf, P. L. and Bing, R. J. **'MYOCARDIAL PROTEIN SYNTHESIS IN CARDIAC HYPERTROPHY**', *J Lab Clin Med* **63**, 244–53. 1964.

Halestrap, A. P. **'The SLC16 gene family – Structure, role and regulation in health and disease**', *Molecular Aspects of Medicine* **34**(2), 337–349. 2013.

Hall, M. and Saggerson, E. D. **'Reversible inactivation by noradrenaline of long-chain fatty acyl-CoA synthetase in rat adipocytes**', *Biochemical Journal* **226**(1), 275–282. 1985.

Hambleton, R., Krall, J., Tikishvili, E., Honeggar, M., Ahmad, F., Manganiello, V. C. and Movsesian, M. A. **'Isoforms of cyclic nucleotide phosphodiesterase PDE3 and their contribution to cAMP hydrolytic activity in subcellular fractions of human myocardium**', *J Biol Chem* **280**(47), 39168–74. 2005.

Han, T., Goralski, M., Gaskill, N., Capota, E., Kim, J., Ting, T. C., Xie, Y., Williams, N. S. and Nijhawan, D. **'Anticancer sulfonamides target splicing by inducing RBM39 degradation via recruitment to DCAF15**', *Science* **356**(6336). 2017.

Han, X., Light, P. E., Giles, W. R. and French, R. J. **'Identification and properties of an ATP-sensitive K+ current in rabbit sino-atrial node pacemaker cells.**',

The Journal of Physiology **490**(2), 337–350. 1996.

Hayes, J. S., Brunton, L. L. and Mayer, S. E. **'Selective activation of particulate cAMP-dependent protein kinase by isoproterenol and prostaglandin E1**', *J Biol Chem* **255**(11), 5113–9. 1980.

Heijman, J., Dewenter, M., El-Armouche, A. and Dobrev, D. **'Function and regulation of serine/threonine phosphatases in the healthy and diseased heart**', *Journal of Molecular and Cellular Cardiology* **64**, 90–98. 2013.

Hentze, M. W. and Preiss, T. **'The REM phase of gene regulation**', *Trends Biochem Sci* **35**(8), 423–6. 2010.

Herzig, S., Raemy, E., Montessuit, S., Veuthey, J.-L., Zamboni, N., Westermann, B., Kunji, E. R. S. and Martinou, J.-C. **'Identification and Functional Expression of the Mitochondrial Pyruvate Carrier**', *Science* **337**(6090), 93–96. 2012.

Hindson, V. J. **'Serine acetyltransferase of Escherichia coli: substrate specificity and feedback control by cysteine**', *Biochem J* **375**(Pt 3), 745–52. 2003.

Hinney, A., Albayrak, ö., Antel, J., Volckmar, A., Sims, R., Chapman, J., Harold, D., Gerrish, A., Heid, I. M. and Winkler, T. W. **'Genetic variation at the CELF1 (CUGBP, elav-like family member 1 gene) locus is genome-wide associated with Alzheimer's disease and obesity**', *American Journal of Medical Genetics Part B: Neuropsychiatric Genetics* **165**(4), 283–293. 2014.

Hochbaum, D., Barila, G., Ribeiro-Neto, F. and Altschuler, D. L. **'Radixin Assembles cAMP Effectors Epac and PKA into a Functional cAMP Compartment: ROLE IN cAMP-DEPENDENT CELL PROLIFERATION***', *Journal of Biological Chemistry* **286**(1), 859–866. 2011.

Holman, G. D. **'Structure, function and regulation of mammalian glucose transporters of the SLC2 family**', *Pflugers Arch* **472**(9), 1155–1175. 2020.

Holman, G. D., Kozka, I. J., Clark, A. E., Flower, C. J., Saltis, J., Habberfield, A. D., Simpson, I. A. and Cushman, S. W. **'Cell surface labeling of glucose transporter isoform GLUT4 by bis-mannose photolabel. Correlation with stimulation of glucose transport in rat adipose cells by insulin and phorbol ester**', *J Biol Chem* **265**(30), 18172–9. 1990.

Hoyos, L. E. and Abdel-Wahab, O. **'Cancer-Specific Splicing Changes and the Potential for Splicing-Derived Neoantigens**', *Cancer Cell* **34**(2), 181–183. 2018.

Huang, A. Z., Delaidelli, A. and Sorensen, P. H. **'RNA modifications in brain tumorigenesis**', *Acta Neuropathologica Communications* **8**(1), 64. 2020.

Hue, L. and Taegtmeyer, H. **'The Randle cycle revisited: a new head for an old hat**', *Am J Physiol Endocrinol Metab* **297**(3), E578–91. 2009.

human protein atlas (2025).

Itabe, H., Yamaguchi, T., Nimura, S. and Sasabe, N. **'Perilipins: a diversity of intracellular lipid droplet proteins**', *Lipids in Health and Disease* **16**(1), 83. 2017.

Jakobs, S., Stephan, T., Ilgen, P. and Brüser, C. **'Light microscopy of mitochondria at the nanoscale**', *Annual review of biophysics* **49**(1), 289–308. 2020.

Jurevicius, J. and Fischmeister, R. **'cAMP compartmentation is responsible for a local activation of cardiac Ca2+ channels by beta-adrenergic agonists**', *Proceedings of the National Academy of Sciences* **93**(1), 295–299. 1996.

Kamel, R., Bourcier, A., Margaria, J. P., Varin, A., Hivonnait, A., Mercier-Nomé, F.,

Mika, D., Ghigo, A., Charpentier, F., Algalarrondo, V., Hirsch, E., Fischmeister, R., Vandecasteele, G. and Leroy, J. **'Cardiac gene therapy with PDE2A limits remodeling and arrhythmias in mouse models of heart failure induced by catecholamines**', *bioRxiv* . 2023.

Kamenetsky, M., Middelhaufe, S., Bank, E. M., Levin, L. R., Buck, J. and Steegborn, C. **'Molecular details of cAMP generation in mammalian cells: a tale of two systems**', *Journal of molecular biology* **362**(4), 623–639. 2006.

Kammoun, H. L., Chabanon, H., Hainault, I., Luquet, S., Magnan, C., Koike, T., Ferré, P. and Foufelle, F. **'GRP78 expression inhibits insulin and ER stress–induced SREBP-1c activation and reduces hepatic steatosis in mice**', *The Journal of clinical investigation* **119**(5), 1201–1215. 2009.

Kaumann, A. J., Galindo-Tovar, A., Escudero, E. and Vargas, M. L. **'Phosphodiesterases do not limit beta1-adrenoceptor-mediated sinoatrial tachycardia: evidence with PDE3 and PDE4 in rabbits and PDE1-5 in rats**', *Naunyn Schmiedebergs Arch Pharmacol* **380**(5), 421–30. 2009.

Kawaguchi, T., Takenoshita, M., Kabashima, T. and Uyeda, K. **'Glucose and cAMP regulate the L-type pyruvate kinase gene by phosphorylation/dephosphorylation of the carbohydrate response element binding protein**', *Proceedings of the National Academy of Sciences* **98**(24), 13710–13715. 2001.

Kessler, G. and Friedman, J. **'Metabolism of Fatty Acids and Glucose**', *Circulation* **98**(13), 1350a–1353. 1998.

Kinderman, F. S., Kim, C., von Daake, S., Ma, Y., Pham, B. Q., Spraggon, G., Xuong, N.-H., Jennings, P. A. and Taylor, S. S. **'A Dynamic Mechanism for AKAP**

Binding to RII Isoforms of cAMP-Dependent Protein Kinase', *Molecular Cell* **24**(3), 397–408. 2006.

Kitayama, H., Sugimoto, Y., Matsuzaki, T., Ikawa, Y. and Noda, M. **'A ras-related gene with transformation suppressor activity**', *Cell* **56**(1), 77–84. 1989.

Klingenberg, M. **'The ADP and ATP transport in mitochondria and its carrier**', *Biochimica et Biophysica Acta (BBA) - Biomembranes* **1778**(10), 1978–2021. 2008.

Kodde, I. F., van der Stok, J., Smolenski, R. T. and de Jong, J. W. **'Metabolic and genetic regulation of cardiac energy substrate preference**', *Comparative Biochemistry and Physiology Part A: Molecular & Integrative Physiology* **146**(1), 26–39. 2007.

Kohno, K., Izumi, H., Uchiumi, T., Ashizuka, M. and Kuwano, M. **'The pleiotropic functions of the Y-box-binding protein, YB-1**', *Bioessays* **25**(7), 691–8. 2003.

Kokkonen, K. and Kass, D. A. **'Nanodomain Regulation of Cardiac Cyclic Nucleotide Signaling by Phosphodiesterases**', *Annual Review of Pharmacology and Toxicology* **57**(Volume 57, 2017), 455–479. 2017.

Kolleritsch, S., Kien, B., Schoiswohl, G., Diwoky, C., Schreiber, R., Heier, C., Maresch, L. K., Schweiger, M., Eichmann, T. O., Stryeck, S., Krenn, P., Tomin, T., Schittmayer, M., Kolb, D., Rülicke, T., Hoefler, G., Wolinski, H., Madl, T., Birner-Gruenberger, R. and Haemmerle, G. **'Low cardiac lipolysis reduces mitochondrial fission and prevents lipotoxic heart dysfunction in Perilipin 5 mutant mice**', *Cardiovasc Res* **116**(2), 339–352. 2020.

Kondadi, A. K., Anand, R., Hänsch, S., Urbach, J., Zobel, T., Wolf, D. M., Segawa, M., Liesa, M., Shirihai, O. S. and Weidtkamp-Peters, S. **'Cristae undergo continuous**

cycles of membrane remodelling in a MICOS-dependent manner', *EMBO reports* **21**(3), e49776. 2020.

Koschinski, A. and Zaccolo, M. **'Activation of PKA in cell requires higher concentration of cAMP than in vitro: implications for compartmentalization of cAMP signalling**', *Scientific reports* **7**(1), 14090. 2017.

Kots, A. Y. and Bian, K. **'Regulation and Pharmacology of the Cyclic GMP and Nitric Oxide Pathway in Embryonic and Adult Stem Cells**', *Cells* **13**(23), 2008. 2024.

Kovanich, D., Van Der Heyden, M. A., Aye, T. T., Van Veen, T. A., Heck, A. J. and Scholten, A. **'Sphingosine kinase interacting protein is an A-kinase anchoring protein specific for type I cAMP-dependent protein kinase**', *Chembiochem* **11**(7), 963–971. 2010.

Kowluru, A., Chen, H.-Q., Modrick, L. M. and Stefanelli, C. **'Activation of Acetyl-CoA Carboxylase by a Glutamate- and Magnesium-Sensitive Protein Phosphatase in the Islet β-Cell**', *Diabetes* **50**(7), 1580–1587. 2001.

Kunji, E. R. S., King, M. S., Ruprecht, J. J. and Thangaratnarajah, C. **'The SLC25 Carrier Family: Important Transport Proteins in Mitochondrial Physiology and Pathology**', *Physiology (Bethesda)* **35**(5), 302–327. 2020.

Langeberg, L. K. and Scott, J. D. **'Signalling scaffolds and local organization of cellular behaviour**', *Nature Reviews Molecular Cell Biology* **16**(4), 232–244. 2015.

LaNoue, K. F., Jeffries, F. M. and Radda, G. K. **'Kinetic control of mitochondrial ATP synthesis**', *Biochemistry* **25**(23), 7667–75. 1986.

Laudette, M., Sainte-Marie, Y., Cousin, G., Bergonnier, D., Belhabib, I., Brun, S., Formoso,

K., Laib, L., Tortosa, F. and Bergoglio, C. **'Cyclic AMP-binding protein Epac1 acts as a metabolic sensor to promote cardiomyocyte lipotoxicity**', *Cell death & disease* **12**(9), 824. 2021.

Laudette, M., Zuo, H., Lezoualc'h, F. and Schmidt, M. **'Epac Function and cAMP Scaffolds in the Heart and Lung**', *J Cardiovasc Dev Dis* **5**(1). 2018.

Laursen, T., Møller, B. L. and Bassard, J.-E. **'Plasticity of specialized metabolism as mediated by dynamic metabolons**', *Trends in Plant Science* **20**(1), 20–32. 2015.

Lazar, A. M., Irannejad, R., Baldwin, T. A., Sundaram, A. B., Gutkind, J. S., Inoue, A., Dessauer, C. W. and Von Zastrow, M. **'G protein-regulated endocytic trafficking of adenylyl cyclase type 9**', *Elife* **9**. 2020.

Lee, J. H., Giannikopoulos, P., Duncan, S. A., Wang, J., Johansen, C. T., Brown, J. D., Plutzky, J., Hegele, R. A., Glimcher, L. H. and Lee, A.-H. **'The transcription factor cyclic AMP–responsive element–binding protein H regulates triglyceride metabolism**', *Nature Medicine* **17**(7), 812–815. 2011.

Lee, S., Hoyt, S., Wu, X., Garvie, C., McGaunn, J., Shekhar, M., Tötzl, M., Rees, M. G., Cherniack, A. D., Meyerson, M. and Greulich, H. **'Velcrin-induced selective cleavage of tRNALeu(TAA) by SLFN12 causes cancer cell death**', *Nature Chemical Biology* **19**(3), 301–310. 2023.

Lefkimmiatis, K. **'cAMP signalling meets mitochondrial compartments**', *Biochemical Society Transactions* **42**(2), 265–269. 2014.

Lefkimmiatis, K., Leronni, D. and Hofer, A. M. **'The inner and outer compartments of mitochondria are sites of distinct cAMP/PKA signaling dynamics**', *Journal of Cell Biology* **202**(3), 453–462. 2013.

Leite, A. R., Angélico-Gonçalves, A., Vasques-Nóvoa, F., Borges-Canha, M., Leite-Moreira, A., Neves, J. S. and Ferreira, J. P. **'Effect of glucagon-like peptide-1 receptor agonists on cardiovascular events in overweight or obese adults without diabetes: A meta-analysis of placebo-controlled randomized trials**', *Diabetes, Obesity and Metabolism* **24**(8), 1676–1680. 2022.

Levitzki, A. **'From epinephrine to cyclic AMP**', *Science* **241**(4867), 800–6. 1988.

Li, D., Liu, X., Zhou, J., Hu, J., Zhang, D., Liu, J., Qiao, Y. and Zhan, Q. **'Long noncoding RNA HULC modulates the phosphorylation of YB-1 through serving as a scaffold of extracellular signal-regulated kinase and YB-1 to enhance hepatocarcinogenesis**', *Hepatology* **65**(5), 1612–1627. 2017.

Li, H., Degenhardt, B., Tobin, D., Yao, Z.-x., Tasken, K. and Papadopoulos, V. **'Identification, localization, and function in steroidogenesis of PAP7: a peripheral-type benzodiazepine receptor-and PKA (RIα)-associated protein**', *Molecular Endocrinology* **15**(12), 2211–2228. 2001.

Li, H. L., Go, S., Chang, J.-C., Verhoeven, A. and Elferink, R. O. **'Soluble adenylyl cyclase, the cell-autonomous member of the family**', *Biochimica et Biophysica Acta (BBA) - Molecular Basis of Disease* **1870**(2), 166936. 2024.

Li, J., Yan, B., Huo, Z., Liu, Y., Xu, J., Sun, Y., Liu, Y., Liang, D., Peng, L., Zhang, Y., Zhou, Z. N., Shi, J., Cui, J. and Chen, Y. H. **'beta2- but not beta1-adrenoceptor activation modulates intracellular oxygen availability**', *J Physiol* **588**(Pt 16), 2987–98. 2010.

Li, L. O., Ellis, J. M., Paich, H. A., Wang, S., Gong, N., Altshuller, G., Thresher, R. J., Koves, T. R., Watkins, S. M., Muoio, D. M., Cline, G. W., Shulman, G. I. and Coleman, R. A. **'Liver-specific Loss of Long Chain Acyl-CoA Synthetase-1 Decreases**

Triacylglycerol Synthesis and α-Oxidation and Alters Phospholipid Fatty Acid Composition, year = 2009, issn = 0021-9258, number = 41, pages = 27816-27826, volume = 284, doi = 10.1074/jbc.M109.022467, type = Journal Article, url = https://doi.org/10.1074/jbc.M109.022467,', *Journal of Biological Chemistry* .

Liang, K. **, 'Mitochondrial CPT1A: Insights into structure, function, and basis for drug development**'.

Liao, Y., Castello, A., Fischer, B., Leicht, S., Föehr, S., Frese, C. K., Ragan, C., Kurscheid, S., Pagler, E., Yang, H., Krijgsveld, J., Hentze, M. W. and Preiss, T. **'The Cardiomyocyte RNA-Binding Proteome: Links to Intermediary Metabolism and Heart Disease**', *Cell Rep* **16**(5), 1456–1469. 2016.

Libby, P. **'The changing landscape of atherosclerosis**', *Nature* **592**(7855), 524–533. 2021.

Lobo, M. J., Reverte-Salisa, L., Chao, Y. C., Koschinski, A., Gesellchen, F., Subramaniam, G., Jiang, H., Pace, S., Larcom, N., Paolocci, E., Pfeifer, A., Zanivan, S. and Zaccolo, M. **'Phosphodiesterase 2A2 regulates mitochondria clearance through Parkin-dependent mitophagy**', *Commun Biol* **3**(1), 596. 2020.

Lobo, M. J. and Zaccolo, M. (2018), *PDE2A*, Springer International Publishing, Cham, pp. 3826–3834.

Lobo, S., Wiczer, B. and Bernlohr, D. **'Functional Analysis of Long-chain Acyl-CoA Synthetase 1 in 3T3-L1 Adipocytes**', *The Journal of biological chemistry* **284**, 18347–56. 2009.

Lohse, C., Bock, A., Maiellaro, I., Hannawacker, A., Schad, L. R., Lohse, M. J. and Bauer,

W. R. **'Experimental and mathematical analysis of cAMP nanodomains**', *PLoS One* **12**(4), e0174856. 2017.

London, E. and Stratakis, C. A. **'The regulation of PKA signaling in obesity and in the maintenance of metabolic health**', *Pharmacology & Therapeutics* **237**, 108113. 2022.

Lopaschuk, G. D., Karwi, Q. G., Tian, R., Wende, A. R. and Abel, E. D. **'Cardiac Energy Metabolism in Heart Failure**', *Circ Res* **128**(10), 1487–1513. 2021.

Lugnier, C. **'Cyclic nucleotide phosphodiesterase (PDE) superfamily: A new target for the development of specific therapeutic agents**', *Pharmacology & Therapeutics* **109**(3), 366–398. 2006.

Lugnier, C., Keravis, T. and Eckly-Michel, A. **'Cross talk between NO and cyclic nucleotide phosphodiesterases in the modulation of signal transduction in blood vessel**', *J Physiol Pharmacol* **50**(4), 639–52. 1999.

Lugnier, C. and Schini, V. B. **'Characterization of cyclic nucleotide phosphodiesterases from cultured bovine aortic endothelial cells**', *Biochem Pharmacol* **39**(1), 75–84. 1990.

Ma, Y. and Taylor, S. **'A 15-residue bifunctional element in D-AKAP1 is required for both endoplasmic reticulum and mitochondrial targeting**', *Journal of Biological Chemistry* **277**(30), 27328–27336. 2002.

Maier, E., Attenberger, F., Tiwari, A., Lettau, K., Rebholz, S., Fehrenbacher, B., Schaller, M., Gani, C. and Toulany, M. **'Dual Targeting of Y-Box Binding Protein-1 and Akt Inhibits Proliferation and Enhances the Chemosensitivity of Colorectal Cancer Cells**', *Cancers (Basel)* **11**(4). 2019.

Malbon, C., Tao, J., Shumay, E. and Wang, H.-Y. **'AKAP (A-kinase anchoring protein) domains: beads of structure–function on the necklace of G-protein signalling**', *Biochemical Society Transactions* **32**(5), 861–864. 2004.

Martinez, S. E., Wu, A. Y., Glavas, N. A., Tang, X.-B., Turley, S., Hol, W. G. and Beavo, J. A. **'The two GAF domains in phosphodiesterase 2A have distinct roles in dimerization and in cGMP binding**', *Proceedings of the National Academy of Sciences* **99**(20), 13260–13265. 2002.

Martins, T. J., Mumby, M. C. and Beavo, J. A. **'Purification and characterization of a cyclic GMP-stimulated cyclic nucleotide phosphodiesterase from bovine tissues**', *Journal of Biological Chemistry* **257**(4), 1973–1979. 1982.

Marvin, J. S., Kokotos, A. C., Kumar, M., Pulido, C., Tkachuk, A. N., Yao, J. S., Brown, T. A. and Ryan, T. A. **'iATPSnFR2: A high-dynamic-range fluorescent sensor for monitoring intracellular ATP**', *Proceedings of the National Academy of Sciences* **121**(21), e2314604121. 2024.

Mashek, D. G. and Coleman, R. A. **'Cellular fatty acid uptake: the contribution of metabolism**', *Current opinion in lipidology* **17**(3), 274–278. 2006.

Maurice, D. H., Ke, H., Ahmad, F., Wang, Y., Chung, J. and Manganiello, V. C. **'Advances in targeting cyclic nucleotide phosphodiesterases**', *Nat Rev Drug Discov* **13**(4), 290–314. 2014.

McCommis, K. S. and Finck, B. N. **'The Hepatic Mitochondrial Pyruvate Carrier as a Regulator of Systemic Metabolism and a Therapeutic Target for Treating Metabolic Disease**', *Biomolecules* **13**(2). 2023.

McGarry, J. D. and Brown, N. F. **'The Mitochondrial Carnitine Palmitoyltransferase**

System — From Concept to Molecular Analysis', *European Journal of Biochemistry* **244**(1), 1–14. 1997.

McGarry, J. D., Leatherman, G. F. and Foster, D. W. **'Carnitine palmitoyltransferase I. The site of inhibition of hepatic fatty acid oxidation by malonyl-CoA**', *J Biol Chem* **253**(12), 4128–36. 1978.

Means, C. K., Lygren, B., Langeberg, L. K., Jain, A., Dixon, R. E., Vega, A. L., Gold, M. G., Petrosyan, S., Taylor, S. S. and Murphy, A. N. **'An entirely specific type I A-kinase anchoring protein that can sequester two molecules of protein kinase A at mitochondria**', *Proceedings of the National Academy of Sciences* **108**(48), E1227–E1235. 2011.

Mehel, H., Emons, J., Vettel, C., Wittköpper, K., Seppelt, D., Dewenter, M., Lutz, S., Sossalla, S., Maier, L. S., Lechêne, P., Leroy, J., Lefebvre, F., Varin, A., Eschenhagen, T., Nattel, S., Dobrev, D., Zimmermann, W. H., Nikolaev, V. O., Vandecasteele, G., Fischmeister, R. and El-Armouche, A. **'Phosphodiesterase-2 is up-regulated in human failing hearts and blunts β-adrenergic responses in cardiomyocytes**', *J Am Coll Cardiol* **62**(17), 1596–606. 2013.

Menard, L., Maughan, D. and Vigoreaux, J. **'The structural and functional coordination of glycolytic enzymes in muscle: evidence of a metabolon?**', *Biology (Basel)* **3**(3), 623–44. 2014.

Mendez Garcia, M. F., Matsuzaki, S., Batushansky, A., Newhardt, R., Kinter, C., Jin, Y., Mann, S. N., Stout, M. B., Gu, H., Chiao, Y. A., Kinter, M. and Humphries, K. M. **'Increased cardiac PFK-2 protects against high-fat diet-induced cardiomyopathy and mediates beneficial systemic metabolic effects**', *iScience* **26**(7), 107131. 2023.

Mengi, S. A. and Dhalla, N. S. **'Carnitine Palmitoyltransferase-I, a New Target for the Treatment of Heart Failure**', *American Journal of Cardiovascular Drugs* **4**(4), 201–209. 2004.

Merrill, R. A., Dagda, R. K., Dickey, A. S., Cribbs, J. T., Green, S. H., Usachev, Y. M. and Strack, S. **'Mechanism of neuroprotective mitochondrial remodeling by PKA/AKAP1**', *PLoS Biol* **9**(4), e1000612. 2011.

Miles, E. W. **'Tryptophan synthase: a multienzyme complex with an intramolecular tunnel**', *Chem Rec* **1**(2), 140–51. 2001.

Milger, K., Herrmann, T., Becker, C., Gotthardt, D., Zickwolf, J., Ehehalt, R., Watkins, P. A., Stremmel, W. and Füllekrug, J. **'Cellular uptake of fatty acids driven by the ER-localized acyl-CoA synthetase FATP4**', *J Cell Sci* **119**(Pt 22), 4678–88. 2006.

Miner, G. E., So, C. M., Edwards, W., Ragusa, J. V., Wine, J. T., Wong Gutierrez, D., Airola, M. V., Herring, L. E., Coleman, R. A., Klett, E. L. and Cohen, S. **'PLIN5 interacts with FATP4 at membrane contact sites to promote lipid droplet-to-mitochondria fatty acid transport**', *Developmental Cell* **58**(14), 1250–1265.e6. 2023.

Mongillo, M., McSorley, T., Evellin, S., Sood, A., Lissandron, V., Terrin, A., Huston, E., Hannawacker, A., Lohse, M. J. and Pozzan, T. **'Fluorescence resonance energy transfer–based analysis of cAMP dynamics in live neonatal rat cardiac myocytes reveals distinct functions of compartmentalized phosphodiesterases**', *Circulation research* **95**(1), 67–75. 2004.

Mongillo, M., Tocchetti, C. G., Terrin, A., Lissandron, V., Cheung, Y. F., Dostmann, W. R., Pozzan, T., Kass, D. A., Paolocci, N., Houslay, M. D. and Zaccolo, M.

'Compartmentalized phosphodiesterase-2 activity blunts beta-adrenergic cardiac inotropy via an NO/cGMP-dependent pathway', *Circ Res* **98**(2), 226–34. 2006.

Mons, N., Decorte, L., Jaffard, R. and Cooper, D. M. **'Ca2+-sensitive adenylyl cyclases, key integrators of cellular signalling**', *Life Sci* **62**(17-18), 1647–52. 1998.

Monterisi, S., Lobo, M. J., Livie, C., Castle, J. C., Weinberger, M., Baillie, G., Surdo, N. C., Musheshe, N., Stangherlin, A., Gottlieb, E., Maizels, R., Bortolozzi, M., Micaroni, M. and Zaccolo, M. **'PDE2A2 regulates mitochondria morphology and apoptotic cell death via local modulation of cAMP/PKA signalling**', *Elife* **6**. 2017.

Moujalled, D., Weston, R., Anderton, H., Ninnis, R., Goel, P., Coley, A., Huang, D. C., Wu, L., Strasser, A. and Puthalakath, H. **'Cyclic-AMP-dependent protein kinase A regulates apoptosis by stabilizing the BH3-only protein Bim**', *EMBO reports* **12**(1), 77–83. 2011.

Movsesian, M. A. **'Beta-adrenergic receptor agonists and cyclic nucleotide phosphodiesterase inhibitors: shifting the focus from inotropy to cyclic adenosine monophosphate**', *Journal of the American College of Cardiology* **34**(2), 318–324. 1999.

Muckenthaler, M. U., Galy, B. and Hentze, M. W. **'Systemic iron homeostasis and the iron-responsive element/iron-regulatory protein (IRE/IRP) regulatory network**', *Annu Rev Nutr* **28**, 197–213. 2008.

Méry, P. F., Pavoine, C., Belhassen, L., Pecker, F. and Fischmeister, R. **'Nitric oxide regulates cardiac Ca2+ current. Involvement of cGMP-inhibited and cGMP-stimulated phosphodiesterases through guanylyl cyclase activation**', *J Biol Chem* **268**(35), 26286–95. 1993.

Nagampalli, R. S. K., Quesñay, J. E. N., Adamoski, D., Islam, Z., Birch, J., Sebinelli, H. G., Girard, R. M. B. M., Ascenção, C. F. R., Fala, A. M., Pauletti, B. A., Consonni, S. R., de Oliveira, J. F., Silva, A. C. T., Franchini, K. G., Leme, A. F. P., Silber, A. M., Ciancaglini, P., Moraes, I., Dias, S. M. G. and Ambrosio, A. L. B. **'Human mitochondrial pyruvate carrier 2 as an autonomous membrane transporter**', *Scientific Reports* **8**(1), 3510. 2018.

Nakagawa, Y., Satoh, A., Yabe, S., Furusawa, M., Tokushige, N., Tezuka, H., Mikami, M., Iwata, W., Shingyouchi, A. and Matsuzaka, T. **'Hepatic CREB3L3 controls whole-body energy homeostasis and improves obesity and diabetes**', *Endocrinology* **155**(12), 4706–4719. 2014.

Neely, J. R. and Morgan, H. E. **'Relationship between carbohydrate and lipid metabolism and the energy balance of heart muscle**', *Annual review of physiology* **36**(1), 413–459. 1974.

Neely, J. R., Rovetto, M. J. and Oram, J. F. **'Myocardial utilization of carbohydrate and lipids**', *Prog Cardiovasc Dis* **15**(3), 289–329. 1972.

Nevzorova, J., Bengtsson, T., Evans, B. A. and Summers, R. J. **'Characterization of the beta-adrenoceptor subtype involved in mediation of glucose transport in L6 cells**', *Br J Pharmacol* **137**(1), 9–18. 2002.

Nevzorova, J., Evans, B. A., Bengtsson, T. and Summers, R. J. **'Multiple signalling pathways involved in beta2-adrenoceptor-mediated glucose uptake in rat skeletal muscle cells**', *Br J Pharmacol* **147**(4), 446–54. 2006.

Ng, Y. H., Koay, Y. C., Marques, F. Z., Kaye, D. M. and O'Sullivan, J. F. **'Leveraging metabolism for better outcomes in heart failure**', *Cardiovascular Research* **120**(15), 1835–1850. 2024.

Nikolaev, V. O., Bunemann, M., Hein, L., Hannawacker, A. and Lohse, M. J. **'Novel Single Chain cAMP Sensors for Receptor-induced Signal Propagation**', *Journal of Biological Chemistry* **279**(36), 37215–37218. 2004.

Nikolaev, V. O., Bünemann, M., Schmitteckert, E., Lohse, M. J. and Engelhardt, S. **'Cyclic AMP imaging in adult cardiac myocytes reveals far-reaching beta1-adrenergic but locally confined beta2-adrenergic receptor-mediated signaling**', *Circ Res* **99**(10), 1084–91. 2006.

Nikolaev, V. O., Moshkov, A., Lyon, A. R., Miragoli, M., Novak, P., Paur, H., Lohse, M. J., Korchev, Y. E., Harding, S. E. and Gorelik, J. **'Beta2-adrenergic receptor redistribution in heart failure changes cAMP compartmentation**', *Science* **327**(5973), 1653–7. 2010.

Nikolaidis, L. A., Poornima, I., Parikh, P., Magovern, M., Shen, Y. T. and Shannon, R. P. **'The effects of combined versus selective adrenergic blockade on left ventricular and systemic hemodynamics, myocardial substrate preference, and regional perfusion in conscious dogs with dilated cardiomyopathy**', *J Am Coll Cardiol* **47**(9), 1871–81. 2006.

Obayashi, E., Luna, R. E., Nagata, T., Martin-Marcos, P., Hiraishi, H., Singh, C. R., Erzberger, J. P., Zhang, F., Arthanari, H., Morris, J., Pellarin, R., Moore, C., Harmon, I., Papadopoulos, E., Yoshida, H., Nasr, M. L., Unzai, S., Thompson, B., Aube, E., Hustak, S., Stengel, F., Dagraca, E., Ananbandam, A., Gao, P., Urano, T., Hinnebusch, A. G., Wagner, G. and Asano, K. **'Molecular Landscape of the Ribosome Pre-initiation Complex during mRNA Scanning: Structural Role for eIF3c and Its Control by eIF5**', *Cell Reports* **18**(11), 2651–2663. 2017.

Olzmann, J. A. and Carvalho, P. **'Dynamics and functions of lipid droplets**', *Nature Reviews Molecular Cell Biology* **20**(3), 137–155. 2019.

Omori, K. and Kotera, J. **'Overview of PDEs and Their Regulation**', *Circulation Research* **100**(3), 309–327. 2007.

Opie, L. H. (2004), *Heart physiology: from cell to circulation*, Lippincott Williams & Wilkins.

Osadchii, O. E. **'Myocardial phosphodiesterases and regulation of cardiac contractility in health and cardiac disease**', *Cardiovasc Drugs Ther* **21**(3), 171–94. 2007.

Pandit, J., Forman, M. D., Fennell, K. F., Dillman, K. S. and Menniti, F. S. **'Mechanism for the allosteric regulation of phosphodiesterase 2A deduced from the X-ray structure of a near full-length construct**', *Proc Natl Acad Sci U S A* **106**(43), 18225–30. 2009.

Papa, A., Zakharov, S. I., Katchman, A. N., Kushner, J. S., Chen, B.-x., Yang, L., Liu, G., Jimenez, A. S., Eisert, R. J., Bradshaw, G. A., Dun, W., Ali, S. R., Rodriques, A., Zhou, K., Topkara, V., Yang, M., Morrow, J. P., Tsai, E. J., Karlin, A., Wan, E., Kalocsay, M., Pitt, G. S., Colecraft, H. M., Ben-Johny, M. and Marx, S. O. **'Rad regulation of CaV1.2 channels controls cardiac fight-or-flight response**', *Nature Cardiovascular Research* **1**(11), 1022–1038. 2022.

Papa, S. **'The NDUFS4 nuclear gene of complex I of mitochondria and the cAMP cascade**', *Biochimica et Biophysica Acta (BBA)-Bioenergetics* **1555**(1-3), 147–153. 2002.

Pavlaki, N., Froese, A., Li, W., De Jong, K. A., Geertz, B., Subramanian, H., Mohagaonkar, S., Luo, X., Schubert, M., Wiegmann, R., Margaria, J. P., Ghigo, A., Kämmerer, S., Hirsch, E., El-Armouche, A., Guan, K. and Nikolaev, V. O. **'Gene therapy with phosphodiesterases 2A and 4B ameliorates heart failure and arrhythmias by**

improving subcellular cAMP compartmentation', *Cardiovasc Res* **120**(9), 1011–1023. 2024.

Pavlaki, N. and Nikolaev, V. O. **'Imaging of PDE2- and PDE3-Mediated cGMP-to-cAMP Cross-Talk in Cardiomyocytes**', *J Cardiovasc Dev Dis* **5**(1). 2018.

Pereira, B., Billaud, M. and Almeida, R. **'RNA-Binding Proteins in Cancer: Old Players and New Actors**', *Trends Cancer* **3**(7), 506–528. 2017.

Pereira, L., Cheng, H., Lao, D. H., Na, L., van Oort, R. J., Brown, J. H., Wehrens, X. H., Chen, J. and Bers, D. M. **'Epac2 mediates cardiac β1-adrenergic-dependent sarcoplasmic reticulum Ca2+ leak and arrhythmia**', *Circulation* **127**(8), 913–22. 2013.

Pereira, L., Rehmann, H., Lao, D. H., Erickson, J. R., Bossuyt, J., Chen, J. and Bers, D. M. **'Novel Epac fluorescent ligand reveals distinct Epac1 vs. Epac2 distribution and function in cardiomyocytes**', *Proc Natl Acad Sci U S A* **112**(13), 3991–6. 2015.

Peterson, L. R. **'Obesity and insulin resistance: effects on cardiac structure, function, and substrate metabolism**', *Current hypertension reports* **8**(6), 451–456. 2006.

Pfanner, N., Van Der Laan, M., Amati, P., Capaldi, R. A., Caudy, A. A., Chacinska, A., Darshi, M., Deckers, M., Hoppins, S. and Icho, T. **'Uniform nomenclature for the mitochondrial contact site and cristae organizing system**', *Journal of Cell Biology* **204**(7), 1083–1086. 2014.

Pidoux, G., Witczak, O., Jarnæss, E., Myrvold, L., Urlaub, H., Stokka, A. J., Küntziger, T. and Taskén, K. **'Optic atrophy 1 is an A-kinase anchoring protein on lipid droplets that mediates adrenergic control of lipolysis**', *Embo j* **30**(21), 4371–86.

2011.

Piquereau, J., Caffin, F., Novotova, M., Prola, A., Garnier, A., Mateo, P., Fortin, D., Huynh le, H., Nicolas, V., Alavi, M. V., Brenner, C., Ventura-Clapier, R., Veksler, V. and Joubert, F. **'Down-regulation of OPA1 alters mouse mitochondrial morphology, PTP function, and cardiac adaptation to pressure overload**', *Cardiovasc Res* **94**(3), 408–17. 2012.

Pollak, N. M., Jaeger, D., Kolleritsch, S., Zimmermann, R., Zechner, R., Lass, A. and Haemmerle, G. **'The Interplay of Protein Kinase A and Perilipin 5 Regulates Cardiac Lipolysis**', *Journal of Biological Chemistry* **290**(3), 1295–1306. 2015.

Pollak, N. M., Schweiger, M., Jaeger, D., Kolb, D., Kumari, M., Schreiber, R., Kolleritsch, S., Markolin, P., Grabner, G. F., Heier, C., Zierler, K. A., Rülicke, T., Zimmermann, R., Lass, A., Zechner, R. and Haemmerle, G. **'Cardiac-specific overexpression of perilipin 5 provokes severe cardiac steatosis via the formation of a lipolytic barrier**', *J Lipid Res* **54**(4), 1092–102. 2013.

Ponsioen, B., Gloerich, M., Ritsma, L., Rehmann, H., Bos, J. L. and Jalink, K. **'Direct spatial control of Epac1 by cyclic AMP**', *Mol Cell Biol* **29**(10), 2521–31. 2009.

Ponsioen, B., Zhao, J., Riedl, J., Zwartkruis, F., van der Krogt, G., Zaccolo, M., Moolenaar, W. H., Bos, J. L. and Jalink, K. **'Detecting cAMP-induced Epac activation by fluorescence resonance energy transfer: Epac as a novel cAMP indicator**', *EMBO Rep* **5**(12), 1176–80. 2004.

Porat-Shliom, N., Harding, O. J., Malec, L., Narayan, K. and Weigert, R. **'Mitochondrial Populations Exhibit Differential Dynamic Responses to Increased Energy Demand during Exocytosis In Vivo**', *iScience* **11**, 440–449. 2019.

Portman, M. A. **'The Adenine Nucleotide Translocator: Regulation And Function During Myocardial Development And Hypertrophy'**, *Clinical and Experimental Pharmacology and Physiology* **29**(4), 334–338. 2002.

Pryde, K. R., Smith, H. L., Chau, K.-Y. and Schapira, A. H. **'PINK1 disables the anti-fission machinery to segregate damaged mitochondria for mitophagy'**, *Journal of Cell Biology* **213**(2), 163–171. 2016.

Pérez-Schindler, J., Philp, A., Baar, K. and Hernández-Cascales, J. **'Regulation of contractility and metabolic signaling by the β2-adrenergic receptor in rat ventricular muscle'**, *Life Sci* **88**(19-20), 892–7. 2011.

Raaijmakers, J. H. and Bos, J. L. **'Specificity in Ras and Rap signaling'**, *J Biol Chem* **284**(17), 10995–9. 2009.

Rambold, A. S., Cohen, S. and Lippincott-Schwartz, J. **'Fatty Acid Trafficking in Starved Cells: Regulation by Lipid Droplet Lipolysis, Autophagy, and Mitochondrial Fusion Dynamics'**, *Developmental Cell* **32**(6), 678–692. 2015.

Randle, P. J., Garland, P. B., Hales, C. N. and Newsholme, E. A. **'The glucose fatty-acid cycle. Its role in insulin sensitivity and the metabolic disturbances of diabetes mellitus'**, *Lancet* **1**(7285), 785–9. 1963.

Ravnskjaer, K., Madiraju, A. and Montminy, M. (2016), *Role of the cAMP Pathway in Glucose and Lipid Metabolism*, Springer International Publishing, Cham, pp. 29–49.

Rehmann, H., Arias-Palomo, E., Hadders, M. A., Schwede, F., Llorca, O. and Bos, J. L. **'Structure of Epac2 in complex with a cyclic AMP analogue and RAP1B'**, *Nature* **455**(7209), 124–7. 2008.

Rehmann, H., Das, J., Knipscheer, P., Wittinghofer, A. and Bos, J. L. **'Structure of the**

cyclic-AMP-responsive exchange factor Epac2 in its auto-inhibited state', *Nature* **439**(7076), 625–628. 2006.

Reinhardt, R. R., Chin, E., Zhou, J., Taira, M., Murata, T., Manganiello, V. C. and Bondy, C. A. **'Distinctive anatomical patterns of gene expression for cGMP-inhibited cyclic nucleotide phosphodiesterases**', *The Journal of clinical investigation* **95**(4), 1528–1538. 1995.

Ren, Z., Chen, S., Pak, S. and Guo, L. **'A mechanism of perhexiline's cytotoxicity in hepatic cells involves endoplasmic reticulum stress and p38 signaling pathway**', *Chem Biol Interact* **334**, 109353. 2021.

Richards, M., Lomas, O., Jalink, K., Ford, K. L., Vaughan-Jones, R. D., Lefkimmiatis, K. and Swietach, P. **'Intracellular tortuosity underlies slow cAMP diffusion in adult ventricular myocytes**', *Cardiovascular research* **110**(3), 395–407. 2016.

Richards, M. R., Harp, J. D., Ory, D. S. and Schaffer, J. E. **'Fatty acid transport protein 1 and long-chain acyl coenzyme A synthetase 1 interact in adipocytes**', *Journal of Lipid Research* **47**(3), 665–672. 2006.

Rickey and Weilch, G. (1995), *Chapter 4 The organization of metabolic pathways in vivo*, Vol. 4, Elsevier, pp. 77–92.

Rinaldi, L., Delle Donne, R., Borzacchiello, D., Insabato, L. and Feliciello, A. **'The role of compartmentalized signaling pathways in the control of mitochondrial activities in cancer cells**', *Biochim Biophys Acta Rev Cancer* **1869**(2), 293–302. 2018.

Rodbell, M., Birnbaumer, L., Pohl, S. L. and Krans, H. M. **'The glucagon-sensitive adenyl cyclase system in plasma membranes of rat liver. V. An obligatory role of guanylnucleotides in glucagon action**', *J Biol Chem* **246**(6), 1877–82. 1971.

Rogne, M., Chu, D.-T., Küntziger, T. M., Mylonakou, M.-N., Collas, P. and Tasken, K. **'OPA1-anchored PKA phosphorylates perilipin 1 on S522 and S497 in adipocytes differentiated from human adipose stem cells**', *Molecular Biology of the Cell* **29**(12), 1487–1501. 2018.

Rosman, G. J., Martins, T. J., Sonnenburg, W. K., Beavo, J. A., Ferguson, K. and Loughney, K. **'Isolation and characterization of human cDNAs encoding a cGMP-stimulated 3',5'-cyclic nucleotide phosphodiesterase**', *Gene* **191**(1), 89–95. 1997.

Rous, S. **'Effect of dibutyryl cAMP on the enzymes of fatty acid synthesis and of glycogen metabolism**', *FEBS Lett* **12**(1), 45–48. 1970.

Rupp, H. and Jacob, R. **'Metabolically-modulated growth and phenotype of the rat heart**', *European heart journal* **13**(suppl_D), 56–61. 1992.

Saha, A. K. and Ruderman, N. B. **'Malonyl-CoA and AMP-activated protein kinase: an expanding partnership**', *Molecular and cellular biochemistry* **253**, 65–70. 2003.

Sakamoto, K. and Holman, G. D. **'Emerging role for AS160/TBC1D4 and TBC1D1 in the regulation of GLUT4 traffic**', *Am J Physiol Endocrinol Metab* **295**(1), E29–37. 2008.

Sandroni, P. B., Fisher-Wellman, K. H. and Jensen, B. C. **'Adrenergic Receptor Regulation of Mitochondrial Function in Cardiomyocytes**', *J Cardiovasc Pharmacol* **80**(3), 364–377. 2022.

Saraiva, F. K. and Sposito, A. C. **'Cardiovascular effects of glucagon-like peptide 1 (GLP-1) receptor agonists**', *Cardiovasc Diabetol* **13**, 142. 2014.

Savkur, R. S., Philips, A. V. and Cooper, T. A. **'Aberrant regulation of insulin**

receptor alternative splicing is associated with insulin resistance in myotonic dystrophy', *Nature genetics* **29**(1), 40–47. 2001.

Schaffer, J. E. and Lodish, H. F. **'Expression cloning and characterization of a novel adipocyte long chain fatty acid transport protein**', *Cell* **79**(3), 427–436. 1994.

Schneider, J. W., Oommen, S., Qureshi, M. Y., Goetsch, S. C., Pease, D. R., Sundsbak, R. S., Guo, W., Sun, M., Sun, H., Kuroyanagi, H., Webster, D. A., Coutts, A. W., Holst, K. A., Edwards, B. S., Newville, N., Hathcock, M. A., Melkamu, T., Briganti, F., Wei, W., Romanelli, M. G., Fahrenkrug, S. C., Frantz, D. E., Olson, T. M., Steinmetz, L. M., Carlson, D. F. and Nelson, T. J. **'Dysregulated ribonucleoprotein granules promote cardiomyopathy in RBM20 gene-edited pigs**', *Nat Med* **26**(11), 1788–1800. 2020.

Schulze, P. C., Drosatos, K. and Goldberg, I. J. **'Lipid Use and Misuse by the Heart**', *Circ Res* **118**(11), 1736–51. 2016.

Schwoch, G., Trinczek, B. and Bode, C. **'Localization of catalytic and regulatory subunits of cyclic AMP-dependent protein kinases in mitochondria from various rat tissues**', *Biochemical Journal* **270**(1), 181–188. 1990.

Scott, J. D., Dessauer, C. W. and Taskén, K. **'Creating order from chaos: cellular regulation by kinase anchoring**', *Annual review of pharmacology and toxicology* **53**(1), 187–210. 2013.

Selbie, L. A. and Hill, S. J. **'G protein-coupled-receptor cross-talk: the fine-tuning of multiple receptor-signalling pathways**', *Trends Pharmacol Sci* **19**(3), 87–93. 1998.

Sen, S., Talukdar, I. and Webster, N. J. **'SRp20 and CUG-BP1 modulate insulin receptor exon 11 alternative splicing**', *Molecular and cellular biology* **29**(3), 871–880. 2009.

Seybold, J., Thomas, D., Witzenrath, M., Boral, S., Hocke, A. C., Bürger, A., Hatzelmann, A., Tenor, H., Schudt, C., Krüll, M., Schütte, H., Hippenstiel, S. and Suttorp, N. **'Tumor necrosis factor-alpha-dependent expression of phosphodiesterase 2: role in endothelial hyperpermeability**', *Blood* **105**(9), 3569–76. 2005.

Seydi, E., Tabbati, Y. and Pourahmad, J. **'Toxicity of atenolol and propranolol on rat heart mitochondria**', *Drug Research* **70**(04), 151–157. 2020.

Sharma, S., Adrogue, J. V., Golfman, L., Uray, I., Lemm, J., Youker, K., Noon, G. P., Frazier, O. and Taegtmeyer, H. **'Intramyocardial lipid accumulation in the failing human heart resembles the lipotoxic rat heart**', *The FASEB Journal* **18**(14), 1692–1700. 2004.

Shen, J. X. and Cooper, D. M. **'AKAP79, PKC, PKA and PDE4 participate in a Gq-linked muscarinic receptor and adenylate cyclase 2 cAMP signalling complex**', *Biochem J* **455**(1), 47–56. 2013.

Sikkel, M. B., Francis, D. P., Howard, J., Gordon, F., Rowlands, C., Peters, N. S., Lyon, A. R., Harding, S. E. and MacLeod, K. T. **'Hierarchical statistical techniques are necessary to draw reliable conclusions from analysis of isolated cardiomyocyte studies**', *Cardiovascular research* **113**(14), 1743–1752. 2017.

Sim, A. T. and Scott, J. D. **'Targeting of PKA, PKC and protein phosphatases to cellular microdomains**', *Cell Calcium* **26**(5), 209–17. 1999.

Singh, G., Pratt, G., Yeo, G. W. and Moore, M. J. **'The Clothes Make the mRNA:**

Past and Present Trends in mRNP Fashion', *Annu Rev Biochem* **84**, 325–54. 2015.

Skroblin, P., Grossmann, S., Schäfer, G., Rosenthal, W. and Klussmann, E. **'Mechanisms of protein kinase A anchoring**', *International review of cell and molecular biology* **283**, 235–330. 2010.

Smith, K. E., Gibson, E. S. and Dell'Acqua, M. L. **'cAMP-dependent protein kinase postsynaptic localization regulated by NMDA receptor activation through translocation of an A-kinase anchoring protein scaffold protein**', *J Neurosci* **26**(9), 2391–402. 2006.

Smith, R. L., Soeters, M. R., Wüst, R. C. I. and Houtkooper, R. H. **'Metabolic Flexibility as an Adaptation to Energy Resources and Requirements in Health and Disease**', *Endocrine Reviews* **39**(4), 489–517. 2018.

Smith, S. **'The animal fatty acid synthase: one gene, one polypeptide, seven enzymes**', *Faseb j* **8**(15), 1248–59. 1994.

Spivey, H. O. and Merz, J. M. **'Metabolic compartmentation**', *Bioessays* **10**(4), 127–30. 1989.

Srere, P. A. **'The metabolon**', *Trends in Biochemical Sciences* **10**(3), 109–110. 1985.

Srivastava, R. K., Srivastava, A. R., Korsmeyer, S. J., Nesterova, M., Cho-Chung, Y. S. and Longo, D. L. **'Involvement of microtubules in the regulation of Bcl2 phosphorylation and apoptosis through cyclic AMP-dependent protein kinase**', *Molecular and cellular biology* . 1998.

Stahl, A., Hirsch, D. J., Gimeno, R. E., Punreddy, S., Ge, P., Watson, N., Patel, S., Kotler,

M., Raimondi, A., Tartaglia, L. A. and Lodish, H. F. **'Identification of the Major Intestinal Fatty Acid Transport Protein**', *Molecular Cell* **4**(3), 299–308. 1999.

Stangherlin, A., Koschinski, A., Terrin, A., Zoccarato, A., Jiang, H., Fields, L. A. and Zaccolo, M. **'Analysis of compartmentalized cAMP: a method to compare signals from differently targeted FRET reporters**', *Methods Mol Biol* **1071**, 59–71. 2014.

Stephenson, D. T., Coskran, T. M., Wilhelms, M. B., Adamowicz, W. O., O'Donnell, M. M., Muravnick, K. B., Menniti, F. S., Kleiman, R. J. and Morton, D. **'Immunohistochemical Localization of Phosphodiesterase 2A in Multiple Mammalian Species**', *Journal of Histochemistry & Cytochemistry* **57**(10), 933–949. 2009.

Stork, P. J. and Schmitt, J. M. **'Crosstalk between cAMP and MAP kinase signaling in the regulation of cell proliferation**', *Trends Cell Biol* **12**(6), 258–66. 2002.

Subramaniam, G., Schleicher, K., Kovanich, D., Zerio, A., Folkmanaite, M., Chao, Y.-C., Surdo, N. C., Koschinski, A., Hu, J., Scholten, A., Heck, A. J., Ercu, M., Sholokh, A., Park, K. C., Klussmann, E., Meraviglia, V., Bellin, M., Zanivan, S., Hester, S., Mohammed, S. and Zaccolo, M. **'Integrated Proteomics Unveils Nuclear PDE3A2 as a Regulator of Cardiac Myocyte Hypertrophy**', *Circulation Research* **132**(7), 828–848. 2023.

Suen, D. F., Norris, K. L. and Youle, R. J. **'Mitochondrial dynamics and apoptosis**', *Genes Dev* **22**(12), 1577–90. 2008.

Sunahara, R. K., Dessauer, C. W. and Gilman, A. G. **'Complexity and diversity of mammalian adenylyl cyclases**', *Annu Rev Pharmacol Toxicol* **36**, 461–80. 1996.

Surapisitchat, J., Jeon, K. I., Yan, C. and Beavo, J. A. **'Differential regulation of endothelial cell permeability by cGMP via phosphodiesterases 2 and 3**', *Circ Res* **101**(8), 811–8. 2007.

Surdo, N. C., Berrera, M., Koschinski, A., Brescia, M., Machado, M. R., Carr, C., Wright, P., Gorelik, J., Morotti, S., Grandi, E., Bers, D. M., Pantano, S. and Zaccolo, M. **'FRET biosensor uncovers cAMP nano-domains at β-adrenergic targets that dictate precise tuning of cardiac contractility**', *Nat Commun* **8**, 15031. 2017.

Sutherland, E. W. and Rall, T. W. **'Fractionation and characterization of a cyclic adenine ribonucleotide formed by tissue particles**', *J Biol Chem* **232**(2), 1077–91. 1958.

Suzuki, Y., Nakano, K., Sugiyama, M. and Imagawa, J. **'betaARK1 inhibition improves survival in a mouse model of heart failure induced by myocardial infarction**', *J Cardiovasc Pharmacol* **44**(3), 329–34. 2004.

Tao, Y., Zhang, Q., Wang, H., Yang, X. and Mu, H. **'Alternative splicing and related RNA binding proteins in human health and disease**', *Signal Transduction and Targeted Therapy* **9**(1), 26. 2024.

Tatman, P. D., Kao, D. P., Chatfield, K. C., Carroll, I. A., Wagner, J. A., Jonas, E. R., Sucharov, C. C., Port, J. D., Lowes, B. D., Minobe, W. A., Huebler, S. P., Karimpour-Fard, A., Rodriguez, E. M., Liggett, S. B. and Bristow, M. R. **'An extensive β1-adrenergic receptor gene signaling network regulates molecular remodeling in dilated cardiomyopathies**', *JCI Insight* **8**(16). 2023.

Taylor, S. S., Buechler, J. A. and Yonemoto, W. **'cAMP-dependent protein kinase: framework for a diverse family of regulatory enzymes**', *Annual review of biochemistry* **59**, 971–1005. 1990.

Taylor, S. S., Zhang, P., Steichen, J. M., Keshwani, M. M. and Kornev, A. P. **'PKA: lessons learned after twenty years'**, *Biochimica et Biophysica Acta (BBA)-Proteins and Proteomics* **1834**(7), 1271–1278. 2013.

Technikova-Dobrova, Z., Sardanelli, A. M., Speranza, F., Scacco, S., Signorile, A., Lorusso, V. and Papa, S. **'Cyclic adenosine monophosphate-dependent phosphorylation of mammalian mitochondrial proteins: enzyme and substrate characterization and functional role'**, *Biochemistry* **40**(46), 13941–13947. 2001.

Thul, P. J., Åkesson, L., Wiking, M., Mahdessian, D., Geladaki, A., Ait Blal, H., Alm, T., Asplund, A., Björk, L., Breckels, L. M., Bäckström, A., Danielsson, F., Fagerberg, L., Fall, J., Gatto, L., Gnann, C., Hober, S., Hjelmare, M., Johansson, F., Lee, S., Lindskog, C., Mulder, J., Mulvey, C. M., Nilsson, P., Oksvold, P., Rockberg, J., Schutten, R., Schwenk, J. M., Sivertsson, A., Sjöstedt, E., Skogs, M., Stadler, C., Sullivan, D. P., Tegel, H., Winsnes, C., Zhang, C., Zwahlen, M., Mardinoglu, A., Pontén, F., von Feilitzen, K., Lilley, K. S., Uhlén, M. and Lundberg, E. **'A subcellular map of the human proteome'**, *Science* **356**(6340), eaal3321. 2017.

Tong, L. **'Acetyl-coenzyme A carboxylase: crucial metabolic enzyme and attractive target for drug discovery'**, *Cellular and Molecular Life Sciences CMLS* **62**(16), 1784–1803. 2005.

Torres-Quesada, O., Mayrhofer, J. E. and Stefan, E. **'The many faces of compartmentalized PKA signalosomes'**, *Cellular signalling* **37**, 1–11. 2017.

Turcani, M. and Rupp, H. **'Etomoxir Improves Left Ventricular Performance of Pressure-Overloaded Rat Heart'**, *Circulation* **96**(10), 3681–3686. 1997.

Uehara, T., Minoshima, Y., Sagane, K., Sugi, N. H., Mitsuhashi, K. O., Yamamoto, N., Kamiyama, H., Takahashi, K., Kotake, Y., Uesugi, M., Yokoi, A., Inoue, A., Yoshida,

T., Mabuchi, M., Tanaka, A. and Owa, T. **'Selective degradation of splicing factor CAPERα by anticancer sulfonamides**', *Nature Chemical Biology* **13**(6), 675–680. 2017.

Ueno, M., Suzuki, J., Hirose, M., Sato, S., Imagawa, M., Zenimaru, Y., Takahashi, S., Ikuyama, S., Koizumi, T., Konoshita, T., Kraemer, F. B. and Ishizuka, T. **'Cardiac overexpression of perilipin 2 induces dynamic steatosis: prevention by hormone-sensitive lipase**', *Am J Physiol Endocrinol Metab* **313**(6), E699–e709. 2017.

Ule, J. and Blencowe, B. J. **'Alternative Splicing Regulatory Networks: Functions, Mechanisms, and Evolution**', *Molecular Cell* **76**(2), 329–345. 2019.

Usui, I., Imamura, T., Babendure, J. L., Satoh, H., Lu, J. C., Hupfeld, C. J. and Olefsky, J. M. **'G protein-coupled receptor kinase 2 mediates endothelin-1-induced insulin resistance via the inhibition of both Galphaq/11 and insulin receptor substrate-1 pathways in 3T3-L1 adipocytes**', *Mol Endocrinol* **19**(11), 2760–8. 2005.

Vallorz, E. L., Blohm-Mangone, K., Schnellmann, R. G. and Mansour, H. M. **'Formoterol PLGA-PEG nanoparticles induce mitochondrial biogenesis in renal proximal tubules**', *The AAPS journal* **23**(4), 88. 2021.

Valsecchi, F., Konrad, C. and Manfredi, G. **'Role of soluble adenylyl cyclase in mitochondria**', *Biochimica et Biophysica Acta (BBA)-Molecular Basis of Disease* **1842**(12), 2555–2560. 2014.

Verma, S. K., Deshmukh, V., Liu, P., Nutter, C. A., Espejo, R., Hung, M.-L., Wang, G.-S., Yeo, G. W. and Kuyumcu-Martinez, M. N. **'Reactivation of fetal splicing programs in diabetic hearts is mediated by protein kinase C signaling**', *Journal of Biological Chemistry* **288**(49), 35372–35386. 2013.

Vettel, C., Lindner, M., Dewenter, M., Lorenz, K., Schanbacher, C., Riedel, M., Lämmle, S., Meinecke, S., Mason, F. E., Sossalla, S., Geerts, A., Hoffmann, M., Wunder, F., Brunner, F. J., Wieland, T., Mehel, H., Karam, S., Lechêne, P., Leroy, J., Vandecasteele, G., Wagner, M., Fischmeister, R. and El-Armouche, A. **'Phosphodiesterase 2 Protects Against Catecholamine-Induced Arrhythmia and Preserves Contractile Function After Myocardial Infarction**', *Circulation Research* **120**(1), 120–132. 2017.

Vinge, L. E., Øie, E., Andersson, Y., Grøgaard, H. K., Andersen, G. and Attramadal, H. **'Myocardial distribution and regulation of GRK and beta-arrestin isoforms in congestive heart failure in rats**', *Am J Physiol Heart Circ Physiol* **281**(6), H2490–9. 2001.

Virshup, D. M. and Shenolikar, S. **'From Promiscuity to Precision: Protein Phosphatases Get a Makeover**', *Molecular Cell* **33**(5), 537–545. 2009.

Völkers, M., Preiss, T. and Hentze, M. W. **'RNA-binding proteins in cardiovascular biology and disease: the beat goes on**', *Nat Rev Cardiol* **21**(6), 361–378. 2024.

Walsh, D. A., Perkins, J. P. and Krebs, E. G. **'An adenosine 3',5'-monophosphate-dependant protein kinase from rabbit skeletal muscle**', *J Biol Chem* **243**(13), 3763–5. 1968.

Wang, H., Robichaux, W. G., Wang, Z., Mei, F. C., Cai, M., Du, G., Chen, J. and Cheng, X. **'Inhibition of Epac1 suppresses mitochondrial fission and reduces neointima formation induced by vascular injury**', *Scientific Reports* **6**(1), 36552. 2016.

Wang, L., Sunahara, R. K., Krumins, A., Perkins, G., Crochiere, M. L., Mackey, M., Bell, S., Ellisman, M. H. and Taylor, S. S. **'Cloning and mitochondrial localization of**

full-length D-AKAP2, a protein kinase A anchoring protein', *Proceedings of the National Academy of Sciences* **98**(6), 3220–3225. 2001.

Watson, W. D., Green, P. G., Lewis, A. J. M., Arvidsson, P., De Maria, G. L., Arheden, H., Heiberg, E., Clarke, W. T., Rodgers, C. T., Valkovič, L., Neubauer, S., Herring, N. and Rider, O. J. **'Retained Metabolic Flexibility of the Failing Human Heart**', *Circulation* **148**(2), 109–123. 2023.

Wechsler, J., Choi, Y.-H., Krall, J., Ahmad, F., Manganiello, V. C. and Movsesian, M. A. **'Isoforms of Cyclic Nucleotide Phosphodiesterase PDE3A in Cardiac Myocytes ***', *Journal of Biological Chemistry* **277**(41), 38072–38078. 2002.

Weissinger, E. M., Eissner, G., Grammer, C., Fackler, S., Haefner, B., Yoon, L. S., Lu, K. S., Bazarov, A., Sedivy, J. M., Mischak, H. and Kolch, W. **'Inhibition of the Raf-1 kinase by cyclic AMP agonists causes apoptosis of v-abl-transformed cells**', *Mol Cell Biol* **17**(6), 3229–41. 1997.

Westermann, B. **'Mitochondrial fusion and fission in cell life and death**', *Nature reviews Molecular cell biology* **11**(12), 872–884. 2010.

Wills, L. P., Trager, R. E., Beeson, G. C., Lindsey, C. C., Peterson, Y. K., Beeson, C. C. and Schnellmann, R. G. **'The β2-adrenoceptor agonist formoterol stimulates mitochondrial biogenesis**', *The Journal of pharmacology and experimental therapeutics* **342**(1), 106–118. 2012.

Wolfgang, M. J. and Lane, M. D. **'The role of hypothalamic malonyl-CoA in energy homeostasis**', *J Biol Chem* **281**(49), 37265–9. 2006.

Wu, Q., Ortegon, A. M., Tsang, B., Doege, H., Feingold, K. R. and Stahl, A. **'FATP1 is an insulin-sensitive fatty acid transporter involved in diet-induced obesity**',

Mol Cell Biol **26**(9), 3455–67. 2006.

Wu, X., Schnitzler, G. R., Gao, G. F., Diamond, B., Baker, A. R., Kaplan, B., Williamson, K., Westlake, L., Lorrey, S., Lewis, T. A., Garvie, C. W., Lange, M., Hayat, S., Seidel, H., Doench, J., Cherniack, A. D., Kopitz, C., Meyerson, M. and Greulich, H. **'Mechanistic insights into cancer cell killing through interaction of phosphodiesterase 3A and schlafen family member 12**', *J Biol Chem* **295**(11), 3431–3446. 2020.

Xu, S., Wang, P., Zhang, H., Gong, G., Gutierrez Cortes, N., Zhu, W., Yoon, Y., Tian, R. and Wang, W. **'CaMKII induces permeability transition through Drp1 phosphorylation during chronic β-AR stimulation**', *Nat Commun* **7**, 13189. 2016.

Xu, Y., Nijhuis, A. and Keun, H. C. **'RNA-binding motif protein 39 (RBM39): An emerging cancer target**', *Br J Pharmacol* **179**(12), 2795–2812. 2022.

Yamamoto, K. K., Gonzalez, G. A., Biggs, W. H., r. and Montminy, M. R. **'Phosphorylation-induced binding and transcriptional efficacy of nuclear factor CREB**', *Nature* **334**(6182), 494–8. 1988.

Yan, C., Miller, C. L. and Abe, J. **'Regulation of phosphodiesterase 3 and inducible cAMP early repressor in the heart**', *Circ Res* **100**(4), 489–501. 2007.

Yasuda, K., Matsunaga, T., Adachi, T., Aoki, N., Tsujimoto, G. and Tsuda, K. **'Adrenergic receptor polymorphisms and autonomic nervous system function in human obesity**', *Trends in Endocrinology & Metabolism* **17**(7), 269–275. 2006.

Yu, S., Wu, Y., Li, C., Qu, Z., Lou, G., Guo, X., Ji, J., Li, N., Guo, M., Zhang, M., Lei, L. and Tai, S. **'Comprehensive analysis of the SLC16A gene family in pancreatic cancer via integrated bioinformatics**', *Scientific Reports* **10**(1), 7315. 2020.

Zaccolo, M., De Giorgi, F., Cho, C. Y., Feng, L., Knapp, T., Negulescu, P. A., Taylor,

S. S., Tsien, R. Y. and Pozzan, T. **'A genetically encoded, fluorescent indicator for cyclic AMP in living cells**', *Nat Cell Biol* **2**(1), 25–9. 2000.

Zaccolo, M. and Movsesian, M. A. **'cAMP and cGMP Signaling Cross-Talk**', *Circulation Research* **100**(11), 1569–1578. 2007.

Zaccolo, M. and Pozzan, T. **'Discrete microdomains with high concentration of cAMP in stimulated rat neonatal cardiac myocytes**', *Science* **295**(5560), 1711–5. 2002.

Zaccolo, M., Zerio, A. and Lobo, M. J. **'Subcellular Organization of the cAMP Signaling Pathway**', *Pharmacological Reviews* **73**(1), 278–309. 2021.

Zadoorian, A., Du, X. and Yang, H. **'Lipid droplet biogenesis and functions in health and disease**', *Nat Rev Endocrinol* **19**(8), 443–459. 2023.

Zhai, K., Gu, L., Yang, Z., Mao, Y., Jin, M., Chang, Y., Yuan, Q., Leblais, V., Wang, H., Fischmeister, R. and Ji, G. **'RNA-binding protein CUGBP1 regulates insulin secretion via activation of phosphodiesterase 3B in mice**', *Diabetologia* **59**(9), 1959–1967. 2016.

Zhan, T., Poppelreuther, M., Ehehalt, R. and Füllekrug, J. **'Overexpressed FATP1, ACSVL4/FATP4 and ACSL1 increase the cellular fatty acid uptake of 3T3-L1 adipocytes but are localized on intracellular membranes**', *PLoS One* **7**(9), e45087. 2012.

Zhang, F., Zhang, L., Qi, Y. and Xu, H. **'Mitochondrial cAMP signaling**', *Cellular and Molecular Life Sciences* **73**(24), 4577–4590. 2016.

Zhao, X., León, I. R., Bak, S., Mogensen, M., Wrzesinski, K., Højlund, K. and Jensen, O. N. **'Phosphoproteome analysis of functional mitochondria isolated from**

resting human muscle reveals extensive phosphorylation of inner membrane protein complexes and enzymes', *Mol Cell Proteomics* **10**(1), M110.000299. 2011.

Zhong, J., Chen, H., Liu, Q., Zhou, S., Liu, Z. and Xiao, Y. **'GLP-1 receptor agonists and myocardial metabolism in atrial fibrillation**', *Journal of Pharmaceutical Analysis* **14**(5), 100917. 2024.

Zhu, J., Yang, Q., Dai, D. and Huang, Q. **'X-ray crystal structure of phosphodiesterase 2 in complex with a highly selective, nanomolar inhibitor reveals a binding-induced pocket important for selectivity**', *J Am Chem Soc* **135**(32), 11708–11. 2013.

Ziegler, M. G., Elayan, H., Milic, M., Sun, P. and Gharaibeh, M. **'Epinephrine and the metabolic syndrome**', *Curr Hypertens Rep* **14**(1), 1–7. 2012.

Zoccarato, A., Surdo, N. C., Aronsen, J. M., Fields, L. A., Mancuso, L., Dodoni, G., Stangherlin, A., Livie, C., Jiang, H. and Sin, Y. Y. **'Cardiac hypertrophy is inhibited by a local pool of cAMP regulated by phosphodiesterase 2**', *Circulation research* **117**(8), 707–719. 2015.

Zou, Z., Tong, F., Faergeman, N. J., Børsting, C., Black, P. N. and DiRusso, C. C. **'Vectorial acylation in Saccharomyces cerevisiae. Fat1p and fatty acyl-CoA synthetase are interacting components of a fatty acid import complex**', *J Biol Chem* **278**(18), 16414–22. 2003.